Institut für Nutzpflanzenwissenschaften und Ressourcenschutz (INRES)
Fachbereich Pflanzenzüchtung

Genetic and molecular analysis of drought stress adaptation in cultivated and wild barley

Dissertation

zur Erlangung des Grades

Doktor der Agrarwissenschaften (Dr. agr.)

der Landwirtschaftlichen Fakultät

der Rheinischen Friedrich-Wilhelms-Universität Bonn

vorgelegt von

Asis Shrestha

aus

Sindhuli, Nepal

Bonn 2020

Angefertigt mit Genehmigung der Landwirtschaftlichen Fakultät der Universität Bonn

Referent:	PD Dr. Ali Ahmad Naz
Koreferent:	Prof. Dr. Gabriel Schaaf
Fachnahes Mitglied:	Prof. Dr. Michael Frei
Prüfungsvorsitz:	Prof. Dr. Jens Léon
Tag der mündlichen Prüfung:	21.09.2020

Acknowledgment

First, I would like to express my sincere gratitude to PD Dr. Ali Naz for providing this fantastic opportunity to work under his supervision and excellent guidance throughout the Doctoral research. I am grateful to Prof. Dr. Jens Léon for his support and guidance during my research. I am also thankful to Prof. Dr. Gabriel Schaaf for being my second supervisor, sharing the research ideas and providing valuable comments on my thesis. I also thank him for providing the experimental facility. I would also like to thank Prof. Dr. Michael Frei for sharing his research ideas and accepting my request to be part of the examination committee.

I would like to thank Prof. Dr. Florian Grundler and his team (Molekulare Phytomedizin) for sharing the experimental facilities. My sincere appreciation goes to Prof. Dr. Shahid Siddique and Dr. Illys Mohammad for their support and technical guidance to perform heterologous expression. Dr. Samer Habash and Dr. Zoran Radkovic showed me the techniques to culture Arabidopsis plants.

My sincere gratitude also goes to Dr. Jochen Kumlehn, and his team (Reproductive biology, IPK, Gatersleben) for their support during my research stay in IPK. Special thank you to Dr. Götz Hensel for his guidance in developing CRISPR constructs and coordinating barley transformation work. Also, I would like to send my appreciation to the technical staff who did transformation and sent us T_1 seeds.

I would also like to thank Dr. Fabio Fiorani (Head, Jülich Plant Phenotyping Centre) for helping me with the non-invasive phenotyping of Arabidopsis.

I would also like to thank the members of Ökophysiologie der Pflanzenernährung, especially Phillip Gaugler, for helping with protein purification.

I am also grateful to Thuy Huu Nguyen from Pflanzenbau, who helped me with photosynthesis measurement.

I also send my appreciation to the staff of Campus Kleinaltendorf for helping me to manage the experiment inside the rainout shelter. I would also send my sincere appreciation to the staff managing the greenhouse and climate chamber, especially Josef Bauer, Jörg Nettekoven and Thomas Gerhardt, for helping to organize experiments.

I would also take this opportunity to thank Graduiertenkolleg (GRK2064) for providing financial support for my research work. I am grateful to colleagues and PIs of GRK2064 for fruitful discussion during progress seminars.

I would also like to thank the Department of Plant Breeding and its technical/administrative staff for their support and experimental facility. Special thanks to Karola Müller for taking care of crossing. I am also grateful to Karin Woitol and Martina Brodeßer for organizing the laboratory materials. Karin Woitol also read my thesis and gave excellent feedback to improve the thesis. I would like to thank Dr. Shumaila Muzammil and Dr. Said Dadshani for the collaborative work and fruitful discussion. My sincere appreciation and a big round of applause go to Alexander Fendel, Stina Kullik, Anteneh Adebay, Daniel Kingsley Cudjoe and Jan Bendorf for their hard work and significant contribution to this doctoral work. Marius Denkler helped me to prepare Figure S19. I am also grateful to Michael Schneider for helping to process the RNAseq data and fruitful scientific discussion. I am also thankful to Md. Kamruzzaman and Richard Lange for helping me during the experiments. I would also like to acknowledge Patrice Ahossi Koua and Dr. Benedict Oyiga for reading and providing critical comments on my thesis.

Finally, I must express my gratitude to my family for their love and encouragement throughout my studies. This work would not have been possible without these wonderful people. Thank you all.

Table of contents

Summary

Drought tolerance breeding is an integral part of modern-day agriculture for sustained crop production. In this study, we employed forward and reverse genetics tools to understand and improve drought stress adaptation in barley (*Hordeum vulgare* L.). Using the forward genetics approach, we identified a novel allele of pyrroline-5-carboxylate synthase 1 (*HvP5cs1*) from wild barley ISR42-8 (*H. vulgare* spp. *spontaneum*). The putative functional mutations were detected in the *HvP5cs1* promoter across ABA-responsive elements (ABREs) between ISR42-8 and cultivar Scarlett. Thereafter, allele mining of the *HvP5cs1* promoter region in a barely diversity panel comprised of wild barley, landraces and cultivars identified novel variants of *cis*-acting elements. Proline measurements and expression analyses in the haplotypes based on promoter variation illustrated the significance of ABRE and MYB binding elements for *HvP5cs1* transcriptional regulation.

Next, we quantified the *HvP5cs1* promoter activity of ISR42-8 and Scarlett through transient expression of promoter::GUS construct in Arabidopsis protoplast (Col-0). GUS expression analysis revealed greater activation of ISR42-8 promoter than Scarlett upon ABA application. To test the role of ABRE binding factors (ABFs), we evaluated *HvP5cs1* promoter activity of ISR42-8 in protoplast of loss-of-function *abf1 abf2 abf3 abf4* quadruple mutant in Arabidopsis. Notably, ISR42-8 promoter activity diminished in the protoplast of the *abf1 abf2 abf3 abf4* quadruple mutant indicating the promoter activity is regulated in an ABF-dependent manner.

Then, we developed a near-isogenic line (NIL-143) *QPro.S42-1H* in cultivated barley Scarlett through marker-assisted backcrossing (BC6). NIL-143 preserved the genetic competence of ISR42-8 to accumulate proline in higher concentrations under drought conditions. Under drought stress, NIL-143 maintained superior membrane integrity, reduced pigment damage, and sustained photosynthetic health compared to Scarlett. Further, NIL-143 presented a remarkable improvement in drought stress recovery than Scarlett. The introgression of *QPro.S42-1H* enhanced yield attributes in NIL-143 compared to Scarlett under drought stress in field conditions.

Hereafter, we generated barley mutant lines of putative ABFs using the CRISPR/Cas9 system in the background of cultivated barley Golden Promise. ABFs belongs to basic leucine zipper family, and four putative orthologs were identified in barley. We targeted the conserved C-terminus end, and site-directed mutation events were detected at the target site in HORVU3Hr1G084360 (*HvAbi5*) and HORVU6Hr1G080670 (*HvAbf*). Three allelic mutants were detected for HvABI5, resulting in a translational frameshift. One allelic mutant with 3 bp deletion in HvABF caused a loss of serine from the conserved domain. The morphological and

physiological evaluation revealed that *hvabf* and *hvabi5* were more sensitive to drought stress than wild type. Global transcriptome profiling demonstrated that stress-inducible genes were downregulated in *hvabf* and *hvabi5* compared to wild type.

As a proof of concept, stress-inducible proline synthesis was evaluated in Col-0 and the *abf1 abf2 abf3 abf4* quadruple mutant at different stress scenarios. Upon ABA application, *P5CS1* mRNA expression and shoot proline content were significantly more upregulated in Col-0 as compared to the *abf1 abf2 abf3 abf4* quadruple mutant.

In conclusion, the present data uncover the genetic regulation of drought-inducible proline accumulation and its role in drought stress adaptation in barley.

Kurzfassung

Die Züchtung auf Trockentoleranz in Nutzpflanzen ist ein wesentlicher Teil der modernen Landwirtschaft für eine nachhaltige Nutzpflanzenproduktion. In dieser Studie haben wir, zum weiteren Verständnis der Anpassungsfähigkeit von Gerste (*Hordeum vulgare* L.) an Trockenstress, Werkzeuge der Vorwärts- sowie Rückwärts-Genetik benutzt. Durch die Vorwärts-Genetik gezielte Herangehensweise, konnten wir ein neues Allel der pyrroline-5-carboxylate synthase 1 (*HvP5cs1*) der Wildgerste ISR42-8 (*H. vulgare* spp. *spontaneum*) identifizieren. Die vermeintlich funktionellen Mutationen wurden in dem *HvP5cs1* Promotor in ABA-responsive elements (ABREs) zwischen ISR42-8 und der Kulturgerste Scarlett gefunden. Daraus resultierende nachfolgende Untersuchungen der *HvP5cs1* Promotorregion an diversen Gerstenarten, zeigten neue Varianten *cis*-wirkender Elemente. Durch Promotorvariation gebildete Haplotypen, verdeutlichten anhand von Genexpressionsanalysen sowie Prolinmessungen die Signifikanz von ABRE und MYB cis-Elementen für die transkriptionelle Regulation von *HvP5cs1*.

Als Nächstes haben wir die Aktivität des *HvP5cs1* Promotors von ISR42-8 und Scarlett durch eine vorübergehende Expression eines GUS-Reportersystems in einem Protoplasten der Acker-Schmalwand (*Arabidopsis thaliana*) (Col-0) quantifiziert. Unter der Zugabe von ABA, zeigte die Expressionsanalyse dieses Systems eine verstärkte Aktivität des ISR42-8 Promotors im Vergleich zu Scarlett. Zur Bestimmung der Aufgabe von ABRE binding factors (ABFs), haben wir die Aktivität des *HvP5cs1* Promotors von ISR42-8 in einem Protoplasten des Acker-Schmalwand (*Arabidopsis thaliana*) Funktionsverlustmutanten *abf1 abf2 abf3 abf4* untersucht. Dabei verringerte sich die Aktivität des ISR42-8 Promotors in besagter Mutante und zeigt damit eine Art Abhängigkeit der Promotoraktivität von regulierenden ABFs.

Als Nächstes haben wir mit Hilfe markergestützter Rückkreuzungen (BC6) eine auf der Kulturgerste Scarlett basierende, nahezu isogene Linie (NIL-143) *QPro.S42-1H* entwickelt. NIL-143 bewahrte die genetische Fähigkeit der Wildgerste ISR42-8 zur gesteigerten Prolinakkumulation unter trockenen Bedingungen. Unter der Belastung durch Trockenstress, zeigte NIL-143, verglichen mit Scarlett, eine überlegene Membranintegrität, reduzierte Schäden der Blattpigmente und eine anhaltende photosynthetische Aktivität. Des Weiteren zeigte NIL-143, im Gegensatz zu Scarlett, eine bemerkenswert verbesserte Genesung der durch Trockenstress induzierten Schäden. Ebenso verbesserten sich durch die Einbringung von *QPro.S42-1H* in NIL-143 Ertragsparameter unter Trockenstress in Feldbedingungen im Vergleich zu Scarlett.

Nachfolgend haben wir Gerstemutanten von vermeintlichen ABF Genen der Kulturgerste Golden Promise mit Hilfe des CRISPR/Cas9-Systems erstellt. ABFs gehören zur Familie der

Leucin-Zipper, von denen vier mutmaßliche Orthologe in Gerste identifiziert wurden. Wir konzentrierten uns hier auf das Ende des C-Terminus und entdeckten ortsspezifische Mutationen (site-directed mutation events) an der Zielsequenz (target site) in HORVU3Hr1G084360 (*HvAbi5*) und HORVU6Hr1G080670 (*HvAbf*). In HvABI5 wurden drei Allelmutanten gefunden, die zu einer Leserasterverschiebung führen. Ein Allelmutant, mit einer 3 Basenpaar großen Deletion in HvABF, verursachte einen Verlust von Serin aus der konservierten Domäne. Morphologische und physiologische Auswertungen zeigten, dass *hvabf* und *hvabi5* sensitiver gegenüber Trockenstress im Vergleich zum Wildtyp reagierten. Das Zusammenführen globaler Transkriptome verdeutlichte, dass die, im Gegensatz zum Wildtyp durch Stress ausgelösten Gene in *hvabf* und *hvabi5* heruntergeregelt wurden.

Als Proof of Concept wurde die durch Stress induzierte Synthese von Prolin in Col-0 sowie dem Funktionsverlustmutanten *abf1 abf2 abf3 abf4* in unterschiedlichen Stressszenarios ermittelt. Unter der Zugabe von ABA, steigerte sich in Col-0 die Expression der *P5CS1* mRNA sowie des sich im Spross befindlichen Prolingehalts signifikant im Vergleich zum Funktionsverlustmutanten *abf1 abf2 abf3 abf4*.

Zusammengefasst, decken die vorliegenden Daten die genetische Regulation der durch Trockenheit induzierten Prolinakkumulation sowie dessen Rolle in der Anpassung von Gerste an Trockenstress auf.

List of figures

List of tables

List of supplementary tables

List of supplementary figures

List of abbreviations

A	CO_2 assimilation rate
ABA	abscisic acid
ABI	abscisic acid insensitive
ABRE	abscisic acid-responsive elements
AREB/ABF	abscisic acid-responsive element binding factors
BC	Backcross
BHT	2,6-di-tert-butyl-4-methyl pheno
bZIP	basic-domain leucine zipper
CRISPR	clustered regularly interspaced palindromic repeat
CBF	C-repeat and low-temperature element binding factors
CE	coupling element
C_i	intracellular CO_2 concentration
CRI	carotenoid index
CRT	C-repeat and low-temperature elements
Ctr	Carter index
DEG	differentially expressed gene
DRE	dehydration responsive elements
DREB	dehydration responsive element binding factors
DSB	double-stranded break
E	transpiration rate
EC	electrical conductivity
EL	electrolyte leakage
FW	fresh weight
GFP	green fluorescent protein
GM	Gitelson and Merzyak index
GP	Golden Promise
g_s	stomatal conductance
GSA	glutamate-semialdehyde
GUS	beta-glucuronidase
J_{max}	the maximum rate of electron transport during ribulose-1,5-biphosphate regeneration
Lic	Lichtenthaler index
MDA	Malondialdehyde
NAC	derived from the initials of three genes no apical meristem, Arabidopsis NAC domain-containing protein and cup-shaped cotyledon which possess conserved NAC domain
NHEJ	non-homologous end-joining
NDVI	normalized difference vegetation index
NIL	near-isogenic line
OSAVI	optimized soil adjusted vegetation index
P5C	pyrroline-5-carboxylate
P5CDH	pyrroline-5-carboxylate dehydrogenase
P5CR	pyrroline-5-carboxylate reductase
P5CS	pyrroline-5-carboxylate synthase
PAM	protospacer adjancent motif
PDH	proline dehydrogenase

PLA	projected leaf area
PP2C	protein phosphatase 2C
PRI	photochemical reflectance index
PS	Protospacer
RDVI	renormalized differences vegetation index
RGR	relative growth rate
ROS	reactive oxygen species
RWC	relative water content
sgRNA	single guide RNA
SIPI	structure intensive pigment index
SnRK	sucrose non-fermenting related protein kinases
SPAD	soil plant analysis development chlorophyll meter
SPRI	simple ratio pigment index
SR	simple ratio index
TALEN	transcription activator-like effector nucleases
TBA	thiobarbituric acid
TCA	trichloroacetic acid
V_{cmax}	maximum carboxylation rate of rubisco
VI	vegetation index
Y(II)	effective quantum yield of photosystem II at steady-state photosynthesis under light conditions
ZMI	Zarco-Tejada and Miller index
ZFN	Zinc finger nuclease

Note: The gene symbol is written in block letters and italics (e.g., *P5CS1*) for Arabidopsis. For other plant species, gene symbol is indicated in italics with initials of the genus (capital letter) and species (small letter) followed by the abbreviation of annotation in sentence case (e.g., *HvP5cs1*). Proteins are indicated in block letters (e.g., P5CS1 or HvP5CS1). Gene and protein mentioned in general context are indicated in rules followed for Arabidopsis.

Chapter 1. General introduction

1.1. Effect of drought on crop production

Drought is defined as a period when precipitation is below the normal condition causing water shortage (Dai, 2011). It is classified into three major categories, namely, meteorological drought, hydrological drought, and agricultural drought. Meteorological drought is reduced precipitation over long periods while hydrological drought is the shrinkage of lakes, river flow and ground-water levels. Agricultural drought is the period during a cropping season when the rainfall and soil moisture cannot meet the evapotranspiration demand of the crops to maintain optimum growth and production (Trenberth *et al.*, 2014; Dai, 2011).

Short-term and prolonged dry periods occurred in several instances in history, which was primarily linked to tropical oceanic temperature fluctuations. However, the global change in temperature due to greenhouse gas emission and land-use change are the main divers of recent drought events. The drying tendency over the last eight decades resulted in severe crop damage and economic loss (Figure 1.1; Wang *et al*., 2018). The global temperature has increased approximately by 1°C compared to 1880 and projected to rise by 0.2°C per decade (IPCC 2014). Several prediction studies revealed that the drought evens would be more frequent and severe in the future owing to decreased precipitation and increased evaporation (Trenberth *et al.*, 2014; Dhanyalakshmi *et al.*, 2019; Sheffield and Wood, 2008). Remarkably, the impact of the drought will be more severe in developing worlds such as Africa and Asia due to the lack of technical means and infrastructures to cope with climate disasters (Wang *et al.*, 2018). However, Lesk *et al.* (2016) pointed out that the recent drought events caused greater crop damage (8-11%) in developed countries than developing nations. Wang *et al.* (2018) reported that in 1987, 2002, and 2007 all the countries across the globe experienced severe drought and crop failure. In addition, the dry and warm climate facilitates insect-pest outbreak leaving the trails of large-scale crop failures (Thomson *et al.*, 2010).

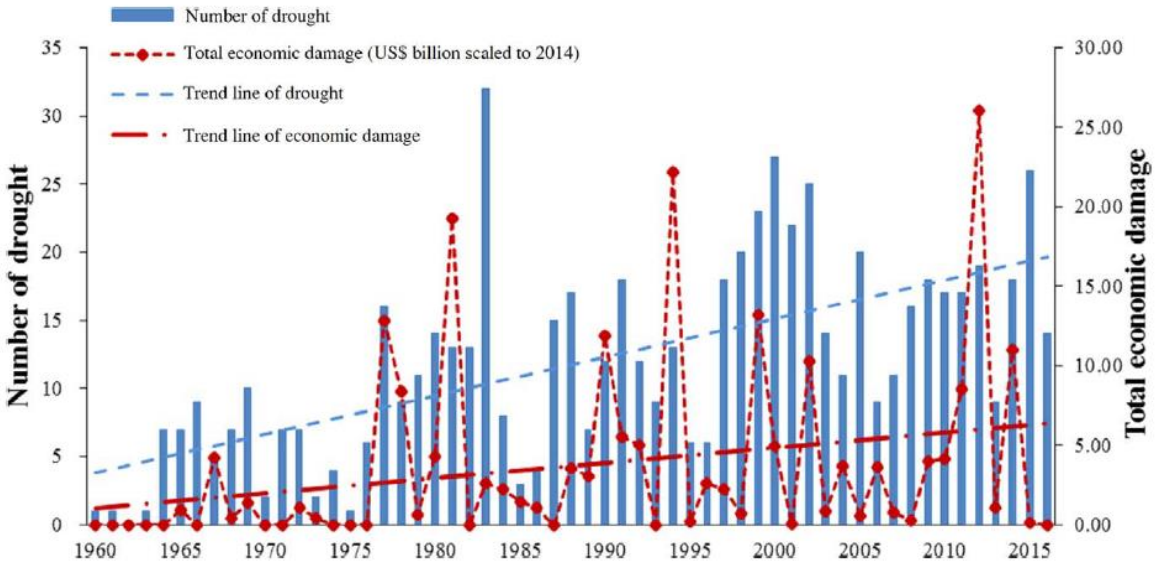

Figure 1.1. The trend of drought event and economic loss from 1960 to 2015. Source: Wang *et al.*, 2018.

The recent trend in temperature and precipitation showed a negative effect on the yield of major cereal crops such as wheat, barley and maize (Figure 1.2; Lobell and Field, 2007; Li *et al.*, 2009). From 1983 to 2009, around 75% of arable land experienced drought-related yield deficits (Kim *et al.*, 2019). Lobell *et al.* (2011) reported a global yield deficit of 3.8%, 5.5% and 1.7% of maize, wheat and soybean, respectively, due to high temperature and drought between 1980 and 2008. Matiu *et al.* (2017) also reported more than a 9% reduction in yield of soybean, maize and wheat in 2014 compared to the early 1960s. Daryanto *et al.* (2017) analyzed the yield data of maize and wheat from field drought experiments on a global scale and concluded that a 40% reduction in irrigation might cause around 39% and 21% grain yield loss in maize and wheat, respectively. A similar study showed that drought-related grain yield reduction was around 28% and 25% in wheat and rice, respectively (Zhang *et al.*, 2018). The future prediction of crop production is not encouraging, as Leng and Hall (2019) reported that published drought models in the literature would result in substantial yield loss in major crops by the end of the 21st century. Li *et al.* (2009) predicted extreme conditions where the yield of major crops will reduce by more than 50% in 2050 and approximately 90% in 2100. Therefore, the current situation demands urgent mitigation strategies to cope with high temperatures and drier soil, such as the re-use of wastewater, construction of reservoirs and the development of adapted cultivars.

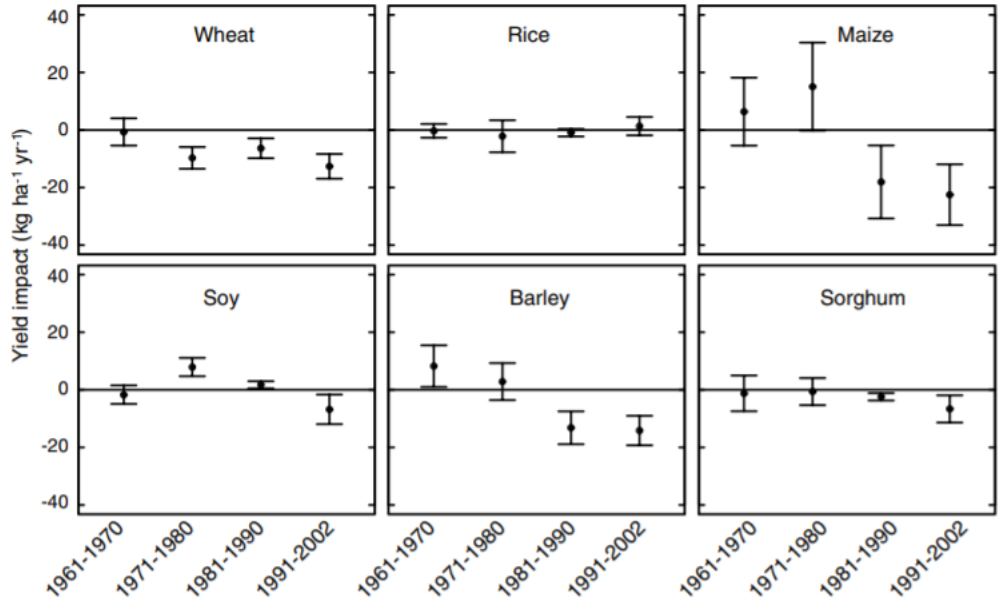

Figure 1.2. Impact of climate change (temperature and precipitation) on the grain yield of six major crops. The negative value indicates yield loss. Source: Lobell and Field, 2007.

1.2. Plant response to drought stress

Terrestrial plants are exposed to different abiotic stresses, including salt, heat, cold and water stress. Under water-limiting conditions, plants make several morphological, physiological and molecular adjustments to maximize water use efficiency (Shinozaki *et al.*, 2003; Osakabe *et al.*, 2014). Plants achieve drought resistance by escaping or avoiding the drought period, tolerate the unwanted biochemical changes induced by water stress, and its ability to recover after stress (Zhou *et al.*, 2016). Plants tend to accelerated reproductive growth and flower early to escape the drought period (Shavrukov *et al.*, 2017). As the transpiration rate exceeds the water uptake, the initial response of most plants is to avoid water-stress is by closing its stomata (Mata and Lamattina, 2001). Abscisic acid (ABA) is the positive regulator of stomatal closure during drought stress. ABA-induced alteration of stomatal conductance involves Ca^{2+} influx in the guard cells, which triggers K^+ efflux from the guard cells. The outward movement of K^+ anions results in reduced guard cell turgor pressure causing stomatal closure (Daszkowska-Golec and Szarejko, 2013; Schroeder *et al.*, 2001). Besides, plants adopt morphological adjustments such as rapid leaf rolling (Price and Tomos, 1997), modification of root system for drought avoidance (Uga *et al.*, 2013; Uga *et al.*, 2011; Ashraf *et al.*, 2019), wax content (Xue *et al.*, 2017) and root suberization (Schreiber, 2010). In addition, plants activate reactive oxygen species (ROS) scavenging pathways (Laxa *et al.*, 2019; Mittler, 2002) and synthesize protective proteins such as dehydrins, late embryogenesis abundant proteins and heat shock proteins to cope with environmental stresses (Bartels and Sunkar, 2005). Another key feature of drought tolerance is osmotic adjustment, which is achieved by the

accumulation of compatible solutes such as proline, glycine betaine, and soluble sugars (Blum *et al.*, 1999; Blum, 2017).

The drought resistance process discussed above is achieved through the transactivation of stress-responsive genes (Osakabe *et al.*, 2014). In general, the drought stress response can be divided into ABA-dependent and ABA-independent pathways (Nakashima *et al.*, 2009). Chemical signals such as ABA sensed by specific receptors activate transcription factors, which are the master regulator of stress-inducible genes (Fujita *et al.*, 2009). Stress inducible genes harbors *cis*-elements in its promoter region and transcription factors bind to the *cis*-elements recruiting the transcription initiation complex. The promoter region of ABA-inducible genes contains ABA-responsive elements (ABRE). ABRE are the targets of ABRE binding factors (ABFs). ABFs belong to the basic-domain leucine zipper (bZIP) transcription family and transactivates ABA-responsive genes (Fujita *et al.*, 2005; Yoshida *et al.*, 2010; Yoshida *et al.*, 2015). Four ABFs (ABF1, AREB1/ABF2, ABF3, and AREB2/ABF4) were identified through yeast one-hybrid screening and electrophoretic mobility shift assay, and their transactivation property was verified by heterologous expression of *lacZ* in yeast (Uno *et al.*, 2000; Choi *et al.*, 2000). The role of ABFs has been illustrated in osmotic stress tolerance in Arabidopsis (Fujita *et al.*, 2005; Yoshida *et al.*, 2010; Yoshida *et al.*, 2015) and crop species (Wang *et al.*, 2016; Joshi *et al.*, 2016; Nakashima *et al.*, 2009).

Dehydration responsive elements (DRE) and C-repeat and low-temperature elements (CRT) are the major class of ABA-independent regulatory elements (Liu *et al.*, 1998). DRE binding factors (DREB) contains APETALA2/ethylene responsive element and binds to DRE/CRT domains (Nakashima *et al.*, 2009). Stockinger *et al.* (1997) demonstrated that CRT element-binding factor 1 (CBF1) binds to the DRE element through yeast one-hybrid and electrophoretic mobility shift assay. Similarly, the affinity of DREB1A and DREB2A towards DRE was demonstrated through yeast one-hybrid screen as well as a transient assay in Arabidopsis mesophyll protoplast (Liu *et al.*, 1998). They also showed that DREB1A was induced by cold while DREB2A was induced by drought stress. Transgenic lines over-expression DREB1A and DREB1B exhibited enhanced stress tolerance (Liu *et al.*, 1998). In Arabidopsis, DREB1 expression is induced by cold stress, while DREB2 expression is induced by water and salt stress (Nakashima *et al.*, 2009). Since then, the regulatory pathway involving DREB genes and its role in osmotic stress tolerance has been demonstrated in several crop species (Zhuang *et al.*, 2015; Shavrukov *et al.*, 2016; Agarwal *et al.*, 2007; Mizoi *et al.*, 2013; Yang *et al.*, 2020).

NAC transcription factor is one of the largest transcription factor families involved in developmental processes, and its role in abiotic stress tolerance has been illustrated in several

studies (Shao *et al.*, 2015). Also, MYB, WRKY, zinc finger proteins, and bHLH are other indispensable regulators of a complex pathway of drought response (Tripathi *et al.*, 2014; Baldoni *et al.*, 2015). Plant response to drought is a dynamic process that involves significant crosstalk at single perception and transduction to transactivation of target genes shaping drought stress resistance.

1.3. Role of proline in drought tolerance

Proline accumulation under stress conditions is conserved in unicellular to multicellular organisms (Hu *et al.*, 1992). Proline is attributed to several protective roles in stressed cells such as osmotic adjustment, plasma membrane integrity, redox balance and (ROS) detoxification. Proline accumulation is a general response of plants to a wide range of abiotic stress, including water, salinity, cold, heat, heavy metal toxicity and nutrient deficiency. Therefore, it is one of the widely studied molecules in the field of plant science (Kishor *et al.*, 2005; Szabados and Savouré, 2010).

1.3.1. How does plant accumulate proline?

Plants achieve the accumulation of free proline in the cytosol through increased biosynthesis and decreased degradation. The proline metabolic process under stress and the normal developmental process is also illustrated in Figure 1.3. The precursor molecule of proline biosynthesis is glutamate and ornithine; however, glutamate accounts for the majority of proline synthesis in plants (Kishor *et al.*, 2005). The first step of the proline biosynthetic pathway involves the reduction of glutamate to glutamate-semialdehyde (GSA), which is simultaneously converted to pyrroline-5-carboxylate (P5C). This process is catalyzed by a gamma-glutamyl kinase and GSA dehydrogenase in *E. coli* (Deutch *et al.*, 1984). However, Hu *et al.* (1992) discovered that a single enzyme pyrolline-5-carboxylate synthetase (P5CS) possesses both glutamyl kinase and dehydrogenase activity and catalyzes the first two steps of proline biosynthesis in plants. P5C is further reduced to proline by enzyme P5C reductase (P5CR) (Szoke *et al.*, 1992; Verbruggen *et al.*, 1993). Savouré *et al.* (1995) found that the expression of the *P5CS* gene was osmotically regulated, and transcript increase upon salt treatment in Arabidopsis. Yoshiba *et al.* (1995) showed that the *P5CS* gene was upregulated by osmotic stress but not *P5CR*, which indicated that the conversion of glutamate to P5C is the rate-limiting step of proline biosynthesis. In higher plants, there are mostly two closely related homologs of P5CS, namely P5CS1 and P5CS2 (Strizhov *et al.*, 1997; Ginzberg *et al.*, 1998). Fujita *et al.* (1998) found that only one P5CS homolog of tomato was induced under osmotic stress, and Strizhov *et al.* (1997) also observed a similar trend in Arabidopsis. Székely *et al.* (2008) demonstrated that *p5cs1* knock-out mutant showed hypersensitivity to salinity,

while *p5cs2* showed embryo abortion in Arabidopsis. They also showed that P5CS2 was localized to the cytosol, while P5CS1 was localized to the chloroplast in Arabidopsis. Plants can synthesize proline *via* the ornithine pathway, where ornithine is converted to GSA and P5C by ornithine-delta-aminotransferase (Delauney *et al*., 1993; Roosens *et al*., 1998). Nevertheless, proline synthesis from glutamate is the major proline biosynthesis pathway in plants (Verslues and Sharma, 2010). Proline degradation is also a two-step process, where proline is oxidized to P5C producing by proline dehydrogenase (PDH) (Kiyosue *et al.*, 1996). P5C is subsequently oxidized to glutamate by P5C dehydrogenase (P5CDH) (Forlani *et al.*, 1997). PDH has a mitochondrial location and downregulated upon water stress and upregulated by external proline application and rehydration (Kiyosue *et al.*, 1996; Verbruggen *et al.*, 1996). P5CDH is also localized to mitochondria, and induced by P5C, therefore protecting the cells from proline toxicity (Forlani *et al.*, 1997). Altogether, the proline anabolic pathway is upregulated, while the proline catabolism is down-regulated under stress conditions leading to proline accumulation in the cytosol.

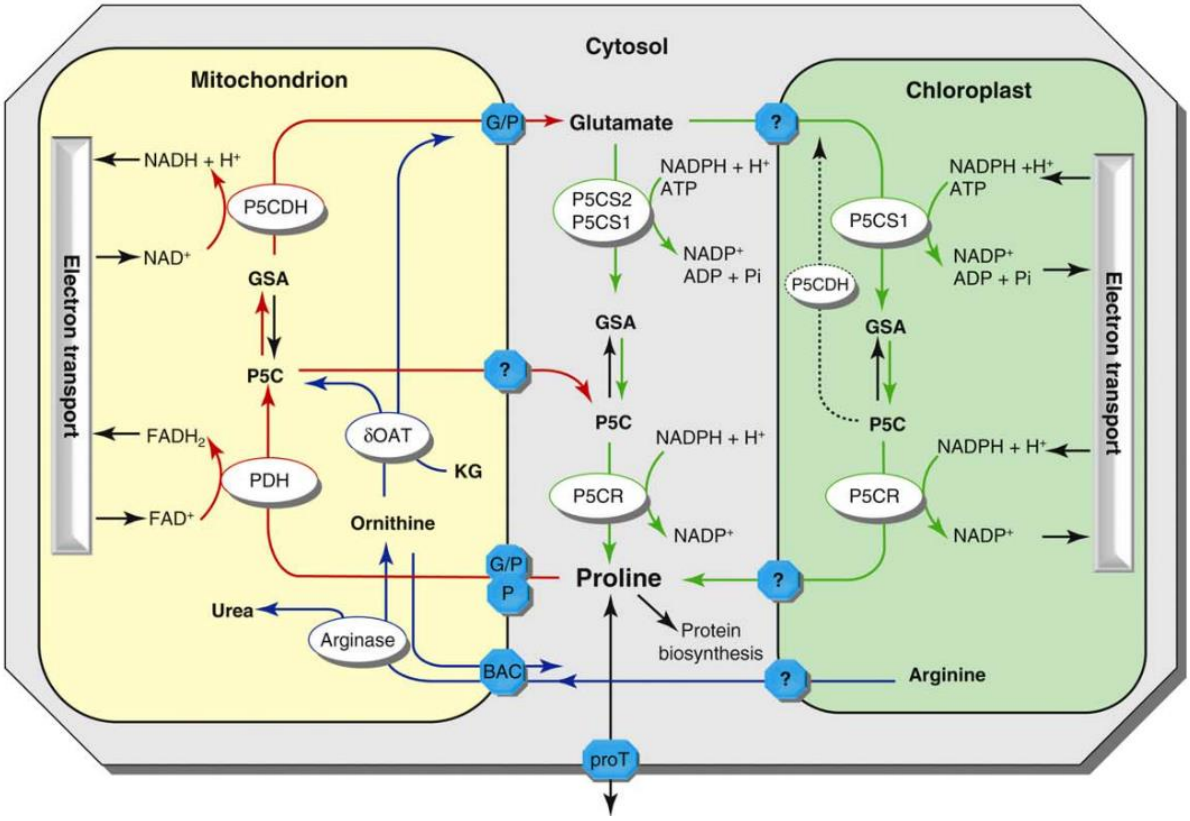

Figure 1.3. A schematic model of proline accumulation in plants. Green lines indicate the biosynthetic pathway, and the red lines indicate the catabolic pathway. BAC, basic amino acid transporter involved in arginine and ornithine exchange; Glu, glutamate; G/P, mitochondrial glutamate/proline antiporter; GSA, glutamate semialdehyde; KG, alpha-ketoglutarate; P, mitochondrial proline transporter; Pi, inorganic phosphate; ProT, plasma membrane proline transporter. Source: Szabados and Savouré, 2010.

1.3.2. How does proline help in drought stress tolerance?

Proline is a proteinogenic amino acid with a diverse role in plant development processes and stress adaptation (Kishor *et al.*, 2005). Besides stress tolerance, proline regulates plant development processes, such as flowering, pollen fertility, root development and embryo development (Kishor *et al.*, 2015). Proline plays a vital role in floral transition and pollen development. Low proline mutants tend to flower late and proline over-expression mutant flowers earlier in Arabidopsis (Mattioli *et al.*, 2018; Székely *et al.*, 2008). It has been shown that proline accumulates in high concentrations in pollen and is essential for pollen maturity (Mattioli *et al.*, 2018) and embryo development (Funck *et al.*, 2012; Székely *et al.*, 2008). The accumulation of proline in maturing pollen might be linked to its widely accepted protective function under stress conditions. Previous studies have described the multi-faceted significance of free proline accumulation under abiotic stress such as osmotic adjustment, ROS detoxification, stress recovery and cellular signaling (Szabados and Savouré, 2010).

Osmotic adjustment is the most widely accepted, but equally contested role of proline accumulation. Proline and other non-toxic compatible solutes are highly soluble in water and help to decrease the osmotic potential preventing the efflux of water from the cytosol (Kishor *et al.,* 2005). Kishor *et al.* (1995) showed that transgenic plants overexpressing *Vigna aconitifolia VaP5cs* resulted in higher osmotic tolerance producing more biomass compared to wild type under salt stress. Székely *et al.* (2008) also found that low proline accumulating mutants showed reduced osmotic adjustment compared to wild type. Verslues and Bray (2004) also found a positive correlation between proline accumulation and osmotic adjustment in Arabidopsis. Although several studies illustrated the osmoprotective role of proline, some studies contested its function as an osmolyte. They argued that the reported amount of accumulated proline alone in the plants might not be enough to induce osmotic adjustment. Instead the collective compatible solutes such as glycine betaine, soluble sugar accumulation should be considered while drawing conclusions on osmotic adjustment potential of the plants (Forlani *et al.*, 2019; Kishor and Sreenivasulu, 2014; Rejeb *et al.*, 2015). However, they did not deny that proline imparts other protective functions, including the stress recovery process. Another major protective role of proline is molecular chaperon activity, protecting macromolecules such as protein and lipids (Rajendrakumar *et al.*, 1994; Chattopadhyay *et al.*, 2004). Rajendrakumar *et al.* (1994) showed that proline helped to maintain the structural integrity of M4 lactate dehydrogenase during a freeze-thaw cycle and heat stress. It might interact with the hydrophobic backbone of the protein and prevent protein aggregation during stress. The chaperone activity of proline was also illustrated in the work of Chattopadhyay *et al.* (2004). They showed that protein aggregation due to heat treatment was reduced in a

dnaK-deficient mutant of *E. coli* expressing high proline. Sharma and Dubey (2005) demonstrated that osmolyte accumulation, including proline, might offer a protective role in nitrate reductase activity in rice under drought and aluminum toxicity. The addition of proline restored RNase activity in the aluminum and polyethylene glycol treated rice sap (Mishra and Dubey, 2006).

Proline is also involved in maintaining plasma membrane integrity through the protection of membrane proteins, phospholipid layer, and ROS detoxification (Hare *et al.*, 1998; Rudolph *et al.*, 1986; Szabados and Savouré, 2010). Gadallah (1999) reported that the external application of proline and glycine betaine enhanced cell membrane stability and chlorophyll content in salt-stressed bean plants. Knock-out mutant of *P5CS1* (*p5cs1*) in Arabidopsis showed significant oxidative damage and chlorophyll degradation compared to wild type (Székely *et al.*, 2008). Likewise, Fedina *et al.* (2003) discovered that increased proline accumulation in barley seedling exposed to ultraviolet radiation might prevent chlorophyll degradation. Alia and Mohanty (1997) demonstrated that proline contributed to the reduction of lipid peroxidation in the chloroplast of *Brassica juncea* exposed to UV radiation. They illustrated that proline was able to scavenge singlet oxygen in the thylakoid membrane of *Brassica juncea* exposed to high illumination. Alia and Matysik (2001) further illustrated the role of proline in scavenging singlet oxygen in the thylakoid membrane and proposed a non-enzymatic quenching of ROS. However, these studies did not provide conclusive evidence if proline is involved in non-enzymatic detoxification of single oxygen or activates the enzymatic pathway of ROS scavenging. The work of Öztürk and Demir (2002) revealed that proline protects the activity of ROS scavengers such as catalases and peroxidases rather than direct detoxification of ROS. In a separate study, it was shown that proline was involved in the scavenging of hydroxyl radicals by producing delta-pyrroline, which is the precursor molecule of aminobutyric acid biosynthesis (Signorelli *et al.*, 2015; Signorelli *et al.*, 2014).

Proline biosynthesis is a reductive process, and both P5CS1 and P5CR require NADPH that regenerates $NADP^+$ (Szabados and Savouré, 2010). $NADP^+$ regeneration is depleted during the stress conditions breaking the electron transport chain that might trigger ROS accumulation in photosystem I (Szabados and Savouré, 2010; Kishor *et al.*, 2005). The upregulation of the proline biosynthesis pathway under drought might contribute to maintaining $NADP^+$ pool to sustain photosynthesis under stress conditions (de Ronde *et al.*, 2004; Hare and Cress, 1997). This hypothesis was supported by the results of Sharma *et al.* (2011), where they showed that $NADP^+$/NADPH ratio was lower in *p5cs1* mutant compared to wild type under low water potential. Also, the overexpression of *P5CR* in soybean increased the $NADP^+$ pool in transgenic soybean under stress conditions (de Ronde *et al.*, 2004). In addition to the protective function, proline catabolism potentially contributes to the stress recovery process

(Szabados and Savouré, 2010). The reduction of proline to glutamate generated ATP molecules, which provide much-needed energy for growth resumption (Hare and Cress, 1997; Hare *et al.*, 1998). Blum and Ebercon (1981) showed that proline accumulation during drought stress in sorghum and wheat was proportional to stress recovery and dark respiration rate. Similarly, Itai and Paleg (1982) reported a positive effect of external proline accumulation on the stress recovery in barley.

Overall, the vast research in the field of proline suggests that proline is a universal response of plants to stress. The published data suggest that proline, together with other accumulated compatible solutes, might prevent the withdrawal of water from the cytosol during drought stress. However, there is compelling evidence that proline is involved in ROS detoxification and chaperon activity. Also, the role of proline in maintaining redox balance during stress and facilitating stress recovery is described through several *in vitro* experiments as well as a transgenic approach.

1.4. Barley: a model plant for studying drought stress tolerance

Barley is classified as genus *Hordeum* under the grass family *Poaceae.* Barley was one of the earliest domesticated crops and *Hordeum vulgare* L. spp. *spontaneum* C. Koch (referred to as wild barley in the following text) is considered as the wild progenitor of cultivated barley (*Hordeum vulgare* L.) (Harlan and Zohary, 1966). The Fertile Crescent from Israel and Jordan, the southeast region of Turkey and the hilly region of Iraq and Iran are considered as the primary center of origin of barley (Dawson *et al.*, 2015). The wild progenitor is still widespread in these sites of early domestication, which occurred around 10,000 years ago (Badr *et al.*, 2000). Wild barley and cultivated barley show significant similarities, including a diploid genome with an equal number of chromosomes and a high success rate of hybridization (Dawson *et al.*, 2015). The major differences are the narrow leaves, brittle rachis and loss of germination inhibition, which are used as domestication traits in evolutionary studies. Row type (two versus six) and presence or absence of hulls are other critical domestication related traits (Dai *et al.*, 2012). Although the monophyletic origin of barley is widely accepted, barley might have gone through the second wave of domestication. This hypothesis is supported by the fact that more than 95% of the gene pool linked to naked barely is concentrated in the Tibetan plateau and hilly regions of Nepal (Taketa *et al.*, 2004). Apart from the Fertile Crescent, Tibetan plateau and Himalayas are considered as a secondary center of barley domestication. Based on the variation in domestication traits, the diversity of cultivars grown in Europe is primarily contributed by domestication in the Fertile Crescent (Morrell and Clegg, 2007).

The domestication and breeding for modern varieties for intensive agriculture systems have resulted in a loss of genetic diversity, which is essential for tolerance breeding (Tanksley and McCouch, 1997). There are several instances where introgression of a wild allele from primary and secondary gene pool proved beneficial for drought tolerance in barley (Tuberosa and Salvi, 2006; Lakew *et al.*, 2011). For example, Kalladan *et al.* (2013) found that introgression of exotic alleles from wild accession HS584 improved yield performance of cultivated barley under drought conditions. Also, a barley landrace Tadmor contributed several QTLs linked to osmotic adjustment in cultivated barley grown under water-limited conditions (Teulat *et al.*, 2001; Teulat *et al.*, 1998). Similarly, Baum *et al.* (2003) identified QTLs from wild barley and a variety adapted to the Mediterranean environment that contributed favorable alleles for agronomic traits such as plant height, tiller number, days to heading and grain yield under drought stress. Similarly, Talame *et al.* (2004) identified 42 QTLs from wild barley, which contributed to the adaptation of introgression lines to a harsh growing environment in Tunisia and Morocco. The utility of wild barley was also illustrated in a work of (Wiegmann *et al.*, 2019). They evaluated the yield performance of a subset of HEB-25 nested association mapping population developed from a cross between 25 diverse wild barley and a German cultivar Barke (Maurer *et al.*, 2015) across five different locations in UK, Germany, Australia, UAE and Jordan. They found that the yield performance of HEB-25 was relatively stable across the growing environment and stress treatment compared to local checks. Similarly, advanced backcross line developed from the genetic cross of German cultivar, Scarlett and wild barely, ISR42-8 (von Korff *et al.*, 2004; Schmalenbach *et al.*, 2009) highlighted the importance of exotic allele for improved drought tolerance in cultivar (Honsdorf *et al.*, 2014; Muzammil *et al.*, 2018).

Barley is one of the major crops grown across the globe from the highlands of Nepal and Ethiopia, in Tibetan plateau to warm and dry areas in Israel, Jordan and Morocco (Badr *et al.*, 2000). Therefore, it offers a unique resource to study diverse abiotic stresses such as drought, salinity, heat and cold stress in a single genus. In addition, the barley germplasm diversity is conserved across different countries *in situ* as well as *ex situ* gene banks (Dawson *et al.*, 2015). The rich diversity in germplasm and adaptive environmental signatures offers the opportunity to conduct genome-wide association studies, allele mining for specific locus, development of bi-parental, as well as a multi-parent mapping population. Besides, the international barley genome sequencing consortium has released whole-genome sequence assembly and well-curated gene models (Beier *et al.*, 2017). Plus, the genetic similarity between wild and cultivated barley (Dawson *et al.*, 2015) makes crossing much easier compared to crops such as rice, wheat and maize, which facilitates genetic studies and

introgression of favorable genes. To summarize, the wide range adaptability, genetic and genomic resources makes barley an excellent crop model to study abiotic stress tolerance.

1.5. Aim of the study

As indicated in the above section, stress-inducible proline biosynthesis supports plant to achieve drought tolerance *via* multiple physiological adjustments (Kishor *et al*., 2005). However, the majority of the studies were done in model plant species (Savouré *et al*., 1997; Sharma *et al.,* 2011; Strizhov *et al.* 1997; Székely *et al.* 2008; Verslues and Bray, 2006) or *in vitro* cell cultures (Alia and Matysik, 2001, Chattopadhyay *et al*., 2004). The research in crop species also primarily focused on the generation of transgenic lines over-expressing the stress-inducible proline biosynthesis pathway (Kishor *et al*., 1995; Su and Wu 2004; Zhu *et al*., 1998). In other studies, the researcher compared the proline accumulation in previously characterized tolerant and susceptible crop varieties. In doing so, the researcher could not detect a similar effect observed in the transgenic plants. Therefore, there are mixed views on the actual utility of proline in stress adaptation in crop plants. However, some studies neatly displayed the potential of proline to cope with stress (Szabados and Savouré, 2010; Verslues and Sharma, 2010). Yet, we have not found a single case where natural allele controlling proline accumulation being utilized in plant breeding.

In our research group, we are making a conscious effort to identify genetic loci controlling proline accumulation in barley diversity. Therefore, the current study was planned to achieve the following objectives.

- To dissect the genetic factors controlling drought-inducible proline accumulation in barley
- Molecular and functional characterization of candidate genes associated with proline accumulation in barley
- Evaluate the near-isogenic line carrying exotic allele from wild barley under drought stress

The result of the study is divided into three chapters

Chapter 2: Genetic and molecular analysis of proline mediated drought stress tolerance in barley

Chapter 3: Site-directed mutagenesis of drought stress-related ABA-responsive element binding factors in barley using CRISPR RNA/Cas9 system

Chapter 4: Role of ABA-responsive element binding factors in proline biosynthesis and drought adaptation in *Arabidopsis thaliana*

1.6. References

Agarwal, P., Agarwal, P.K., Nair, S., Sopory, S.K. and Reddy, M.K. (2007) Stress-inducible DREB2A transcription factor from *Pennisetum glaucum* is a phosphoprotein and its phosphorylation negatively regulates its DNA-binding activity. *Mol. Genet. Genomics*, **277**, 189–198.

Alia, M.P. and Matysik, J. (2001) Effect of proline on the production of singlet oxygen. *Amino Acids*, **21**, 195–200.

Alia, S.P.P. and Mohanty, P. (1997) Involvement of proline in protecting thylakoid membranes against free radical-induced photodamage. *J. Photochem. Photobiol. B Biol.*, **38**, 253–257.

Ashraf, A., Rehman, O.U., Muzammil, S., Léon, J., Naz, A.A., Rasool, F., Ali, G.M., Zafar, Y. and Khan, M.R. (2019) Evolution of deeper rooting 1-like homoeologs in wheat entails the C-terminus mutations as well as gain and loss of auxin response elements. *PLoS One*, **14**.

Badr, A., M, K., Sch, R., Rabey, H. El, Effgen, S., Ibrahim, H.H., Pozzi, C., Rohde, W. and Salamini, F. (2000) On the origin and domestication history of barley (*Hordeum vulgare*). *Mol. Biol. Evol.*, **17**, 499–510.

Baldoni, E., Genga, A. and Cominelli, E. (2015) Plant MYB transcription factors: Their role in drought response mechanisms. *Int. J. Mol. Sci.*, **16**, 15811–15851.

Bartels, D. and Sunkar, R. (2005) Drought and salt tolerance in plants. *CRC. Crit. Rev. Plant Sci.*, **24**, 23–58.

Baum, M., Grando, S., Backes, G., Jahoor, A., Sabbagh, A. and Ceccarelli, S. (2003) QTLs for agronomic traits in the Mediterranean environment identified in recombinant inbred lines of the cross “Arta” x *H. spontaneum* 41-1. *Theor. Appl. Genet.*, **107**, 1215–1225.

Beier, S., Himmelbach, A., Colmsee, C., *et al*. (2017) Construction of a map-based reference genome sequence for barley, *Hordeum vulgare* L. *Sci. Data*, **4**, 170044.

Blum, A. (2017) Osmotic adjustment is a prime drought stress adaptive engine in support of plant production. *Plant Cell Environ.*, **40**, 4–10.

Blum, A. and Ebercon, A. (1981) Cell membrane stability as a measure of drought and heat tolerance in wheat. *Crop Sci.*, **21**, 43–47.

Blum, A., Zhang, J. and Nguyen, H.T. (1999) Consistent differences among wheat cultivars in osmotic adjustment and their relationship to plant production. *F. Crop. Res.*, **64**, 287–291.

Chattopadhyay, M.K., Kern, R., Mistou, M.Y., Dandekar, A.M., Uratsu, S.L. and Richarme, G. (2004) The chemical chaperone proline relieves the thermosensitivity of a dnaK deletion mutant at 42°C. *J. Bacteriol.*, **186**, 8149–8152.

Choi, H.I., Hong, J.H., Ha, J.O., Kang, J.Y. and Kim, S.Y. (2000) ABFs, a family of ABA responsive element binding factors. *J. Biol. Chem.*, **275**, 1723–1730.

Dai, A. (2011) Drought under global warming: A review. *Wiley Interdiscip. Rev. Clim. Chang.*, **2**, 45–65.

Dai, F., Nevo, E., Wu, D., *et al*. (2012) Tibet is one of the centers of domestication of cultivated barley. *Proc. Natl. Acad. Sci.*, **109**, 16969–16973.

Daryanto, S., Wang, L. and Jacinthe, P.A. (2017) Global synthesis of drought effects on cereal, legume, tuber and root crops production: A review. *Agric. Water Manag.*, **179**, 18–33.

Daszkowska-Golec, A. and Szarejko, I. (2013) Open or close the gate - Stomata action under the control of phytohormones in drought stress conditions. *Front. Plant Sci.*, **4**, 1–16.

Dawson, I.K., Russell, J., Powell, W., Steffenson, B., Thomas, W.T.B. and Waugh, R. (2015) Barley: A translational model for adaptation to climate change. *New Phytol.*, **206**, 913–931.

de Ronde, J.A., Cress, W.A., Krüger, G.H.J., Strasser, R.J. and Staden, J. Van (2004) Photosynthetic response of transgenic soybean plants, containing an Arabidopsis P5CR gene, during heat and drought stress. *J. Plant Physiol.*, **161**, 1211–1224.

Dhanyalakshmi, K.H., Mounashree, D.C., Vidyashree, D.N., Earanna, N. and Nataraja, K.N. (2019) Options and opportunities for manipulation of drought traits using endophytes in crops. *Plant Physiol. Reports*, **24**, 555–562.

Delauney, A.J., *et al*. (1993) Cloning of ornithine delta- aminotransferase cDNA from Vigna aconitifolia by trans- complementation in *Escherichia coli* and regulation of proline biosynthesis. *J. Biol. Chem*., **268**, 18673–18678.

Fedina, I.S., Grigorova, I.D. and Georgieva, K.M. (2003) Response of barley seedlings to UV-B radiation as affected by NaCl. *J. Plant Physiol.*, **160**, 205–208.

Forlani, G., Scainelli, D. and Nielsen, E. (1997) Δ1-pyrroline-5-carboxylate dehydrogenase from cultured cells of potato: Purification and properties. *Plant Physiol.*, **113**, 1413–1418.

Forlani, G., Trovato, M., Funck, D. and Signorelli, S. (2019) Regulation of proline accumulation and its molecular and physiological functions in stress defence. In M. A. Hossain, V. Kumar, D. J. Burritt, M. Fujita, and P. S. A. Mäkelä, eds. Osmoprotectant-mediated abiotic stress tolerance in plants: Recent advances and future perspectives. Cham: Springer International Publishing, pp. 73–97.

Fujita, T., Maggio, A., Garcia-Rios, M., Bressan, R.A. and Csonka, L.N. (1998) Comparative analysis of the regulation of expression and structures of two evolutionary divergent genes for Δ1-pyrroline-5-carboxylate synthetase from tomato. *Plant Physiol.*, **118**, 661–674.

Fujita, Y., Fujita, M. and Satoh, R. (2005) AREB1 is a transcription activator of novel ABRE-dependent ABA signaling that enhances drought stress tolerance in Arabidopsis. *Plant Cell*, **17**, 3470–3488.

Fujita, Y., Nakashima, K., Yoshida, T., *et al*. (2009) Three SnRK2 protein kinases are the main positive regulators of abscisic acid signaling in response to water stress in Arabidopsis. *Plant Cell Physiol.*, **50**, 2123–2132.

Funck, D., Winter, G., Baumgarten, L. and Forlani, G. (2012) Requirement of proline synthesis during Arabidopsis reproductive development. *BMC Plant Biol.*, **12**, 1–12.

Gadallah, M.A.A. (1999) Effects of proline and glycinebetaine on *Vicia faba* responses to salt stress. *Biol. Plant.*, **42**, 249–257.

Ginzberg, I., Stein, H., Kapulnik, Y., Szabados, L., Strizhov, N., Schell, J., Koncz, C. and Zilberstein, A. (1998) Isolation and characterization of two different cDNAs of Δ1-pyrroline-5-carboxylate synthase in alfalfa, transcriptionally induced upon salt stress. *Plant Mol. Biol.*, **38**, 755–764.

Hare, P.D. and Cress, W.A. (1997) Metabolic implications of stress-induced proline accumulation in plants. *Plant Growth Regul.*, **21**, 79–102.

Hare, P.D., Cress, W.A. and Staden, J. Van (1998) Dissecting the roles of osmolyte accumulation during stress. *Plant, Cell Environ.*, **21**, 535–553.

Harlan, J.R. and Zohary, D. (1966) Distribution of wild wheats and barley - The present distribution of wild forms may provide clues to the regions of early cereal domestication. *Science.*, **153**, 1074–1080.

Honsdorf, N., March, T.J., Berger, B., Tester, M. and Pillen, K. (2014) High-throughput phenotyping to detect drought tolerance QTL in wild barley introgression lines. *PLoS One*, **9**.

Hu, C.A., Delauney, A.J. and Verma, D.P. (1992) A bifunctional enzyme (delta 1-pyrroline-5-carboxylate synthetase) catalyzes the first two steps in proline biosynthesis in plants. *Proc. Natl. Acad. Sci.*, **89**, 9354–8.

IPCC. (2014) Climate change 2014: synthesis report. IPCC, Geneva, Switzerland.

Itai, C. and Paleg, L.G. (1982) Responses of water-stressed *Hordeum distichum* L. and *Cucumis sativus* to proline and betaine. *Plant Sci. Lett.*, **25**, 329–335.

Joshi, R., Wani, S.H., Singh, B., Bohra, A., Dar, Z.A., Lone, A.A., Pareek, A. and Singla-Pareek, S.L. (2016) Transcription factors and plants response to drought stress: Current understanding and future directions. *Front. Plant Sci.*, **7**, 1–15.

Kalladan, R., Worch, S., Rolletschek, H., Harshavardhan, V.T., Kuntze, L., Seiler, C., Sreenivasulu, N. and Röder, M.S. (2013) Identification of quantitative trait loci contributing to yield and seed quality parameters under terminal drought in barley advanced backcross lines. *Mol. Breed.*, **32**, 71–90.

Kim, W., Iizumi, T. and Nishimori, M. (2019) Global patterns of crop production losses associated with droughts from 1983 to 2009. *J. Appl. Meteorol. Climatol.*, **58**, 1233–1244.

Kishor, P.B., Sangam, S., Amrutha, R.N., *et al*. (2005) Regulation of proline biosynthesis, degradation, uptake and transport in higher plants: Its implications in plant growth and abiotic stress tolerance. *Curr. Sci.*, **88**, 424–438.

Kishor, P.B. and Sreenivasulu, N. (2014) Is proline accumulation per se correlated with stress tolerance or is proline homeostasis a more critical issue? *Plant, Cell Environ.*, **37**, 300–311.

Kishor, P.B., Hong Z., Miao G.H., Hu C.A. and Verma, D.P. (1995) Overexpression of delta1-pyrroline-5-carboxylate synthetase increases proline production and confers osmotolerance in transgenic plants. *Plant Physiol.*, **108**, 1387–1394.

Kishor, P.B.K., Hima K.P., Sunita, M.S.L. and Sreenivasulu, N. (2015) Role of proline in cell wall synthesis and plant development and its implications in plant ontogeny. *Front. Plant Sci.*, **6**, 1–17.

Kishor, P.B.K., Sangam, S., Amrutha, R.N., *et al*. (2005) Regulation of proline biosynthesis, degradation, uptake and transport in higher plants: Its implications in plant growth and abiotic stress tolerance. *Curr. Sci.*, **88**, 424–438.

Kiyosue, T., Yoshiba, Y., Yamaguchi-Shinozaki, K. and Shinozaki, K. (1996) A nuclear gene encoding mitochondrial proline dehydrogenase, an enzyme involved in proline metabolism, is upregulated by proline but downregulated by dehydration in Arabidopsis. *Plant Cell*, **8**, 1323–1335.

von Korff, M., Wang, H., Léon, J. and Pillen, K. (2004) Development of candidate introgression lines using an exotic barley accession (*Hordeum vulgare* ssp. *spontaneum*) as donor. *Theor. Appl. Genet.*, **109**, 1736–1745.

Lakew, B., Eglinton, J., Henry, R.J., Baum, M., Grando, S. and Ceccarelli, S. (2011) The potential contribution of wild barley (*Hordeum vulgare* ssp. *spontaneum*) germplasm to drought tolerance of cultivated barley (*H. vulgare* ssp. *vulgare*). *F. Crop. Res.*, **120**, 161–168.

Laxa, M., Liebthal, M., Telman, W., Chibani, K. and Dietz, K.J. (2019) The role of the plant antioxidant system in drought tolerance. *Antioxidants*, **8**.

Leng, G. and Hall, J. (2019) Crop yield sensitivity of global major agricultural countries to droughts and the projected changes in the future. *Sci. Total Environ.*, **654**, 811–821.

Lesk, C., Rowhani, P. and Ramankutty, N. (2016) Influence of extreme weather disasters on global crop production. *Nature*, **529**, 84–87.

Li, Y., Ye, W., Wang, M. and Yan, X. (2009) Climate change and drought: a risk assessment of crop-yield impacts. *Clim. Res.*, **39**, 31–46.

Liu, Q., Kasuga, M., Sakuma, Y., Abe, H., Miura, S., Yamaguchi-Shinozaki, K. and Shinozaki, K. (1998) Two transcription factors, DREB1 and DREB2, with an EREBP/AP2 DNA binding domain separate two cellular signal transduction pathways in drought- and low-

temperature-responsive gene expression, respectively, in Arabidopsis. *Plant Cell*, **10**, 1391–1406.

Lobell, D.B. and Field, C.B. (2007) Global scale climate-crop yield relationships and the impacts of recent warming. *Environ. Res. Lett.*, **2**.

Lobell, D.B., Schlenker, W. and Costa-Roberts, J. (2011) Climate trends and global crop production since 1980. *Science (80-.).*, **333**, 616–620.

Mata, C.G. and Lamattina, L. (2001) Nitric oxide induces stomatal closure and enhances the adaptive plant responses against drought stress. *Plant Physiol.*, **126**, 1196–1204.

Matiu, M., Ankerst, D.P. and Menzel, A. (2017) Interactions between temperature and drought in global and regional crop yield variability during 1961-2014. *PLoS One*, **12**, 1–23.

Mattioli, R., Biancucci, M., Shall, A., Mosca, L., Costantino, P., Funck, D. and Trovato, M. (2018) Proline synthesis in developing microspores is required for pollen development and fertility. *BMC Plant Biol.*, **18**, 1–15.

Maurer, A., Draba, V., Jiang, Y., Schnaithmann, F., Sharma, R., Schumann, E., Kilian, B., Reif, J.C. and Pillen, K. (2015) Modelling the genetic architecture of flowering time control in barley through nested association mapping. *BMC Genomics*, **16**, 1–12.

Mishra, S. and Dubey, R.S. (2006) Inhibition of ribonuclease and protease activities in arsenic exposed rice seedlings: Role of proline as enzyme protectant. *J. Plant Physiol.*, **163**, 927–936.

Mittler, R. (2002) Oxidative stress, antioxidants and stress tolerance. *Trends Plant Sci.*, **7**, 405–410.

Mizoi, J., Ohori, T., Moriwaki, T., *et al*. (2013) GmDREB2A;2, a canonical dehydration-responsive element-binding protein2-type transcription factor in soybean, is posttranslationally regulated and mediates dehydration-responsive element-dependent gene expression. *Plant Physiol.*, **161**, 346–361.

Morrell, P.L. and Clegg, M.T. (2007) Genetic evidence for a second domestication of barley (*Hordeum vulgare*) east of the Fertile Crescent. *Proc. Natl. Acad. Sci.*, **104**, 3289–3294.

Muzammil, S., Shrestha, A., Dadshani, S., Pillen, K., Siddique, S., Léon, J. and Naz, A.A. (2018) An ancestral allele of pyrroline-5-carboxylate synthase1 promotes proline accumulation and drought adaptation in cultivated barley. *Plant Physiol.*, **178**, 771–782.

Nakashima, K., Ito, Y. and Yamaguchi-Shinozaki, K. (2009) Transcriptional regulatory networks in response to abiotic stresses in Arabidopsis and grasses. *Plant Physiol.*, **149**, 88–95.

Osakabe, Y., Osakabe, K., Shinozaki, K. and Tran, L.S.P. (2014) Response of plants to water stress. *Front. Plant Sci.*, **5**, 1–8.

Öztürk, L. and Demir, Y. (2002) *In vivo* and *in vitro* protective role of proline. *Plant Growth Regul.*, **38**, 259–264.

Deutch, A. H., Rushlow, K. E. & Smith, C. J. (1984) Analysis of the *Escherichia coli* proBA locus by DNA and protein sequencing. *Nucleic Acids Res.*, **12**, 6337-6355.

Price, A.H. and Tomos, A.D. (1997) Genetic dissection of root growth in rice (*Oryza sativa* L.). II: Mapping quantitative trait loci using molecular markers. *Theor. Appl. Genet.*, **95**, 143–152.

Rajendrakumar, C.S.V., Reddy, B.V.B. and Reddy, A.R. (1994) Proline-protein interactions: protection of structural and functional integrity of M4 lactate dehydrogenase. *Biochem. Biophys. Res. Commun.*, **201**, 957–963.

Rejeb, K. Ben, Lefebvre-De Vos, D., Disquet, I. Le, Leprince, A.S., Bordenave, M., Maldiney, R., Jdey, A., Abdelly, C. and Savouré, A. (2015) Hydrogen peroxide produced by NADPH oxidases increases proline accumulation during salt or mannitol stress in *Arabidopsis thaliana*. *New Phytol.*, **208**, 1138–1148.

Roosens, N.H., *et al*. (1998) Isolation of the ornithine-delta- aminotransferase cDNA and effect of salt stress on its expression in *Arabidopsis thaliana*. *Plant Physiol*., **117**, 263–271

Rudolph, A.S., Crowe, J.H. and Crowe, L.M. (1986) Effects of three stabilizing agents-Proline, betaine, and trehalose-on membrane phospholipids. *Arch. Biochem. Biophys.*, **245**, 134–143.

Savouré, A., Hua, X.J., Bertauche, N., Montagu, M. Van and Verbruggen, N. (1997) Abscisic acid-independent and abscisic acid-dependent regulation of proline biosynthesis following cold and osmotic stresses in *Arabidopsis thaliana*. *Mol. Gen. Genet.*, **254**, 104–109.

Savouré, A., Jaoua, S., Hua, X.J., Ardiles, W., Montagu, M. Van and Verbruggen, N. (1995) Isolation, characterization, and chromosomal location of a gene encoding the Δ1-pyrroline-5-carboxylate synthetase in *Arabidopsis thaliana*. *FEBS Lett.*, **372**, 13–19.

Schmalenbach, I., Léon, J. and Pillen, K. (2009) Identification and verification of QTLs for agronomic traits using wild barley introgression lines. *Theor. Appl. Genet.*, **118**, 483–497.

Schreiber, L. (2010) Transport barriers made of cutin, suberin and associated waxes. *Trends Plant Sci.*, **15**, 546–553.

Schroeder, J.I., Allen, G.J., Hugouvieux, V., Kwak, J.M. and Waner, D. (2001) Guard cell transduction. *Annu. Rev. Plant Physiol. Plant Mol. Biol.*, **52**, 627–658.

Shao, H., Wang, H. and Tang, X. (2015) NAC transcription factors in plant multiple abiotic stress responses: Progress and prospects. *Front. Plant Sci.*, **6**, 1–8.

Sharma, P. and Shanker Dubey, R. (2005) Modulation of nitrate reductase activity in rice seedlings under aluminium toxicity and water stress: Role of osmolytes as enzyme protectant. *J. Plant Physiol.*, **162**, 854–864.

Sharma, S., Villamor, J.G. and Verslues, P.E. (2011) Essential role of tissue-specific proline synthesis and catabolism in growth and redox balance at low water potential. *Plant Physiol.*, **157**, 292–304.

Shavrukov, Y., Baho, M., Lopato, S. and Langridge, P. (2016) The TaDREB3 transgene transferred by conventional crossings to different genetic backgrounds of bread wheat improves drought tolerance. *Plant Biotechnol. J.*, **14**, 313–322.

Shavrukov, Y., Kurishbayev, A., Jatayev, S., Shvidchenko, V., Zotova, L., Koekemoer, F., Groot, S. De, Soole, K. and Langridge, P. (2017) Early flowering as a drought escape mechanism in plants: How can it aid wheat production? *Front. Plant Sci.*, **8**, 1–8.

Sheffield, J. and Wood, E.F. (2008) Projected changes in drought occurrence under future global warming from multi-model, multi-scenario, IPCC AR4 simulations. *Clim. Dyn.*, **31**, 79–105.

Shinozaki, K., Yamaguchi-Shinozaki, K. and Seki, M. (2003) Regulatory network of gene expression in the drought and cold stress responses. *Curr. Opin. Plant Biol.*, **6**, 410–417.

Signorelli, S., Coitiño, E.L., Borsani, O. and Monza, J. (2014) Molecular mechanisms for the reaction between •OH radicals and proline: Insights on the role as reactive oxygen species scavenger in plant stress. *J. Phys. Chem. B*, **118**, 37–47.

Signorelli, S., Dans, P.D., Coitiño, E.L., Borsani, O. and Monza, J. (2015) Connecting proline and γ-aminobutyric acid in stressed plants through non-enzymatic reactions. *PLoS One*, **10**, 1–14.

Stockinger, E.J., Gilmour, S.J. and Thomashow, M.F. (1997) *Arabidopsis thaliana* CBF1 encodes an AP2 domain-containing transcriptional activator that binds to the C-repeat/DRE, a cis-acting DNA regulatory element that stimulates transcription in response to low temperature and water deficit. *Proc. Natl. Acad. Sci.*, **94**, 1035–1040.

Strizhov, N., Abrahám, E., Okrész, L., Blickling, S., Zilberstein, A., Schell, J., Koncz, C. and Szabados, L. (1997) Differential expression of two P5CS genes controlling proline accumulation during salt-stress requires ABA and is regulated by ABA1, ABI1 and AXR2 in Arabidopsis. *Plant J.*, **12**, 557–569.

Su, J. and Wu, R. (2004) Stress-inducible synthesis of proline in transgenic rice confers faster growth under stress conditions than that with constitutive synthesis. *Plant Sci.*, **166**, 941–948.

Szabados, L. and Savouré, A. (2010) Proline: a multifunctional amino acid. *Trends Plant Sci.*, **15**, 89–97.

Székely, G., Ábrahám, E., Cséplo, Á., *et al*. (2008) Duplicated P5CS genes of Arabidopsis play distinct roles in stress regulation and developmental control of proline biosynthesis. *Plant J.*, **53**, 11–28.

Szoke, A., Miao, G.H., Hong, Z. and Verma, D.P.S. (1992) Subcellular location of Δ1-pyrroline-5-carboxylate reductase in root/nodule and leaf of soybean. *Plant Physiol.*, **99**, 1642–1649.

Taketa, S., Kikuchi, S., Awayama, T., Yamamoto, S., Ichii, M. and Kawasaki, S. (2004) Monophyletic origin of naked barley inferred from molecular analyses of a marker closely linked to the naked caryopsis gene (nud). *Theor. Appl. Genet.*, **108**, 1236–1242.

Talame, V., Sanguineti, M.C., Chiapparino, E., *et al*. (2004) Identification of *Hordeum spontaneum* QTL alleles improving field performance of barley grown under rainfed conditions. *Ann. Appl. Biol.*, **144**, 309–319.

Tanksley, S.D. and McCouch, S.R. (1997) Seed banks and molecular maps: Unlocking genetic potential from the wild. *Science (80-.).*, **277**, 1063–1066.

Teulat, B., Borries, C. and This, D. (2001) New QTLs identified for plant water status, water-soluble carbohydrate and osmotic adjustment in a barley population grown in a growth-chamber under two water regimes. *Theor. Appl. Genet.*, **103**, 161–170.

Teulat, B., This, D., Khairallah, M., Borries, C., Ragot, C., Sourdille, P., Leroy, P., Monneveux, P. and Charrier, A. (1998) Several QTLs involved in osmotic-adjustment trait variation in barley (*Hordeum vulgare* L.). *Theor. Appl. Genet.*, **96**, 688–698.

Thomson, L.J., Macfadyen, S. and Hoffmann, A.A. (2010) Predicting the effects of climate change on natural enemies of agricultural pests. *Biol. Control*, **52**, 296–306.

Trenberth, K.E., Dai, A., Schrier, G. Van Der, Jones, P.D., Barichivich, J., Briffa, K.R. and Sheffield, J. (2014) Global warming and changes in drought. *Nat. Clim. Chang.*, **4**, 17–22.

Tripathi, P., Rabara, R.C. and Rushton, P.J. (2014) A systems biology perspective on the role of WRKY transcription factors in drought responses in plants. *Planta*, **239**, 255–266.

Tuberosa, R. and Salvi, S. (2006) Genomics-based approaches to improve drought tolerance of crops. *Trends Plant Sci.*, **11**, 405–412.

Uga, Y., Okuno, K. and Yano, M. (2011) Dro1, a major QTL involved in deep rooting of rice under upland field conditions. *J. Exp. Bot.*, **62**, 2485–2494.

Uga, Y., Yamamoto, E., Kanno, N., Kawai, S., Mizubayashi, T. and Fukuoka, S. (2013) A major QTL controlling deep rooting on rice chromosome 4. *Sci. Rep.*, **3**.

Uno, Y., Furihata, T., Abe, H., Yoshida, R., Shinozaki, K. and Yamaguchi-Shinozaki, K. (2000) Arabidopsis basic leucine zipper transcription factors involved in an abscisic acid-dependent signal transduction pathway under drought and high-salinity conditions. *Proc. Natl. Acad. Sci.*, **97**, 11632–11637.

Verbruggen, N., Hua, X.J., May, M. and Montagu, M. Van (1996) Environmental and developmental signals modulate proline homeostasis: Evidence for a negative transcriptional regulator. *Proc. Natl. Acad. Sci.*, **93**, 8787–8791.

Verbruggen, N., Villarroel, R. and Montagu, M. Van (1993) Osmoregulation of a pyrroline-5-carboxylate reductase gene in *Arabidopsis thaliana*. *Plant Physiol.*, **103**, 771–781.

Verslues, P.E. and Bray, E.A. (2004) LWR1 and LWR2 are required for osmoregulation and osmotic adjustment in Arabidopsis. *Plant Physiol.*, **136**, 2831–2842.

Verslues, P.E. and Bray, E.A. (2006) Role of abscisic acid (ABA) and *Arabidopsis thaliana* ABA-insensitive loci in low water potential-induced ABA and proline accumulation. *J. Exp. Bot.*, **57**, 201–212.

Verslues, P.E. and Sharma, S. (2010) Proline metabolism and its implications for plant-environment interaction. *Arab. B.*, **8**, e0140.

Wang, J., Li, Q., Mao, X., Li, A. and Jing, R. (2016) Wheat transcription factor TaAREB3 participates in drought and freezing tolerances in Arabidopsis. *Int. J. Biol. Sci.*, **12**, 257–269.

Wang, Z., Li, J., Lai, C., Wang, R.Y., Chen, X. and Lian, Y. (2018) Drying tendency dominating the global grain production area. *Glob. Food Sec.*, **16**, 138–149.

Wiegmann, M., Maurer, A., Pham, A., *et al*. (2019) Barley yield formation under abiotic stress depends on the interplay between flowering time genes and environmental cues. *Sci. Rep.*, **9**, 1–16.

Xue, D., Zhang, X., Lu, X., Chen, G. and Chen, Z.H. (2017) Molecular and evolutionary mechanisms of cuticular wax for plant drought tolerance. *Front. Plant Sci.*, **8**, 1–12.

Yang, Y., Al-Baidhani, H.H.J., Harris, J., *et al*. (2020) DREB/CBF expression in wheat and barley using the stress-inducible promoters of HD-Zip I genes: impact on plant development, stress tolerance and yield. *Plant Biotechnol. J.*, **18**, 829–844.

Yoshiba, Y., Kiyosue, T., Katagiri, T., Ueda, H., Mizoguchi, T., Yamaguchi-Shinozaki, K., Wada, K., Harada, Y. and Shinozaki, K. (1995) Correlation between the induction of a gene for Δ1-pyrroline-5-carboxylate synthetase and the accumulation of proline in *Arabidopsis thaliana* under osmotic stress. *Plant J.*, **7**, 751–760.

Yoshida, T., Fujita, Y., Maruyama, K., Mogami, J., Todaka, D., Shinozaki, K. and Yamaguchi-Shinozaki, K. (2015) Four Arabidopsis AREB/ABF transcription factors function predominantly in gene expression downstream of SnRK2 kinases in abscisic acid signalling in response to osmotic stress. *Plant, Cell Environ.*, **38**, 35–49.

Yoshida, T., Fujita, Y., Sayama, H., Kidokoro, S., Maruyama, K., Mizoi, J., Shinozaki, K. and Yamaguchi-Shinozaki, K. (2010) AREB1, AREB2, and ABF3 are master transcription factors that cooperatively regulate ABRE-dependent ABA signaling involved in drought stress tolerance and require ABA for full activation. *Plant J.*, **61**, 672–685.

Zhang, J., Zhang, S., Cheng, M., Jiang, H., Zhang, X., Peng, C., Lu, X., Zhang, M. and Jin, J. (2018) Effect of drought on agronomic traits of rice and wheat: A meta-analysis. *Int. J. Environ. Res. Public Health*, **15**.

Zhou, L., Liu, Z., Liu, Y., *et al*. (2016) A novel gene OsAHL1 improves both drought avoidance and drought tolerance in rice. *Sci. Rep.*, **6**, 1–15.

Zhu, B., Su, J., Chang, M., Verma, D.P.S., Fan, Y.L. and Wu, R. (1998) Overexpression of a Δ1-pyrroline-5-carboxylate synthetase gene and analysis of tolerance to water- and salt-stress in transgenic rice. *Plant Sci.*, **139**, 41–48.

Zhuang, J., Wang, F., Xu, Z.S. and Xiong, A.S. (2015) Microarray analysis of different expression profiles between wild-type and transgenic rice seedlings overexpression OsDREB1BI gene. *Biol.*, **70**, 760–770.

Chapter 2. Genetic and molecular analysis of proline mediated drought stress tolerance in barley

2.1. Introduction

Drought stress is one of the major threats to global agriculture and crop production. The frequency and intensity of dry periods will increase in the future owing to decreased precipitation and increased evaporation (Trenberth *et al.*, 2014; Dhanyalakshmi *et al.*, 2019; Sheffield and Wood, 2008). Throughout the last four decades, around 75% of arable land experienced drought-related yield deficit, and the yield of major cereal crops like wheat, barley and maize was particularly affected (Kim *et al.*, 2019; Lobell and Field, 2007; Li *et al.*, 2009). Water stress targets several physiological processes such as reduced photosynthesis (Deeba *et al.*, 2012; Muzammil *et al.*, 2018), oxidative stress (Mittler, 2002) and arrested growth (Barnabás *et al.*, 2008) which ultimately lead to declined yield (Chaves and Davies, 2010).

As land plants are regularly exposed to abiotic stresses, they have evolved several morphological, physiological, and molecular mechanisms to cope with the adverse environment, including drought stress (Shinozaki and Yamaguchi-Shinozaki, 2006; Bartels and Sunkar, 2005). One of the widespread tolerance mechanisms across animal and plant species is the accumulation of non-toxic compatible solutes such as proline, soluble sugars, glycine betaine, and low molecular weight organic acids (Hochberg *et al.*, 2013; Bartels and Sunkar, 2005). The main role of compatible solute is to maintain the tissue turgidity and protect the macromolecules in the dehydrating cells. Among the compatible solutes, the accumulation of proline is one of the most apparent responses of plants against drought stress (Szabados and Savouré, 2010; Kishor *et al.*, 2005). Proline primarily facilitates osmotic adjustment (Kishor *et al.*, 2005; Verbruggen *et al.*, 1996) and cell membrane stability in stressed tissues (Mansour, 1998). Proline also acts as reactive oxygen species (ROS) scavenger or activates the antioxidant like superoxide dismutase, catalases, and peroxidase (Signorelli *et al.*, 2014). Also, proline might play a role in cellular homeostasis by maintaining NADPH:$NADP^+$ ratio in the chloroplast (Kishor *et al.*, 2005; Szabados and Savouré, 2010). Previous studies showed that endogenous proline accumulation, as well as exogenous proline application during osmotic stress, contributes to reduced oxidative damage and improved biomass production (Hassine *et al.*, 2008; Székely *et al.*, 2008; Sripinyowanich *et al.*, 2013). Besides stress adaptation, proline also facilitates the stress recovery process (Singh *et al.*, 2000; Singh *et al.*, 1973; Nounjan and Theerakulpisut, 2012).

Although the role of proline in stress adaptation is well described, the utility and genetic regulation of this trait in crops are poorly understood. Former Doctoral student in our research group conducted a QTL mapping for proline accumulation in a set of introgression line population (IL) carrying chromosomal segments of wild barley, ISR42-8, in the background of cultivar, Scarlett. A major QTL (*QPro.S42-1H*) was detected on chromosome 1, where ILs S42IL-143 and S42IL-141 sharing a common wild chromosome segment accumulated significantly higher proline under drought stress. In the current study, we performed the positional cloning of *QPro.S42-1H,* followed by the functional validation of a novel of *HvP5cs1* from ISR42-8. Then, we evaluated the significance of exotic allele (*QPro.S42-1H*) for drought stress adaptation in cultivated barley.

2.2. Materials and methods

2.2.1. Allele mining of *HvP5cs1* promoter in a barley diversity panel

For allele mining of *HvP5cs1* promoter, we selected 60 barley genotypes comprising of wild accessions, landraces, and cultivars. Then, we selected five accessions, namely ISR42-8, HOR9840, ICB181160, Scarlett, and NGB4605, for further analysis. Based on the *HvP5cs1* promoter polymorphisms, the above five genotypes represented the majority of the sequenced accessions. Seeds were pregerminated using a peat-based potting mixture, ED73 classic produced and marketed by Einheitserde, Germany, and two-day-old seedlings were transferred to a pot (8* 8* 7 cm). The pots were filled with an equal volume of the potting mixture containing 60% natural sand and 40% topsoil (Terrasoil; Cordel and Sohn). Plants were grown in an automated climate chamber with 14/10 h light/dark period, 60% relative humidity, 20/18°C day-night temperature, and 100-160 µmol $m^{-2} \cdot s^{-1}$ light intensity. The field capacity of the soil was maintained at 80% under well-watered condition. Pots were weighed twice a day and watered manually to maintain the constant soil moisture. Drought stress was applied by withholding watering to 14-day old seedlings. The weight of pots was recorded each day to ensure the same moisture level in all pots. Fresh samples were harvested 9 d after drought treatment. The samples were snap-frozen in liquid nitrogen and stored at -80°C before proline determination and mRNA extraction. The experiment was performed in eight biological replicates.

2.2.1.1. Proline determination

Proline was measured from shoot samples, according to Bates *et al.* (1973), adapted to a microplate-based protocol (Ábrahám *et al.*, 2010). In short, seedlings were homogenized in liquid nitrogen, and proline was extracted using 1 ml 3% sulphosalicylic acid followed by centrifuging at 12,000 *g* for 5 minutes. The sample extract was incubated for 1 hour at 96°C

with 2.5% ninhydrin and acetic acid at a 1:1:1 ratio. The reaction was stopped on ice, and the proline-ninhydrin reaction product was extracted with 1 ml toluene. The absorbance of chromatophore containing toluene was measured at 520 nm using a microplate reader (TECAN Infinite 200 Pro, TECAN Group Limited, Switzerland). Shoot proline level was determined using a standard curve method and expressed as micrograms per gram fresh weight.

2.2.1.2. *HvP5cs1* mRNA expression analysis using quantitative relative time PCR

RNA was extracted in three biological replicates from control and treatment samples from all five accessions. The RNA concentration and quality were determined by running on 1% Agarose gel and nanodrop (NanoDrop 2000c, Thermo Fischer Scientific, USA) before cDNA synthesis. cDNA was synthesized using the Revertaid H-minus cDNA synthesis kit (Thermo Fischer Scientific, USA) following the manufacturer's instruction. An SYBR green-based qPCR master mix (Thermo Fischer Scientific, USA) was used in the assay with three technical replicates per sample. The qPCR run was set to initial denaturation at 95°C for 3 minutes, followed by 40 cycles (95°C for 15 seconds, 60°C for 1 minute). Specific amplification was analyzed using a melt curve (95°C for 15 seconds, 60°C for 1 minute, 95°C for 15 seconds). Relative mRNA expression of *HvP5cs1* was calculated based on the $2^{-\Delta\Delta Ct}$ method (Livak & Schmittgen 2001). Elongation factor-beta was used as the reference gene for relative quantification. The primers used in the qPCR assay are provided in Table S1.

2.2.2. Transient expression of ISR42-8 and Scarlett *HvP5cs1* promoter

2.2.2.1. Preparation of promoter::reporter constructs and protoplast transfection

Around 1500 bp region upstream of the start codon of ISR42-8 and Scarlett was synthesized commercially by Invitrogen, USA. The promoter was cloned to a Gateway cloning vector pDONR221 (Invitrogen) according to the manufacturer's instructions. The verified promoters were fused with the eGFP-GUS tag in the expression vector pBGWFS7 (Yoo *et al*., 2007). Transient expression analysis using Arabidopsis leaf mesophyll cells (treated with or without ABA) was performed as described previously (Yoo *et al*., 2007; Yoshida *et al*., 2002; Yoshida *et al*., 2015). A luciferase gene under the control of the 35S promoter (Karimi *et al*., 2005) was used as an internal control for beta-glucuronidase (GUS) activity analysis between Col-0 and *abf1 abf2 abf3 abf4* quadruple mutant. The luciferase activity was performed using the Luciferase Assay System (Promega; catalog no. E1500) following the manufacturer's instructions. The *abf1 abf2 abf3 abf4* quadruple mutant was derived from *abf1* (SALK_132819), *areb1/abf2* (SALK_002984), *abf3* (SALK_096965), and *areb2/abf4* (SALK_069523) in Col-0 background (Yoshida *et al*., 2015). Dr. Yamaguchi-Shinozaki's lab

kindly provided the seeds of the *abf1 abf2 abf3 abf4* quadruple mutant. Transfection efficiency was estimated by counting the number of protoplasts producing fluorescence signals through the expression of green fluorescent protein (GFP) (Figure S1).

2.2.2.2. mRNA extraction and expression analysis of reporter genes

RNA was extracted in three biological replicates from control and treatment samples from all five accessions. RNA extraction, cDNA synthesis and qPCR was performed as described in section 2.2.2.3 using StepOne plus real-time PCR system (Applied Biosystems). The 18S ribosomal gene was used as an endogenous control. Relative mRNA expression of GUS and ABF genes was calculated based on Pfaffl's method (Pfaffl, 2001). A list of primer sequences used for expression analysis is shown in Table S1.

2.2.3. Evaluation of NIL-143 and Scarlett for drought stress adaptation

2.2.3.1. Plant materials

In a pot experiment, S42IL-143 showed better reproductive performance compared to Scarlett (Figure S2). Although S42IL-143 showed superior adaptive traits, the wild introgression was not isogenic (BC3) to Scarlett. Therefore, a near-isogenic line (NIL) was developed by marker-assisted backcrossing of S42IL-143 to recurrent parent Scarlett for three generations (BC6), which is referred to as NIL-143 in the further text. Selfing generation two and three of NIL-143 was used in the experiment.

2.2.3.2. Plant growth condition and drought stress treatment at the seedling stage

The growing condition was similar to the conditions described in section 2.2.2.1. The field capacity of the soil was maintained at 80% under well-watered condition. Pots were weighed twice a day and watered manually to maintain the constant soil moisture. Drought stress treatment was applied by withholding watering to 14 d old seedlings. The weight of pots was recorded each day to ensure that the moisture level is the same in all the pots.

2.2.3.3. Electrolyte leakage and relative water content measurement

Cell membrane integrity was determined by evaluating electrolyte leakage (EL) based on Bajji *et al*. (2002). Falcon tubes were filled with 10 ml deionized water, and initial electrical conductivity was recorded (ECi). First, the tip of (around 2 cm) first fully expanded leaf was removed. Then, two leaf sections (around 2 cm each) were cut and placed in a falcon tube with 10 ml double distilled water and stored in the dark at room temperature. Electrical conductivity was measured 24 h of rehydration period (ECf). After the final reading, the

samples were boiled at 100°C for 30 minutes, cooled to room temperature, and total electrical conductivity (ECt) was measured. EL was expressed as (ECf-ECi)/(ECt-ECi)*100. Leaf water status was estimated through relative water content (RWC), according to Ghoulam *et al.* (2002). For RWC measurement, four leaf sections (around 2 cm each) were detached from the first fully expanded leaf, and the fresh weight was recorded (FW). Then, the leaf sections were dipped in a falcon tube filled with 10 ml deionized water for 24 h at room temperature. The leaf sections were removed from the falcon tube, and excess water was wiped with a paper towel before taking the turgor weight (TW). Dry weight was recorded after oven drying at 70°C for 24 h. RWC was estimated as (FW-DW)/(TW-DW) *100.

2.2.3.4. Proline and malondialdehyde determination

Proline was determined according to procedures described in chapter 2 section 2.2.2.3. Oxidative damage of lipid membrane during drought was estimated by determining MDA based concentration using thiobarbituric acid (TBA) method (Hodges *et al.*, 1999) adapted to a microplate-based protocol (Dziwornu *et al.*, 2018) with some modification. Shoot samples were homogenized in liquid nitrogen, and MDA was extracted using 1.5 ml of 0.1% trichloroacetic acid (TCA) followed by centrifuging at 14,000 *g* for 15 minutes at 4°C. Then, 500 µl supernatant was mixed with reaction solution I (0.01% 2,6-di-tert-butyl-4-methyl phenol (BHT) in 20% TCA) and reaction solution II (0.65% TBA, 0.01% BHT in 20% TCA) in a 1:1 ratio. Reaction and sample mix were incubated at 95°C for 30 minutes. The reaction was stopped on ice for five minutes, and the reaction mix was centrifuged at 8000 *g* for 10 minutes at 4°C. The absorbance was measured at 440 nm, 532 nm, and 600 nm using a microplate reader (TECAN Infinite 200 Pro, TECAN Group Limited, Switzerland). MDA concentration was expressed as nanomoles per gram fresh weight.

2.2.3.5. Evaluation of vegetation indices

Vegetation indices (VI) were recorded using portable spectrometric devices like The Soil plant analysis development (SPAD) chlorophyll meter and photon system instrument (PolyPen, RP 410) using manufacturer instructions. SPAD is a handheld device that measures the transmittance of red and infrared light spectrum through a leaf surface clamped to the arm of the device, and the relative SPAD reading is proportional to the chlorophyll content of the leaf (Uddling *et al.*, 2007). PolyPen is also a portable handheld device that has a capacity to take absorbance at a broad range of light spectrum from 380 nm to 1050 nm. In addition to chlorophyll, PolyPen readings reflect the concentration of other pigments like carotenoids and anthocyanin. VIs were scored from 4 d to 8 d after drought stress. The measurements were made in first fully expanded leaves.

2.2.3.6. Evaluation of photosynthetic parameters

Gas exchange measurement was performed using a portable photosynthesis system (LI-6400 XT, LI-COR Biosciences) after 4, 6, and 8 d after drought stress. The measurements were made in the first fully expanded leaves. The A/C_i curve measurement was performed in the middle part of the leaf inside a leaf chamber. The parameters inside the leaf chamber were set as constant photosynthetic active radiation of 1500 µmol m^{-2} s^{-1}, relative humidity approximately 52% and temperature corresponding to leaf temperature. The gas exchange was measured by supplying external CO_2 at varying concentrations (50, 100, 200, 250, 300, 400, 600, 800 and 1000 ppm). The infrared gas exchange analyzer automatically logs the photosynthetic parameters, including the rate of CO_2 assimilation (*A*), intracellular CO_2 (*Ci*), stomatal conductance (g_s), and transpiration rate (*E*). *A*/*Ci* curve was plotted to estimate the maximum carboxylation rate of Rubisco (V_{cmax}) and the maximum rate of electron transport during ribulose-1,5-biphosphate regeneration (J_{max}) using non-linear fitting program according to (Sharke *et al*., 2007; Sharkey, 2016). The estimated V_{cmax} and J_{max} were then adjusted to a temperature of 25 ^{o}C for data presentation. Further, we used a portable fluorometer (MINI-PAM-II, Heinz Walz, Germany) to measure the effective quantum yield of photosystem II at steady-state photosynthesis under light conditions (Y (II)).

2.2.4. Evaluation of stress recovery at the seedling stage

Two-day old seedlings of Scarlett and NIL-143 were transferred to a pot (12 cm diameter and 12 cm height) filled with a potting mixture comprised of 60% natural sand and 40% topsoil (Terrasoil; Cordel and Sohn). All the pots were filled with an equal amount of soil, and the moisture level was maintained at 75 % field capacity. The plants were grown in the greenhouse, and the growing condition was 18-22°C daily mean temperature, 14/10 h light/dark, and 110-150 µmol $m^{-2}{\cdot}s^{-1}$ light intensity. Fifteen seedlings were grown in one pot for 12 d, and the pots were dehydrated by withholding watering. After 12 d of dehydration, the pots were rewatered, and the number of rejuvenated seedlings was recorded. The experiment was performed in five biological replications and repeated two times. The results were further confirmed by repeating the same experiment where Scarlett and NIL-143 were grown in a single pot.

2.2.5. Evaluation of adaptive traits under drought stress in field conditions

The reproductive and physiological performance of Scarlett and NIL-143 was evaluated in a field condition in Campus Kleinaltendorf, Rheinbach, Germany. Row experiment was implemented inside a rain-out shelter. The seeds were sown in a 40 cm rows at a spacing of 2 cm (plant to plant) and 15 cm (row to row). Irrigation was stopped in a drought plot before

heading (BBCH 41). Each genotype was randomly assigned to ten rows in a block. One block was regularly irrigated while irrigation was stopped in another block before heading stage (BBCH 41) to induce drought stress. Water stress was applied for three weeks. We scored VI using not destructive methods using portable spectrometers such as SPAD and PolyPen as described earlier at 7, 14, and 21 d after drought stress. In addition, photosynthetic health was determined by measuring Y (II) was using MiniPam. Matured ears and straw were harvested, and oven-dried at 30°C and 70°C respectively for 72 hours before evaluating the yield and related traits. One plot was also established in the open field to estimate the yield-related traits under rainfed conditions.

2.2.6. Statistical analyses

Statistical significances were analyzed using open-access statistical computing software R. Two-way ANOVA was performed to observe genotype, treatment, and interaction effects. The student's *t*-test was used for the mean comparison between genotypes for a given treatment condition. Multiple mean comparison analysis was done using a Tukey post hoc test. Graphics were prepared using statistical platform R and Prism8.

2.3. Results

We started with the positional cloning of *QPro.S42-1H* in collaboration with former Doctoral student. My contribution was towards marker development and genotyping of recombinants. A high-resolution population (3300 BC4S2 individuals derived from S42IL-143) was genotyped using SNP derived KASP markers on the right and left border of the QTL locus. Eighty-five recombinants were identified between the left and right border markers. Then, we measured proline in 85 recombinants that were exposed to drought stress for 9 d before proline measurement. Further, the selected recombinants were genotyped, developing additional SSLP markers to the left and right of *HvP5cs1* to delimit the region to single-gene resolution. Later, gene-specific markers developed in the promoter region showed cosegregation with the proline phenotype. Based on this output, in the next step, we did the functional analysis of *HvP5cs1* using a barley diversity panel and transient assay

2.3.1. Novel polymorphism was detected in the promoter region of *HvP5cs1*

Allele mining was done to identify the allelic variation in *HvP5cs1* promoter. The promoter region of *HvP5cs1* was sequenced in 60 barley genotypes. In-silico promoter analysis was done to predict *cis*-acting elements using plant promoter analysis navigator (PlantPAN 3.0) and plant cis-acting regulatory DNA elements (PLACE) databases. Several *cis*-acting elements were detected, such as ABRE and related coupling elements (CE), MYB binding motif, NAC binding motif, and dehydration responsive element (DRE). We found novel polymorphisms detected in ABRE and MYB binding motifs. Allele mining revealed mutations across predicted ABRE, CE3, CE1, and MYB motifs among the sequenced barley genotypes. HOR9840 carried a 10 bp deletion allele, which resulted in a loss of predicted CE3. Besides, HOR9480 revealed SNP across predicted CE1 and MYB binding motif. Likewise, 130 bp deletions in NGB4605 resulted in a loss of predicted ABRE and MYB binding motif (Figure S3). To test if promoter variation correlates with proline accumulation, we selected five genotypes that represented the haplotypes based on promoter polymorphisms. Shoot proline level was highest in ISR42-8, while HOR9840, which revealed polymorphisms across multiple DNA binding domains, accumulated the lowest proline under drought stress (Figure 2.1a and b). Proline concentration was around 6-fold lower in HOR9840 than ISR42-8 under drought conditions. Then, we checked the transcription level of *HvP5cs1* using quantitative real-time PCR. Scarlett and NGB4605 revealed similar proline accumulation in response to drought stress. The relative expression of *HvP5cs1* correlated with shoot proline concentration (r^2=0.81) (Figure 2.1c). Hence, allele mining identified novel variation in the *cis*-acting element of the *HvP5cs1* promoter, especially across ABRE and MYB binding motifs.

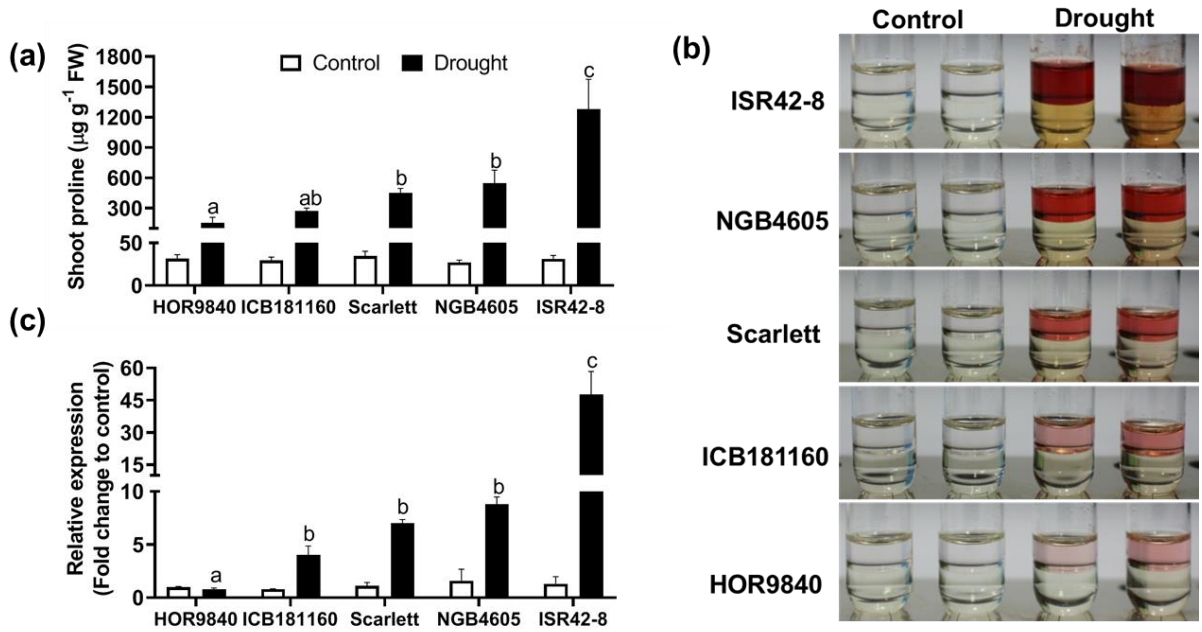

Figure 2.1. Allele mining of barley *HvP5cs1* promoter. Sixty barley genotypes comprised of wild accessions, landraces, and cultivars were sequenced. (a) Shoot proline concentration in barley genotypes selected based on the polymorphism across DNA binding motifs. Indexed letters above the bars indicate significant differences between the genotypes ($P \leq 0.05$), not sharing the same letter under drought conditions. Bars represent mean ± SE (n = 8). (b) Free proline detection from shoot extracts using Ninhydrin reagent. A darker color indicates higher proline concentration in the shoot samples. Two-week-old seedlings were exposed to nine days of drought before proline measurement. (c) Relative mRNA expression of *HvP5cs1* gene. Indexed letters above the bars indicate significant differences between the genotypes ($P \leq 0.05$), not sharing the same letter under drought conditions. Bars represent mean ± SE (n = 3). FW, fresh weight

2.3.2. *HvP5cs1* promoter activity is regulated in an ABF-dependent manner

Recombination and allele mining suggested that the causal mutations controlling drought-inducible proline accumulation may lie in the promoter of *HvP5cs1*. Therefore, we sequenced an approximately 1.5 kb region upstream of ATG in ISR42-8 and Scarlett. The sequence comparison revealed mutations across putative ABREs and related CE3 motifs between Scarlett and ISR42-8 (Figure S3). Based on this, we assumed that these mutations may influence the DNA binding of ABFs in the *HvP5cs1* promoter. To investigate this, we established promoter::reporter constructs for ISR42-8 (pISR::eGFP-GUS) and Scarlett (pSCA::eGFP-GUS). Next, we transiently expressed the pISR::eGFP-GUS or pSCA::eGFP-GUS constructs in protoplasts isolated from Arabidopsis leaf mesophyll cells. We then incubated transfected protoplasts of Col-0 ecotype in the presence of ABA (50 µm) for 4 h and analyzed the expression of *GUS*, *ABF1*, *ABF2*, *ABF3* and *ABF4* via qRT-PCR. The expression of all four ABFs was substantially induced upon ABA treatment in both pISR::eGFP-GUS- and

pSCA::eGFP-GUS-transfected protoplasts. Similarly, expression of the GUS gene was strongly and significantly induced upon ABA treatment in pISR::eGFP-GUS transfected protoplasts; however, only modest up-regulation in GUS expression was observed in pSCA::eGFP-GUS-transfected protoplasts (Figure 2.2a). To determine whether up-regulation of GUS expression in pISR::eGFP-GUS-transfected protoplasts was mediated by ABFs, we transfected this construct into mesophyll protoplasts isolated from the wild-type Arabidopsis (Col-0) and loss-of-function *abf1 abf2 abf3 abf4* quadruple mutant. Notably, we found that the up-regulation of GUS activity upon ABA treatment was significantly impaired in the *abf1 abf2 abf3 abf4* quadruple mutant as compared to the wild type (Figure 2.2b). Taken together, ABA-induced *HvP5cs1* promoter activity differed between ISR42-8 and Scarlett in an ABF-dependent manner.

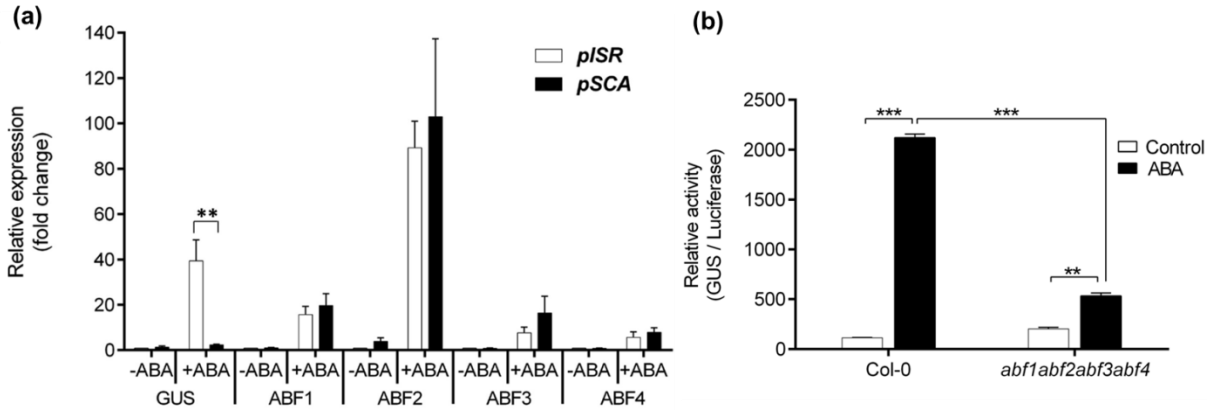

Figure 2.2. *HvP5cs1* promoter activity analysis in Arabidopsis protoplasts upon ABA treatment. (a) Relative expression of GUS, ABF1, ABF2, ABF3, and ABF4 in Arabidopsis Col-0 protoplasts transfected with *HvP5cs1* promoter::reporter constructs of ISR42-8 (pISR::eGFP-GUS) and Scarlett (pSCA::eGFP-GUS). For untreated samples (−ABA), data represent the relative expression of the indicated genes with the value of pISR::eGFP-GUS (Col-0) set to 1. For treated samples (+ABA), data represent the relative expression of the indicated genes with the value of untreated protoplasts set to 1. Bars represent the mean ± SE (n = 3). Asterisks indicate a significant difference between pISR (pISR::eGFP-GUS) and pSCA (pSCA::eGFP-GUS) (***P* ≤ 0.01) using student's *t*-tests. (b) GUS activity of pISR::eGFP-GUS in Arabidopsis mesophyll protoplasts of Col-0 and the *abf1 abf2 abf3 abf4* quadruple mutant. Bars represent the mean ± SE (n = 3). Asterisks indicate significant difference between genotypes under -ABA (control) and +ABA (***P* ≤ 0.01, ****P* ≤ 0.001) using student's *t*-test.

2.3.3. Drought-inducible proline accumulation is superior in NIL-143

NIL-143 is a near-isogenic line where *QPro.S42-1H* is introgressed in Scarlett. *QPro.S42-1H* is a QTL controlling drought-inducible proline accumulation in barley. Therefore, we estimated the proline accumulation in the seedlings of Scarlett and NIL-143 at 4, 5, 6, and 8 d after water stress. We observed a significant treatment effect after 5 d of stress (Table S2). However,

compared to control conditions, the proline accumulation increased only in NIL-143 after 5 d of drought stress. After 6 d, proline concentration in the shoots increased in both Scarlett and NIL-143 under drought conditions. The proline levels in NIL-143 was 2 to 2.5-fold higher than in Scarlett under water stress. The shoot proline content did not differ between NIL-143 and Scarlett under control conditions (Figure 2.3). Taken together, NIL-143 possessed the genetic ability of wild parent, ISR42-8, to accumulate higher proline under drought stress.

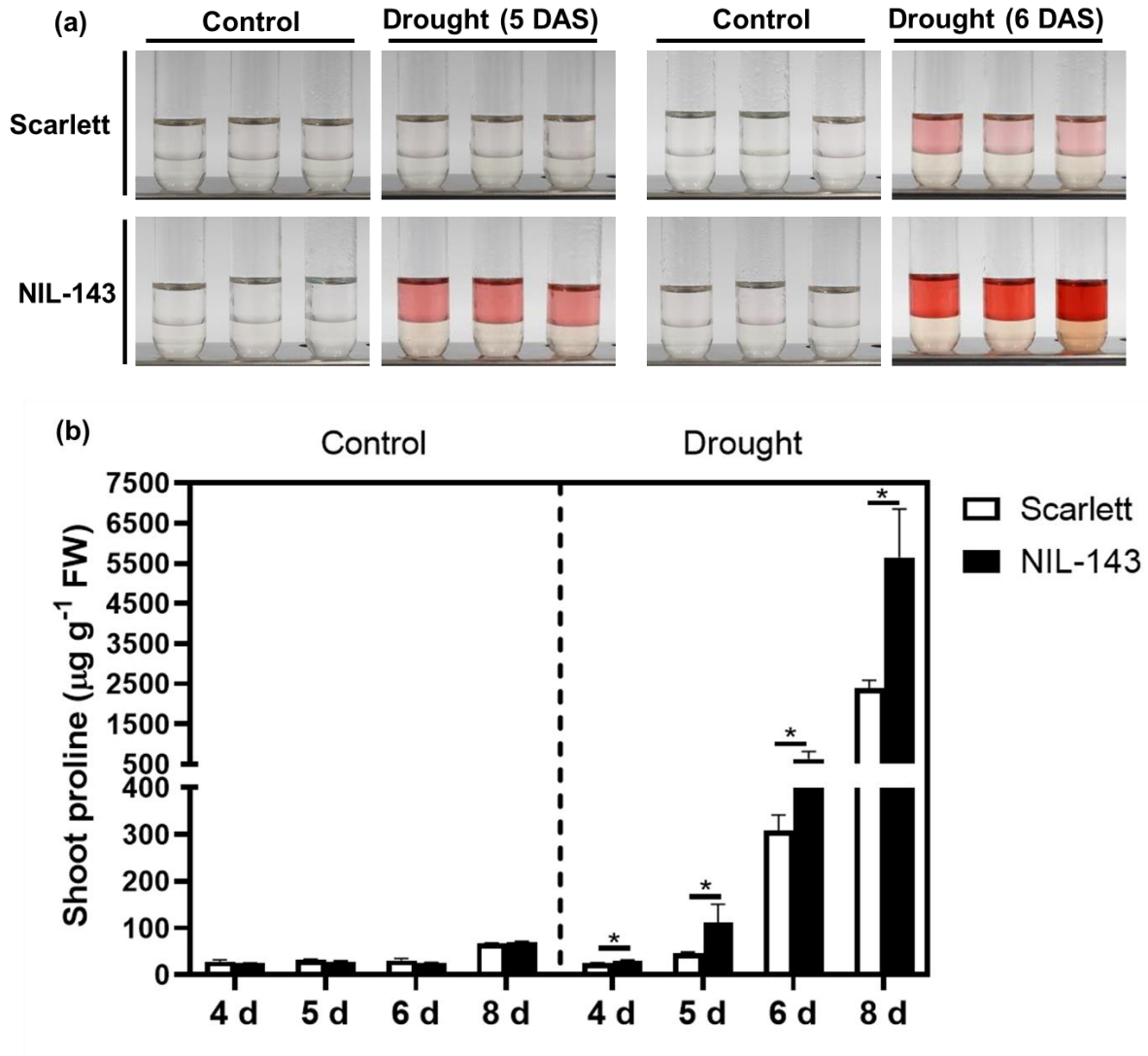

Figure 2.3. Proline accumulation in Scarlett and NIL-143 at the seedling stage in response to drought stress. Drought treatment was applied to two-week-old seedlings by terminating the water supply. Sampling was done at 4, 5, 6 and 8 d after drought stress before proline measurement. (a) Chromatophore indicating a free proline reaction product with ninhydrin. Darker color indicates a higher concentration of proline. (b) Shoot proline concentration under control and drought conditions. The graph represents the mean ± SE (n = 5). Asterisks indicate significant differences between genotypes (*$P \leq 0.05$) using a student's *t*-test. FW, fresh weight

2.3.4. Evaluation of adaptive traits at seedling stage under drought

2.3.4.1. NIL-143 seedling maintains superior membrane stability under drought

To gain insight into the effect of *QPro.S42-1H* into physiological adjustment to the water stress, we measured tissue hydration status and membrane stability. First, we estimated the extent of membrane damage by observing EL at different stages of water stress. EL measurement is based on the hypothesis that the flow of ions from the leaf section immersed in water will be proportional to the damage of the cell membrane. There was a significant treatment effect after 6 d of stress (Table S2). The EL rose by around 1.2 and 2-fold higher in Scarlett than NIL-143 at 6 d and 8 d after drought stress, respectively (Figure 2.4a). Likewise, we observed a significant effect of drought treatment on tissue water status expressed as RWC of leaf tissues. However, we did not observe substantial differences in the tissue hydration between Scarlett and NIL-143. RWC significantly reduced in both lines after 6 d of water stress, and it was marginally (10%) diminished in Scarlett compared to NIL-143 in stressed plants (Figure 2.4b). We also evaluated the extent of oxidative damage through MDA concentration in the shoots. Higher MDA concentration indicates increased lipid peroxidation caused by the overproduction of ROS (Hodges *et al.*, 1999). The shoot MDA content also followed a comparable trend to RWC, and MDA levels were marginally elevated in Scarlett compared to NIL-143 (Figure 2.4c). NIL-143 and Scarlett did not differ for EL, RWC, and MDA concentration under well-watered conditions (Figure 2.4). Overall, compared to Scarlett, NIL-143 displayed improved membrane stability under stress conditions.

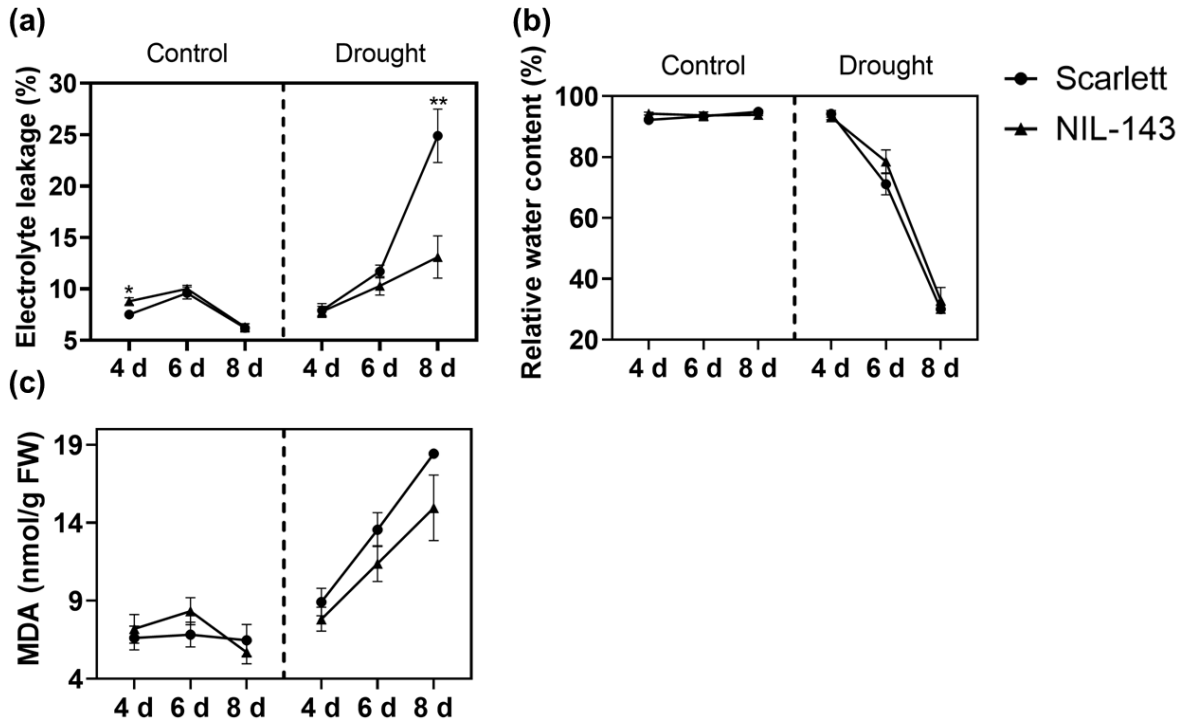

Figure 2.4. Physiological responses of Scarlett and NIL-143 to drought stress at the seedling stage. Effect of drought on (a) Electrolyte leakage, (b) Relative water content, and (c) Malondialdehyde (MDA) concentration. Drought treatment was applied to two-week-old seedlings by terminating the water supply. Sampling was done at 4, 6 and 8 d after drought stress to analyze the biochemical and physiological response of plants to drought stress. Bar indicates mean ± SE (n = 5). Asterisks indicate significant differences between genotypes (*$P \leq 0.05$, **$P \leq 0.01$) using student's *t*-test. FW, fresh weight

2.3.4.2. NIL-143 sustain stay-green character under drought stress

VI is widely used for phenotyping plants grown under drought stress. We employed handheld spectrometric devices like SPAD and PolyPen to score several VIs. At the seedling stage, we observed a significant decrease in SPAD values in plants exposed to drought stress compared to plants under control conditions (Table S2). Markedly, NIL-143 displayed significantly higher SPAD readings compared to Scarlett at 6 and 8 d after drought stress (Figure 2.5a). We also observed a reducing trend for VIs scored using PolyPen. Normalized differences vegetation index (NDVI) and simple ratio index (SR) are comparable indexes to SPAD; hence, the response of NIL-143 and Scarlett to NDVI and SR was identical to SPAD readings (Figure S4). Likewise, other VIs such as structure intensive pigment index (SIPI), Lichtenthaler index 1 (Lic1), and structure intensive pigment index (SIPI) showed a significant treatment effect, and the values decreased in plants grown under drought condition (Table S2). Notably, NIL-143 did not reveal treatment difference for SIPI and Lic1 until 6 d after drought stress, while SIPI and Lic1 continually decreased in Scarlett plants under water stress compared to control

conditions. We observe the most pronounced differences between NIL-143 and Scarlett for SIPI and Lic1 at 8 d after drought stress compared to other VIs (Figure 2.5b and c). Carter index 2 (Ctr2) revealed a different trend as the values increased in plants grown under drought stress compared to well-watered plants (Table S2). Ctr2 readings were significantly higher in Scarlett at 6 and 8 d after stress compared to NIL-143 (Figure 2.5d). In sum, NIL-143 maintained superior VIs compared to Scarlett, indicating reduced chlorophyll damage under water stress conditions.

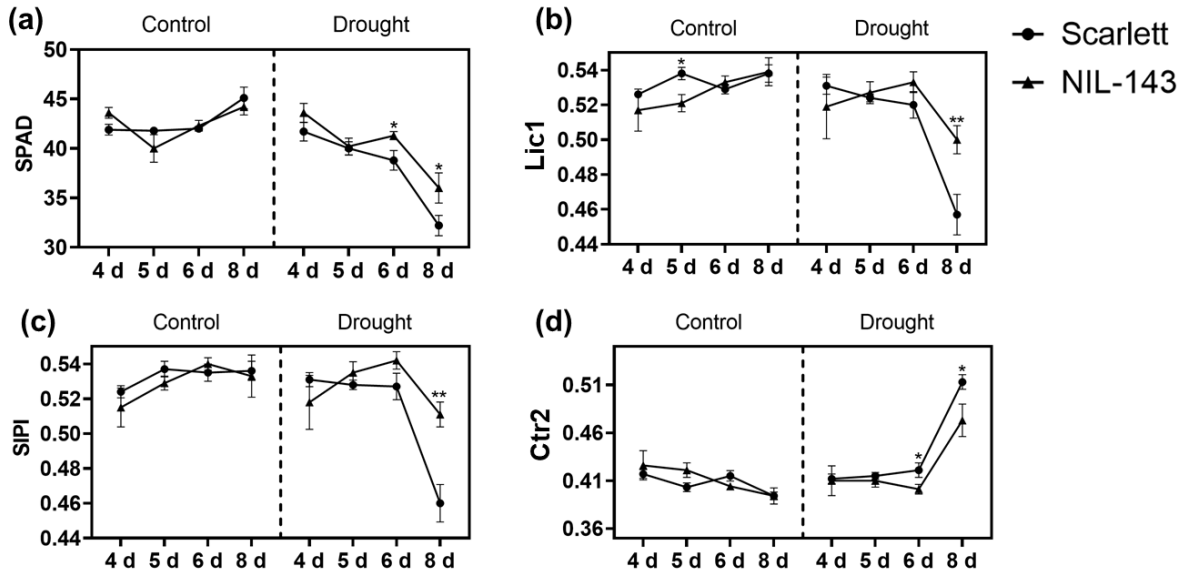

Figure 2.5. Vegetation index of Scarlett and NIL-143 under drought stress at the seedling stage. Effect of water stress on (a) soil plant analysis development (SPAD) chlorophyll meter value, (b) Lichtenthaler index 1 (Lic1), (c) structure intensive pigment index (SIPI), and (d) Carter index 2 (Ctr2). Drought treatment was applied to two-week-old seedlings by terminating the water supply. Vegetation indexes were scored at 4, 5, 6 and 8 d after drought stress using SPAD meter and PolyPen. The graph indicates mean ± SE (n = 5). Asterisks indicate significant differences between genotypes (*$P \leq 0.05$, **$P \leq 0.01$) using student's *t*-test.

2.3.4.3. NIL-143 retain superior photosynthetic health under drought stress

The protective role of proline might be essential to secure the photosynthetic machinery during stress conditions. Therefore, we checked the photosynthetic health of NIL-143 and Scarlett at different stages of drought to learn the potential benefit of *QPro.S42-1H*. First, we measured the Y(II) to learn the plant stress status under light-dependent steady-state photosynthesis. Y(II) is proportional to the CO_2 assimilation rate, and higher values indicate better photosynthesis efficiency (Genty *et al.*, 1989). A sharp decline in Y(II) was noticed in stressed plants in comparison to plants under the control conditions (Table S2). However, the light-adapted quantum photochemical quenching by photosystem II was more effective in NIL-143

under water stress compared to Scarlett (Figure 2.6a). Besides, an infrared gas exchange analyzer was used to estimate the CO_2 uptake (*A*), intracellular CO_2 concentration (C_i), stomatal conductance (g_s), and transpiration rate (*E*). A/C_i response curve was used to estimate V_{cmax} and J_{max}, according to Sharkey *et al.* (2007). The photosynthetic parameters revealed a declining trend under stress conditions (Table S2). Nevertheless, NIL-143 maintained a better photosynthesis rate and stomatal conductance than Scarlett under stress conditions (Figure 2.6b and Figure S5b). Also, the transpiration rate was higher in the stressed plants of NIL-143 than Scarlett (Figure S5a). In addition, CO_2 fixation by rubisco in NIL-143 was superior to Scarlett under water stress (Figure 2.6c). Likewise, the ribulose biphosphate regeneration was diminished in Scarlett compared to NIL-143 at 9 d after stress (Figure 2.6d). We did not detect genotypic differences for photosynthetic traits under control conditions (Figure 2.6 and Figure S5). To summarize, the introgression of *QPro.S42-1H* in NIL-143 was advantageous to maintain a superior photosynthesis rate under water-limited conditions.

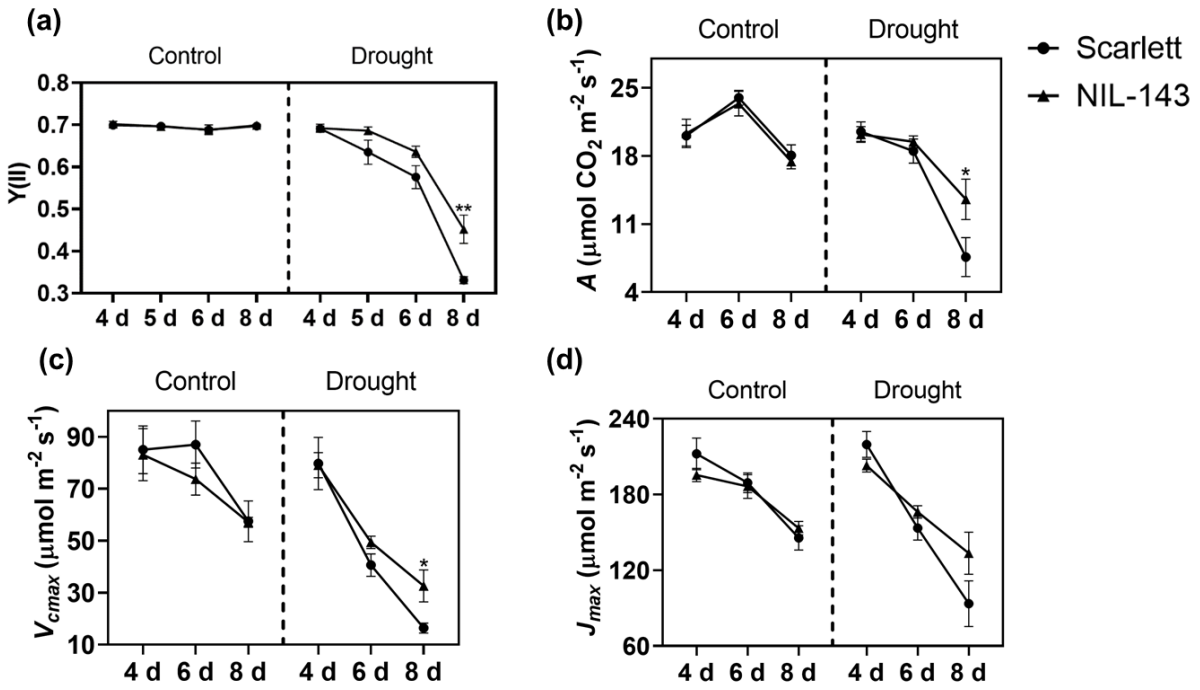

Figure 2.6. Photosynthetic traits in Scarlett and NIL-143 under drought stress at the seedling stage. Effect of water stress on (a) effective quantum yield of photosystem II (Y(II), (b) rate of CO_2 assimilation (*A*), (c) maximum carboxylation rate of rubisco (V_{cmax}), and (d) maximum rate of electron transport (J_{max}). Drought treatment was applied to two-week-old seedlings by terminating the water supply. Photosynthesis related traits were evaluated at 4, 5, 6 and 8 d after drought stress using MiniPam and gas exchange analyzer by LI-COR. The graph indicates mean ± SE (n = 5). Asterisks indicate significant differences between genotypes (**P* ≤ 0.05, ***P* ≤ 0.01) using student's *t*-test.

2.3.5. NIL-143 displayed better stress recovery

In addition to stress adaptation, proline is also known to play a critical role in the stress recovery process. To understand the role of *QPro.S42-1H* on the readjustment of plant growth after stress, we performed recovery experiments in the greenhouse. Two-week-old seedlings grown in pots were dehydrated for 12 d and rewatered to observe the recovery process. Notably, the images recorded 7 d after rewatering indicated that the recovery rate was superior qualitatively and quantitatively in NIL-143 compared to Scarlett (Figure 2.7a and b). We also scored the number of seedlings that rejuvenated successfully after the stress. We detected that only one-third of Scarlett seedlings recovered while, on average, 60% seedlings of NIL-143 recovered after rehydration (Figure 2.7c). Although pot effect was not statistically significant, to rule out the probable environmental effect, we repeated the experiment by growing NIL-143 and Scarlett in single pots. The recovery rate followed a comparable trend in the single pot experiment (Figure S6). Collectively, the introgression of *QPro.S42-1H* in Scarlett demonstrated remarkable improvement in stress recovery.

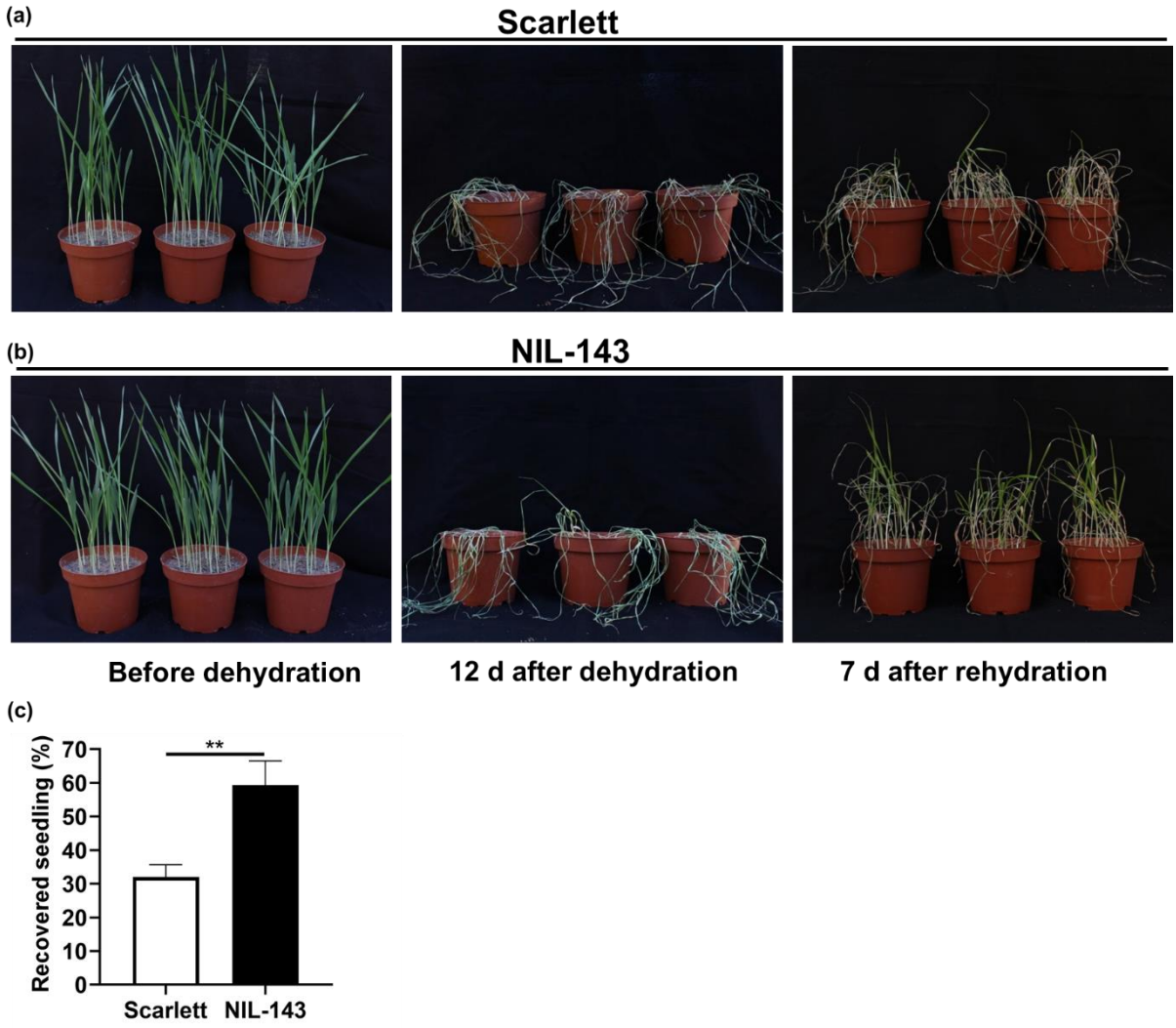

Figure 2.7. Stress recovery in Scarlett and NIL-143 at the seedling stage. Image of representative pots of (a) Scarlett and (b) NIL-143 before the start of dehydration and after rehydration. Fifteen seedlings were grown in a pot for 14 d at 75% field capacity. Two-week-old seedlings were subjected to dehydration stress by withholding the water supply for 12 d. The images were taken 7 d after rewatering using Canon 750D. (c) The percentage of recovered seedlings was determined by counting the number of rejuvenated plants. Scoring was done 14 d after rewatering. The experiment was repeated twice in five biological replicates. The graph represents mean ± SE (n = 10). Asterisks indicate significant differences between genotypes (**$P \leq 0.01$) using student's *t*-test.

2.3.6. NIL-143 displayed superior drought stress adaptation under field conditions

We found that *QPro.S42-1H* plays a significant role in drought adaptation in the seedling stage. However, the experiments were performed in controlled conditions inside automated climate chambers. To investigate the role of *QPro.S42-1H* of drought adaptation in field conditions, we executed a row experiment inside a rainout shelter in the field. We maintained two blocks inside the rainout shelter, and drought stress was induced in one block before heading stage (BBCH 41), and the stress period terminated after 21 d. One block was established outside the rainout shelter to mimic the rainfed system. We scored photosynthetic rate and VI at 7 d intervals during the drought stress. A significant treatment effect was observed in photosynthetic health of the plants under stress expressed as Y(II). The light-dependent photochemical quenching was superior in NIL-143 compared to Scarlett 21 d after drought stress (Figure 2.8a). Similar to seedling stage plants, the VIs measured using SPAD and PolyPen diminished in plants grown under stress conditions compared to irrigated plants (Table S3). Yet, NIL-143 displayed superior VIs under field drought conditions compared to Scarlett (Figure 2.8 and Figure S7). Also, the values for the photochemical reflectance index (PRI), which is an indicator of photosynthetic radiation use efficiency, was better in NIL143 than Scarlett at 21 d after stress (Figure S7e). Consistent with the seedling stage, Carter indexes increased in stressed plants, and Ctr2 values were significantly higher in Scarlett at 21 d after drought stress compared to NIL-143 (Figure 2.8f).

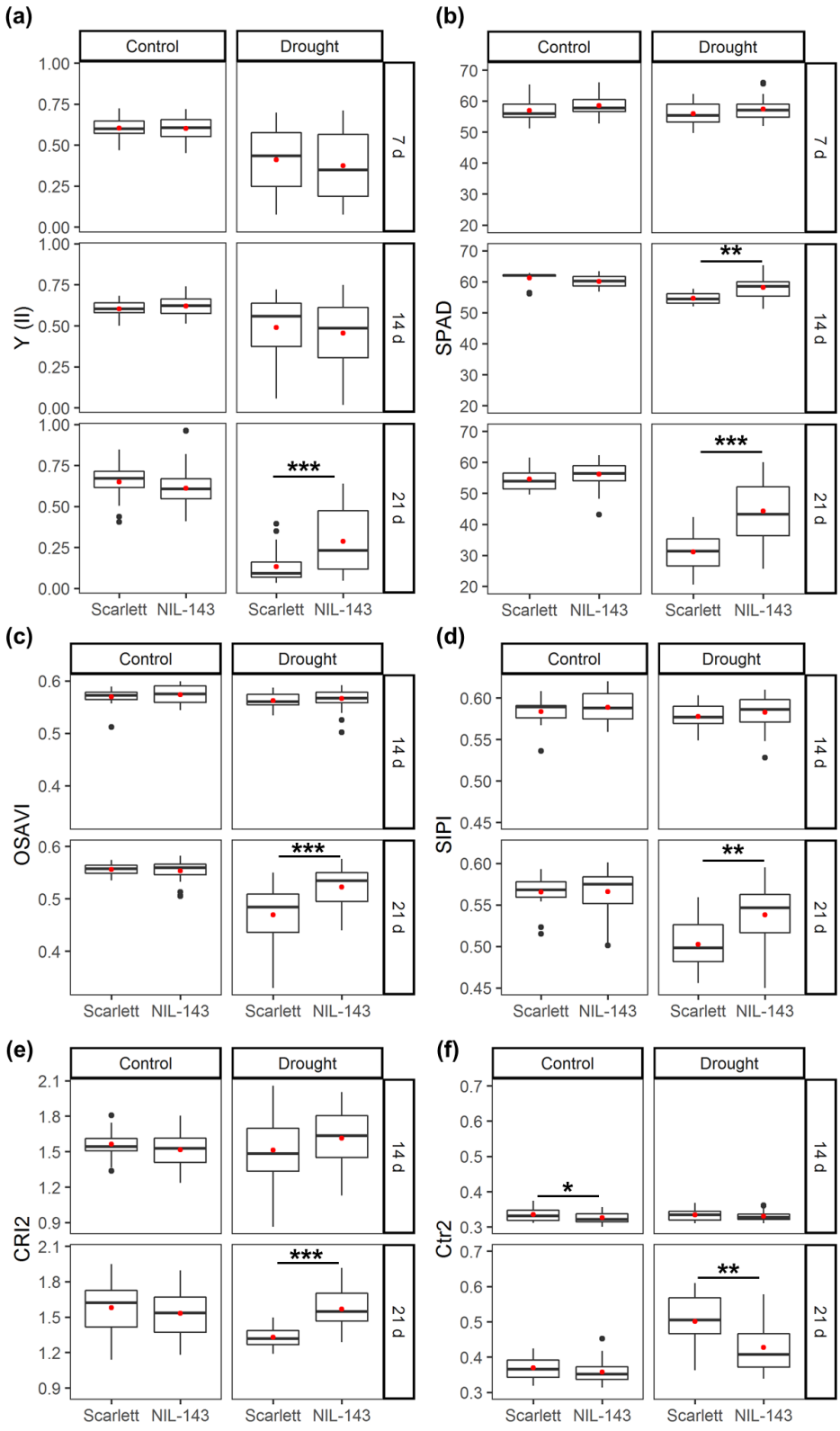

Figure 2.8. Vegetation index and photosynthetic parameters of Scarlett and NIL-143 in field conditions. Effect of drought stress on (a) effective quantum yield of photosystem II (Y(II)) (b) soil plant analysis development (SPAD) chlorophyll meter value (c) optimized soil-adjusted vegetation index (OSAVI) (d) structure intensive pigment index (SIPI) (e) carotenoid reflectance index 2 (CRI2) and (f) Carter index

2 (Ctr2). Scarlett and NIL-143 were grown in 40 cm rows inside a rainout shelter. One plot was regularly irrigated, while drought stress was applied to another plot for 21 d at the heading stage (BBCH 41). Vegetation indexes and photosynthetic traits were scored at 7, 14 and 21 d after stress. The red dot indicates the mean of the distribution. Asterisks indicate significant differences between genotypes (*$P \leq 0.05$, **$P \leq 0.01$, ***$P \leq 0.001$) using student's *t*-test (n = 19 to 45).

To learn the contribution of *QPro.S42-1H* on the yield-related performance under stress conditions, we evaluated several yield attributes under control, drought, and rainfed conditions. Biomass traits such as tiller number and weight of straw per plant decreased under drought conditions in both Scarlett and NIL-143 (Figure 2.9a and f). Similarly, reproductive traits such as ear number, grain weight, 1000 kernel weight were significantly lower in stressed plants than plants in irrigated plots (Figure 2.9b-d). However, NIL-143 showed superior performance for yield-related traits, including grain number per ear, grain size, and grain weight per plant. Notably, in comparison to Scarlett, grain weight per plant, grain number per ear, and grain size was 35%, 18%, and 7% greater in NIL-143, respectively (Figure 2.9b-d). Also, the harvest index increased in NIL-143 compared to Scarlett under drought conditions (Figure 2.9g). Although the majority of yield-related traits were diminished under stress conditions, the grain number per ear and harvest index did not differ between the treatments (Figure 2.9c and g). Besides, biomass and yield attributing traits did not differ between plants grown under irrigated plots and rainfed conditions in the open field. Likewise, the reproductive traits did not differ between Scarlett and NIL-143 under irrigated and rainfed conditions (Figure S8 and Table S4). The yield data indicated that *QPro.S42-1H* impart a positive effect on the reproductive performance under stress environment.

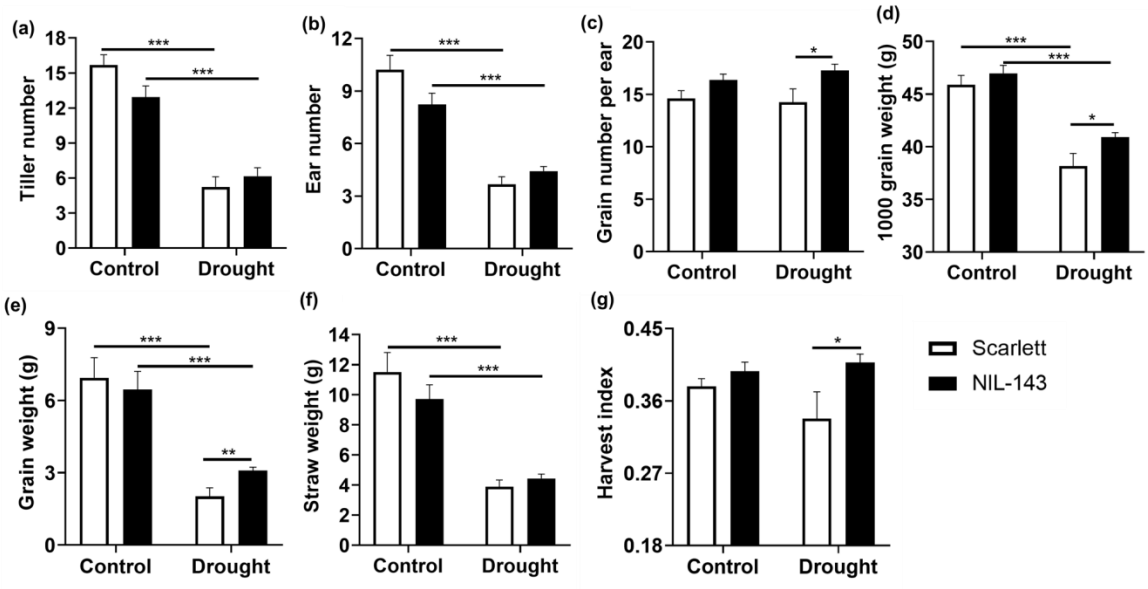

Figure 2.9. Yield and related traits of Scarlett and NIL-143 under field conditions. Effect of drought stress on (a) tiller number, (b) ear number per plant, (c) grain number per ear, (d) 1000-kernel weight, (e) grain weight per plant (f) straw weight per plant, and (g) harvest index. Scarlett and NIL-143 were grown in 40 cm rows inside a rainout shelter and open field. Inside rainout shelter, one plot was regularly irrigated, while drought stress was applied to another plot for 21 d at the heading stage (BBCH 41). Matured panicles and straw were harvested, and oven-dried at 37°C for 72 h. The experiment was performed at Campus Kleinaltendorf, Rheinbach, Germany. The graph represents the mean ± SE (n = 10). Asterisks indicate significant differences between genotypes (*$P \leq 0.05$, **$P \leq 0.01$, ***$P \leq 0.001$) using a student's *t*-test.

2.4. Discussion

The aim of the study was to characterize the previously identified *HvP5cs1* locus. Positional cloning of *QPro.S42-1H* identified allelic variation between ISR42-8 and Scarlett at *HvP5cs1* locus that controlled proline accumulation and *HvP5cs1* expression in barley. The allelic variation was found across the ABRE motif in the *HvP5cs1* promoter. ABREs are present in stress-inducible gens, and ABFs bind to ABREs to regulate ABA-responsive gene expression (Choi *et al*., 2000; Uno *et al*., 2000). The ABF gene family is expressed in vegetative tissues in response to ABA and osmotic stress in Arabidopsis, suggesting a fundamental role in ABA-mediated drought stress tolerance (Fujita *et al.*, 2013). Shen *et al*. (1996) showed in a transient assay that the truncated promoter of HVA1 comprised of ABREs or the combination of an ABRE with one of several non-ACGT ABREs (CE1 and CE3) across the promoter region successfully induced the expression of reporter gene upon ABA treatment. TRAB1 (ABRE binding bZIP protein of rice displayed strong binding affinity to CE3 in electrophoretic mobility shift assay, indicating CE3 might be functionally equivalent to ABRE with ACGT as core sequence (Hobo *et al.,* 1999). These researchers also claimed that a single copy of an ABRE was insufficient to activate ABA-responsive genes. First, we performed allele mining through sequence analysis of *HvP5cs1* promoter in barley diversity panel to identify novel *cis*-acting elements. Allele mining identified barley genotype such as HOR9840, with loss of multiple *cis*-acting elements (ABRE, CE3, and MYB binding motifs). Shoot proline accumulation, and *HvP5cs1* expression was lowest in HOR9840, further confirming the value of ABRE and MYB binding factors in *HvP5cs1* activation. The result is in line with the well-established notion that cooperative action of multiple transcription factors is necessary for transactivation of response genes (Biłas et al., 2016). Next, we used a transient system (Arabidopsis protoplast) to express the GUS reporter gene fused to ISR42-8 and Scarlett promoter under ABA induction. The GUS expression was significantly upregulated when fused with ISR42-8 promoter (pISR::eGFP-GUS) compared to Scarlett (pSCA::eGFP-GUS) in ABA treated protoplasts. To test if Arabidopsis ABFs regulate the pISR::eGFP-GUS under ABA, we transfected pISR::eGFP-GUS in the protoplast of Col-0 and the *abf1 abf2 abf3 abf4* quadruple mutant. Notably, GUS activity was strongly impaired in and the *abf1 abf2 abf3 abf4* compared to Col-0. Transient expression assays indicated that the *HvP5cs*1 promoter might be regulated in ABF dependent manner. Although ABF regulates a plethora of ABA-inducible genes (Yoshida *et al*., 2015), our result showed for the first time that ABF might regulate *P5CS1* transcription.

Another major objective of this work was to dissect the significance of drought-inducible QTL, *QPro.S42-1H,* for drought stress adaptation in barley. Drought stress is one of the most critical environmental stresses affecting the modern agriculture system. Plants respond to water

stress at a morphological, physiological, and molecular level (Cattivelli *et al.*, 2008). In this study, we investigated the role of genetic loci linked to enhanced proline accumulation on physiological adaptation and yield sustainability traits under stress conditions. We detected a drought-inducible QTL (*QPro.S42-1H*) from wild barley ISR42-8, which regulates proline biosynthesis under drought conditions in cultivated background. A NIL-143 was developed where *QPro.S42-1H* was introgressed in the Scarlett background. NIL-143 and Scarlett were screened under different growing environment (climate chamber and field conditions) and growth stages (seedling and reproductive) for adaptive response against water-limited conditions.

Physiological processes like photosynthesis, degradation of chlorophyll pigment, oxidative stress, and membrane damage are often associated with drought stress (Shinozaki and Yamaguchi, 1997). Here we measured several physiological parameters such as leaf water status, photosynthetic health of plants, chlorophyll reflectance, and membrane stability. First, we measured the ability of NIL-143 to accumulate proline under drought stress conditions. Fine mapping of *QPro.S42-1H* revealed a *P5cs1* allele that controlled proline accumulation in barley (Muzammil *et al.*, 2018). As expected, the proline level in the shoot of NIL-143 was consistently higher compared to Scarlett under different stages of stress treatment. Then, we examined if the proline accumulation phenotype correlates with the stress adaptation at vegetative and reproductive stages. Proline is one of the critical compatible solutes which impart osmotic adjustment in osmotically stressed cells in a wide range of species, including prokaryotes and eukaryotes (Kishor *et al.*, 2005; Miller *et al.*, 1991; Graham and Wilkinson, 1992; Amin *et al.*, 1995; Sawahel and Hassan, 2002). It can also act as a molecular chaperon and protect the macromolecules in dehydrating cells (Rajendrakumar *et al.*, 1994; Chattopadhyay *et al.*, 2004). We observed that NIL-143 maintained superior membrane integrity compared to Scarlett under drought stress measured as EL. Also, the MDA levels were partially low in NIL-143 at severe drought stress compared to Scarlett. Although NIL-143 maintained a higher transpiration rate, the RWC did not differ between NIL-143 and Scarlett. These results are supported by the observation of Bandurska, (2000), where he found that high proline accumulating barley accession revealed greater membrane stability under osmotic stress. As we did not observe greater differences in RWC, the membrane integrity might be due to the protection of membrane proteins phospholipid layer (Hare *et al.*, 1998; Rudolph *et al.*, 1986; Szabados and Savouré, 2010). It can also be attributed to the role of proline in ROS scavenging directly by non-enzymatic ROS detoxification or through the activation of the antioxidant pathway (Alia and Matysik, 2001; Signorelli *et al.*, 2014; Signorelli *et al.*, 2015). Collectively, these observations indicated that the introgression of *QPro.S42-1H*

in cultivated barley improved its physiological and biochemical adaptive response to drought stress.

Water stress damages the photosynthetic pigments such as chlorophyll, and the rate of photosynthesis and plant growth is compromised (Yordanov *et al.*, 2000). Non-destructive measurement of VIs, which is proportional to chlorophyll content, is widely used to determine plant health under stress conditions (Maire *et al.*, 2004). SPAD and NDVI are the most commonly used VIs to interpret the chlorophyll content of the leaves. These VIs are derived from the ratio of transmittance of infrared to red (maximum chlorophyll absorption range) light through the leaf surface (Uddling *et al.*, 2007; Main *et al.*, 2011). We found a significant treatment interaction effect for these traits at seedling as well as at the reproductive stage. SPAD and NDVI values indicated that Scarlett incurred more significant damage to chlorophyll pigments than NIL-143 under stress conditions. Other comparable indexes like SR and RDVI also showed similar responses to drought. In addition, an optimized soil-adjusted vegetation index (OSAVI), which corrects the soil background (Rondeaux *et al.*, 1996), also showed a comparable pattern to SPAD and NDVI. Besides, we also analyzed other VIs based on the ratio of the narrow spectral range such as Lic1, Ctr, SIPI, Gitelson and Merzlyak index 2 (GM2), simple ratio pigment index (SPRI), and Zarco-Tejada and Miller index (ZMI). Except for Ctr, all other indexes showed a decreasing trend under drought, and NIL-143 recorded VIs compared with Scarlett under stress conditions. However, Ctr indexes (Ctr1 and Ctr2) increased with water stress, and Scarlett plants under stress displayed the highest Ctr values. These results are in agreement with Carter (1994), who showed that the increased value of Ctr indexes reflects plant stress. Also, the degradation of another photosynthetic pigment carotenoid in Scarlett surpassed NIL-143 under stress conditions, as indicated by CTR2. The slow and reduced degradation of photosynthetic pigment is supported by previous studies where proline accumulation was associated with decreased chlorophyll damage in different plant species (Hayat *et al.*, 2012). Gadallah (1999) showed that the external application of proline and glycine betaine enhanced cell membrane stability, and chlorophyll content in salt-stressed bean plants. Knock-out mutant *p5cs1* in Arabidopsis showed considerable oxidative damage and chlorophyll degradation compared to wild type (Székely *et al.*, 2008). Likewise, Fedina *et al.* (2003) showed that increased proline accumulation in barley seedling exposed to ultraviolet radiation might prevent chlorophyll degradation. Likewise, Hassine *et al*. (2008) reported a positive correlation between photosynthesis rate and proline accumulation in *Atriplex halimus* under osmotic stress. The reduced damage of chlorophyll in NIL-143 can be linked to the previous findings that predominantly P5CS1 activity was localized to chloroplast (Székely *et al.*, 2008), and around one-fifth of P5CR activity was detected in the chloroplast (Szoke *et al.*, 1992). Next, we measured the photosynthetic traits to estimate the effect of

drought stress on active photosynthesis. Gas exchange parameters such as *A*, g_s, and *E* were evaluated. NIL-143 maintained better *E* and *A* under stress conditions than Scarlett. Long and Bernacchi (2003) and Sharkey *et al.* (2007) described that A/C_i response curve could be used to derive additional photosynthetic processes, including V_{cmax} and J_{max}. Although V_{cmax} and J_{max} reduced substantially in drought-stressed plants compared to control conditions, NIL-143 revealed superior V_{cmax} and J_{max} than Scarlett under stress conditions. Genty *et al.* (1989) described that Y(II) is proportional to the CO_2 assimilation rate, and the Y(II) scores can be used to access plant stress (Yuan *et al.*, 2016). The light-adapted quantum photochemical quenching by photosystem II measure as Y(II) was more effective in NIL-143 under water stress compared to Scarlett. Higher photosynthesis rate in NIL-143 might be explained by the previous finding, where proline reduced the damage of the thylakoid membrane by scavenging ROS generated in photosystem II (Alia and Mohanty, 1997). Also, proline biosynthesis is a reductive process, and both P5CS1 and P5CR require NADPH that regenerate $NADP^+$. The upregulation of proline biosynthesis pathway under drought might contribute to maintaining $NADP^+$ pool to sustain photosynthesis under stress conditions (Szabados and Savouré, 2010; de Ronde *et al.*, 2004; Kishor *et al.*, 2005; Hare and Cress, 1997). In conclusion, the VI and photosynthesis data suggested that high proline accumulating NIL-143 was able to protect the photosynthetic apparatus, thus sustained active photosynthesis under drought stress than Scarlett.

In addition to the protective function, proline catabolism potentially contributes to the stress recovery process (Szabados and Savouré, 2010). The degradation of proline after stress release also presents numerous functions, including cellular signaling and stress recovery (Kishor and Sreenivasulu, 2014). The oxidation of proline to glutamate is also a two-step reaction that uses FAD as an electron acceptor. FAD is reduced to $FADH_2$, which enters the electron transport chain, thereby producing ATP molecule), which provides much-needed energy for growth resumption (Hare *et al.*, 1998; Szabados and Savouré, 2010). Therefore, the oxidation of proline to glutamate generates ATP molecules, which provides much-needed energy for growth resumption (Hare and Cress, 1997; Hare *et al.*, 1998). Blum and Ebercon (1976) showed that proline accumulation during drought stress in sorghum was proportional to stress recovery rate and dark respiration rate. Similarly, Itai and Paleg (1982) reported a positive effect of external proline accumulation on the rate of stress recovery in barley. In our study, high proline accumulating NIL-143 showed enhanced stress recovery compared to Scarlett, which aligns with previous findings. Because NIL-143 surpassed Scarlett concerning stress adaptation as well as stress recovery, we evaluated the response of Scarlett and its isogenic line carrying *QPro.S42-1H* for yield-related traits in field conditions. The yield attributing traits such as grain numbers per ear, grain size, grain weight per plant, and harvest

index were enhanced in NIL-143 compared to Scarlett under drought conditions in the field. Blum (2017) reported that osmotic adjustment is one of the critical determinants of crop production under stress environments. González *et al.* (2008) also found a positive correlation between the osmotic adjustment capacity and grain yield in barley. Likewise, Blum *et al.* (1999) also reported a positive effect of osmotic adjustment towards grain yield and biomass production. Therefore, improved reproductive performance of NIL-143 might be related to the ability to accumulate proline at higher concentrations compared to Scarlett that potentially reinforce the adaptive response to stress and stress recovery in NIL-143.

The study illustrated that *HvP5cs1* promoter harbors *cis*-elements such as ABRE and related elements, MYB binding factors, NAC binding factors and DRE and promoter variation were detected, especially across ABRE and MYB-binding motifs. The promoter variation was connected to the differences in transcriptional activation of *HvP5cs1* and subsequent proline accumulation in barley. Furthermore, the study provides necessary evidence on the significance of *QPro.S42-1H* on drought adaptation in cultivated barley. We also showed that proline accumulation was enhanced in NIL-143 compared to Scarlett under drought conditions. As the significance of proline towards stress tolerance and recovery is well documented, the adaptive superiority of NIL-143 might also be linked to its proline phenotype. However, our study focused on the evaluation of adaptive response rather than examining the molecular dissection of proline mediated cellular and subcellular adjustments. Therefore, NIL-143 serves as an excellent genetic material to explore the mechanistic process of proline mediated osmoregulation, redox balance, photosynthetic adjustments and cellular signaling during the recovery process in crop.

2.5. References

Ábrahám, E., Hourton-cabassa, C., Erdei, L. and Szabados, L. (2010) Methods for determination of proline in plants. In R. Sunkar, ed. *Plant Stress Tolerance.* New York: Humana Press. pp. 333-340.

Alia, M.P. and Matysik, J. (2001) Effect of proline on the production of singlet oxygen. *Amino Acids*, **21**, 195–200.

Alia, S.P.P. and Mohanty, P. (1997) Involvement of proline in protecting thylakoid membranes against free radical-induced photodamage. *J. Photochem. Photobiol. B Biol*., **38**, 253–257.

Amin, U.S., Lash, T.D. and Wilkinson, B.J. (1995) Proline betaine is a highly effective osmoprotectant for *Staphylococcus aureus*. Arch. Microbiol., **163**, 138–142.

Ashraf, A., Rehman, O.U., Muzammil, S., Léon, J., Naz, A.A., Rasool, F., Ali, G.M., Zafar, Y. and Khan, M.R. (2019) Evolution of deeper rooting 1-like homoeologs in wheat entails the C-terminus mutations as well as gain and loss of auxin response elements. *PLoS One*, **14**.

Bajji, M., Kinet, J.M. and Lutts, S. (2002) The use of the electrolyte leakage method for assessing cell membrane stability as a water stress tolerance test in durum wheat. *Plant Growth Regul*., **36**, 61–70.

Bandurska, H. (2000) Does proline accumulated in leaves of water deficit stressed barley plants confine cell membrane injury? I. Free proline accumulation and membrane injury index in drought and osmotically stressed plants. *Acta Physiol. Plant*., **22**, 409–415.

Barnabás, B., Jäger, K. and Fehér, A. (2008) The effect of drought and heat stress on reproductive processes in cereals. *Plant, Cell Environ*., **31**, 11–38.

Bartels, D. and Sunkar, R. (2005) Drought and salt tolerance in plants. *CRC. Crit. Rev*. *Plant Sci*., **24**, 23–58.

Bates, L.S., Waldren, R.P. and Teare, I.D. (1973) Rapid determination of free proline for water-stress studies*. Plant Soil*, **39**, 205–207.

Biłas, R., Szafran, K., Hnatuszko-Konka, K. and Kononowicz, A.K. (2016) Cis-regulatory elements used to control gene expression in plants. *Plant Cell Tissue Organ Cult.*, **127**, 269–287.

Blum A and Ebercon A (1976) Genotypic responses in sorghum to drought stress. III. Free proline accumulation and drought resistance. *Crop Sci.,* **16**, 428–431

Blum, A. (2017) Osmotic adjustment is a prime drought stress adaptive engine in support of plant production. *Plant Cell Environ*., **40**, 4–10.

Blum, A., Zhang, J. and Nguyen, H.T. (1999) Consistent differences among wheat cultivars in osmotic adjustment and their relationship to plant production. *F. Crop. Res*., **64**, 287–291.

Carter, G.A. (1994) Ratios of leaf reflectances in narrow wavebands as indicators of plant stress. *Int. J. Remote Sens*., **15**, 517–520.

Cattivelli, L., Rizza, F., Badeck, F.W., Mazzucotelli, E., Mastrangelo, A.M., Francia, E., Marè, C., Tondelli, A. and Stanca, A.M. (2008) Drought tolerance improvement in crop plants: An integrated view from breeding to genomics. *F. Crop. Res.*, **105**, 1–14.

Chattopadhyay, M.K., Kern, R., Mistou, M.Y., Dandekar, A.M., Uratsu, S.L. and Richarme, G. (2004) The chemical chaperone proline relieves the thermosensitivity of a dnaK deletion mutant at 42°C. *J. Bacteriol*., **186**, 8149–8152.

Chaves, M. and Davies, B. (2010) Drought effects and water use efficiency: Improving crop production in dry environments. *Funct. Plant Biol*., **37**.

Deeba, F., Pandey, A.K., Ranjan, S., Mishra, A., Singh, R., Sharma, Y.K., Shirke, P.A. and Pandey, V. (2012) Physiological and proteomic responses of cotton (*Gossypium herbaceum* L.) to drought stress. *Plant Physiol. Biochem*., **53**, 6–18.

de Ronde, J.A., Cress, W.A., Krüger, G.H.J., Strasser, R.J. and Staden, J. Van (2004) Photosynthetic response of transgenic soybean plants, containing an Arabidopsis P5CR gene, during heat and drought stress. *J. Plant Physiol.,* **161**, 1211–1224.

Dhanyalakshmi, K.H., Mounashree, D.C., Vidyashree, D.N., Earanna, N. and Nataraja, K.N. (2019) Options and opportunities for manipulation of drought traits using endophytes in crops. *Plant Physiol*. *Reports*, **24**, 555–562.

Dziwornu, A.K., Shrestha, A., Matthus, E., Ali, B., Wu, L.-B. and Frei, M. (2018) Responses of contrasting rice genotypes to excess manganese and their implications for lignin synthesis. *Plant Physiol. Biochem*., **123**, 252–259.

Fedina, I.S., Grigorova, I.D. and Georgieva, K.M. (2003) Response of barley seedlings to UV-B radiation as affected by NaCl. *J. Plant Physiol*., **160**, 205–208.

Fujita, Y., Yoshida, T. and Yamaguchi-Shinozaki, K. (2013) Pivotal role of the AREB/ABF-SnRK2 pathway in ABRE-mediated transcription in response to osmotic stress in plants. *Physiol. Plant*., **147**, 15–27.

Gadallah, M.A.A. (1999) Effects of proline and glycinebetaine on *Vicia faba* responses to salt stress. *Biol. Plant.,* **42**, 249–257.

Genty, B., Briantais, J.-M. and Baker, N.R. (1989) The relationship between the quantum yield of photosynthetic electron transport and quenching of chlorophyll fluorescence. *Biochim. Biophys. Acta - Gen. Subj*., **990**, 87–92.

Ghoulam, C., Foursy, A. and Fares, K. (2002) Effects of salt stress on growth, inorganic ions and proline accumulation in relation to osmotic adjustment in five sugar beet cultivars. *Environ. Exp. Bot*., **47**, 39–50.

González, A., Martín, I. and Ayerbe, L. (2008) Yield and osmotic adjustment capacity of barley under terminal water-stress conditions. *J. Agron. Crop Sci.,* **194**, 81–91.

Graham, J.E. and Wilkinson, B.J. (1992) *Staphylococcus aureus* osmoregulation: Roles for choline, glycine betaine, proline, and taurine. *J. Bacteriol*., 174, 2711–2716.

Hare, P.D. and Cress, W.A. (1997) Metabolic implications of stress-induced proline accumulation in plants. *Plant Growth Regul*., **21**, 79–102.

Hare, P.D., Cress, W.A. and Staden, J. Van (1998) Dissecting the roles of osmolyte accumulation during stress. *Plant, Cell Environ*., **21**, 535–553.

Hassine, A. Ben, Ghanem, M.E., Bouzid, S. and Lutts, S. (2008) An inland and a coastal population of the Mediterranean xero-halophyte species *Atriplex halimus* L. differ in their ability to accumulate proline and glycinebetaine in response to salinity and water stress. *J. Exp. Bot*., **59**, 1315–1326.

Hayat, S., Hayat, Q., Alyemeni, M.N., Wani, A.S., Pichtel, J. and Ahmad, A. (2012) Role of proline under changing environments: A review. Plant Signal. Behav., **7**.

Hochberg, U., Degu, A., Toubiana, D., Gendler, T., Nikoloski, Z., Rachmilevitch, S. and Fait, A. (2013) Metabolite profiling and network analysis reveal coordinated changes in grapevine water stress response. *BMC Plant Biol*., **13**.

Hobo, T., Asada, M., Kowyama, Y. and Hattori, T. (1999) ACGT-containing abscisic acid response element (ABRE) and coupling element 3 (CE3) are functionally equivalent. *Plant J.*, **19**, 679–689.

Hodges, D.M., DeLong, J.M., Forney, C.F. and Prange, R.K. (1999) Improving the thiobarbituric acid-reactive-substances assay for estimating lipid peroxidation in plant tissues containing anthocyanin and other interfering compounds. *Planta*, **207**, 604–611.

Itai, C. and Paleg, L.G. (1982) Responses of water-stressed *Hordeum distichum* L. and *Cucumis sativus* to proline and betaine. *Plant Sci. Lett*., **25**, 329–335.

Kim, W., Iizumi, T. and Nishimori, M. (2019) Global patterns of crop production losses associated with droughts from 1983 to 2009. *J. Appl. Meteorol. Climatol*., **58**, 1233–1244.

Kishor, P.B.K., Sangam, S., Amrutha, R.N., *et al*. (2005) Regulation of proline biosynthesis, degradation, uptake and transport in higher plants: Its implications in plant growth and abiotic stress tolerance. *Curr. Sci*., **88**, 424–438.

Kishor, P.B.K. and Sreenivasulu, N. (2014) Is proline accumulation per se correlated with stress tolerance or is proline homeostasis a more critical issue? *Plant, Cell Environ.*, **37**, 300–311.

Laxa, M., Liebthal, M., Telman, W., Chibani, K. and Dietz, K.J. (2019) The role of the plant antioxidant system in drought tolerance. *Antioxidants*, **8**.

Li, Y., Ye, W., Wang, M. and Yan, X. (2009) Climate change and drought: a risk assessment of crop-yield impacts. *Clim. Res*., **39**, 31–46.

Lobell, D.B. and Field, C.B. (2007) Global scale climate-crop yield relationships and the impacts of recent warming. *Environ. Res. Lett*., 2.

Long, S.P. and Bernacchi, C.J. (2003) Gas exchange measurements, what can they tell us about the underlying limitations to photosynthesis? Procedures and sources of error. *J. Exp. Bot.,* **54**, 2393–2401.

Main, R., Cho, M.A., Mathieu, R., O'Kennedy, M.M., Ramoelo, A. and Koch, S. (2011) An investigation into robust spectral indices for leaf chlorophyll estimation. ISPRS J. Photogramm. *Remote Sens.*, **66**, 751–761.

Maire, G. L., François, C. and Dufrêne, E. (2004) Towards universal broad leaf chlorophyll indices using PROSPECT simulated database and hyperspectral reflectance measurements. *Remote Sens. Environ*., **89**, 1–28.

Mansour, M.M.F. (1998) Protection of plasma membrane of onion epidermal cells by glycinebetaine and proline against NaCl stress. *Plant Physiol. Biochem*., **36**, 767–772.

Miller, K.J., Zelt, S.C. and Bae, J.H. (1991) Glycine betaine and proline are the principal compatible solutes of *Staphylococcus aureus*. *Curr. Microbiol*., **23**, 131–137.

Mittler, R. (2002) Oxidative stress, antioxidants and stress tolerance. *Trends Plant Sci*., **7**, 405–410.

Livak K.J., Schmittgen T.D. (2001) Analysis of relative gene expression data using real-time quantitative PCR and the 2CT method. *Methods*, **25**: 402–408.

Muzammil, S., Shrestha, A., Dadshani, S., Pillen, K., Siddique, S., Léon, J. and Naz, A.A. (2018) An ancestral allele of pyrroline-5-carboxylate synthase1 promotes proline accumulation and drought adaptation in cultivated barley. *Plant Physiol*., **178**, 771–782.

Nounjan, N. and Theerakulpisut, P. (2012) Effects of exogenous proline and trehalose on physiological responses in rice seedlings during salt-stress and after recovery. *Plant, Soil Environ.,* **58**, 309–315.

Pfaffl, M.W. (2001) A new mathematical model for relative quantification in real-time RT-PCR. *Nucleic Acids Res*., **29**.

Rajendrakumar, C.S.V., Reddy, B.V.B. and Reddy, A.R. (1994) Proline-protein interactions: protection of structural and functional integrity of M4 lactate dehydrogenase. *Biochem. Biophys. Res. Commun*., **201**, 957–963.

Rondeaux, G., Steven, M. and Baret, F. (1996) Optimization of soil-adjusted vegetation indices. *Remote Sens. Environ*., **55**, 95–107.

Rudolph, A.S., Crowe, J.H. and Crowe, L.M. (1986) Effects of three stabilizing agents-proline, betaine, and trehalose on membrane phospholipids. *Arch. Biochem. Biophys.*, **245**, 134–143.

Sawahel, W.A. and Hassan, A.H. (2002) Generation of transgenic wheat plants producing high levels of the osmoprotectant proline*. Biotechnol. Lett*., **24**, 721–725.

Sharkey, T.D. (2016) What gas exchange data can tell us about photosynthesis. *Plant. Cell Environ*., **39**, 1161–1163.

Sharkey, T.D., Bernacchi, C.J., Farquhar, G.D. and Singsaas, E.L. (2007) Fitting photosynthetic carbon dioxide response curves for C3 leaves. *Plant, Cell Environ*., **30**, 1035–1040.

Sheffield, J. and Wood, E.F. (2008) Projected changes in drought occurrence under future global warming from multi-model, multi-scenario, IPCC AR4 simulations. *Clim. Dyn.*, **31**, 79–105.

Shen, Q., Zhang, P. and Ho, T.H.D. (1996) Modular nature of abscisic acid (ABA) response complexes: composite promoter units that are necessary and sufficient for ABA induction of gene expression in barley. *Plant Cell*, **8**, 1107–1 119.

Shinozaki, K. and Yamaguchi-Shinozaki, K. (1997) Gene expression and signal transduction in water-stress response. *Plant Physiol*., **115**, 327–334.

Shinozaki, K. and Yamaguchi-Shinozaki, K. (2006) Gene networks involved in drought stress response and tolerance. *J. Exp. Bot.,* **58**, 221–227

Signorelli, S., Coitiño, E.L., Borsani, O. and Monza, J. (2014) Molecular mechanisms for the reaction between •OH radicals and proline: Insights on the role as reactive oxygen species scavenger in plant stress. *J. Phys. Chem. B*, **118**, 37–47.

Signorelli, S., Dans, P.D., Coitiño, E.L., Borsani, O. and Monza, J. (2015) Connecting proline and γ-aminobutyric acid in stressed plants through non-enzymatic reactions. *PLoS One*, **10**, 1–14.

Singh, D.K., Sale, P.W.G., Pallaghy, C.K. and Singh, V. (2000) Role of proline and leaf expansion rate in the recovery of stressed white clover leaves with increased phosphorus concentration*. New Phytol*., **146**, 261–269.

Singh, I.N., Paleg, I.G. and Aspinall, D. (1973) Stress metabolism I. Nitrogen metabolism and growth in the barley plant during water stress*. Aust. J. Biol. Sci*., **26**, 45–56.

Sripinyowanich, S., Klomsakul, P., Boonburapong, B., Bangyeekhun, T., Asami, T., Gu, H., Buaboocha, T. and Chadchawan, S. (2013) Exogenous ABA induces salt tolerance in indica rice (*Oryza sativa* L.): The role of OsP5CS1 and OsP5CR gene expression during salt stress. *Environ. Exp. Bot.,* **86**, 94–105.

Szabados, L. and Savouré, A. (2010) Proline: a multifunctional amino acid. *Trends Plant Sci.,* **15**, 89–97.

Székely, G., Ábrahám, E., Cséplo, Á., *et al*. (2008) Duplicated P5CS genes of Arabidopsis play distinct roles in stress regulation and developmental control of proline biosynthesis. *Plant J*., **53**, 11–28.

Szoke, A., Miao, G.H., Hong, Z. and Verma, D.P.S. (1992) Subcellular location of Δ1-pyrroline-5-carboxylate reductase in root/nodule and leaf of soybean*. Plant Physiol*., **99**, 1642–1649.

Trenberth, K.E., Dai, A., Schrier, G. Van Der, Jones, P.D., Barichivich, J., Briffa, K.R. and Sheffield, J. (2014) Global warming and changes in drought. *Nat. Clim. Chang*., **4**, 17–22.

Uddling, J., Gelang-Alfredsson, J., Piikki, K. and Pleijel, H. (2007) Evaluating the relationship between leaf chlorophyll concentration and SPAD-502 chlorophyll meter readings. *Photosynth. Res*., **91**, 37–46.

Uno, Y., Furihata, T., Abe, H., Yoshida, R., Shinozaki, K. and Yamaguchi-Shinozaki, K. (2000) Arabidopsis basic leucine zipper transcription factors involved in an abscisic acid-dependent signal transduction pathway under drought and high-salinity conditions. *Proc. Natl. Acad. Sci.*, **97**, 11632–11637.

Verbruggen, N., Hua, X.J., May, M. and Montagu, M. Van (1996) Environmental and developmental signals modulate proline homeostasis: Evidence for a negative transcriptional regulator. *Proc. Natl. Acad. Sci*., **93**, 8787–8791.

Yoo, S.D., Cho, Y.H. and Sheen, J. (2007) Arabidopsis mesophyll protoplasts: A versatile cell system for transient gene expression analysis. *Nat. Protoc.*, **2**, 1565–1572.

Yordanov, I., Velikova, V. and Tsonev, T. (2000) Plant responses to drought, acclimation, and stress tolerance. *Photosynthetica*, **38**, 171–186.

Yoshida, T., Fujita, Y., Maruyama, K., Mogami, J., Todaka, D., Shinozaki, K. and Yamaguchi-Shinozaki, K. (2015) Four Arabidopsis AREB/ABF transcription factors function predominantly in gene expression downstream of SnRK2 kinases in abscisic acid signalling in response to osmotic stress. *Plant, Cell Environ*., **38**, 35–49.

Yoshida, R., Hobo, T., Ichimura, K., Mizoguchi, T., Takahashi, F., Aronso, J., Ecker, J.R., Shinozaki, K. (2002) ABA-activated SnRK2 protein kinase is required for dehydration stress signaling in Arabidopsis. *Plant Cell Physiol,* **43**, 1473–1483

Yuan, X.K., Yang, Z.Q., Li, Y.X., Liu, Q. and Han, W. (2016) Effects of different levels of water stress on leaf photosynthetic characteristics and antioxidant enzyme activities of greenhouse tomato. *Photosynthetica*, **54**, 28–39.

Chapter 3. Site-directed mutagenesis of drought stress-related ABA-responsive element binding factors in barley using CRISPR RNA/Cas9

3.1. Introduction

Drought stress is one of the significant limiting factors for crop production. Water stress activates morphological, physiological and molecular responses affecting the growth and development of plants (Bartels and Sunkar 2005; Finkelstein *et al.*, 2002). Abscisic acid (ABA) signaling plays a pivotal role in plant development processes as well as the stress response. ABA content in the plant increases under several abiotic stress, including drought and trigger stomatal closure and expression of stress-inducible genes (Shinozaki and Yamaguchi, 2006). It has been illustrated that the activation of ABA-induced genes involves four major steps. The fundamental units of ABA signal transduction include pyrabactin resistance (PYR)/ pyrabactin resistance-like (PYL) regulatory component of ABA receptors, protein phosphatase 2C (PP2C), sucrose non-fermenting related protein kinases (SnRK2) and ABA-responsive element (ABRE) binding factors (ABF) (Umezawa *et al.*, 2010). PP2C interacts with SnRK2 in the absence of ABA and prevents the activation of SnRK2. However, under stress conditions, ABA is perceived by PYR/PYL, which forms a complex with PP2C leading to autophosphorylation of SnRK2s (Ma *et al.*, 2009; Fujii *et al.*, 2009). SnRK2 phosphorylates the downstream transcription factor (Fujii *et al.*, 2009; Yoshida *et al.*, 2006), ABFs, which regulates the transcription of ABA-inducible genes (Yoshida *et al.*, 2010; Yoshida *et al.*, 2015).

ABA-inducible genes comprise multiple ABRE (ACGTTGG/TC) or related coupling elements (CE). ABREs are characterized by ACGT as core sequence, while non-ACGT ABREs are also identified to be equally crucial for ABA-responsiveness (Hobo *et al.*, 1999). It was demonstrated by *in vitro* assays that ACGT-containing ABRE, CE1 (TGCCAC) and CE3 (ACGCGTG) elements function as ABA-response complex (ABRC) and regulate the ABA-responsive expression of reporter genes fused to minimal promoters (Shen *et al.*, 1996; Shen and Ho, 1995). ABFs and ABI5 can bind to the ABREs present in the promoter of stress response genes and regulate the transcription of ABA inducible genes. ABFs and ABI5 belong to the group A member of the basic-domain leucine zipper (bZIP) transcription family and have four conserved domains. It has three N-terminal phosphorylation domain and one C-terminal basic domain with 16 conserved amino acid residues (Furihata *et al*., 2006; Jakoby *et al*., 2002).

Genome editing is a powerful tool for gene functional analysis. Recently, a bacterial defense system, clustered regulatory interspaced short palindromic repeats (CRISPR) RNA and associated Cas9 protein has been engineered to introduce site-directed mutagenesis in plants (Marzec and Hensel, 2018). CRISPR RNA/Cas9 system utilizes DNA-RNA interaction and recruits Cas9 protein, which makes a double-stranded break at the target site. The endogenous cell machinery makes an error during the repair of a double-stranded break (DSB), introducing insertion and deletion at the target site (Belhaj *et al.*, 2015). A small non-coding RNA referred to as single guide RNA (sgRNA) can be custom designed that can bind to the target site. Then, the transformation of plant tissues with sgRNA and Cas9 expression vector will introduce mutation events in a gene of interest. The application of CRISPR RNA/Cas9 guided genome editing in plants has been demonstrated by several groups. It has been used in the field of fundamental research as well as to improve agronomic traits in plants (Kumlehn *et al.*, 2018). Lawrenson *et al.* (2015) illustrated that the mutation event generated through CRISPR RNA/Cas9 directed genome editing is heritable in barley.

In barley, the promoter region of ABA-inducible late embryogenesis abundant (LEA) gene, HVA22 contains ACGT-ABRE, CE3 and CE1 forming an ABRC3. GUS reporter gene fused to ABRC3 was transiently expressed in barley aleurone cells and leaf segments. GUS activity was strongly upregulated under ABA induction (Shen *et al.*, 1996; Shen and Ho, 1995). Schoonheim *et al.* (2009) showed that the co-transfection of barley bZIP protein with GUS reporter fused to ABRC3 enhanced the GUS activity in aleurone tissues. In chapter 1, we also discussed that ABRE might be critical for transcriptional regulation of *HvP5cs1*. Allele mining of *HvP5cs1* promoter revealed multiple mutations across ABRE motifs between ISR42-8 (accumulate proline in very high concentration) and other barley accessions. We also demonstrated that ABA-induced *HvP5cs1* promoter activity of ISR42-8 was regulated in ABF dependent manner. Nonetheless, barley bZIP proteins that regulate ABA-inducible genes are poorly understood. Here we employed CRISPR RNA/Cas9 system to generate mutant alleles of barley genes belonging to bZIP family. The genes were selected on the basis of homology to ABFs from Arabidopsis. Then, the mutant lines were phenotyped under drought stress. A comprehensive RNAseq analysis was performed for transcriptome profiling of barley ABF mutants under drought stress.

3.2. Materials and Methods

3.2.1. Selection of putative HvABFs and generation of plant expression CRISPR RNA-Cas9 vector

Four ABF transcription factors are critical for the activation of osmotic stress response in Arabidopsis (Yoshida *et al*., 2015). We performed phylogenetic analysis using MEGA X (Kumar *et al.*, 2018) based on protein sequence similarity between ABF genes of Arabidopsis and barley genes annotated as bZIP domain-containing protein. We found four orthologs in barley, namely HORVU6Hr1G080670 (HvABF), HORVU7Hr1G035500, HORVU5Hr1G068230, and HORVU3Hr1G084360 (HvABI5) (Figure 3.1a). HvABF and HvABI5 are designated to respective genes based on the gene annotation indicated in the barley genome explorer database. The protospacer sequence was designed based on the reference sequence of HvABF and HvABI5 to prepare a single guide RNA to induce site-directed mutagenesis in barley. One suitable candidate, each for HvABI5 (sgRNAbZIP-PS3) and HvABF (sgRNAbZIP-PS4), was detected on exon 1. Then, this region was sequenced in Golden Promise to confirm no mismatch existed between barley reference, Morex, and Golden Promise. Both sgRNAbZIP-PS3 and sgRNAbZIP-PS4 identified all four genes in question as potential off-targets (Figure 3.1 b-e). Therefore, sgRNAbZIP-PS3 and sgRNAbZIP-PS4 were ideal candidates as it could also potentially induce mutations in HORVU7Hr1G035500 and HORVU5Hr1G068230. The protospacer sequence was synthesized and assembled to pSH91 through a restriction (*BsaI*) and ligation approach. The validated clones were digested with (*SfiI*) and ligated to plant expression vector (p6ID35STE9) with the Cas9 expression system and hygromycin as a plant selection agent (Figure 3.1 f). As the vectors are not published, the vector backbone is indicated in Figure S9. Immature barley embryos from Golden Promise were transformed with binary vectors housing sgRNAbZIP-PS3 and sgRNAbZIP-PS4, according to Marthe *et al.* (2015). The vectors and lab facilities for vector construction were kindly provided by Dr. Jochen Kumlehn, Reproductive Biology Group, IPK, Gatersleben. Barley transformation and embryo culture were done in the same lab under the supervision of Dr. Götz Hensel.

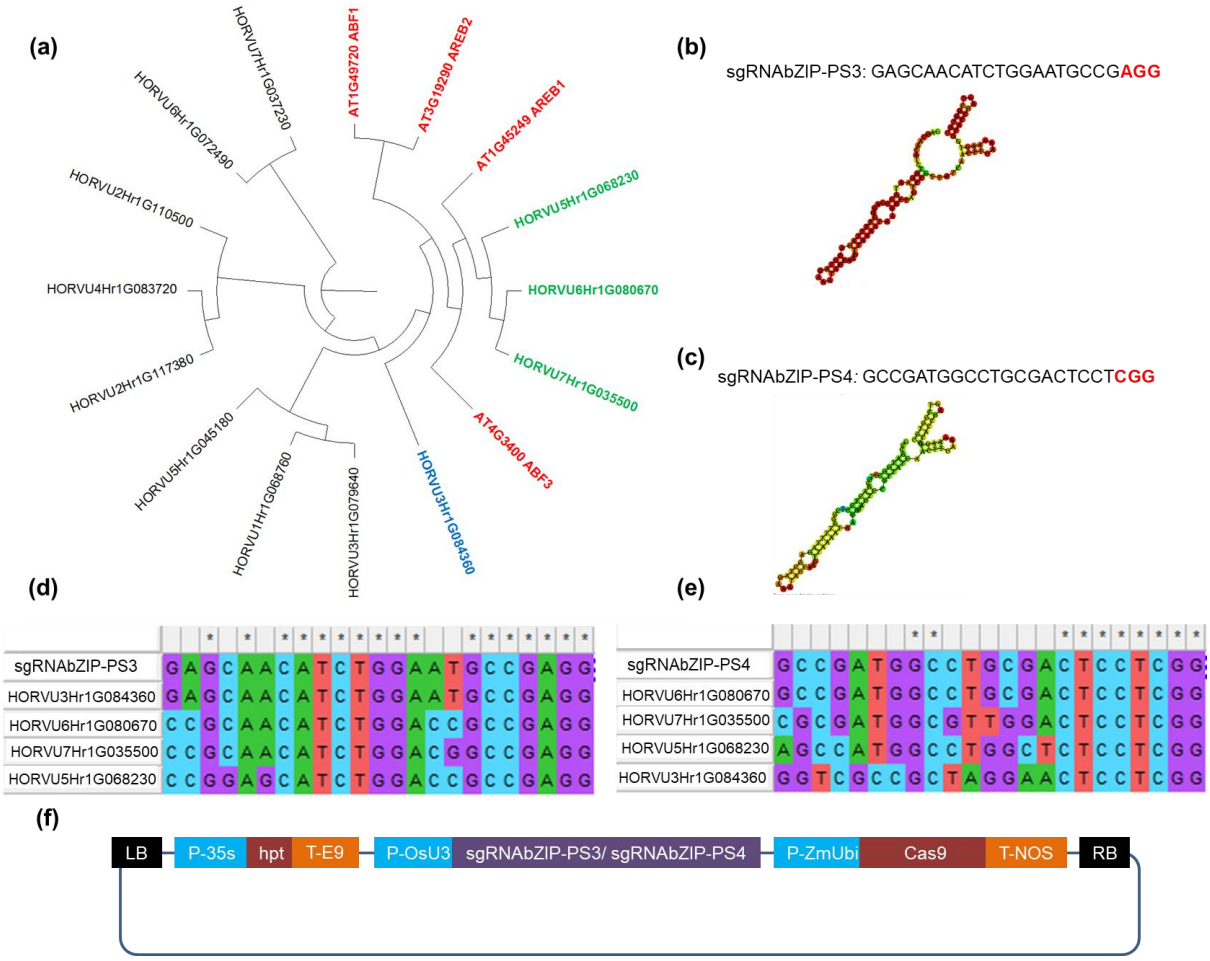

Figure 3.1. Selection of barley bZIP genes and plasmid construction for CRISPR RNA/Cas9 induced gene knock-out. (a) Evolutionary relationship of Arabidopsis ABFs with barley bZIP proteins. The phylogenetic analysis was performed using MEGA X, and the Neighbor-Joining method was inferred for tree construction. (b and c) protospacer sequences used for site-directed mutagenesis. The nucleotides indicated in red font color are protospacer adjacent motif (PAM). The protospacer sequence was designed using the Deskgen website (www.deskgen.com), and the secondary structure of the single guide RNA (sgRNA) was analyzed using the RNAfold server of the Institute of Theoretical Chemistry, the University of Vienna (www.rna.tbi.univie.ac). (d and e) The alignment of sgRNAbZIP-PS3 and sgRNAbZIP-PS4, indicating target and off-target sites. (f) The simplified diagram of a binary vector with CRISPR RNA-Cas9 expression system used for barley transformation. sgRNA was fused to rice U3 (P-OsU3) promoter, while Cas9 protein from *Streptococcus pyogenies* was driven by maize ubiquitin promoter (P-ZmUbi6) and terminated by nopaline synthase terminator (T-NOS). The binary construct contains the hygromycin as plant selection driven by 35s promoter (P-35s) and 35s terminator (T-35s).

3.2.2. Genotyping of T_0, T_1 and T_2 generation

Genomic DNA for 31 regenerated T_0 progenies tested positive for T-DNA insertion was received from Dr. Götz Hensel from IPK. The mutation events in T_0 progenies were detected by Sanger sequencing for both target and off-target sites. We were able to detect mutation events in six T_0 progenies for HvABI5, and only one T_0 progeny for HvABF (Figure S10). No off-target mutagenesis was detected for both sgRNAbZIP-PS3 and sgRNAbZIP-PS4. Then, 48 T_1 progenies from the seven T_0 progenies showing mutations events were screened for the presence of T-DNA. Eight T_1 progenies for selected T_0 pipeline that tested negative for T-DNA insertion were genotyped by Sanger sequencing to detect the site-directed mutagenesis in both target and off-target sites. The positive T_1 progeny for mutation events were selfed to obtain T_2 seeds. Finally, T_2 progenies for each pipeline were again genotyped for the absence of T-DNA as a confirmation and sequenced to identify transgene-free T_2 progenies homozygous for mutation events. Verified T_2 progenies were selfed to obtain the seeds from individuals carrying homozygous mutant alleles to characterize the mutants under drought stress. The mutant lines for HORVU6Hr1G080670 (HvABF) and HORVU3Hr1G084360 (HvABI5) are indicated as *hvabf* and *hvabi5* in the following text.

3.2.3. Evaluation of *hvabi5* and *hvabf* mutants under drought stress

Seeds were pregerminated using a peat-based potting mixture, ED73 classic produced and marketed by Einheitserde, Germany, and two-day-old seedlings were transferred to a pot (8 x 8 x 7 cm). The pots were filled with an equal volume of with potting mixture containing 60% natural sand and 40% topsoil (Terrasoil; Cordel and Sohn). The plants were grown in the greenhouse, and the growing condition was 18-22°C daily mean temperature, 14/10 h light/dark, and 110-150 µmol $m^{-2} \cdot s^{-1}$ light intensity. The field capacity of the soil was maintained at 80% under well-watered condition. Pots were weighed twice a day and watered manually to maintain the constant soil moisture. Drought stress treatment was applied by withholding watering to 14 d old seedlings. The weight of pots was recorded each day to ensure the same moisture level in all the pots. Electrolyte leakage (EL) and relative water content (RWC) measurements were made at 6 d and 9 d after stress. Cell membrane integrity was determined by evaluating electrolyte leakage (EL) based on Bajji *et al*. (2002). Falcon tubes were filled with 10 ml deionized water, and initial electrical conductivity was recorded (ECi). First, the tip of (around 2 cm) first fully expanded leaf was removed. Then, two leaf sections (around 2 cm each) were cut and placed in a falcon tube with 10 ml double distilled water and stored in the dark at room temperature. Then, electrical conductivity was measured after 24 h of rehydration period (ECf). After the final reading, the samples were boiled at 100°C for 30 minutes, cooled to room temperature, and total electrical conductivity (ECt) was

measured. EL was expressed as (ECf-ECi)/(ECt-ECi)*100. Leaf water status was estimated through relative water content (RWC), according to Ghoulam *et al.* (2002). For RWC measurement, four leaf sections (around 2 cm each) were detached from the first fully expanded leaf, and the fresh weight was recorded (FW). Then, the leaf sections were dipped in a falcon tube filled with 10 ml deionized water for 24 h at room temperature. The leaf sections were removed from the falcon tube, and excess water was wiped with a paper towel before taking the turgor weight (TW). Dry weight was recorded after oven drying at 70°C for 24 h. RWC was estimated as (FW-DW)/(TW-DW) *100. Fresh samples were harvested, snap-frozen in liquid nitrogen and stored at -80°C before proline and malondialdehyde (MDA) determination. The experiment was performed in four biological replicates.

3.2.3.1. Proline determination

Proline was measured from shoot samples, according to Bates *et al.* (1973) adapted to a microplate-based protocol (Ábrahám *et al.*, 2010). In short, seedlings were homogenized in liquid nitrogen, and proline was extracted using 1 ml 3% sulphosalicylic acid followed by centrifuging at 12,000 *g* for 5 minutes. The sample extract was incubated for 1 hour at 96°C with 2.5% ninhydrin and acetic acid at a 1:1:1 ratio. The reaction was stopped on ice, and the proline-ninhydrin reaction product was extracted with 1 ml toluene. The absorbance of chromatophore containing toluene was measured at 520 nm using a microplate reader (TECAN Infinite 200 Pro, TECAN Group Limited, Switzerland). Shoot proline level was determined using a standard curve method and expressed as micrograms per gram fresh weight.

3.2.3.2. Malondialdehyde determination

Oxidative damage of lipid membrane during drought was estimated by determining MDA based concentration using thiobarbituric acid (TBA) method (Hodges *et al.*, 1999) adapted to a microplate-based protocol (Dziwornu *et al.*, 2018) with some modification. Shoot samples were homogenized in liquid nitrogen, and MDA was extracted using 1.5 ml of 0.1% trichloroacetic acid (TCA) followed by centrifuging at 14,000 *g* for 15 minutes at 4°C. Then, 500 µl supernatant was mixed with reaction solution I (0.01% 2,6-di-tert-butyl-4-methyl phenol (BHT) in 20% TCA) and reaction solution II (0.65% TBA, 0.01% BHT in 20% TCA) in a 1:1 ratio. Reaction and sample mix were incubated at 95°C for 30 minutes. The reaction was stopped on ice for five minutes, and the reaction mix was centrifuged at 8000 *g* for 10 minutes at 4°C. The absorbance was measured at 440 nm, 532 nm, and 600 nm using a microplate reader (TECAN Infinite 200 Pro, TECAN Group Limited, Switzerland). MDA concentration was expressed as nanomoles per gram fresh weight.

3.2.4. RNAseq analysis of *hvabf* and *hvabi5* under drought stress

We conducted transcriptome profiling of wild type, *hvabf,* and *hvabi5* under control and drought stress. The growing environment and stress treatment were identical to the conditions described in chapter 3, section 3.2.3. Fresh shoot samples were collected 7 d after stress treatment, flash-frozen in liquid nitrogen, and stored at -80°C before RNA extraction.

Shoot materials were homogenized in liquid nitrogen, and RNA was extracted using Monarch RNA miniprep kit (New England Biolabs, USA) following the manufacturer's instruction. The RNA concentration and quality were determined by running on 1% Agarose gel and using nanodrop (NanoDrop 2000c, Thermo Fischer Scientific, USA) before shipping. RNA integrity was further verified by using Bioanalyzer (Agilent 2100, Agilent Technologies, USA). The samples that passed RNA integrity numbers (≥6.3) were used for library preparation. Library preparation and sequencing were outsourced to Novogen Europe.

The quality control or raw sequencing reads was performed using FastQC (Andrews 2010), and the adaptor sequence and reads less than 70 bp were trimmed using Trimmomatic. Trimmed reads were aligned to the barley reference genome sequence (ftp://ftp.ensemblgenomes.org/pub/plants/release-36/fasta/hordeum_vulgare/dna/; Hv_IBSC_PGSB_v2) using HISAT2 (Pertea *et al.*, 2016). The unmapped reads were filtered before further processing. To be selected as a mapped read, ≥80% of the length of a read should have mapped to the reference sequence sharing ≥ 90% identity. On average, more than 80% trimmed reads mapped to the reference, and the unmapped reads were filtered before further processing (Table S5). Differential gene expression (DEG) analysis was performed using edgeR package (Chen *et al.*, 2016). First, the read count for the uniquely mapped sequence was normalized to a sequencing depth of a sample and expressed as log count per million. Based on the normalized expression value, a strong correlation was detected for three biological replicates for each accession under all treatment conditions (Figure S11). A negative binomial distribution was fitted before DEG estimation, which was expressed as a log2 fold change of drought to control. Quasi-likelihood F-test was applied, and $P \leq 0.05$ was set as a significance threshold (Chen *et al.,* 2016). Multiple testing correction was performed for the significant DEGs list to control the false discovery rate to $P \leq 0.05$, according to Benjamini and Hochberg (1995).

Gene ontology (GO) enrichment analysis for DEGs was performed using a web-based software agriGO v2.0 (Tian *et al.*, 2017). First, we performed a singular enrichment analysis (SEA) to identify the over-represented GO terms based on Fischer's exact test. SEA was performed separately for upregulated and downregulated DEGs categories. The resulting *P*-

value was corrected for multiple testing by adjusting the false discovery rate to $P \leq 0.05$ (Benjamini and Hochberg, 1995). For the cross-comparison of co-represented networks between wild type and mutants, we performed SEACOMPARE analysis with the SEA results (Tian *et al.*, 2017).

3.2.5. Statistical analyses

Statistical significances were analyzed using open-access statistical computing software R. Two-way ANOVA was performed to observe genotype, treatment, and interaction effects. The student's *t*-test was used for the mean comparison between genotypes for a given treatment condition. Multiple mean comparison analysis was done using a Tukey post hoc test. Graphics were prepared using statistical platform R and Prism8.

3.3. Results

3.3.1. CRISPR RNA/Cas9 induced site-directed mutagenesis in putative barley ABFs

Table 3.1. Summary of frequency of genome-editing events and transgenerational segregation of transgene and allelic mutations. T-DNA, transfer DNA.

Gene	T_0 line	T_0 mutation type	Number of T_1 plants screened for T-DNA	Plants without T-DNA	Number of T-DNA free plants used for sequencing	Number of T1 plants with a homozygous mutation
HvAbf	BG815E33	Heterozygous	48	16	8	3
HvAbi5	BG815E7	Homozygous	48	18	4	4
HvAbi5	BG815E8	Homozygous	48	16	4	4
HvAbi5	BG815E11	Heterozygous	48	19	8	2
HvAbi5	BG815E12	Homozygous	48	8	4	4
HvAbi5	BG815E14	Heterozygous	48	16	8	1
HvAbi5	BG815E24	Heterozygous	48	22	8	4
HvAbi5	BG815E34	Heterozygous	48	22	8	1

Site-directed mutagenesis in the 31 T_0 progenies was detected by direct sequencing of the target sites. We detected mutation events in seven T_0 progenies for the target site of sgRNAbZIP-PS3 (Figure S10). All detected mutations were present in HvABI5, and off-target genome editing was absent in all 31 T_0 progenies for sgRNAbZIP-PS3. Similarly, no off-target mutation events were detected in 31 T_0 progenies for sgRNAbZIP-PS4, and only one T_0 plant showed potential genome editing events. We also detected a homozygous mutation event in three T_0 progenies in HvABI5 (Figure S10a, c and g). Then, T_1 seeds from eight T_0 progenies were germinated in 96 well plates, and 48 individuals from each pipeline were genotyped for the presence of T-DNA. For all pipelines, we obtained transgene-free T_1 plants fitting to the Mendelian segregation principle, indicating single T-DNA insertion (Table 3.1). To detect mutation at the target site, we sequenced eight transgene-free plants from all T_1 pipelines. We obtained at least one to maximum three transgene-free individuals with a homozygous base editing (insertion or deletion) already in T_1 generation. We sequenced the target site of four individuals from three different transgene-free T_1 pipelines derived from T_0 individuals carrying a homozygous mutation and found that all four progenies were homozygous for 1 bp deletion (Table 3.1). We also sequenced the off-target sites in all the individuals and did not detect any off-target activity. We detected three allelic mutants for HvABI5 with 1 bp insertion, 1 bp deletion, and 4 bp deletion, which were named as *hvabi5-1*, *hvabi5-2*, and *hvavi5-3* (Figure

3.2a). All three allelic mutants resulted in a translational frameshift mutation. We found only one allelic mutant for HvABF with 3 bp deletion that caused the deletion of serine from the conserved domain (Figure 3.2c). This allelic mutant is named as *hvabf* in the following text. Leaf samples were pooled from the T_2 plants used for drought screening, genotyped for T-DNA insertion, and sequenced to verify mutations. We did not detect any false positives.

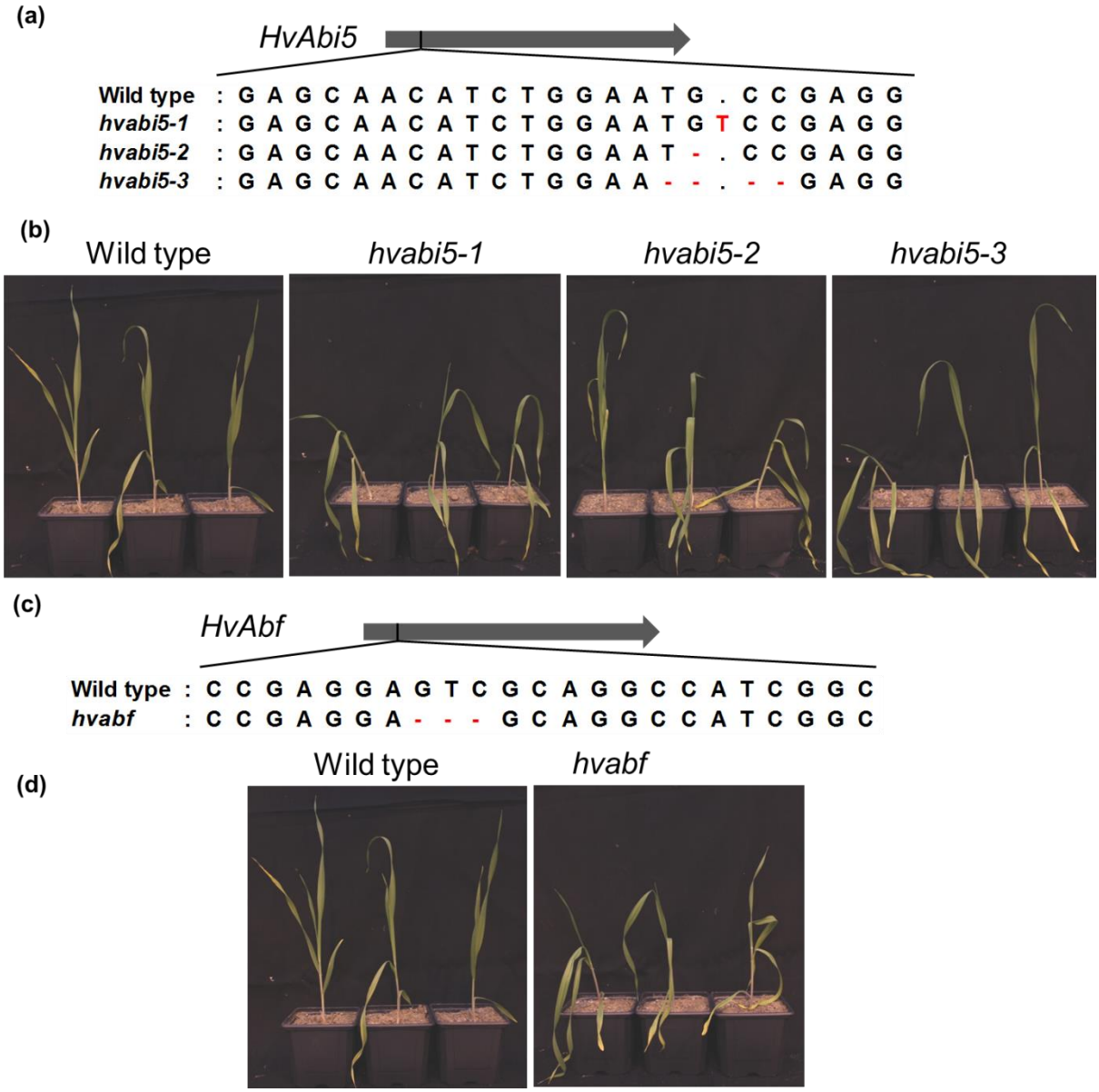

Figure 3.2. Sequence analysis of target sites of barley T_2 progenies of *hvabf* and *hvabi5* allelic mutants. (a) The mutation events in *HvAbi5* with one bp insertion (*hvabi5-1*), one bp deletion (*hvabi5-2*), and four bp deletion (*hvabi5-3*). These mutations resulted in gene knock-out owing to a translational frameshift. (b) The phenotype of wild type and *hvabi5* mutants under drought stress (c) The mutation event in *HvAbf* with three bp deletion (*hvabf*). The mutation resulted in the deletion of serine in a conserved domain. (d) The phenotype of wild type and *hvabf* mutant under drought stress. Drought stress was applied to 14 d old seedlings, and the moisture level on control pots was maintained at 80% field

capacity throughout the experiment. The pictures were taken 7 d after drought treatment using Canon D750.

3.3.2. Physiological and biochemical response of *hvabi5* and *hvabf* to drought stress

bZIP transcription factors are one of the critical regulators of drought response in plants. Therefore, we screened wild type and mutants to characterize morphological, physiological, and biochemical traits under control and drought conditions. We did not observe any morphological and reproductive growth differences in the T_1 generation. The same was true for T_2 seedlings under control condition. However, under drought conditions, all allelic mutant of *hvabi5* and *hvabf* showed wilting symptoms earlier than wild type (Figure 3.2b and d). First signs of wilting were observed 6 d after stress while visual differences between wild type and mutants were distinct at 7 d after stress. We checked the tissue water status by estimating relative RWC and observed a significant treatment and genotype treatment interaction effect at 6 d after stress (Figure 3.3a and Table S6). RWC was higher in wild type compared to *hvabi5* and *hvabf* under water stress (Figure 3.3a and b). Then, we estimated the membrane integrity measured as electrolyte leakage, which showed a significant treatment effect as EL was higher in plants exposed to drought stress. Although statistically not significant, EL was around 15% lower in wild type compared *hvabf* and *hvabi5* allelic mutant at 9 d after water stress (Figure 3.3c and d). Likewise, lipid peroxidation measured as MDA concentration also revealed a similar response to drought, where *hvabf* and *hvabi5* allelic mutants showed marginally higher values compared to wild type under drought conditions (Figure 3.3e and f, Table S6). In contrast, drought-inducible proline concentration measured around 2.3 and 2.6 times higher in *hvabf* and *hvabi5* allelic mutant compared to wild type. However, proline accumulation was induced upon drought treatment in both wild type and mutants (Figure 3.3g and h). We did not observe genotypic differences for measured traits under control conditions (Table S6). To conclude, *hvabf* and *hvabi5* allelic mutants were sensitive to drought stress compared to the wild type.

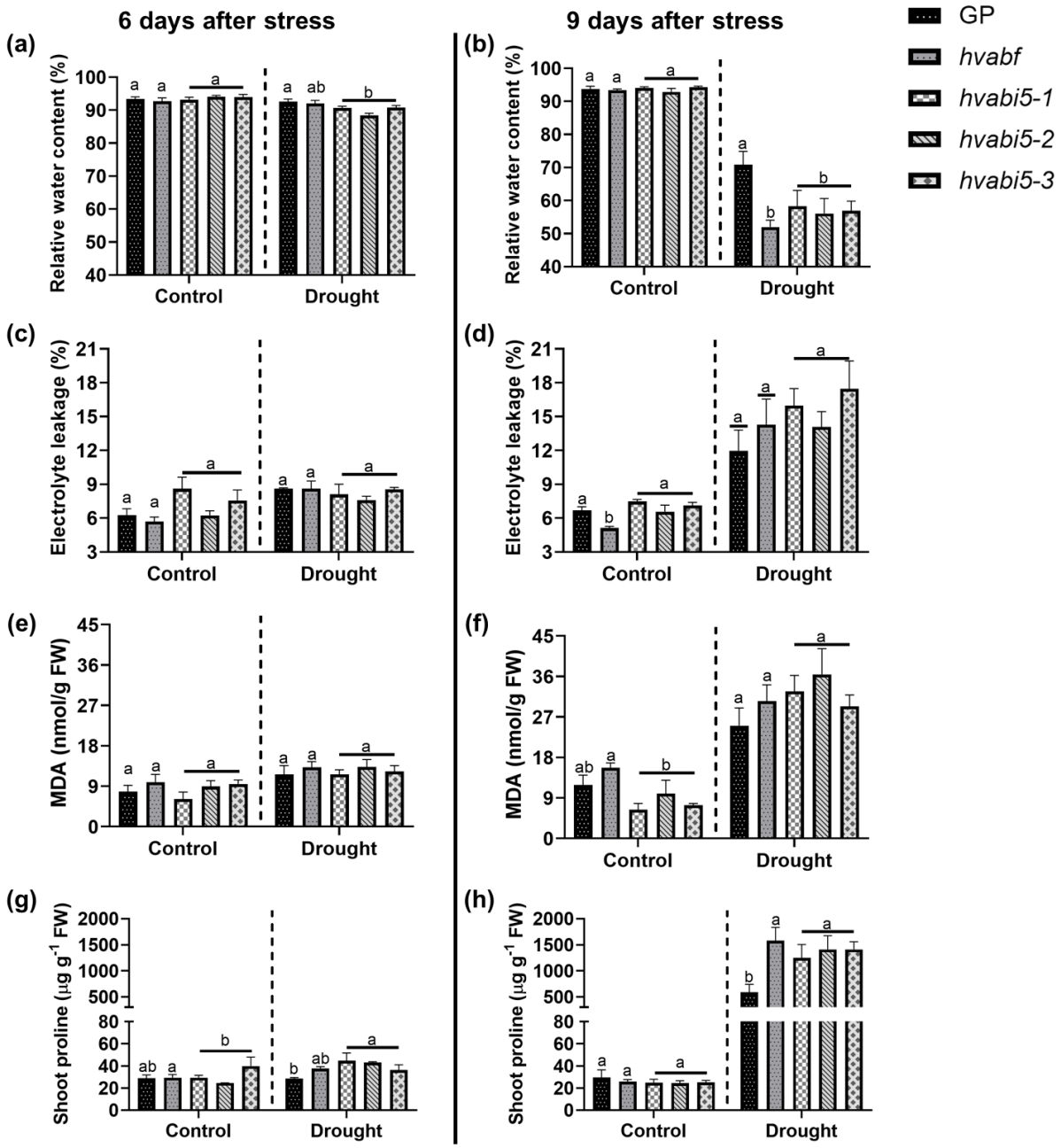

Figure 3.3. Morphological and physiological response of wild type, *hvabf*, and *hvabi5* to drought stress. The effect of drought stress on (a-b) relative water content at 6 d and 9 d; (c-d) electrolyte leakage at 6 d and 9 d; (e-f) malondialdehyde (MDA) concentration at 6 d and 9 d; (g-h) shoot proline concentration at 6 d and 9 d after stress. Drought stress was applied to 14 d old seedlings, and the moisture level on control pots was maintained at 80% field capacity throughout the experiment. Bar indicates mean ± SE (n = 4). Indexed letters above the box indicate a significant difference between the genotypes ($P \leq 0.05$) using TukeyHSD test. FW, fresh weight; GP, Golden Promise

3.3.3. Transcriptome analysis of *hvabi5* and *hvabf* mutants in barely

Next, we performed a genome-wide transcriptome analysis of *hvabf* and *hvabi5* to understand the genetic networks that are differentially regulated compared to wild type. A total of 19422 genes were co-expressed in all the lines at both control and drought conditions (Figure 3.4a). In general, the number of DEGs was higher in mutants than wild type. Compared to wild type, the number of down-regulated genes was much higher in mutants. Forty-six and 86 genes were exclusively upregulated and down-regulated in wild type compared to mutants (Figure 3.4b and c). Next, we performed GO enrichment analysis to identify the significant biological process represented in the up and downregulated gene networks. The gene network involved in protein phosphorylation and kinase activity was downregulated under stress conditions in both wild type and mutants. Notably, the gene network involved in transmembrane transport of nitrogenous compounds was exclusively downregulated in wild type, while transmembrane transport of organic acid and divalent metal transport was only downregulated in *hvabi5*. GO term enrichment analysis revealed that the biological process, such as response to wounding, response to acid chemical, and anatomical structure development, was exclusively upregulated in wild type. The gene network involved in response to water stress was the most significantly upregulated process under drought stress in wild type compared to mutants and *hvabf* in particular (Table S7).

Next, we analyzed the DEGs between wild type and mutants under drought conditions. A total of 111 were differentially regulated between wild type and *hvabf*, while 82 DEGs were detected between wild type and *hvabi5* (Data submitted as electronic file). Then, we looked into the top twenty most significantly up and downregulated genes (Figure 3.5). We found that genes coding for peroxidases (HORVU1Hr1G016840 and HORVU3Hr1G083190) were upregulated in wild type compared to *hvabf*. Besides, VRN-H1 (HORVU5Hr1G095630) and oxidoreductases (HORVU5Hr1G015140 and HORVU0Hr1G0108809) were also upregulated in the wild type. Genes coding for histone 3 (HORVU6Hr1G011520) and ubiquitin-like domain-containing protein (HORVU4Hr1G061900) were downregulated in wild type than *hvabf* (Table S8). Likewise, in comparison to *hvabi5,* oxidoreductase (HORVU0Hr1G010880), and defense response (HORVU5Hr1G028140) and stress signaling (HORVU6Hr1G090470) were upregulated in wildtype. Genes coding for a ubiquitin-like domain-containing protein (HORVU6Hr1G010420 and HORVU4Hr1G061900) were downregulated in wild type than *hvabi5* (Table S9).

We also checked the expression pattern of genes involved in proline metabolic pathways. The expression of *HvP5cs1* and *HvP5cs2* was highly upregulated under drought conditions in all accessions. *HvP5cs1* showed the highest level of expression compared to other genes.

Although *HvP5cs2* is not known to be drought-inducible, not only was it highly induced under drought, but the expression level was diminished in wild type compared to mutants. The expression of *HvP5cr* was also induced by drought. As genes involved in proline catabolism are known to be downregulated under osmotic stress, we also observed strong suppression of *HvPdh* under drought stress in both wild type and mutants. In contrast, the expression of P5C dehydrogenase (*HvP5cdh*) was induced under drought stress (Figure 3.6). In summary, the drought sensitivity of *hvabf* and *hvabi5* allelic mutant can be linked to the downregulation of critical stress-responsive genes.

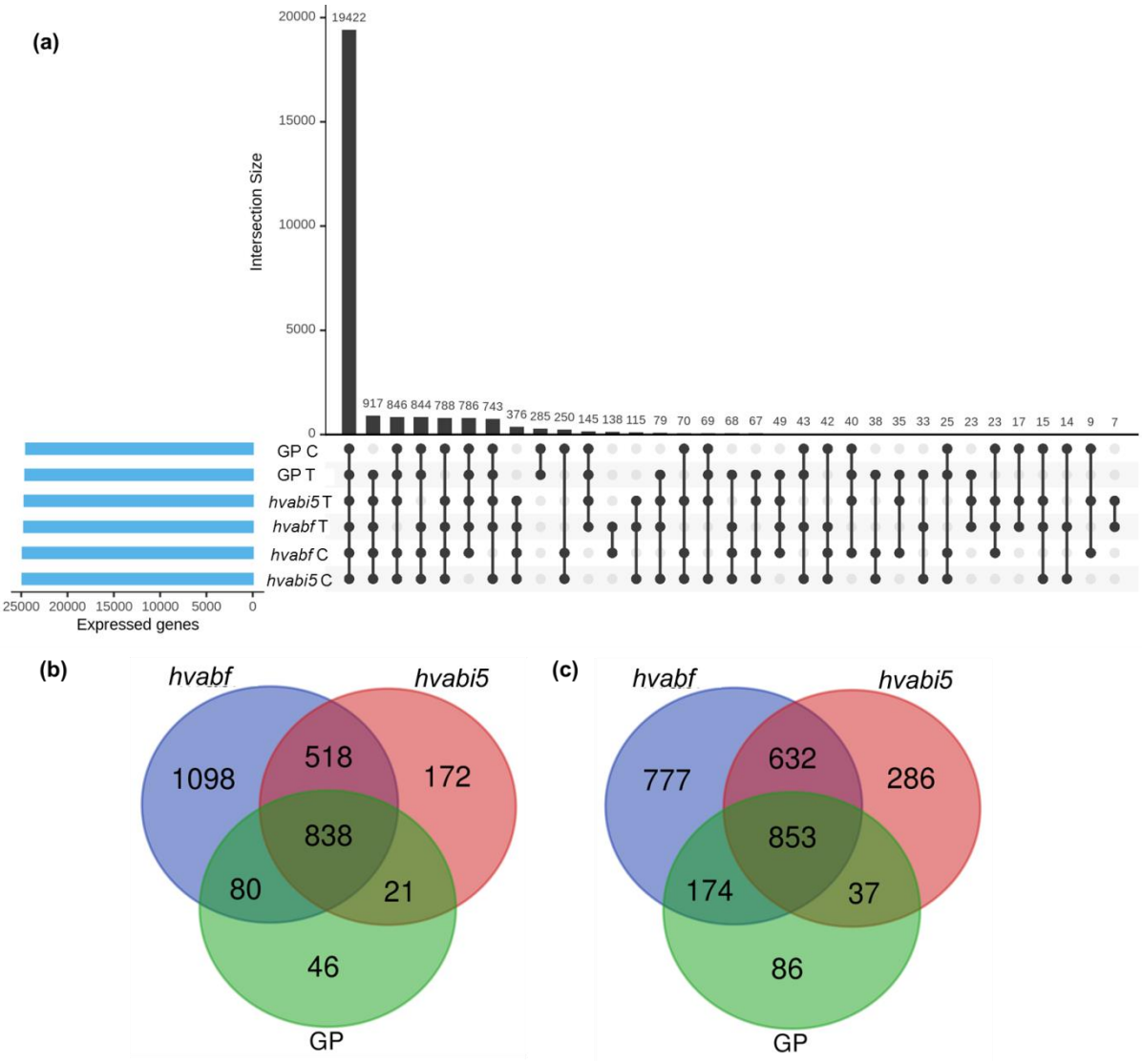

Figure 3.4. Overview of co-expressed and differentially expressed genes of wild type, *hvabf* and *hvabi5.* (a) The number of expressed genes detected in genotypes grown under control conditions, C and stress treatment, T. The nodes indicate the overlap between different combinations, and the bar indicates the number of co-expressed genes for the combination. Blue bars indicate the total number of expressed

genes for a genotype in a given growing condition (C or T). Venn diagram showing the overlap of (b) upregulated (c) downregulated genes between wild type and mutants under drought stress. GP, Golden Promise

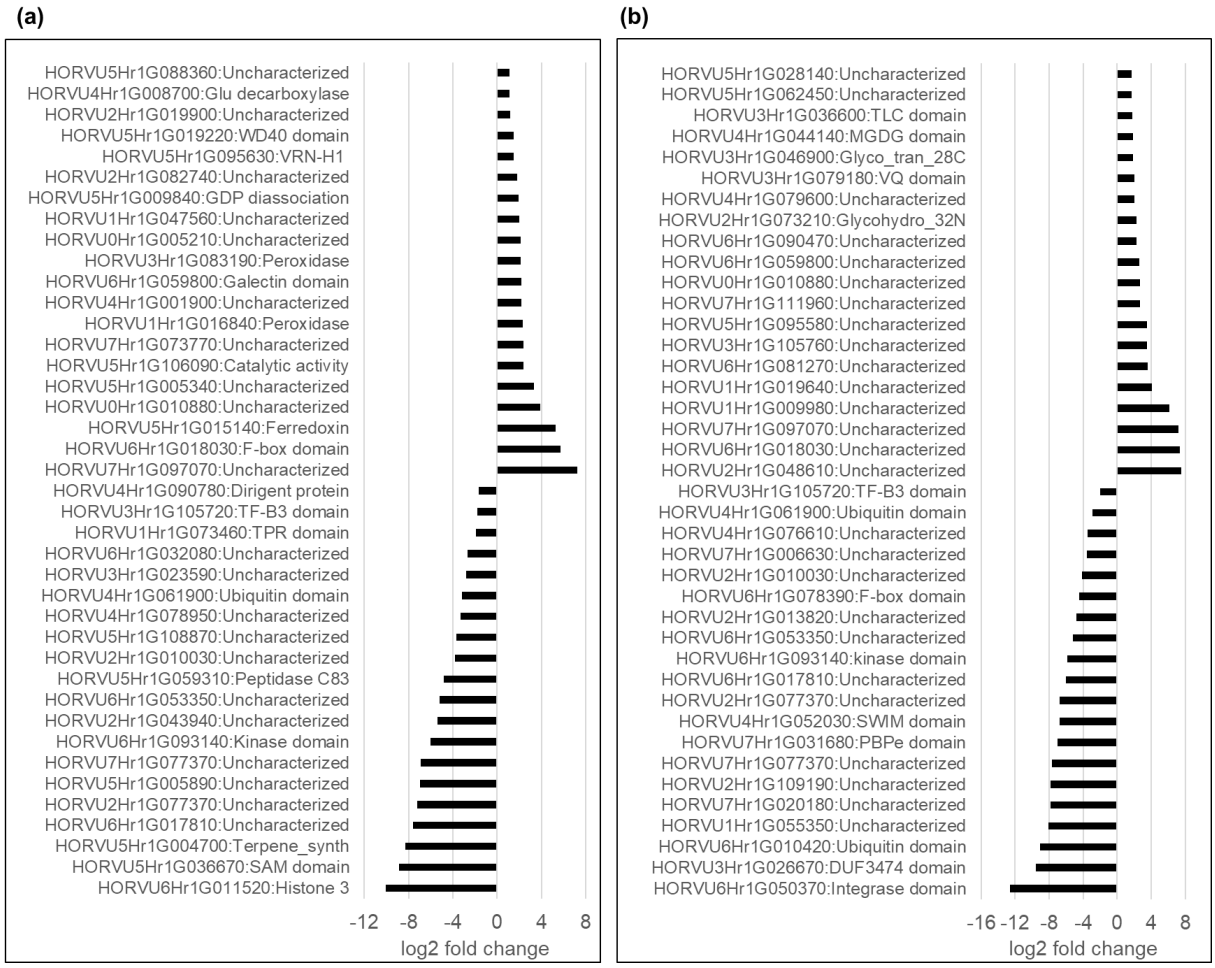

Figure 3.5. Differentially expressed genes between wild type and mutants under drought conditions in barley. Top twenty upregulated and downregulated genes in wild type compared to (a) *hvabf* and (b) *hvabi5* under drought stress. Top twenty genes were selected based on the *P*-value obtained from the quasi-likelihood F-test. Gene identifier and keywords for functional annotation is indicated for each gene. A detailed ontology classification is presented in Table S8 and S9.

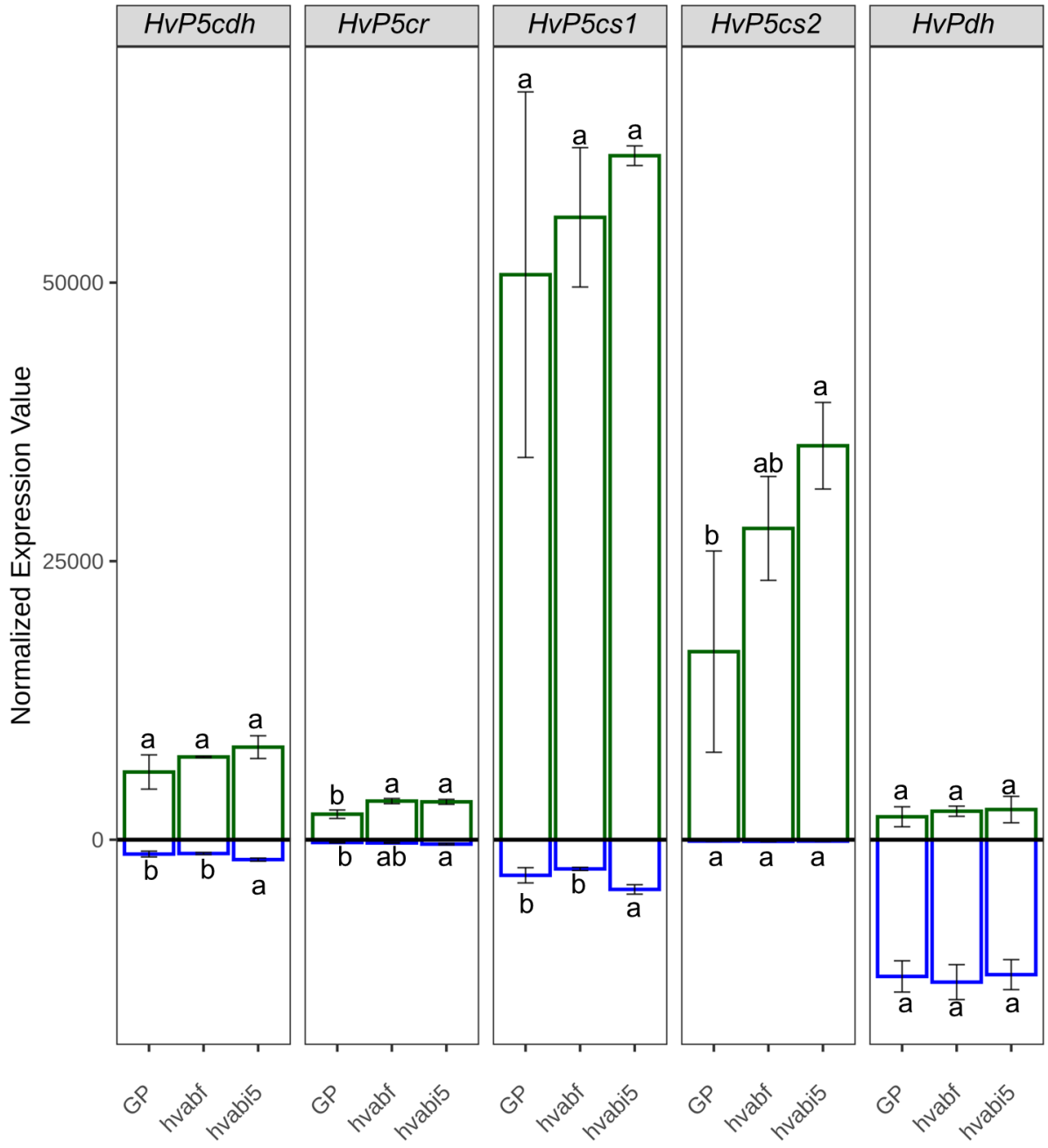

Figure 3.6. Normalized expression values of genes involved in the proline metabolic pathway. Blue and green bars indicate the normalized expression value under control and drought conditions, respectively. Letter not sharing the same letter are significantly different based on TukeHSD test ($P \leq 0.05$). GP, Golden Promise

3.4. Discussion

The aim of the study was to generate and characterize the knock-out mutant of genes related to the ABF family in barley. CRISPR RNA and associated Cas9 is a bacterial defense mechanism that has been engineered for genome editing in different plant species (Pacher and Puchta, 2017; Kumlehn *et al.*, 2018). CRISPR RNA/Cas9 system relies on the interaction between small non-coding RNA (sgRNA) and DNA that recruits Cas9 endonuclease. Cas9 makes DSBs, and the DNA repair by endogenous cell machinery is error-prone, causing mutations on the cleavage site. Therefore, custom-designed sgRNA can be capitalized to generate mutagenesis events at the target site (Belhaj *et al.*, 2015). In our study, we also employed CRISPR RNA/Cas9 to generate allelic mutants of barley genes annotated as bZIP transcription factors that displayed homology to ABFs. We targeted four genes with two sgRNAs. The sgRNAbZIP-PS3 and sgRNAbZIP-PS4 were specific to HORVU3Hr1G084360 (*HvAbi5*) and HORVU6Hr1G080670 (*HvAbf*), respectively, whereas 5^{l} mismatch existed for other genes (HORVU7Hr1G035500 and HORVU5Hr1G068230). The sgRNA was designed on the conserved phosphorylation domain because it is well-established that ABFs undergo post-translational phosphorylation to achieve transactivation property (Furihata *et al*. 2006; Uno *et al*., 2000). In previous studies, it has been demonstrated that the 3^{l} mismatch successfully prevents off-target activity, but the 5^{l} mismatch might not prevent off-target base editing (Lawrenson *et al.*, 2015; Upadhyay *et al.*, 2013). Though, we did not detect any off-target activity after direct sequencing of T_0 and T_1 progenies. There are successful instances where multiplexing and co-transfection resulted in genome editing in multi-sites (Wang *et al.*, 2017). In order to obtain multi-site genome editing, we also co-transfected immature embryos of barely with two sgRNAs with no evidence of multi-site editing in both T_0 and T_1 progenies. Nevertheless, we detected biallelic mutations in three T_0 progenies for *HvAbi5*. Biallelic mutants were also detected in rice and grapes (Zhou *et al.*, 2014; Wang *et al.*, 2018). We detected three different allelic mutants in *hvabi5,* resulting in a translational frameshift. In *hvabf,* only one allelic mutant with three base pair deletion was detected, resulting in loss of serine in the conserved phosphorylation domain.

ABFs are involved in the activation of drought stress-responsive genes, and knock-out mutants of ABFs in Arabidopsis are sensitive to drought stress (Yoshida *et al*., 2015). The sensitivity of mutants might be linked to the repression of stress-responsive genes knock-out mutants under drought stress (Yoshida *et al*., 2010). The role of ABFs in osmotic stress tolerance is also demonstrated in other crops such as rice, wheat, and soybean using a transgenic approach (Nakashima *et al.*, 2009; Joshi *et al.*, 2016; Shinozaki *et al.*, 2003). Overexpression of OsbZIP46, belonging to the ABF family, enhanced drought tolerance in rice

(Tang *et al.*, 2012). Wang *et al.* (2016) showed that overexpression of wheat bZIP protein sharing homology with ABFs resulted in enhanced osmotic stress tolerance in transgenic Arabidopsis plants. Also, Hossain *et al.* (2010a) demonstrated that osabf2 mutant of rice revealed reduced survival and chlorophyll content under osmotic stress compared to wild type. The same group also showed that the *osabf1* knock-out mutant was sensitive to drought and salinity stress Hossain *et al.* (2010b). Likewise, overexpression of ABF2 and ABF3 resulted in multiple stress tolerance as transgenic lines displayed better stress survival, reduced oxidative damage and upregulation of ABA-responsive (Kim *et al.*, 2004a; Kim *et al.*, 2004b). We also made morphological and physiological phenotyping of *hvabf* and *hvabi5* allelic mutants under drought stress. Both barley mutant lines were sensitive to drought compared to wild type. Both *hvabf* and *hvabi5* allelic mutants wilted faster compared to wild type, which was also reflected in tissue water status measure as RWC. Therefore, it will be interesting to measure stomatal conductance and aperture in wild type, *hvabf,* and *hvabi5* mutants under osmotic stress. It was also illustrated that the rate of water loss from the detached leaf of the wild type was slightly reduced than ABF knock-out mutants in Arabidopsis (Yoshida *et al.*, 2010). Similarly, the transpiration rate was reduced in rice lines overexpressing OsbZIP23 under drought stress (Xiang *et al.*, 2008). Although a single gene of bZIP transcription family was knocked-out in *hvabf* and *hvabi5* allelic mutants, a distinct drought susceptible phenotype was observed in the mutants. It has been demonstrated that ABFs form homo and heterodimers for efficient DNA binding. The N-terminus conserved domain with 16 amino acid residue and leucine repeat region have distinct functions. Leucine zipper region is involved in dimerization and basic domain binds to the DNA (Jakoby *et al*., 2002; Vysotskii *et al*., 2013). Therefore, a translational frameshift mutation in *hvabi5* mutant might interfere with the dimerization process blocking the expression of ABA-inducible genes. However, in *hvabf* a single amino acid deleted in predicted HvABF. Furihata *et al*. (2006) showed that single and multi-site substitution of serine to alanine in the phosphorylation domain of AREB1 suppressed the transactivation property of AREB1. Hence, the loss of serine in HvABF might result in the loss of function mutation. However, it requires further investigation using the *in vitro* kinase assay. Transcriptome profiling under drought stress revealed that the number of up and downregulated genes were higher in mutants compared to wild type. Genes involved in organic acid and divalent metal transport was downregulated only in *hvabi5* under drought stress. GO enrichment analysis revealed that among upregulated genes, the biological process involved in stress response was over-represented in wild type compared to *hvabf* and *hvabi5* mutants. Similarly, genes involved in signal transduction and peroxidases were upregulated in the wild type under drought stress. Our results agree with previous findings where stress-responsive genes were upregulated in plants overexpressing ABFs and suppressed in ABF knock-out mutants (Yoshida *et al.*, 2015; Yoshida *et al.*, 2010; Fujita *et al.*,

2005). These results indicated that the function of ABF transcription factors in mediating drought stress tolerance is conserved across the plant species.

To test if *HvAbf* and *HvAbi5* might regulate proline accumulation under drought stress, we measured proline concentration in *hvabf* and *hvabi5* allelic mutants. Schoonheim *et al.* (2009) demonstrated that *HvAbi5* was able to transactivate the reporter gene fused to the ABRC3 complex when co-transfected in barley aleurone cells. We also showed through *in vitro* assay that the *HvP5cs1* promoter is regulated in ABF-dependent manner upon ABA treatment (Muzammil *et al.*, 2018). We discovered that shoot proline level was higher in *hvabf* and *hvabi5* allelic mutants than wild type under drought conditions. Also, proline biosynthetic genes such as *HvP5cs1* and *HvP5cs2* were strongly induced in wild type, *hvabf,* and *hvabi5* allelic mutants. This is different from what has been reported in Arabidopsis where *P5CS1* is stress-inducible, and *P5CS2* serves a house-keeping function (Székely *et al.*, 2008). However, Hur *et al.* (2004) discovered that both *OsP5cs1* and *OsP5cs2* were highly induced under osmotic stress in rice, and *OsP5c1* is a housekeeping gene. Because we did not measure proline in *hvabf* and *hvabi5* under ABA-application due to time constraints, it will be difficult to conclude if *hvabf* and *hvabi5* will differ in proline response under ABA application. Therefore, the systematic evaluation of *hvabf* and *hvabi5* under controlled stress such as external ABA application, moderate and acute water stress should be prioritized.

To summarize, we demonstrated the power of the CRISPR RNA/Cas9 system for gene functional analysis in crops. Besides, the role of ABFs on drought stress adaptation is conserved across the plant species. However, it is necessary to provide experimental evidence on the direct physical interaction between *HvAbf* and *HvAbi5* and ABREs.

3.5. References

Ábrahám, E., Hourton-Cabassa, C., Erdei, L. and Szabados, L. (2010) Methods for determination of proline in plants. In R. Sunkar, ed. Plant stress tolerance. New York: Humana Press, pp. 333-340.

Andrews, S. (2010). FastQC: A quality control tool for high throughput sequence data. Available online at: http://www.bioinformatics.babraham.ac.uk/projects/fastqc/

Bajji, M., Kinet, J.M. and Lutts, S. (2002) The use of the electrolyte leakage method for assessing cell membrane stability as a water stress tolerance test in durum wheat. *Plant Growth Regul.*, **36**, 61–70.

Bartels, D. and Sunkar, R. (2005) Drought and salt tolerance in plants. *CRC. Crit. Rev. Plant Sci.*, **24**, 23–58.

Bates, L.S., Waldren, R.P. and Teare, I.D. (1973) Rapid determination of free proline for water-stress studies. *Plant Soil*, **39**, 205–207.

Belhaj, K., Chaparro-Garcia, A., Kamoun, S., Patron, N.J. and Nekrasov, V. (2015) Editing plant genomes with CRISPR/Cas9. *Curr. Opin. Biotechnol.*, **32**, 76–84.

Benjamini, Y. and Hochberg, Y. (1995) Controlling the false discovery rate: A practical and powerful approach to multiple testing. , **57**, 289–300.

Chen, Y., Lun, A.T.L. and Smyth, G.K. (2016) From reads to genes to pathways: differential expression analysis of RNA-seq experiments using Rsubread and the edgeR quasi-likelihood pipeline. *F1000Research*, **5**, 1438.

Choi, H.I., Hong, J.H., Ha, J.O., Kang, J.Y. and Kim, S.Y. (2000) ABFs, a family of ABA responsive element binding factors. *J. Biol. Chem.*, **275**, 1723–1730.

Dziwornu, A.K., Shrestha, A., Matthus, E., Ali, B., Wu, L. and Frei, M. (2018) Responses of contrasting rice genotypes to excess manganese and their implications for lignin synthesis. *Plant Physiol. Biochem.*, **123**, 252–259.

Finkelstein, R.R., Gampala, S.S.L. and Rock, C.D. (2002) Abscisic acid signaling in seeds and seedlings. *Plant Cell*, **14**, 15–46.

Fujii, H., Chinnusamy, V., Rodrigues, A., et al. (2009) *In vitro* reconstitution of an abscisic acid signalling pathway. *Nature*, **462**, 660–664.

Fujita, Y., Fujita, M. and Satoh, R. (2005) AREB1 is a transcription activator of novel ABRE-dependent ABA signaling that enhances drought stress tolerance in Arabidopsis. *Plant Cell*, **17**, 3470–3488.

Furihata, T., Maruyama, K., Fujita, Y., Umezawa, T., Yoshida, R., Shinozaki, K. and Yamaguchi-Shinozaki, K. (2006) Abscisic acid-dependent multisite phosphorylation regulates the activity of a transcription activator AREB1. *Proc. Natl. Acad. Sci. U. S. A.*, **103**, 1988–1993.

Ghoulam, C., Foursy, A. and Fares, K. (2002) Effects of salt stress on growth, inorganic ions and proline accumulation in relation to osmotic adjustment in five sugar beet cultivars. *Environ. Exp. Bot.*, **47**, 39–50.

Hobo, T., Asada, M., Kowyama, Y. and Hattori, T. (1999) ACGT-containing abscisic acid response element (ABRE) and coupling element 3 (CE3) are functionally equivalent. *Plant J.*, **19**, 679–689.

Hodges, D.M., DeLong, J.M., Forney, C.F. and Prange, R.K. (1999) Improving the thiobarbituric acid-reactive-substances assay for estimating lipid peroxidation in plant tissues containing anthocyanin and other interfering compounds. *Planta*, **207**, 604–611.

Hossain, M.A., Cho, J. Il, Han, M., Ahn, C.H., Jeon, J.S., An, G. and Park, P.B. (2010a) The ABRE-binding bZIP transcription factor OsABF2 is a positive regulator of abiotic stress and ABA signaling in rice. *J. Plant Physiol.*, **167**, 1512–1520.

Hossain, M.A., Lee, Y., Cho, J.I., et al. (2010b) The bZIP transcription factor OsABF1 is an ABA responsive element binding factor that enhances abiotic stress signaling in rice. *Plant Mol. Biol.*, **72**, 557–566.

Hur, J., Jung, K.H., Lee, C.H. and An, G. (2004) Stress-inducible OsP5CS2 gene is essential for salt and cold tolerance in rice. *Plant Sci.*, **167**, 417–426.

Jakoby, M., Weisshaar, B., Dröge-Laser, W., Vicente-Carbajosa, J., Tiedemann, J., Kroj, T. and Parcy, F. (2002) bZIP transcription factors in Arabidopsis. *Trends Plant Sci.*, **7**, 106–111.

Joshi, R., Wani, S.H., Singh, B., Bohra, A., Dar, Z.A., Lone, A.A., Pareek, A. and Singla-Pareek, S.L. (2016) Transcription factors and plants response to drought stress: Current understanding and future directions. *Front. Plant Sci.*, **7**, 1–15.

Kim, J.B., Kang, J.Y. and Soo, Y.K. (2004a) Over-expression of a transcription factor regulating ABA-responsive gene expression confers multiple stress tolerance. *Plant Biotechnol. J.*, **2**, 459–466.

Kim, S., Kang, J.Y., Cho, D.I., Park, J.H. and Soo, Y.K. (2004b) ABF2, an ABRE-binding bZIP factor, is an essential component of glucose signaling and its overexpression affects multiple stress tolerance. *Plant J.*, **40**, 75–87.

Kumar, S., Stecher, G., Li, M., Knyaz, C. and Tamura, K. (2018) MEGA X: Molecular evolutionary genetics analysis across computing platforms. *Mol. Biol. Evol.*, **35**, 1547–1549.

Kumlehn, J., Pietralla, J., Hensel, G., Pacher, M. and Puchta, H. (2018) The CRISPR/Cas revolution continues: From efficient gene editing for crop breeding to plant synthetic biology. *J. Integr. Plant Biol.*, **60**, 1127–1153.

Lawrenson, T., Shorinola, O., Stacey, N., Li, C., Østergaard, L., Patron, N., Uauy, C. and Harwood, W. (2015) Induction of targeted, heritable mutations in barley and *Brassica oleracea* using RNA-guided Cas9 nuclease. *Genome Biol.*, **16**, 258.

Ma, Y., Szostkiewicz, I., Korte, A., Moes, D., Yang, Y., Christmann, A. and Grill, E. (2009) Regulators of PP2C. *Science (80-.).*, **324**, 1064–1069.

Marthe, C., Kumlehn, J. and Hensel, G. (2015) Barley (*Hordeum vulgare* L.) transformation using immature embryos. In *Agrobacterium Protocols: Third Edition*. pp. 71–83.

Marzec, M. and Hensel, G. (2018) Targeted base editing systems are available for plants. *Trends Plant Sci.*, **23**, 955–957.

Muzammil, S., Shrestha, A., Dadshani, S., Pillen, K., Siddique, S., Léon, J. and Naz, A.A. (2018) An ancestral allele of pyrroline-5-carboxylate synthase1 promotes proline accumulation and drought adaptation in cultivated barley. *Plant Physiol.*, **178**, 771–782.

Nakashima, K., Ito, Y. and Yamaguchi-Shinozaki, K. (2009) Transcriptional regulatory networks in response to abiotic stresses in arabidopsis and grasses. *Plant Physiol.*, **149**, 88–95.

Pacher, M. and Puchta, H. (2017) From classical mutagenesis to nuclease-based breeding – directing natural DNA repair for a natural end-product. *Plant J.*, **90**, 819–833.

Pertea, M., Kim, D., Pertea, G.M., Leek, J.T. and Salzberg, S.L. (2016) RNA-seq experiments with HISAT , StringTie and Ballgown. *Nat. Protoc.*, **11**, 1650–1667.

Schoonheim, P.J., Costa Pereira, D. Da and Boer, A.H. De (2009) Dual role for 14-3-3 proteins and ABF transcription factors in gibberellic acid and abscisic acid signalling in barley (*Hordeum vulgare*) aleurone cells. *Plant, Cell Environ.*, **32**, 439–447.

Shinozaki, K. and Yamaguchi-Shinozaki, K. (2006) Gene networks involved in drought stress response and tolerance. *J. Exp. Bot.*, **58**, 221–227.

Shinozaki, K., Yamaguchi-Shinozaki, K. and Seki, M. (2003) Regulatory network of gene expression in the drought and cold stress responses. *Curr. Opin. Plant Biol.*, **6**, 410–417.

Shen, Q., Zhang, P. and Ho, T.H.D. (1996) Modular nature of abscisic acid (ABA) response complexes: composite promoter units that are necessary and sufficient for aba induction of gene expression in barley. *Plant Cell*, **8**, 1107–1 119.

Shen Q., and Ho T.H.D. (1995) Functional dissection of an abscisic acid (ABA)-inducible gene reveals two independent ABA-responsive complexes each containing a G-box and a novel cis-acting element. *Plant Cell*, **7**, 295–307.

Székely, G., Ábrahám, E., Cséplo, Á., et al. (2008) Duplicated P5CS genes of Arabidopsis play distinct roles in stress regulation and developmental control of proline biosynthesis. *Plant J.*, **53**, 11–28.

Tang, N., Zhang, H., Li, X., Xiao, J. and Xiong, L. (2012) Constitutive activation of transcription factor OsbZIP46 improves drought tolerance in rice. *Plant Physiol.*, **158**, 1755–1768.

Tian, T., Liu, Y., Yan, H., You, Q., Yi, X., Du, Z., Xu, W. and Su, Z. (2017) AgriGO v2.0: A GO analysis toolkit for the agricultural community, 2017 update. *Nucleic Acids Res.*, **45**, W122–W129.

Umezawa, T., Nakashima, K., Miyakawa, T., Kuromori, T., Tanokura, M., Shinozaki, K. and Yamaguchi-Shinozaki, K. (2010) Molecular basis of the core regulatory network in ABA responses: Sensing, signaling and transport. *Plant Cell Physiol.*, **51**, 1821–1839.

Uno, Y., Furihata, T., Abe, H., Yoshida, R., Shinozaki, K. and Yamaguchi-Shinozaki, K. (2000) Arabidopsis basic leucine zipper transcription factors involved in an abscisic acid-dependent signal transduction pathway under drought and high-salinity conditions. *Proc. Natl. Acad. Sci.*, **97**, 11632–11637.

Upadhyay, S.K., Kumar, J., Alok, A. and Tuli, R. (2013) RNA-Guided genome editing for target gene mutations in wheat. *G3 Genes, Genomes, Genet.*, **3**, 2233–2238.

Vysotskii, D.A., Vries-van Leeuwen, I.J. de, Souer, E., Babakov, A. V. and Boer, A.H. de (2013) ABF transcription factors of *Thellungiella salsuginea*: Structure, expression profiles and interaction with 14-3-3 regulatory proteins. *Plant Signal. Behav.*, **8**, 64–70.

Wang, J., Li, Q., Mao, X., Li, A. and Jing, R. (2016) Wheat transcription factor TaAREB3 participates in drought and freezing tolerances in Arabidopsis. *Int. J. Biol. Sci.*, **12**, 257–269.

Wang, M., Mao, Y., Lu, Y., Tao, X. and Zhu, J. kang (2017) Multiplex gene editing in rice using the CRISPR-Cpf1 system. *Mol. Plant*, **10**, 1011–1013.

Wang, Xianhang, Tu, M., Wang, D., Liu, J., Li, Y., Li, Z., Wang, Y. and Wang, Xiping (2018) CRISPR/Cas9-mediated efficient targeted mutagenesis in grape in the first generation. *Plant Biotechnol. J.*, **16**, 844–855.

Xiang, Y., Tang, N., Du, H., Ye, H. and Xiong, L. (2008) Characterization of OsbZIP23 as a key player of the basic leucine zipper transcription factor family for conferring abscisic acid sensitivity and salinity and drought tolerance in rice. *Plant Physiol.*, **148**, 1938–1952.

Yoshida, R., Umezawa, T., Mizoguchi, T., Takahashi, S., Takahashi, F. and Shinozaki, K. (2006) The regulatory domain of SRK2E/OST1/SnRK2.6 interacts with ABI1 and integrates abscisic acid (ABA) and osmotic stress signals controlling stomatal closure in Arabidopsis. *J. Biol. Chem.*, **281**, 5310–5318.

Yoshida, T., Fujita, Y., Maruyama, K., Mogami, J., Todaka, D., Shinozaki, K. and Yamaguchi-Shinozaki, K. (2015) Four Arabidopsis AREB/ABF transcription factors function predominantly in gene expression downstream of SnRK2 kinases in abscisic acid signalling in response to osmotic stress. *Plant, Cell Environ.*, **38**, 35–49.

Yoshida, T., Fujita, Y., Sayama, H., Kidokoro, S., Maruyama, K., Mizoi, J., Shinozaki, K. and Yamaguchi-Shinozaki, K. (2010) AREB1, AREB2, and ABF3 are master transcription factors that cooperatively regulate ABRE-dependent ABA signaling involved in drought stress tolerance and require ABA for full activation. *Plant J.*, **61**, 672–685.

Zhou, H., Liu, B., Weeks, D.P., Spalding, M.H. and Yang, B. (2014) Large chromosomal deletions and heritable small genetic changes induced by CRISPR/Cas9 in rice. *Nucleic Acids Res.*, **42**, 10903–10914.

Chapter 4. Role of ABA-responsive element binding factors in proline biosynthesis and drought adaptation in *Arabidopsis thaliana*

4.1. Introduction

Higher plants have evolved several physiological mechanisms to cope with environmental stresses like drought (Shinozaki and Yamaguchi, 2006). Osmotic adjustment by maintaining cell turgidity is one of the critical adaptive measures to accomplish drought tolerance (Bartels and Sunkar, 2005; Szabados and Savouré, 2010; Blum, 2017). To achieve an osmotic balance plant accumulates compatible solutes like proline, soluble sugars, glycine betaine, and low molecular weight organic acids, which are essential to maintain membrane stability and protect macromolecule structure and activity during osmotic stress (Szabados and Savouré, 2010; Forlani *et al.*, 2019). Among those, the accumulation of proline is one of the most apparent responses of plants against drought stress. The primary role of proline is to maintain membrane stability and protect macromolecule structure and activity during osmotic stress (Szabados & Savouré 2010; Forlani *et al.* 2019). Proline also acts as reactive oxygen species (ROS) scavenger or activates the antioxidant like superoxide dismutase, catalases, and peroxidase (Alia and Matysik, 2001; Signorelli *et al.*, 2014; Signorelli *et al.*, 2015). Therefore, understanding the genetic mechanisms modulating proline accumulation is highly essential for its utility in developing drought stress adaptation in plants.

The major genes involved in proline metabolic pathways are well documented. *P5CS1* transcription is considered as a hallmark for cytosolic proline deposition under drought stress conditions. In the past, some research groups studied the genetic regulation of *P5CS1* transcription activity in Arabidopsis (Székely *et al.*, 2008). GUS activity assay of transgenic Arabidopsis plants expressing GUS gene fused to truncated *P5CS1* promoter suggested that MYC binding motif might be critical for *P5CS1* transcription under dehydration (Yoshiba *et al.*, 1999). Later, Jae *et al.* (2005) validated the role of MYB-like transcription factor for the upregulation of *P5CS1* expression *via* Ca^{2+} signaling under salinity in Arabidopsis. In addition, epigenetic control of *P5CS1* was illustrated in a recent study where decreased methylation of chromatin in the ANAC055 promoter in *cau1* mutant was associated with increased the *P5CS1* expression and proline accumulation under dehydration stress (Fu *et al.*, 2018). Apart from osmotic stress, a recent study showed that the MYB-like transcription factor regulates the transcription of *P5CS1* in Arabidopsis seedling exposed to phosphorus deficiency (Aleksza *et al.*, 2017). These data suggest a complex genetic regulation of *P5CS1* transcription and proline accumulation under different stress scenarios.

Drought stress response is generally divided into ABA-dependent and ABA-independent signals (Savouré et al. 1997, Szabados & Savouré 2010). ABA-responsive elements (ABREs) containing ACGT core sequence are one of the critical regulatory elements found in the promoter of osmotic-stress-responsive genes. Also, non-ACGT containing ABREs referred to as coupling elements (CE1 and CE3), are present in clusters with one or more ACGT-containing ABRE in the promoter of ABA-inducible genes and function as a complex (Shen *et al*., 1996). ABREs are the direct target of ABRE binding factors (AREBs/ABFs), which belong to the basic-domain leucine zipper (bZIP) transcription family and transactivates ABA-responsive genes (Fujita *et al.*, 2005; Yoshida *et al.*, 2010; Yoshida *et al.*, 2015). The binding of ABFs (ABF1, ABF2, ABF3 and ABF4) to ABREs was demonstrated through yeast one-hybrid screening and electrophoretic mobility shift assay (Choi *et al*., 2000; Uno *et al.*, 2000). Although ABF transcription factors are a fundamental component of ABA-driven transcription cascade, their role in modulating proline accumulation and proline mediated drought stress adaptation remained enigmatic.

Recently, we isolated a new *HvP5cs1* allele from wild barley that modulated drought-inducible proline accumulation in cultivated barley. Polymorphisms across ABA-responsive element (ABRE) motifs in *HvP5cs1* promoter between wild barley, ISR42-8 and Scarlett explained the variation in drought-inducible shoot proline content. Heterologous expression of *HvP5cs1* promoter:GUS constructs in Arabidopsis protoplast (Col-0) revealed higher activation of wild barley promoter upon ABA treatment compared to Scarlett. However, the promoter activity of ISR42-8 significantly reduced in the protoplast of quadruple mutants of ABF1, AREB1/ABF2, ABF3, and AREB2/ABF4 (*abf1 abf2 abf3 abf4*) upon ABA treatment (Muzammil *et al.*, 2018). Therefore, the present study aimed to dissect the critical role of ABFs in proline biosynthesis under ABA signaling. The availability of quadruple mutant in Arabidopsis was capitalized for phenotypic, biochemical, and molecular screening under external ABA application, acute dehydration, terminal drought and constant drought stress.

4.2. Materials and methods

4.2.1. Plant materials and growth conditions

We used *Arabidopsis thaliana* ecotype Col-0 and quadruple mutant of four ABF transcription factors (*abf1 abf2 abf3 abf4*) in the study. The a*bf1 abf2 abf3 abf4* quadruple mutant was developed in the lab of Prof. Dr. Yamaguchi through genetic crosses between T-DNA insertion lines SALK_043079 (*abf1*), SALK_002984 (*areb1/abf2*), SALK_096965 (*abf3*), SALK_069523 (*areb2/abf4*). Prof. Dr. Yamaguchi kindly provided seeds of *abf1 abf2 abf3 abf4* quadruple

mutant. We analyzed the presence/absence of gene expression by semi-quantitative PCR (Figure S12).

4.2.2. ABA treatment

Seeds were plated in half-strength MS media agar plates (2mM MES and pH 5.7). Plates were stratified at 4°C and transferred to a growth chamber at 22/20°C day/night temperature, 10/14 light/dark period, and 100-150 µmol m^{-2} s^{-1} light intensity. For ABA treatment, 15 d old seedlings were transferred to the semi-solid MS media (0.2% Agar) supplemented with 50 µM ABA (Sigma Aldrich, A1049). For the control condition, seedlings were transferred to semi-solid MS media agar plates without ABA (Figure S13a). We collected fresh samples at 24, 48, 72 and 96 h of ABA treatment. Seedlings were snap-frozen in liquid nitrogen and stored at -80°C before proline measurement and RNA extraction. The experiment was performed in six biological replicates.

4.2.3. Acute dehydration treatment

Seeds were sown in a plastic pot (6cm*6cm*7cm) filled with a peat-based potting mixture, ED73 classic produced and marketed by Einheitserde, Germany. The pots were stratified at 4°C for three days and transferred to the greenhouse. After germination, the seedlings were thinned, maintaining 8 to 10 seedlings per pot. The water level was maintained at 1.5 times the dry weight of the soil. For dehydration, 15 d old seedlings were removed from the pots and soil adhered to the roots were washed off with water. Then, the seedlings were placed above the parafilm. Seedlings placed above wet filter paper were used as control samples (Figure S13b). The samples were collected at 1, 2 and 3 h of dehydration, snap-frozen in liquid nitrogen, and stored at -80°C before proline determination and RNA extraction. The experiment was performed in six biological replicates.

4.2.4. Drought stress treatment in pots

The growing conditions were identical to dehydration treatment. The pots were gradually dehydrated by applying terminal drought to 21-day-old seedlings for one week, and morphological and physiological traits were evaluated. Shoot fresh weight was recorded and dried at 70°C for 24 h before taking the dry weight.

Cell membrane integrity was determined by evaluating electrolyte leakage (EL) based on Bajji *et al*. (2002). Falcon tubes were filled with 10 ml deionized water, and initial electrical conductivity was recorded (ECi). Rosettes were detached and placed in a falcon tube with 10 ml double distilled water and stored in the dark at room temperature. Then, electrical conductivity was measured 24 h of rehydration period (ECf). After the final reading, the

samples were boiled at 100°C for 30 minutes, cooled to room temperature, and total electrical conductivity (ECt) was measured. EL was expressed as (ECf-ECi)/(ECt-ECi)*100. Leaf water status was estimated through relative water content (RWC), according to Ghoulam *et al.* (2002). For RWC measurement, rosettes were detached and the fresh weight was recorded (FW). Then, the rosettes were dipped in a falcon tube filled with 10 ml deionized water for 24 h at room temperature. The rosettes were removed from the falcon tube, and excess water was wiped with a paper towel before taking the turgor weight (TW). Dry weight was recorded after oven drying at 70°C for 24 h. RWC was estimated as (FW-DW)/(TW-DW) *100. The experiment was performed in six biological replicates. Fresh samples were collected, snap-frozen in liquid nitrogen, and stored at -80°C before malondialdehyde (MDA) and proline analysis. The experiment was performed in six biological replicates.

4.2.4.1. Proline determination

Proline was measured from shoot samples, according to Bates *et al.* (1973) adapted to a microplate-based protocol (Ábrahám *et al.*, 2010). In short, seedlings were homogenized in liquid nitrogen, and proline was extracted using 1 ml 3% sulphosalicylic acid followed by centrifuging at 12,000 *g* for 5 minutes. The sample extract was incubated for 1 hour at 96°C with 2.5% ninhydrin and acetic acid at a 1:1:1 ratio. The reaction was stopped on ice, and the proline-ninhydrin reaction product was extracted with 1 ml toluene. The absorbance of chromatophore containing toluene was measured at 520 nm using a microplate reader (TECAN Infinite 200 Pro, TECAN Group Limited, Switzerland). Shoot proline level was determined using a standard curve method and expressed as micrograms per gram fresh weight.

4.2.4.2. Malondialdehyde determination

Oxidative damage of lipid membrane during drought was estimated by determining MDA based concentration using thiobarbituric acid (TBA) method (Hodges *et al.*, 1999) adapted to a microplate-based protocol (Dziwornu *et al.*, 2018) with some modification. Shoot samples were homogenized in liquid nitrogen, and MDA was extracted using 1.5 ml of 0.1% trichloroacetic acid (TCA) followed by centrifuging at 14,000 *g* for 15 minutes at 4°C. Then, 500 µl supernatant was mixed with reaction solution I (0.01% 2,6-di-tert-butyl-4-methyl phenol (BHT) in 20% TCA) and reaction solution II (0.65% TBA, 0.01% BHT in 20% TCA) in a 1:1 ratio. Reaction and sample mix were incubated at 95°C for 30 minutes. The reaction was stopped on ice for five minutes, and the reaction mix was centrifuged at 8000 *g* for 10 minutes at 4°C. The absorbance was measured at 440 nm, 532 nm, and 600 nm using a microplate

reader (TECAN Infinite 200 Pro, TECAN Group Limited, Switzerland). MDA concentration was expressed as nanomoles per gram fresh weight.

4.2.5. Evaluation of shoot growth and rosette morphology under constant drought stress

The above-ground morphology of wild type and the *abf1 abf2 abf3 abf4* quadruple mutant was phenotyped in the GROWSCREEN-FLURO system, according to (Barboza-Barquero *et al.*, 2015). Stratified seeds were pre-germinated, and 7-day-old seedlings were transferred to a pot (6cm*6cm*7cm). Plants were grown under controlled conditions at 22/20°C day/night temperature, 10/14 h light/dark period, and 150 µmol m^{-2} s^{-1} light intensity. Two sets of wild type and the *abf1 abf2 abf3 abf4* quadruple mutant plants were grown in 20 biological replicates in a completely randomized design for control and moderate drought conditions. During the establishment phase of one week after transplanting, plants were grown under well-watered conditions maintaining 60% volumetric moisture content (VMC). At 24 d, when VMC reached 30%, the control pots were rewatered while the irrigation was stopped in drought set. Drought stress was induced by withholding irrigation at 24 d until 36 d after seeding. A constant drought was applied by maintaining 10% VMC. The first measurement was done at 16 d after seeding. Then, three additional measurements were done between 20 d and 23 d after seeding. After 26 d, the measurements were done every day until 30 d and between 33 d and 36 d after seeding. Plants from drought treatment were rewatered at 36 d after seeding when shoot growth was ceased in the *abf1 abf2 abf3 abf4* quadruple mutant. Data were recorded at 40 d and 41 d after seeding to evaluate the recovery process. Plants were harvested to record shoot fresh and dry weight at 41 d after seeding. Projected leaf area, rosette morphology, and growth rate were estimated according to (Barboza-Barquero *et al.* 2015).

4.2.6. *P5CS1* mRNA expression analysis using quantitative RT-PCR

RNA was extracted from ABA and dehydration experiments from control and treatment samples for all time points. Arabidopsis shoots were homogenized in liquid nitrogen, and RNA was extracted using Monarch RNA miniprep kit (New England Biolabs, USA) following the manufacturer's instruction. The RNA concentration and quality were determined by running on 1% Agarose gel and nanodrop (NanoDrop 2000c, Thermo Fischer Scientific, USA) before cDNA synthesis.

cDNA was synthesized using the LunaScript super RT mix (New England Biolabs, USA) following the manufacturer's instruction. Quantitative real-time PCR (qPCR) was performed in 96-well plates using a 7500 fast real-time PCR system (Applied Biosystems, USA). A SYBR

green-based Luna Universal qPCR master mix was used in the assay with three technical replicates per sample. The qPCR run was set to initial denaturation at 95°C for 3 minutes, followed by 40 cycles (95°C for 15 seconds, 60°C for 1 minute). Specific amplification was analyzed using a melt curve (95°C for 15 seconds, 60°C for 1 minute, 95°C for 15 seconds). Relative mRNA expression of *P5CS1* was calculated based on the $2^{-\Delta\Delta Ct}$ method (Livak & Schmittgen 2001). qPCR experiment was performed in three biological replicates. Primers used in for qPCR assay are provided in Table S10.

4.3. Results

We performed *in silico* analysis of DNA binding motif across the promoter of the *P5CS1* gene. The motifs were predicted from plant promoter analysis navigator (PlantPAN 3.0) and plant cis-acting regulatory DNA elements (PLACE) databases. We detected four fundamental categories of regulatory motifs that are targets of ABF, MYC, MYB, and WRKY transcription factors. Notably, three ABREs were present within 500 bp upstream of the start codon of *P5CS1* in Arabidopsis (Figure S14). There are four ABFs (ABF1, AREB1/ABF2, ABF3, and AREB2/ABF4) characterized in Arabidopsis that possess conserved N-terminal and C-terminal (basic leucine zipper) domains (Figure S15). To test the role of ABFs on *P5CS1* expression and proline accumulation, we used *abf1 abf2 abf3 abf4* quadruple mutant and wild type Col-0 and performed a series of experiments such as external ABA application, acute dehydration, terminal drought stress, and constant drought stress.

4.3.1. ABFs are involved in proline accumulation upon ABA treatment in Arabidopsis

As ABFs are driven under ABA signals, first, we evaluated the role of ABFs on proline biosynthesis under external ABA application. Fifteen-day-old seedlings were transferred to semisolid media (0.2%) supplemented with ABA. We measured proline after 24, 48, 72 and 96 h of ABA application in wild type and the *abf1 abf2 abf3 abf4* quadruple mutant. The plants transferred to 0.2% media without external ABA were used as control. Shoot proline concentration in wild type significantly increased already at 24 h of ABA treatment (Table S11). Proline levels increased rapidly with increasing duration of ABA application in wild type. At 96 h of ABA application, shoot proline was six-fold higher in wild type compared to non-treated plants. In contrast, the *abf1 abf2 abf3 abf4* quadruple mutant showed a steady increase in proline with the duration of ABA treatment compared to non-treated plants (Figure 4.1a). In the *abf1 abf2 abf3 abf4* quadruple mutant, a significant difference in proline concentration between ABA treated and non-treated samples were only observed after 72 h. However, the shoot proline levels in wild type were significantly higher than the *abf1 abf2 abf3 abf4* quadruple mutant at all the sampling times (Table S11). Proline concentration was two and three-fold higher in wild type compared to the *abf1 abf2 abf3 abf4* quadruple mutant at 72 and 96 h of ABA application, respectively. Shoot proline concentration did not differ between wild type and the *abf1 abf2 abf3 abf4* quadruple mutant in non-treated conditions (Figure 4.1a and Table S11).

To test if the observed proline accumulation under ABA-application correlates with the activation of *P5CS1*, we evaluated the relative expression of *P5CS1* in wild type and the *abf1 abf2 abf3 abf4* quadruple mutant after 24, 48, 72 and 96 h of ABA application. *P5CS1*

expression was significantly upregulated in wild type upon ABA treatment. Compared to untreated plants, the expression of *P5CS1* in wild type was 7, 15, 18 and 21-fold higher at 24, 48, 72 and 96 h in treated samples, respectively. Also, the *abf1 abf2 abf3 abf4* quadruple mutant showed a significant increase in the expression of *P5CS1* after 48 h. However, the expression level in wild type was around four-fold higher at 24 and 48 h and six-fold higher at 72 and 96 h compared to the *abf1 abf2 abf3 abf4* quadruple mutant in ABA treated samples (Figure 4.1b and Table S11). These data suggest that ABA-application mediates proline biosynthesis in an ABF-dependent manner.

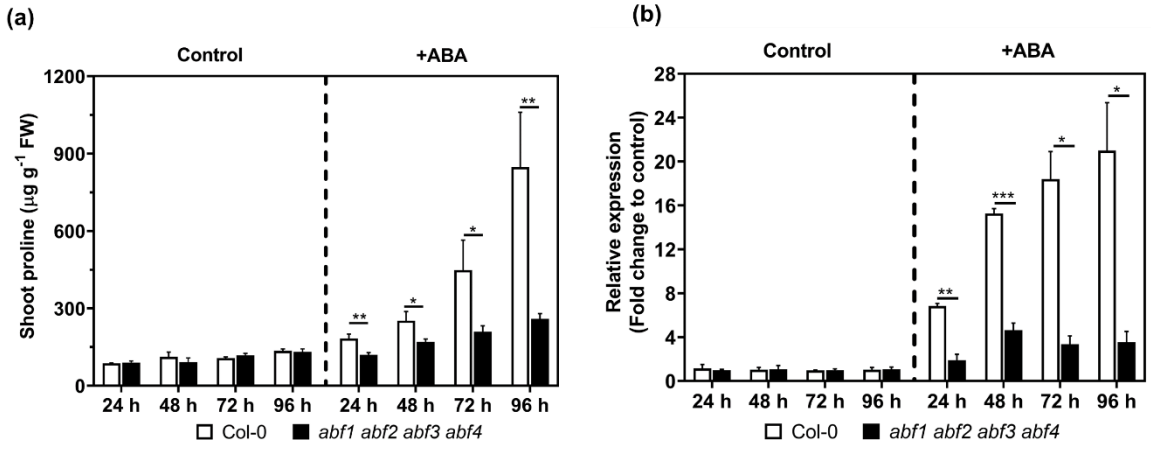

Figure 4.1. Proline accumulation and *P5CS1* expression in response to external ABA application in wild type and the *abf1 abf2 abf3 abf4* quadruple mutant. (a) Shoot proline concentration in Arabidopsis after 24, 48, 72 and 96 h of ABA (50 µM) treatment. Before sampling, 15-day-old seedlings were cultivated on MS medium with and without ABA. The graph represents the mean ± SE (n = 8). (b) Relative mRNA expression of *P5CS1* after 24, 48, 72 and 96 h of ABA treatment. The graph represents mean ± SE (n = 3). Asterisks indicate significant differences between genotypes (**P* ≤ 0.05, ***P* ≤ 0.01, ****P* ≤ 0.001) using student's *t*-test. FW, fresh weight

4.3.2. Proline determination and *P5CS1* expression under acute dehydration

To test the role of ABFs on instantaneous proline synthesis during tissue desiccation, we performed acute dehydration stress and measured *P5CS1* activation and proline concentration in the shoots. Fifteen-day-old Arabidopsis seedlings were placed on the parafilm, and samples were collected at 1, 2 and 3 h after dehydration. Shoot proline concentration significantly increased in wild type after dehydration (Table S12). Proline levels at 1, 2 and 3 h were 1.6, 2.5 and 5 times higher in dehydrated samples in wild type compared to control conditions, respectively (Figure 4.2a). Higher proline levels were also detected in dehydrated shoots of the *abf1 abf2 abf3 abf4* quadruple mutant compared to control plants, although the significant differences can be observed only after 3 h (Table S12). Nevertheless,

the shoot proline concentration was significantly higher in wild type than the *abf1 abf2 abf3 abf4* quadruple mutant after 2 h (25%) and 3 h (63%) of acute dehydration (Figure 4.2a). Similar to ABA treatment, we observed significant upregulation of *P5CS1* upon dehydration in wild type. The relative expression of *P5CS1* in wild type was 2.5 to 4-fold higher compared to the *abf1 abf2 abf3 abf4* quadruple mutant in dehydrated tissues (Figure 4.2b and Table S12). The result indicated that ABF mediated stress-inducible proline accumulation is an instantaneous response of plants to osmotic stress.

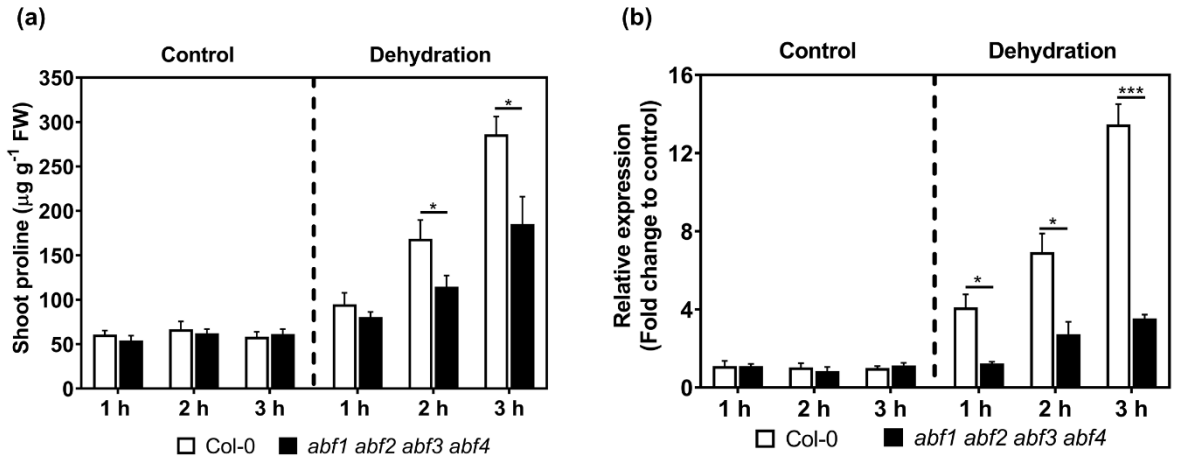

Figure 4.2. Proline accumulation and *P5CS1* expression in response to acute dehydration in wild type and the *abf1 abf2 abf3 abf4* quadruple mutant. (a) Shoot proline concentration in Arabidopsis at 1, 2 and 3 h of acute dehydration. Fifteen-day-old seedlings were removed from the soil and placed over parafilm after washing the roots. The graph represents the mean ± SE (n = 6). (b) Relative mRNA expression of *P5CS1* after 1, 2 and 3 h of acute dehydration. The graph represents the mean ± SE (n = 3). Asterisks indicate significant differences between genotypes (*$P \leq 0.05$, ***$P \leq 0.001$) using student's *t*-test. FW, fresh weight

4.3.3. Variation of proline accumulation and adaptive traits under drought stress

To mimic the natural drought scenario, we evaluated the morphological and physiological response of plants to terminal drought stress. Terminal drought was applied to 21 d old seedlings, and shoot proline concentration was measured at 4, 5, 6 and 7 d after stress treatment. Compared to plants grown under well-watered conditions, proline concentration increased significantly in drought-stressed plants after 5 d (Table S13). At 5 d, shoot proline was significantly higher (2-fold) in wild type compared to the *abf1 abf2 abf3 abf4* quadruple mutant. However, the shoot proline rose to a similar level between wild type and the *abf1 abf2 abf3 abf4* quadruple mutant at 6 d and 7 d under drought stress (Figure 4.3b). The result indicates that ABFs might be critical for early drought stress response concerning proline

biosynthesis. Moreover, the data suggests that under drought stress, both ABA-dependent and ABA-independent pathways are critical for proline accumulation in Arabidopsis.

We also evaluated the morphological and physiological response of the *abf1 abf2 abf3 abf4* quadruple mutant to drought stress. After 7 d of drought stress, wild type did not wilt, whereas the *abf1 abf2 abf3 abf4* quadruple mutant plants showed severe wilting (Figure 4.3a). Shoot fresh and dry weight were measured from plants under control and drought conditions. The growth of the *abf1 abf2 abf3 abf4* quadruple mutant was severely affected by drought compared to wild type (Figure 4.3a). Shoot fresh and dry weight significantly reduced in both wild type and the *abf1 abf2 abf3 abf4* quadruple mutant under drought stress (Table S14). Fresh weight and dry weight were three and two times higher in wild type compared to the *abf1 abf2 abf3 abf4* quadruple mutant after one week of drought (Figure 4.3c and d). Tissue water status measured as RWC decreased in both wild type and the *abf1 abf2 abf3 abf4* quadruple mutant under drought stress (Table S14). However, RWC was 31% percent higher in wild type compared to the *abf1 abf2 abf3 abf4* quadruple mutant (Figure 4.3e). Similarly, the extent of cell membrane integrity estimated as EL increased significantly under drought in both wild type and the *abf1 abf2 abf3 abf4* quadruple mutant (Table S14). However, the extent of cell membrane damage was significant and two-fold higher in the *abf1 abf2 abf3 abf4* quadruple mutant compared to wild type plants grown under water stress (Figure 4.3f). Oxidative stress can be estimated by determining lipid peroxidation in the tissues quantified as malondialdehyde (MDA) concentration (Hodges *et al.* 1999). MDA levels were measured from the fresh tissues harvested one week after drought stress. MDA levels significantly increased in the *abf1 abf2 abf3 abf4* quadruple mutant under drought conditions (Table S14). The concentration was 78% higher in the *abf1 abf2 abf3 abf4* quadruple mutant compared to wild type (Figure 4.3g). These results indicated that ABF transcription factors are vital for drought stress adaptation in Arabidopsis.

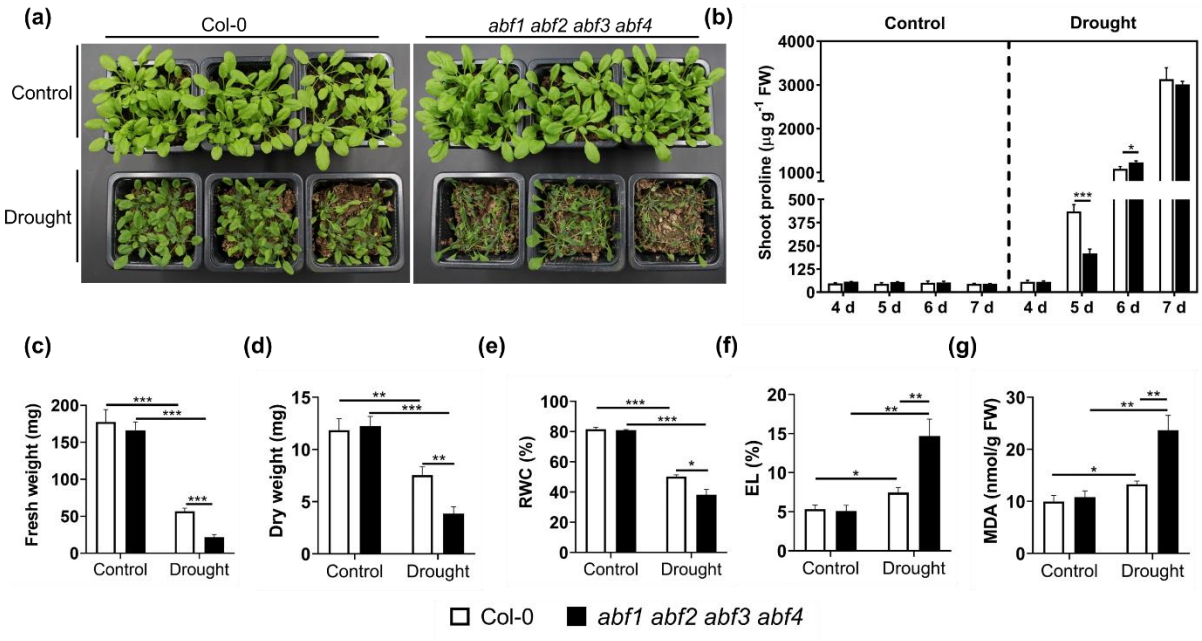

Figure 4.3. Morphological and physiological responses of wild type and the *abf1 abf2 abf3 abf4* quadruple mutant to drought stress. (a) Effect of drought on the growth of wild type and the *abf1 abf2 abf3 abf4* quadruple mutant. (b) Shoot proline concentration at 4, 5, 6 and 7 d after drought stress. Terminal drought was applied to 21-day-old seedlings. Pictures were taken 7 d after the drought using Canon D750. The effect of drought on (c) fresh weight (d) dry weight (e) relative water content (RWC) (f) electrolyte leakage (EL) and (g) malondialdehyde concentration (MDA). The analyses were done in samples collected at 7 d after drought (Bar indicates mean ± SE (n = 6). Asterisks indicate significant differences between genotypes (*$P \leq 0.05$, **$P \leq 0.01$, ***$P \leq 0.001$) using student's *t*-test. FW, fresh weight

4.3.4. High-resolution growth rate analysis under constant drought stress

Plant growth is suppressed under water stress; therefore, the growth rate is one of the crucial markers of plant response to drought. We maintained constant drought stress to test the plant growth under water stress conditions. Two sets of plants of wild type and the *abf1 abf2 abf3 abf4* quadruple mutant were grown in 20 biological replicates in a completely randomized design (Figure 4.4).

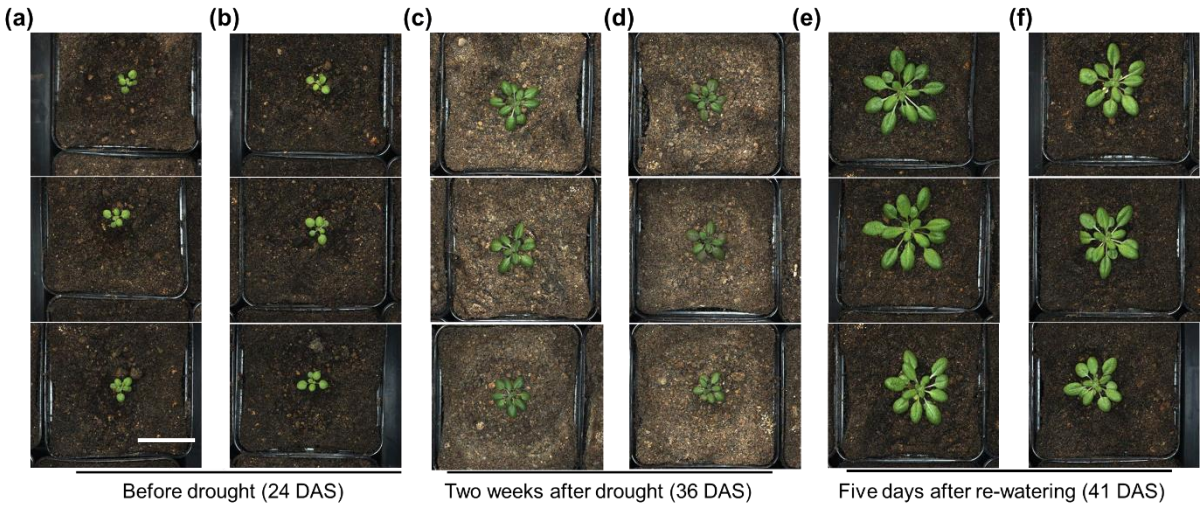

Figure 4.4. Representative pictures of wild type and the *abf1 abf2 abf3 abf4* quadruple mutant during constant drought treatment. The images of three representative plants of (a) Col-0 and (b) *abf1 abf2 abf3 abf4* quadruple mutant at 24 d after sowing (DAS). The images of three representative plants of (c) Col-0 and (d) *abf1 abf2 abf3 abf4* quadruple mutant after at 12 d of drought stress. Watering was stopped at 24 DAS, maintaining 10% volumetric moisture content and the. Images of three representative plants of (e) Col-0 and (f) *abf1 abf2 abf3 abf4* quadruple mutant at 5 d after re-watering. The pots under drought stress were re-watered when the further increase in the projected leaf area was ceased in the *abf1 abf2 abf3 abf4* quadruple mutant at 36 d after stress. The white scale bar corresponds to 30 mm.

One set was grown under well-watered condition (60% VMC). Water stress was applied to another set by withholding watering at 24 d after seeding (10% VMC). Rosette images recorded in the GROWSCREEN-FLURO setup were analyzed to derive different growth-related parameters, including PLA. The growth rate was recorded over the vegetation period, and the pots were rewatered at 36 d after sowing when no further increase in PLA was observed in the *abf1 abf2 abf3 abf4* quadruple mutant. Plant growth rate and rosette morphology were recorded from 16 d to 41 d after sowing. The PLA of the wild type was around 15% lower compared to the *abf1 abf2 abf3 abf4* quadruple mutant at four weeks after seeding in a well-watered condition. In contrast, PLA reduced significantly in the *abf1 abf2 abf3 abf4* quadruple mutant compared to the wild type under water stress (Figure 4.5a and b). At 29 d and 36 d, PLA was 17% and 54% higher in wild type compared to the *abf1 abf2 abf3 abf4* quadruple mutant under drought stress. Plants were rewatered at 36 d after seeding when further growth was ceased in the *abf1 abf2 abf3 abf4* quadruple mutant. After rewatering, both wild type and the *abf1 abf2 abf3 abf4* quadruple mutant recovered at a similar rate and PLA was 45% higher at 41 d in wild type (Figure 4.5a and b). When averaged over the drought period, PLA significantly reduced in both wild type and the *abf1 abf2 abf3 abf4* quadruple

mutant compared to well-watered conditions. However, the PLA of wild type plants was significantly higher than the *abf1 abf2 abf3 abf4* quadruple mutant (Figure S16a).

We also estimated the relative growth rate (RGR) per day for plants grown under control and water-stressed conditions. Under the water stress, RGR decreased in wild type and the *abf1 abf2 abf3 abf4* quadruple mutants compared to the control conditions. Although the RGR was marginally higher in mutants in well-watered pots, wild type maintained remarkably higher shoot growth rate compared to the *abf1 abf2 abf3 abf4* quadruple mutant under moderate water stress (Figure 4.5c and d). At 41 d, plants were harvested for fresh and dry biomass determination. Compared to wild type, the fresh and dry weight of the *abf1 abf2 abf3 abf4* quadruple mutant was marginally higher (15% and 18% respectively) under control conditions. Nevertheless, compared to the wild type, the shoot biomass significantly reduced in mutants under moderate drought conditions. Shoot fresh and dry weight was 47% and 44% higher in wild type compared to the *abf1 abf2 abf3 abf4* quadruple mutant (Figure S16b). The growth rate derived from plant images showed a good correlation with the biomass data.

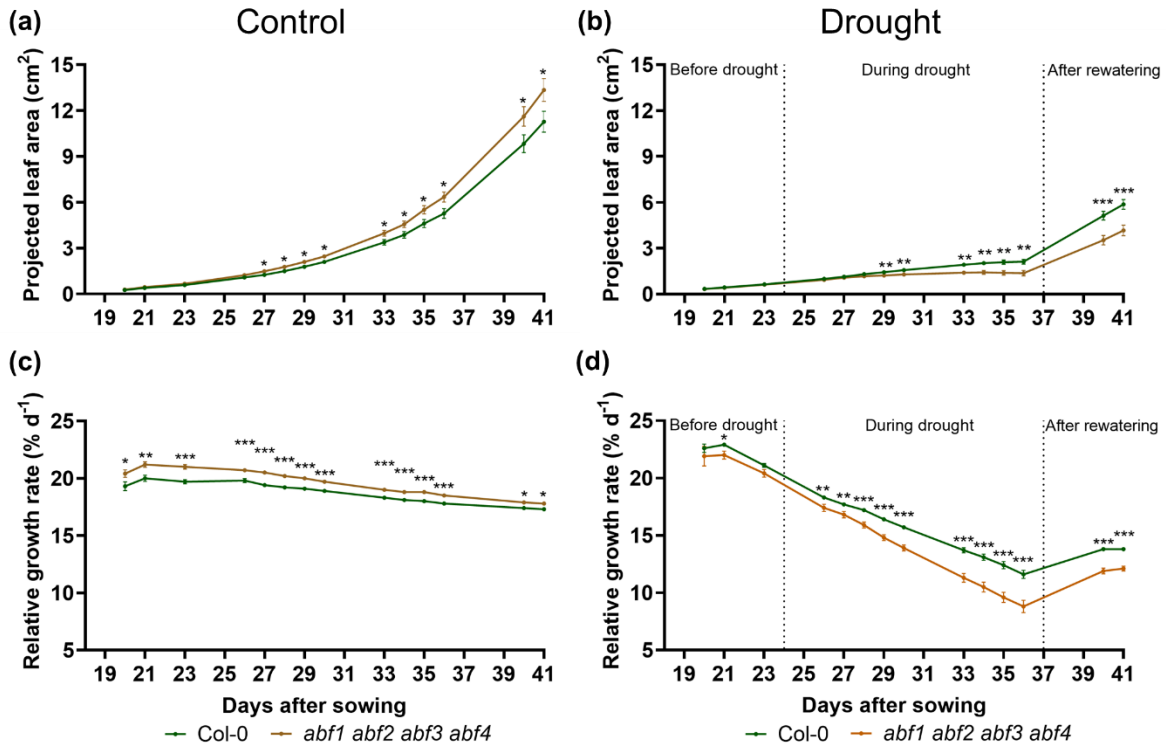

Figure 4.5. Shoot growth of wild type and the *abf1 abf2 abf3 abf4* quadruple mutant under constant drought stress. Projected leaf area (PLA) under (a) control and (b) drought conditions. Watering was stopped at 24 d after seeding, and moderate drought (10% volumetric moisture content) was maintained until 36 d. PLA was recorded every day after drought treatment, and the plants were re-watered when no further increase in PLA was observed under drought conditions. Relative growth rate (RGR) per day under (c) control and (d) drought conditions. RGR per day was estimated by change in PLA between

consecutive days. The points on the line graph represent mean ± SE (n = 20). Asterisks indicate significance difference between genotypes (*$P \leq 0.05$, **$P \leq 0.01$, ***$P \leq 0.001$) using student's *t*-test.

Compared to the wild type, the rosette circumference of the *abf1 abf2 abf3 abf4* quadruple mutant was significantly larger under control conditions (Figure 4.6a). However, rosette circumference significantly decreased in the *abf1 abf2 abf3 abf4* quadruple mutant compared to wild type under water stress (Figure 4.6b). When averaged over the drought period, the rosette circumference decreased in wild type and mutant compared to control conditions (Figure 4.6c). Similarly, the circular size of rosette was bigger in wild type compared to the *abf1 abf2 abf3 abf4* quadruple mutant under drought stress (Figure S17). Also, constant drought resulted in a more compact rosette and petiole size in the *abf1 abf2 abf3 abf4* quadruple mutant, which can be explained by a reduced growth rate (Figure S18e and f). Rosette stockiness and excentricity did not differ under moderate drought stress between wild type and the *abf1 abf2 abf3 abf4* quadruple mutant (Figure S18a-d). In conclusion, the rosette morphology data indicated that the *abf1 abf2 abf3 abf4* quadruple mutant is sensitive to drought stress.

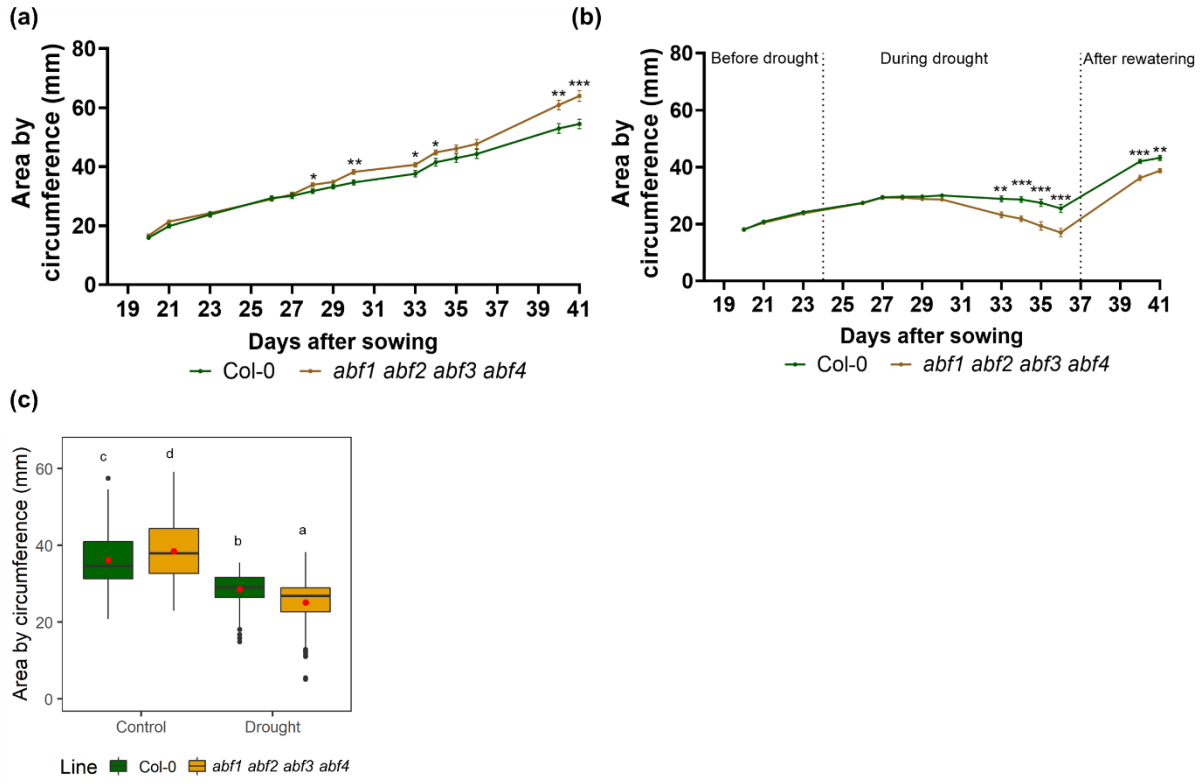

Figure 4.6. Rosette morphology of wild type and the *abf1 abf2 abf3 abf4* quadruple mutant under constant drought stress. Rosette circumference under (a) control and (b) drought conditions. Watering was stopped at 24 d after seeding, and moderate drought (10% volumetric moisture content) was maintained until 36 d. PLA was recorded every day after drought treatment, and the plants were re-watered when no further increase in PLA was observed under drought conditions. The points on the

line graph represent mean ± SE (n = 20). Asterisks indicate significance difference between genotypes (*$P \leq 0.05$, **$P \leq 0.01$, ***$P \leq 0.001$) using student's *t*-test. (c) Boxplot for rosette circumference between 26 d and 36 d (duration of drought). The red dot indicates the mean of the distribution. Indexed letters above the box indicate a significant difference between the genotypes ($P \leq 0.05$) using TukeyHSD test.

4.4. Discussion

The study aimed to evaluate the role of ABF in proline accumulation under different stress scenarios. ABFs belong to the basic-domain leucine zipper (bZIP) transcription family and binds to ABREs to transactivate ABA-responsive genes (Yoshida *et al*. 2010, Yoshida *et al*. 2015). In the present study, we scanned the *P5CS1* promoter region and detected three ABREs within 500 bp upstream of the start codon. Transgenic rice plants transformed with *Vigna aconitifolia VaP5cs* under the control of an ABA-inducible promoter complex (described in Shen *et al*., 1995) accumulated higher proline compared to wild type under osmotic stress (Su and Wu 2004; Zhu *et al*., 1998). Similarly, the proline concentration of transgenic wheat plants transformed with the same construct was 2-fold higher than in wild type under water stress (Vendruscolo *et al*., 2007). Therefore, we measured proline concentration and *P5CS1* expression in the *abf1 abf2 abf3 abf4* quadruple mutant under ABA application and water stress conditions. Stress inducible proline response is generally divided in ABA-dependent and ABA-independent signals (Savouré *et al*., 1997; Szabados and Savouré 2010). Strizhov *et al.* (1997) reported that *P5CS1* mRNA was not induced by salt stress in ABA deficient mutant *aba1-1*. They also evaluated the knock-out mutant of ABA insensitive 1 (ABI1) and found that *P5CS1* mRNA expression was 2-fold higher in wild type than *abi1-1* under salt stress. However, the *P5CS1* mRNA level was similar between the wild type and other ABI mutants (*abi2-1* and *abi3-1*). Also, Savouré *et al.* (1997) found that proline accumulation was reduced in *aba1-1* and *abi1-1* compared to wild type under salt stress. Verslues and Bray (2006) reported reduced proline accumulation in *abi1-1* compared to wild type under low water stress. Also, Sharma and Verslues (2010) discovered that proline accumulation was reduced by 2-fold in another ABA deficient mutant *aba2-1*. Taken together, the ABA-driven signal for proline induction is controlled by ABA insensitive 1 (ABI1) regulatory pathway in Arabidopsis. ABI1 belongs to protein phosphatase 2C and controls the ABA responsiveness in reproductive and vegetative tissues (Gosti *et al.*, 1999; Rodriguez *et al.*, 1998). Uno *et al*. (2000) found that ABI1 and ABI2 are required for the full activation of ABFs. We observed that the rhizosphere application of ABA resulted in increased induction of *P5CS1* mRNA and subsequent proline accumulation in wild type compared to the *abf1 abf2 abf3 abf4* quadruple mutant. Similar to ABA treatment, the *P5CS1* transcription and consequential proline accumulation in dehydrated shoots were significantly higher in wild type compared to the *abf1 abf2 abf3 abf4* quadruple mutant under acute dehydration. Under, terminal drought, we observed that wild

type accumulated less proline compared to the *abf1 abf2 abf3 abf4* quadruple mutant at the earlier stage of terminal drought. However, the shoot proline content swelled to a comparable level between wild type and the *abf1 abf2 abf3 abf4* quadruple mutant at later stages of drought stress. It has been suggested that that chemical drought signaling under ABA might control the initial drought stress response (Schachtman and Goodger, 2008). Our data also imply that the ABA-dependent pathway might dominate drought-inducible proline biosynthesis at the earlier stage of drought stress. At a later stage, both ABA-dependent and ABA-independent pathways are critical for proline accumulation. Altogether, this study submits evidence that ABFs are the key regulators of proline accumulation under ABA signaling in Arabidopsis.

The sensitivity of the *abf1 abf2 abf3 abf4* quadruple mutant to drought was demonstrated by Yoshida *et al*. (2015). However, they only evaluated the number of surviving plants after drought recovery. The *abf* mutants of Arabidopsis also maintained a slightly higher transpiration rate under drought stress (Kim *et al*., 2004; Yoshida *et al*., 2010). In the current study, we made a series of morphological and biochemical measurements to assess the role of ABFs in drought tolerance in Arabidopsis. Wild type revealed diminished membrane damage and oxidative stress and improved tissue turgidity compared to the *abf1 abf2 abf3 abf4* quadruple mutant. Also, the *abf1 abf2 abf3 abf4* quadruple mutant wilted earlier than wild type under terminal drought. At the earlier stage, the shoot proline concentration in wild type was two-fold higher compared to quadruple mutant, which might trigger early damage to cell machinery in low proline accumulating *abf1 abf2 abf3 abf4* quadruple mutant. Previous studies have also demonstrated that proline accumulation correlated with reduced oxidative damage during osmotic stress (Alia and Matysik 2001; Hong *et al.*, 2000; Verslues and Bray, 2004; Ghaffari *et al.*, 2019). Proline contributes to ROS scavenging directly by non-enzymatic ROS detoxification or through the activation of the antioxidant pathway (Alia and Matysik 2001; Signorelli *et al.*, 2014; Signorelli *et al.*, 2015). Furthermore, exogenous proline application during osmotic stress contributes to reduced oxidative damage and improved biomass production (Hassine *et al.*, 2008; Székely *et al.*, 2008; Sripinyowanich *et al.*, 2013). On the other hand, transcriptome analysis revealed that several stress-inducible genes, late embryogenesis abundant and dehydrin family, were suppressed in the *abf1 abf2 abf3 abf4* quadruple mutant under osmotic stress (Yoshida *et al*., 2015). Therefore, it is more likely that the drought sensitivity is caused by the suppression of downstream stress-responsive genes than a modest difference in proline concentration between wild type and the *abf1 abf2 abf3 abf4* quadruple mutant. Additionally, we performed a non-destructive measurement of growth-related parameters using a fluorescence-based screening system, GROWSCREEN FLUORO (Jansen *et al.*, 2009). This approach was successfully utilized to dissect the differences in the

growth rate of Arabidopsis accessions under controlled drought environments (Barboza-Barquero *et al.*, 2015; Jansen *et al.*, 2009; Bangash *et al.*, 2019). Under well-watered conditions, RGR and PLA were similar or higher in the *abf1 abf2 abf3 abf4* quadruple mutant compared to wild type. Yoshida *et al.* (2015) reported that flowering is delayed in the *abf1 abf2 abf3 abf4* quadruple mutant and produced more rosettes than wild type before bolting. Arabidopsis is a facultative long-day plant, and a long day promotes flowering while a short day (below 12 h of light) delays flower initiation (Pouteau and Albertini, 2009). Because the experiment was performed under short-day conditions (10 h), it might have caused the increased RGR and PLA in the quadruple mutant compared to wild type cultivated under control condition. However, wild type maintained superior RGR and PLA of rosette compared to the *abf1 abf2 abf3 abf4* quadruple mutant under drought stress. Besides, constant water stress resulted in suppression of the rosette morphological traits such as circle size and area by circumference in the *abf1 abf2 abf3 abf4* quadruple mutant compared to wild type. The rosette morphology data indicated that the *abf1 abf2 abf3 abf4* quadruple mutant was susceptible to water stress.

In conclusion, our study provided new insights into the role of ABFs in proline biosynthesis at different drought scenarios in Arabidopsis. The results of the ABA-application experiment indicated that ABFs are the major transcriptional regulators of proline biosynthesis under the chemical stimulus at an early stage of drought-related stress. Likewise, proline biosynthesis under acute dehydration was comparable to ABA-treatment, indicating that ABA-mediated chemical signaling seems the earliest response against drought stress. The dynamics of proline accumulation under terminal drought suggested that the ABA-driven ABFs perhaps regulate earlier response to proline accumulation under water stress. However, under severe drought stress, proline regulation might be influenced by ABA-independent transcriptional components. Comparisons of transcription response, proline expression and phenotypic (adaptive) responses suggested that early proline accumulation seems critical for stress adaptation. This study provides strong evidence that ABFs are one of the transcriptional regulators of stress-inducible *P5CS1* activation and subsequent proline accumulation.

4.5. References

Ábrahám, E., Hourton-Cabassa, C., Erdei, L. and Szabados, L. (2010) Methods for determination of proline in plants. In R. Sunkar, ed. Plant stress tolerance. New York: Humana Press, pp. 333-340.

Aleksza, D., Horváth, G. V., Sándor, G. and Szabados, L. (2017) Proline accumulation is regulated by transcription factors associated with phosphate starvation. *Plant Physiol.*, **175**, 555–567.

Alia, M.P. and Matysik, J. (2001) Effect of proline on the production of singlet oxygen. *Amino Acids*, **21**, 195–200.

Bajji, M., Kinet, J.M. and Lutts, S. (2002) The use of the electrolyte leakage method for assessing cell membrane stability as a water stress tolerance test in durum wheat. *Plant Growth Regul.*, **36**, 61–70.

Bangash, S.A.K., Müller-Schüssele, S.J., Solbach, D., Jansen, M., Fiorani, F., Schwarzländer, M., Kopriva, S. and Meyer, A.J. (2019) Low-glutathione mutants are impaired in growth but do not show an increased sensitivity to moderate water deficit. *PLoS One*, **14**, 1–19.

Barboza-Barquero, L., Nagel, K.A., Jansen, M., *et al*. (2015) Phenotype of *Arabidopsis thaliana* semi-dwarfs with deep roots and high growth rates under water-limiting conditions is independent of the GA5 loss-of-function alleles. *Ann. Bot.*, **116**, 321–331.

Bartels, D. and Sunkar, R. (2005) Drought and Salt Tolerance in Plants. *CRC. Crit. Rev. Plant Sci.*, **24**, 23–58.

Bates, L.S., Waldren, R.P. and Teare, I.D. (1973) Rapid determination of free proline for water-stress studies. *Plant Soil*, **39**, 205–207.

Blum, A. (2017) Osmotic adjustment is a prime drought stress adaptive engine in support of plant production. *Plant Cell Environ.*, **40**, 4–10.

Choi, H.I., Hong, J.H., Ha, J.O., Kang, J.Y. and Kim, S.Y. (2000) ABFs, a family of ABA responsive element binding factors. *J. Biol. Chem.*, **275**, 1723–1730.

Dziwornu, A.K., Shrestha, A., Matthus, E., Ali, B., Wu, L. and Frei, M. (2018) Responses of contrasting rice genotypes to excess manganese and their implications for lignin synthesis. *Plant Physiol. Biochem.*, **123**, 252–259.

Forlani, G., Trovato, M., Funck, D. and Signorelli, S. (2019) Regulation of proline accumulation and its molecular and physiological functions in stress defence. In M. A. Hossain, V. Kumar, D. J. Burritt, M. Fujita, and P. S. A. Mäkelä, eds. *Osmoprotectant*-mediated abiotic stress tolerance in plants: recent advances and future perspectives. Cham: Springer International Publishing, pp. 73–97.

Fu, Y., Ma, H., Chen, S., Gu, T. and Gong, J. (2018) Control of proline accumulation under drought via a novel pathway comprising the histone methylase CAU1 and the transcription factor ANAC055. *J. Exp. Bot.*, **69**, 579–588.

Fujita, Y., Fujita, M. and Satoh, R. (2005) AREB1 is a transcription activator of novel ABRE-dependent ABA signaling that enhances drought stress tolerance in Arabidopsis. *Plant Cell*, **17**, 3470–3488.

Ghaffari, H., Tadayon, M.R., Nadeem, M., Cheema, M. and Razmjoo, J. (2019) Proline-mediated changes in antioxidant enzymatic activities and the physiology of sugar beet under drought stress. *Acta Physiol. Plant.*, **41**, 1–13.

Ghoulam, C., Foursy, A. and Fares, K. (2002) Effects of salt stress on growth, inorganic ions and proline accumulation in relation to osmotic adjustment in five sugar beet cultivars. *Environ. Exp. Bot.*, **47**, 39–50.

Gosti, F., Beaudoin, N., Serizet, C., Webb, A.A.R., Vartanian, N. and Giraudat, J. (1999) ABI1 protein phosphatase 2C is a negative regulator of abscisic acid signaling. *Plant Cell*, **11**, 1897–1909.

Hassine, A. Ben, Ghanem, M.E., Bouzid, S. and Lutts, S. (2008) An inland and a coastal population of the Mediterranean xero-halophyte species *Atriplex halimus* L. differ in their ability to accumulate proline and glycinebetaine in response to salinity and water stress. *J. Exp. Bot*., **59**, 1315–1326.

Hodges, D.M., DeLong, J.M., Forney, C.F. and Prange, R.K. (1999) Improving the thiobarbituric acid-reactive-substances assay for estimating lipid peroxidation in plant tissues containing anthocyanin and other interfering compounds. *Planta*, **207**, 604–611.

Hong, Z., Lakkineni, K., Zhang, Z. and Verma, D.P.S. (2000) Removal of feedback inhibition of Δ1-pyrroline-5-carboxylate synthetase results in increased proline accumulation and protection of plants from osmotic stress. *Plant Physiol.*, **122**, 1129–1136.

Jae, H.Y., Chan, Y.P., Jong, C.K., *et al*. (2005) Direct interaction of a divergent CaM isoform and the transcription factor, MYB2, enhances salt tolerance in Arabidopsis. *J. Biol. Chem.*, **280**, 3697–3706.

Jansen, M., Gilmer, F., Biskup, B., *et al*. (2009) Simultaneous phenotyping of leaf growth and chlorophyll fluorescence via Growscreen Fluoro allows detection of stress tolerance in *Arabidopsis thaliana* and other rosette plants. *Funct. Plant Biol.*, **36**, 902–914.

Kim, S., Kang, J.Y., Cho, D.I., Park, J.H. and Soo, Y.K. (2004) ABF2, an ABRE-binding bZIP factor, is an essential component of glucose signaling and its overexpression affects multiple stress tolerance. *Plant J.*, **40**, 75–87.

Livak K.J., Schmittgen T.D. (2001) Analysis of relative gene expression data using real-time quantitative PCR and the 2CT method. *Methods*, **25**: 402–408.

Muzammil, S., Shrestha, A., Dadshani, S., Pillen, K., Siddique, S., Léon, J. and Naz, A.A. (2018) An ancestral allele of pyrroline-5-carboxylate synthase1 promotes proline accumulation and drought adaptation in cultivated barley. *Plant Physiol.*, **178**, 771–782.

Pouteau, S. and Albertini, C. (2009) The significance of bolting and floral transitions as indicators of reproductive phase change in Arabidopsis. J. Exp. Bot., 60, 3367–3377.

Rodriguez, P.L., Benning, G. and Grill, E. (1998) ABI2, a second protein phosphatase 2C involved in abscisic acid signal transduction in Arabidopsis. *FEBS Lett.*, **421**, 185–190.

Savouré, A., Hua, X.J., Bertauche, N., Montagu, M. Van and Verbruggen, N. (1997) Abscisic acid-independent and abscisic acid-dependent regulation of proline biosynthesis following cold and osmotic stresses in *Arabidopsis thaliana*. *Mol. Gen. Genet.*, **254**, 104–109.

Schachtman, D.P. and Goodger, J.Q.D. (2008) Chemical root to shoot signaling under drought. *Trends Plant Sci.*, **13**, 281–287.

Sripinyowanich, S., Klomsakul, P., Boonburapong, B., Bangyeekhun, T., Asami, T., Gu, H., Buaboocha, T. and Chadchawan, S. (2013) Exogenous ABA induces salt tolerance in indica rice (*Oryza sativa* L.): The role of OsP5CS1 and OsP5CR gene expression during salt stress. *Environ. Exp. Bot.*, **86**, 94–105.

Sharma, S. and Verslues, P.E. (2010) Mechanisms independent of abscisic acid (ABA) or proline feedback have a predominant role in transcriptional regulation of proline metabolism during low water potential and stress recovery. *Plant, Cell Environ.*, **33**, 1838–1851.

Shen, Q. and Ho, T.H. D. (1995) Functional dissection of an abscisic acid (ABA)-inducible gene reveals two independent ABA-responsive complexes each containing a G-box and a novel cis-acting element. *Plant Cell*, **7**, 295–307.

Shen, Q., Zhang, P. and Ho, T.H.D. (1996) Modular nature of abscisic acid (ABA) response complexes: composite promoter units that are necessary and sufficient for ABA induction of gene expression in barley. *Plant Cell*, **8**, 1107–1 119.

Shinozaki, K. and Yamaguchi-Shinozaki, K. (2006) Gene networks involved in drought stress response and tolerance. *J. Exp. Bot.*, **58**, 221–227.

Signorelli, S., Coitiño, E.L., Borsani, O. and Monza, J. (2014) Molecular mechanisms for the reaction between •OH radicals and proline: Insights on the role as reactive oxygen species scavenger in plant stress. *J. Phys. Chem. B.*,**118**, 37–47.

Signorelli, S., Dans, P.D., Coitiño, E.L., Borsani, O. and Monza, J. (2015) Connecting proline and γ-aminobutyric acid in stressed plants through non-enzymatic reactions. *PLoS One*, **10**, 1–14.

Strizhov, N., Abrahám, E., Okrész, L., Blickling, S., Zilberstein, A., Schell, J., Koncz, C. and Szabados, L. (1997) Differential expression of two P5CS genes controlling proline accumulation during salt-stress requires ABA and is regulated by ABA1, ABI1 and AXR2 in Arabidopsis. *Plant J.*, **12**, 557–569.

Su, J. and Wu, R. (2004) Stress-inducible synthesis of proline in transgenic rice confers faster growth under stress conditions than that with constitutive synthesis. *Plant Sci*., 166, 941–948.

Szabados, L. and Savouré, A. (2010) Proline: a multifunctional amino acid. *Trends Plant Sci.*, **15**, 89–97.

Székely, G., Ábrahám, E., Cséplo, Á., *et al*. (2008) Duplicated P5CS genes of Arabidopsis play distinct roles in stress regulation and developmental control of proline biosynthesis. *Plant J.*, **53**, 11–28.

Uno, Y., Furihata, T., Abe, H., Yoshida, R., Shinozaki, K. and Yamaguchi-Shinozaki, K. (2000) Arabidopsis basic leucine zipper transcription factors involved in an abscisic acid-dependent signal transduction pathway under drought and high-salinity conditions. *Proc. Natl. Acad. Sci.*, **97**, 11632–11637.

Vendruscolo, E.C.G., Schuster, I., Pileggi, M., Scapim, C.A., Molinari, H.B.C., Marur, C.J. and Vieira, L.G.E. (2007) Stress-induced synthesis of proline confers tolerance to water deficit in transgenic wheat. *J. Plant Physiol.*, **164**, 1367–1376.

Verslues, P.E. and Bray, E.A. (2006) Role of abscisic acid (ABA) and *Arabidopsis thaliana* ABA-insensitive loci in low water potential-induced ABA and proline accumulation. *J. Exp. Bot.*, **57**, 201–212.

Yoshiba, Y., Nanjo, T., Miura, S., Yamaguchi-Shinozaki, K. and Shinozaki, K. (1999) Stress-responsive and developmental regulation of Δ1-Pyrroline-5-carboxylate synthetase 1 (P5CS1) gene expression in *Arabidopsis thaliana*. *Biochem. Biophys. Res. Commun.*, **261**, 766–772.

Yoshida, T., Fujita, Y., Maruyama, K., Mogami, J., Todaka, D., Shinozaki, K. and Yamaguchi-Shinozaki, K. (2015) Four Arabidopsis AREB/ABF transcription factors function predominantly in gene expression downstream of SnRK2 kinases in abscisic acid signalling in response to osmotic stress. *Plant, Cell Environ.*, **38**, 35–49.

Yoshida, T., Fujita, Y., Sayama, H., Kidokoro, S., Maruyama, K., Mizoi, J., Shinozaki, K. and Yamaguchi-Shinozaki, K. (2010) AREB1, AREB2, and ABF3 are master transcription factors that cooperatively regulate ABRE-dependent ABA signaling involved in drought stress tolerance and require ABA for full activation. *Plant J.*, **61**, 672–685.

Zhu, B., Su, J., Chang, M., Verma, D.P.S., Fan, Y.L. and Wu, R. (1998) Overexpression of a Δ1-pyrroline-5-carboxylate synthetase gene and analysis of tolerance to water- and salt-stress in transgenic rice. *Plant Sci*., **139**, 41–48.

Chapter 5. General discussion

5.1. Exotic allele of *HvP5cs1* mediates proline accumulation and drought adaptation in barley

In the current work, we did the functional characterization of an exotic allele of *HvP5cs1* from wild barley, ISR42-8, and identified novel variants of *cis*-elements that might regulate *HvP5cs1* transcription (chapter 2). Then, we generated genetic materials through the site-directed mutagenesis of possible *trans*-acting elements using the CRISPR RNA/Cas9 tool in barley (chapter 3). Finally, based on the results of chapter 2, we investigated the role of ABFs in Arabidopsis as a proof of concept (chapter 4).

We started with the positional cloning of previously identified QTL (*QPro.S42-1H*) for proline accumulation in barley. A series of markers were developed across the QTL interval, which helped to delimit the region to a single gene, *HvP5cs1,* using a high-resolution population derived from S42IL-143. It has been shown in several studies that P5CS1 catalyzes the rate-limiting step of reduction of glutamate to proline in plants, especially under stress conditions (Szabados and Savouré, 2010). A marker developed on the *HvP5cs1* promoter region cosegregated with proline concentration measured in the recombinants indicating the *cis*-regulation. In fact, we identified mutations across ABRE and related elements across the *HvP5cs1* promoter in barley accessions. No barley genotype (wild or cultivars) accumulated more proline than ISR42-8. Heterologous expression analysis of *HvP5cs1* promoter from ISR42-8 and Scarlett also confirmed that wild barley promoter was highly responsive to ABA and regulated in ABF-dependent manner. Several studies demonstrated the role of ABA in proline induction. For instance, ABA application successfully induced proline accumulation in barley and rice leaf (Chou *et al.*, 1991; Pesci 1987, Stewart *et al.*, 1986). Also, in maize seedling, drought stress and ABA application induced proline accumulation in root tissues (Dallmier and Stewart, 1992). Therefore, as described in chapter 4, we utilized the *abf1 abf2 abf3 abf4* quadruple mutant in Arabidopsis to understand the role of ABFs on proline accumulation. Shoot proline accumulation, and *P5CS1* expression was impaired in the *abf1 abf2 abf3 abf4* quadruple mutant compared to wild type upon ABA application, which was a proof of concept that ABFs are the possible regulators of ABA-driven proline biosynthesis in plants. Drought stress response is a complex process that involves ABA-dependent and ABA-independent signal transduction and significant cross-talk between the two pathways (Shinozaki and Yamaguchi-Shinozaki, 2006). It was also reflected in the result of chapter 4 where proline levels did not differ between wild type and the *abf1 abf2 abf3 abf4* quadruple

under severe drought stress. These results also explained our observation of allele mining experiment in barley. The proline level under drought was 5-fold higher than control conditions in the lowest proline accumulating accession, HOR9840. It carried multiple mutations across ABREs and MYB binding motifs in *HvP5cs1* promoter. Other *cis*-acting elements such as MYC, WRKY, and DRE elements were present in a highly conserved 5′ untranslated region of *HvP5cs1* in all barley accessions (Figure S19). These observations suggested that proline accumulation under drought stress is a complex trait regulated by multiple *cis*- and *trans*-acting elements. Furthermore, wild barley, ISR42-8 harbors a unique promoter allele that regulates elevated *HvP5cs1* expression and proline accumulation compared to other barley accessions tested in the study. In chapter 3, we targeted putative *trans*-acting elements that might be involved in ABA-driven proline biosynthesis in barley using the CRISPR RNA/Cas9 system. Targeted base-editing was observed in HORVU3Hr1G084360 (*HvAbi5*) and HORVU6Hr1G080670 (*HvAbf*). Therefore, *hvabi5* and *hvabf* can be used in future experiments to understand how HvABFs regulate proline accumulation in barley.

In chapter 2, we also evaluated the proline-mediated drought stress adaptation in NIL-143. The positive effect of accumulated proline in stressed plants is often linked to osmotic adjustment (OA). However, very few studies attempted to check if the proline levels in the cells are biologically significant to reduce the osmotic potential of cytosol preventing efflux of water. Kishor *et al.* (1995) showed that compared to wild type, transgenic Arabidopsis plants overexpressing *VaP5cs* gene of *Vigna aconitifolia* accumulated 10 to 18-fold more proline under osmotic stress. They estimated the osmotic potential of cell sap and found the solute potential was lower in the over-expression line than wild type, which does not support the hypothesis of proline role in OA. A comprehensive study on maize showed the OA capacity of proline where a maize hybrid maintained low water potential in the root apex, preventing the outward flow of water under moderate osmotic stress (Sharp *et al.*, 1990; Voetberg and Sharp, 1991). They found that proline accumulated in very high concentration in the root apex under which contributed 50% OA in the region. Many researchers often estimate the tissue water status through relative water content (RWC), which is proportional to the OA in the stressed tissue. We also estimated the OA capacity of high proline accumulating NIL-143 through RWC measurement. Although proline accumulation in NIL-143 was two-fold higher than Scarlett, a minor improvement in RWC was observed in NIL-143. Nevertheless, NIL-143 maintained superior transpiration and photosynthesis rate sustaining marginally higher RWC compared to Scarlett under drought stress. These results might be accounted for improved OA.

Another widely accepted function of proline is its effectiveness in serving as a molecular chaperon and reactive oxygen species (ROS) scavenging. Transgenic tobacco plants transformed with *VaP5cs1* under the control of native promoter accumulated 2-fold more

proline and showed salt tolerance by reduced oxidative damage, higher germination rate, and plant vigor (Hong *et al.*, 2000). Similarly, Zhang *et al.* (2015) demonstrated that soybean plant overexpressing *VaP5cs1* resulted in enhanced salt tolerance by producing more biomass and reduced oxidative damage. Also, in our study, the malondialdehyde (MDA) level was slightly lower in NIL-143 compared to Scarlett under stress conditions. In addition, we observed a significant difference in membrane stability between NIL-143 and Scarlett under drought conditions. The other distinct advantage of proline was observed in the slow and reduced degradation of photosynthetic pigments, such as chlorophyll and carotenoids in NIL-143, compared to Scarlett. As superior pigment retention under stress was the most stable trait in NIL-143 across different stress environments (growth chamber and field) and growth stages (vegetative and reproductive), the oxidative stress measurement in NIL-143 and Scarlett should be revisited. Measurement of a wide range of ROS and enzymatic ROS scavenging systems should be prioritized. Also, *in vitro* assay in cell cultures derived from Scarlett and NIL-143 will contribute to the understanding of the mechanism behind superior protective features gained in NIL-143. Because ROS has a damaging effect on multiple cellular components (Mittler, 2002), it will be essential to analyze traits, such as mitochondrial and nuclear DNA integrity, in addition to lipid peroxidation. Also, *in vitro* assay in cell cultures derived from Scarlett and NIL-143 will contribute to the understanding of the mechanism behind superior protective features gained in NIL-143. Furthermore, NIL-143 was able to maintain a better photosynthesis rate than Scarlett at the vegetative and reproductive stages under drought conditions. The fact that stress-inducible proline biosynthesis is localized to chloroplast further validate the significance of inflated P5CS1 and P5CR activity to protect the chlorophyll pigment, chloroplast structures and photosynthetic health under stress condition (Székely *et al.*, 2008; Szoke *et al.*, 1992). Through repeated experiments, we demonstrated that the recovery rate in NIL-143 was superior to Scarlett. So far, the assumption is that more proline in NIL-143 translates to more energy generation for growth resumption as the genetic loci controlling proline degradation should be the same in both NIL-143 and Scarlett. Yet, it is necessary to confirm this as both proline catabolism proteins are present in chromosome 1, and *HvP5cdh* is very close to QTL interval (*QPro.S42-1H*). This unique adaptive advantage of *QPro.S42-1H* during stress and after stress release translated into yield performance, where NIL-143 surpassed Scarlett for yield attributing traits under field drought conditions. Traits such as grain size, grain number per ear, gain per plant, and harvest index were enhanced in NIL-143 compared to Scarlett. Although our study demonstrated a positive correlation between stress adaptation and proline accumulation, the molecular mechanism of proline-mediated stress tolerance requires further investigation. The next step might prioritize understanding the subcellular localization of accumulated proline. As excess proline might be phytotoxic, it will be necessary to understand how the proline synthesized in the chloroplast is distributed

across the cell organelles. Besides, the functional complementation test in Scarlett using ISR42-8 promoter:*HvP5cs1 (pISR:HvP5cs1)* construct might provide the necessary proof of the functional significance of *pISR:HvP5cs1*.

Nevertheless, our study is one of the very rare, if not the first instance in plant breeding, where a natural allele controlling elevated stress-inducible proline accumulation is introgressed in a cultivar. Most of the transgenic plants over-expressing drought inducible *P5CS* homolog with native promoter showed a 2 to 10-fold increase in proline accumulation under stress conditions. We also observed that NIL-143 accumulated 2 to 2.5-fold higher proline compared to Scarlett. Therefore, we might carefully conclude the positive effect of proline to boost drought adaptation in barley. But, we also want to point out the fact that *QPro.S42-1H* is rich in stress-responsive genes. Out of 122 genes in the interval, 44 annotated genes are highly relevant for abiotic stress response. Genes coding for MYB (HORVU1Hr1G072430, HORVU1Hr1G073300, HORVU1Hr1G073310, HORVU1Hr1G073940, HORVU1Hr1G073320), NAC (HORVU1Hr1G073900), bZIP (HORVU1Hr1G072090, HORVU1Hr1G072120) and other class of transcription factors were abundant in the QTL locus. Other relevant gene families such as auxin transporter and response, calcium ion channels, cytochrome P450, zinc finger proteins were located around *HvP5cs1* locus in the QTL interval (Table S15). Therefore, it requires careful investigation to estimate the genetic contribution of these genes, which might cosegregate with a wild allele of *HvP5cs1* in NIL-143. Regardless, NIL-143 is a naturally created overexpression line over Scarlett to explore the fundamental research questions regarding proline function. Moreover, our work provides compelling evidence on the utility of wild gene pool in general and proline in particular to revamp drought adaptation in crops.

5.2. CRISPR RNA/Cas9 system channels a new era of functional genomics

Gene functional analysis in crops heavily relied on mutagenic agents such as ultraviolet irradiation and chemicals (Pacher and Puchta, 2017). However, multiple and random mutation events created by such techniques require extensive screening, often time-consuming, and introduce undesirable effects (Kumlehn *et al.*, 2018). In the past two decades, new techniques have evolved, which allowed plant researchers to introduce targeted mutations in the plant genome (Kamburova *et al.*, 2017). Precise genome editing started in plants in the mid-90s when Kim *et al.* (1996) engineered an artificial zinc finger nuclease (ZFN) by coupling *FokI* with two zinc finger proteins to introduce a double-stranded break (DSB) in the specific genomic location. One decade later, another genome-editing tool, namely transcription activator-like effector nucleases (TALEN) was discovered, which relies on the interaction of TALE protein with a single base pair. The TALE protein complex constitutes repeat-variable

diresidue, which could be engineered to define the target specificity (Moscou and Bogdanove, 2009). Recently, another bacterial defense system known as clustered regularly interspaced palindromic repeat (CRISPR) RNA associated Cas 9 protein was customized to induce site-directed mutagenesis in plants. CRISPR RNA/ Cas9 system offers an elegant solution to create mutation events in targeted genomic loci with greater ease compared to previous genome editing tools (Pacher and Puchta, 2017; Voytas, 2013; Belhaj *et al.*, 2013; Kumlehn *et al.*, 2018). CRISPR RNA/Cas9 has a comparative advantage over ZFN and TALEN because the later tools rely on DNA-protein interaction. At the same time, the mechanism of target DNA recognition in CRISPR RNA/Cas9 is based on RNA-DNA interaction (Belhaj *et al.*, 2015). The site-directed mutagenesis using the tools, as mentioned above, relies on (DSB) made by the nuclease and the repair of DNA breaks by endogenous cell machinery. Once the DSB is made at the target site by the nuclease, the cell will try to repair the DNA through homology-directed repair and non-homologous end joining (NHEJ) (Belhaj *et al.*, 2015). NHEJ is the primary repair process that is error-prone and results in random mutations in the target site. HDR utilizes the homologous chromosome as a template and makes a perfect repair. HDR can be utilized to insert the desired gene or DNA sequence to the chromosome; however, the success rate is meager. Therefore, the NHEJ process has been capitalized to create knock-out mutants through translational frameshift mutations or large deletions (Kumlehn *et al.,* 2018). Since the discovery of the CRISPR RNA/Cas9 system, several groups investigated the utility of this technique in plant research. The work varied from answering fundamental questions to practical application in crop improvement. The work of Wang *et al.* (2014) illustrated the power of genome editing, where they knock-out six homologs of MLO1 locus in wheat. The knock-out mutants were resistant to powdery mildew. Similarly, other groups also demonstrated the efficacy of the CRISPR system to improve monogenic traits, such as disease resistance (Zhang *et al.*, 2017; Ma *et al.*, 2018). Rodríguez *et al*. (2017) took genome editing to the next level, where they presented the potential of the CRISPR system to manipulate quantitative traits in tomato.

Table 5.1. Application of CRISPR RNA/Cas9 system in plant research.

Plant species	Application	Citation
Arabidopsis and tobacco	Demonstrated the efficacy of CRISPR RNA/Cas9 system in a transient system as well as *in planta*	(Li *et al.*, 2013)
Arabidopsis, tobacco, rice, and sorghum	Demonstrated the efficacy of CRISPR RNA/Cas9 system in the transient system as well as *in planta*	(Jiang *et al.*, 2013)

Tobacco	Demonstrated the efficacy of CRISPR RNA/Cas9 system in a transient system Evidence of large deletions using two sgRNA	(Belhaj *et al.*, 2013)
Arabidopsis and rice	Demonstrated the efficacy of CRISPR RNA/Cas9 system in a transient system in model species and crops	(Feng *et al.*, 2013)
Tobacco and wheat	Demonstrated the efficacy of CRISPR RNA/Cas9 system in a transient system in wheat $3^{/}$ mismatch resulted in no off-target activity, and $5^{/}$ mismatch reduced editing events	(Upadhyay *et al.*, 2013)
Tobacco	Demonstrated the efficacy of CRISPR RNA/Cas9 system in a transient system as well as *in planta*	(Gao *et al.*, 2015)
Arabidopsis	Demonstrated the efficacy of CRISPR RNA/Cas9 system *in planta* Checked the transgenerational segregation of mutation event	(Jiang *et al.*, 2014)
Arabidopsis	Demonstrated the efficacy of CRISPR RNA/Cas9 system *in planta* targeting several genes Checked the transgenerational segregation of mutation event	(Feng *et al.*, 2014)
Arabidopsis	Demonstrated the efficacy of CRISPR RNA/Cas9 system *in planta* Checked the transgenerational segregation of mutation event	(Fauser *et al.*, 2014)
Wheat	Targeted MLO locus with TALEN and CRISPR RNA/Cas9 system Mutations were heritable, and edited plants were resistant to powdery mildew	(Wang *et al.*, 2014)
Rice and wheat	Demonstrated the efficacy of CRISPR RNA/Cas9 system *in planta*	(Shan *et al.*, 2013)
Maize	Demonstrated the efficacy of TALEN and CRISPR RNA/Cas9 system in a transient system	(Liang *et al.*, 2014)
Rice	Demonstrated the efficacy of CRISPR RNA/Cas9 system *in planta*	(Miao *et al.*, 2013)

Rice	Demonstrated the efficacy of CRISPR RNA/Cas9 system in a transient system	(Xie and Yang, 2013)
Rice	Demonstrated the efficacy of CRISPR RNA/Cas9 system *in planta* Detected biallelic mutation in T_0 progenies	(Zhang *et al.*, 2014)
Rice	Demonstrated the efficacy of CRISPR RNA/Cas9 system *in planta* Deletion of large segments using multiple sgRNA Detected biallelic mutation in T_0 progenies	(Zhou *et al.*, 2014)
Rice	Demonstrated the efficacy of CRISPR RNA/Cas9 system *in planta* Detected biallelic mutation in T_0 progenies Knock-out of OsBEL resulted in herbicide resistance	(Xu *et al.*, 2014)
Tomato	Demonstrated the efficacy of CRISPR RNA/Cas9 system *in planta* Deletion of large segments using two flanking sgRNA	(Brooks *et al.*, 2014)
Rice	Demonstrated the efficacy of CRISPR RNA/Cas9 system in a transient system and *in planta*	(Shan *et al.*, 2014)
Rice	Validated the function of OsNCED3 in salt and drought tolerance	(Huang *et al.*, 2018)
Rice	Demonstrated how multiplexing helps in targeting multigene family	(Wang *et al.*, 2017)
Maize	Demonstrated promoter swap could be performed using the CRISPR system Introduced inducible promoter upstream of AGROS8 resulted in drought stress tolerance	(Shi *et al.*, 2017)
Tobacco	Transfer of prokaryote immune system to tobacco confers resistance to geminiviruses	(Baltes *et al.*, 2015)
Cucumber	Knock-out of elF4E resulted in tolerance to cucumber vein yellowing virus and potyviruses	(Chandrasekaran *et al.*, 2016)
Rice	Knock-out of sugar transport OsSWEET13 resulted in bacterial blight and rice blast resistance	(Zhou *et al.*, 2015)

Tomato	Knock-out of MLO SlMlo1 resulted in powdery mildew resistance	(Nekrasov *et al.*, 2017)
Citrus	Knock-out of CsLob1 results in citrus canker resistance	(Jia *et al.*, 2017)
Grape	Detected biallelic mutant in first-generation for VvWRKY52 Knock-out mutant resulted in resistance to *Botrytis cinereal*	(Wang *et al.*, 2018)
Wheat	Developed protocol to produce transgene-free T_0 progenies carrying homozygous mutants	(Zhang *et al.*, 2016)
Barley and mustard	Demonstrated the efficacy of CRISPR RNA/Cas9 system *in planta* Checked the transgenerational segregation of mutation event Produced dwarf and semi-dwarf mustard plants by knocking-out BolC.GA4a	(Lawrenson *et al.*, 2015)
Rice	Knock-out of OsSEC3A resulted in dwarf growth and enhanced resistance to *Magnaporthe oryzae*	(Ma *et al.*, 2018)
Rice	Knock-out of OsER1 and OsER2 resulted in dwarf plants	(Zhang *et al.*, 2018)
Rapeseed	Knock-out of CLAVATA genes resulted in semi-dwarf plants	(Yang *et al.*, 2018)
Tomato	Knock-out of SP5G results in accelerated flowering	(Soyk *et al.*, 2017)
Rice	Knock-out of Gn1a, DEP1, GS3, and IPA1 improved yield attributing traits	(Li *et al.*, 2016)
Wheat	Knockdown of TaERD1 resulted in powdery mildew resistance	(Zhang *et al.*, 2017)
Tomato	Demonstrated the manipulation of quantitative traits is possible through CRISPR RNA/Cas9 system One of the significant achievements thus far using the CRISPR system	(Rodríguez *et al.*, 2017)
Rapeseed	Knock-out of ALC family increased resistance to pod shattering	(Braatz *et al.*, 2017)

In chapter 3, we base-editing of putative HvABFs in barley using the CRISPR RNA/Cas9 system. We detected three allelic mutants for HORVU3Hr1G084360 (*HvAbi5*), resulting in frame-shift mutation, while only one allelic mutant with 3 bp deletion was detected in HORVU6Hr1G080670 (*HvAbf*). Next, we evaluated the physiological and transcriptomic response of *hvabi5* and *hvabf* to drought stress. The mutants (*hvabi5* and *hvabf*) were more sensitive to drought stress compared to wild type. The sensitivity of mutants (*hvabi5* and *hvabf*) to drought stress also reflected in the transcriptome data where relevant genes involved in stress signaling and ROS detoxification were downregulated in the mutants. In chapter 4, we also observed that the growth rate was compromised in the *abf1 abf2 abf3 abf4* mutants compared to wild type. Furthermore, These data indicated that the role of ABFs in drought stress adaptation is conserved across the plant species. Moreover, the result of chapter 3 displayed the power of site-directed mutagenesis using the CRISPR RNA/Cas9 system for gene functional analysis in crops.

The recent advancement in genome editing has made reverse genetics screen in crop genetics more attractive. A research lab with a basic molecular biology facility can readily use this approach. In the past, the unavailability of whole-genome sequence information for crop species was the major setback to use this approach, which is no more a constraint. At least one reference genome is available for all major crop species, and more will come thick and fast. The elegant work of several research groups has already shown the power of genome editing to answer the fundamental questions as well as to improve agronomically essential traits in a wide range of crops. It can also be used to create diverse alleles for the gene or trait of interest, which is a cornerstone of plant breeding and genetics. Also, the prospect of generating transgene-free base-edited plants make the CRISPR system a tool of choice for engineering nutritional, industrial, and agronomic traits. Although the manifold application of the technique, there are also obstacles, such as screening of off-target activity and plant regeneration through tissue culture, which will determine the progress of genome editing. There is no doubt about the utility of genome editing in basic research, but applied research will continue to face ethical and regulatory challenges.

5.3. References

Baltes, N.J., Hummel, A.W., Konecna, E., Cegan, R., Bruns, A.N., Bisaro, D.M. and Voytas, D.F. (2015) Conferring resistance to geminiviruses with the CRISPR-Cas prokaryotic immune system. *Nat. Plants*, **1**, 4–7.

Belhaj, K., Chaparro-Garcia, A., Kamoun, S. and Nekrasov, V. (2013) Plant genome editing made easy: targeted mutagenesis in model and crop plants using the CRISPR/Cas system. *Plant Methods*, **9**, 39.

Belhaj, K., Chaparro-Garcia, A., Kamoun, S., Patron, N.J. and Nekrasov, V. (2015) Editing plant genomes with CRISPR/Cas9. *Curr. Opin. Biotechnol.*, **32**, 76–84.

Braatz, J., Harloff, H.J., Mascher, M., Stein, N., Himmelbach, A. and Jung, C. (2017) CRISPR-Cas9 targeted mutagenesis leads to simultaneous modification of different homoeologous gene copies in polyploid oilseed rape (*Brassica napus*). *Plant Physiol.*, **174**, 935–942.

Brooks, C., Nekrasov, V., Lipppman, Z.B. and Eck, J. Van (2014) Efficient gene editing in tomato in the first generation using the clustered regularly interspaced short palindromic repeats/CRISPR-associated9 system. *Plant Physiol.*, **166**, 1292–1297.

Chandrasekaran, J., Brumin, M., Wolf, D., Leibman, D., Klap, C., Pearlsman, M., Sherman, A., Arazi, T. and Gal-On, A. (2016) Development of broad virus resistance in non-transgenic cucumber using CRISPR/Cas9 technology. *Mol. Plant Pathol.*, **17**, 1140–1153.

Chou, I.T., Chen, C.T. and Kao, C.H. (1991) Characteristics of the induction of the accumulation of proline by abscisic acid and isobutyric acid in detached rice leaves. *Plant Cell Physiol.*, **32**, 269–272.

Dallmier, K.A. and Stewart, C.R. (1992) Effect of exogenous abscisic acid on proline dehydrogenase activity in maize (*Zea mays* L.). *Plant Physiol.*, **99**, 762–764.

Fauser, F., Schiml, S. and Puchta, H. (2014) Both CRISPR/Cas-based nucleases and nickases can be used efficiently for genome engineering in *Arabidopsis thaliana*. *Plant J.*, **79**, 348–359.

Feng, Z., Mao, Y., Xu, N., *et al*. (2014) Multigeneration analysis reveals the inheritance, specificity, and patterns of CRISPR/Cas-induced gene modifications in Arabidopsis. *Proc. Natl. Acad. Sci..*, **111**, 4632–4637.

Feng, Z., Zhang, B., Ding, W., *et al*. (2013) Efficient genome editing in plants using a CRISPR/Cas system. *Cell Res.*, **23**, 1229–1232.

Gao, J., Wang, G., Ma, S., Xie, X., Wu, X., Zhang, X., Wu, Y., Zhao, P. and Xia, Q. (2015) CRISPR/Cas9-mediated targeted mutagenesis in *Nicotiana tabacum*. *Plant Mol. Biol.*, **87**, 99–110.

Hong, Z., Lakkineni, K., Zhang, Z. and Verma, D.P.S. (2000) Removal of feedback inhibition of Δ1-pyrroline-5-carboxylate synthetase results in increased proline accumulation and protection of plants from osmotic stress. *Plant Physiol.*, **122**, 1129–1136.

Huang, Y., Guo, Y., Liu, Y., *et al*. (2018) 9-Cis-Epoxycarotenoid Dioxygenase 3 regulates plant growth and enhances multi-abiotic stress tolerance in rice. *Front. Plant Sci.*, **9**.

Jia, H., Zhang, Y., Orbović, V., Xu, J., White, F.F., Jones, J.B. and Wang, N. (2017) Genome editing of the disease susceptibility gene CsLOB1 in citrus confers resistance to citrus canker. *Plant Biotechnol. J.*, **15**, 817–823.

Jiang, W., Zhou, H., Bi, H., Fromm, M., Yang, B. and Weeks, D.P. (2013) Demonstration of CRISPR/Cas9/sgRNA-mediated targeted gene modification in Arabidopsis, tobacco, sorghum and rice. *Nucleic Acids Res.*, **41**, 1–12.

Jiang, W.Z., Yang, B. and Weeks, D.P. (2014) Efficient CRISPR/Cas9-mediated gene editing in *Arabidopsis thaliana* and inheritance of modified genes in the T2 and T3 generations. *PLoS One*, **9**, 21–26.

Kamburova, V.S., Nikitina, E. V., Shermatov, S.E., Buriev, Z.T., Kumpatla, S.P., Emani, C. and Abdurakhmonov, I.Y. (2017) Genome editing in plants: An overview of tools and applications. *Int. J. Agron.*, **2017**.

Kim, Y.G., Cha, J. and Chandrasegaran, S. (1996) Hybrid restriction enzymes: Zinc finger fusions to Fok I cleavage domain. *Proc. Natl. Acad. Sci.*, **93**, 1156–1160.

Kishor, P.B., Hong Zonglie, Miao Guo-Hua, Hu Chein-An, A. and Verma, D.P. (1995) Overexpression of delta1-pyrroline-5-carboxylate synthetase increases proline production and confers osmotolerance in transgenic plants. *Plant Physiol.*, **108**, 1387–1394.

Kumlehn, J., Pietralla, J., Hensel, G., Pacher, M. and Puchta, H. (2018) The CRISPR/Cas revolution continues: From efficient gene editing for crop breeding to plant synthetic biology. *J. Integr. Plant Biol.*, **60**, 1127–1153.

Lawrenson, T., Shorinola, O., Stacey, N., Li, C., Østergaard, L., Patron, N., Uauy, C. and Harwood, W. (2015) Induction of targeted, heritable mutations in barley and *Brassica oleracea* using RNA-guided Cas9 nuclease. *Genome Biol.*, **16**, 258.

Li, M., Li, X., Zhou, Z., *et al*. (2016) Reassessment of the four yield-related genes Gn1a, DEP1, GS3, and IPA1 in rice using a CRISPR/Cas9 system. *Front. Plant Sci.*, **7**, 1–13.

Li, W., Teng, F., Li, T. and Zhou, Q. (2013) Simultaneous generation and germline transmission of multiple gene mutations in rat using CRISPR-Cas systems. *Nat. Biotechnol.*, **31**, 684–686.

Liang, Z., Zhang, K., Chen, K. and Gao, C. (2014) Targeted mutagenesis in *Zea mays* using TALENs and the CRISPR/Cas System. *J. Genet. Genomics*, **41**, 63–68.

Ma, J., Chen, J., Wang, M., Ren, Y., Wang, S., Lei, C., Cheng, Z. and Sodmergen (2018) Disruption of OsSEC3A increases the content of salicylic acid and induces plant defense responses in rice. *J. Exp. Bot.*, **69**, 1051–1064.

Miao, J., Guo, D., Zhang, J., Huang, Q., Qin, G., Zhang, X., Wan, J., Gu, H. and Qu, L.J. (2013) Targeted mutagenesis in rice using CRISPR-Cas system. *Cell Res.*, **23**, 1233–1236.

Mittler, R. (2002) Oxidative stress, antioxidants and stress tolerance. *Trends Plant Sci.*, **7**, 405–410.

Moscou, M.J. and Bogdanove, A.J. (2009) A simple cipher governs DNA recognition by TAL effectors. *Science (80-.).*, **326**, 1501.

Nekrasov, V., Wang, C., Win, J., Lanz, C., Weigel, D. and Kamoun, S. (2017) Rapid generation of a transgene-free powdery mildew resistant tomato by genome deletion. *Sci. Rep.*, **7**, 1–6.

Pacher, M. and Puchta, H. (2017) From classical mutagenesis to nuclease-based breeding – directing natural DNA repair for a natural end-product. *Plant J.*, **90**, 819–833.

Pesci, P. (1987) ABA-induced proline accumulation in barley leaf segments: Dependence on protein synthesis. *Physiol. Plant.*, **71**, 287–291.

Rodríguez, D.L., Lemmon, Z.H., Man, J., Bartlett, M.E. and Lippman, Z.B. (2017) Engineering quantitative trait variation for crop improvement by genome editing. *Cell*, **171**, 470-480.e8.

Shan, Q., Wang, Y., Li, J., *et al*. (2013) Targeted genome modification of crop plants using a CRISPR-Cas system. *Nat. Biotechnol.*, **31**, 686–688.

Shan, Q., Wang, Y., Li, J. and Gao, C. (2014) Genome editing in rice and wheat using the CRISPR/Cas system. *Nat. Protoc.*, **9**, 2395–2410.

Sharma, S. and Verslues, P.E. (2010) Mechanisms independent of abscisic acid (ABA) or proline feedback have a predominant role in transcriptional regulation of proline metabolism during low water potential and stress recovery. *Plant, Cell Environ.*, **33**, 1838–1851.

Sharp, R.E., Hsiao, T.C. and Silk, W.K. (1990) Growth of the maize primary root at low water potentials: II. Role of growth and deposition of hexose and potassium in osmotic adjustment. *Plant Physiol.*, **93**, 1337–1346.

Shi, J., Gao, H., Wang, H., Lafitte, H.R., Archibald, R.L., Yang, M., Hakimi, S.M., Mo, H. and Habben, J.E. (2017) ARGOS8 variants generated by CRISPR-Cas9 improve maize grain yield under field drought stress conditions. *Plant Biotechnol. J.*, **15**, 207–216.

Shinozaki, K. and Yamaguchi-Shinozaki, K. (2006) Gene networks involved in drought stress response and tolerance. *J. Exp. Bot.*, **58**, 221–227.

Soyk, S., Müller, N.A., Park, S.J., *et al*. (2017) Variation in the flowering gene SELF PRUNING 5G promotes day-neutrality and early yield in tomato. *Nat. Genet.*, **49**, 162–168.

Stewart, C.R., Voetberg, G. and Rayapati, P.J. (1986) The effects of benzyladenine, cycloheximide, and cordycepin on wilting-induced abscisic acid and proline accumulations and abscisic acid- and salt-induced proline accumulation in barley leaves. *Plant Physiol.*, **82**, 703–707.

Szabados, L. and Savouré, A. (2010) Proline: a multifunctional amino acid. *Trends Plant Sci.*, **15**, 89–97.

Székely, G., Ábrahám, E., Cséplo, Á., *et al*. (2008) Duplicated P5CS genes of Arabidopsis play distinct roles in stress regulation and developmental control of proline biosynthesis. *Plant J.*, **53**, 11–28.

Szoke, A., Miao, G.H., Hong, Z. and Verma, D.P.S. (1992) Subcellular location of Δ1-pyrroline-5-carboxylate reductase in root/nodule and leaf of soybean. *Plant Physiol.*, **99**, 1642–1649.

Upadhyay, S.K., Kumar, J., Alok, A. and Tuli, R. (2013) RNA-Guided genome editing for target gene mutations in wheat. *G3 Genes, Genomes, Genet.*, **3**, 2233–2238.

Voetberg, G.S. and Sharp, R.E. (1991) Growth of the maize primary root at low water potentials: III. Role of increased proline deposition in osmotic adjustment. *Plant Physiol.*, **96**, 1125–1130.

Voytas, D.F. (2013) Plant genome engineering with sequence-specific nucleases. *Annu. Rev. Plant Biol.*, **64**, 327–350.

Wang, M., Mao, Y., Lu, Y., Tao, X. and Zhu, J. (2017) Multiplex gene editing in rice using the CRISPR-Cpf1 system. *Mol. Plant*, **10**, 1011–1013.

Wang, Xianhang, Tu, M., Wang, D., Liu, J., Li, Y., Li, Z., Wang, Y. and Wang, Xiping (2018) CRISPR/Cas9-mediated efficient targeted mutagenesis in grape in the first generation. *Plant Biotechnol. J.*, **16**, 844–855.

Wang, Y., Cheng, X., Shan, Q., Zhang, Y., Liu, J., Gao, C. and Qiu, J.L. (2014) Simultaneous editing of three homoeoalleles in hexaploid bread wheat confers heritable resistance to powdery mildew. *Nat. Biotechnol.*, **32**, 947–951.

Xie, K. and Yang, Y. (2013) RNA-Guided genome editing in plants using a CRISPR-Cas system. *Mol. Plant*, **6**, 1975–1983.

Xu, R., Li, H., Qin, R., Wang, L., Li, L., Wei, P. and Yang, J. (2014) Gene targeting using the Agrobacterium tumefaciens-mediated CRISPR-Cas system in rice. *Rice*, **7**, 7–10.

Yang, Y., Zhu, K., Li, H., Han, S., Meng, Q., Khan, S.U., Fan, C., Xie, K. and Zhou, Y. (2018) Precise editing of CLAVATA genes in Brassica napus L. regulates multilocular silique development. *Plant Biotechnol. J.*, **16**, 1322–1335.

Zhang, G.C., Zhu, W.L., Gai, J.Y., Zhu, Y.L. and Yang, L.F. (2015) Enhanced salt tolerance of transgenic vegetable soybeans resulting from overexpression of a novel Δ1-pyrroline-5-

carboxylate synthetase gene from Solanum torvum Swartz. *Hortic. Environ. Biotechnol.*, **56**, 94–104.

Zhang, Hui, Zhang, J., Wei, P., *et al*. (2014) The CRISPR/Cas9 system produces specific and homozygous targeted gene editing in rice in one generation. *Plant Biotechnol. J.*, **12**, 797–807.

Zhang, Y., Bai, Y., Wu, G., Zou, S., Chen, Y., Gao, C. and Tang, D. (2017) Simultaneous modification of three homoeologs of TaEDR1 by genome editing enhances powdery mildew resistance in wheat. *Plant J.*, **91**, 714–724.

Zhang, Y., Li, S., Xue, S., Yang, S., Huang, J. and Wang, L. (2018) Phylogenetic and CRISPR/Cas9 studies in deciphering the evolutionary trajectory and phenotypic impacts of rice ERECTA genes. *Front. Plant Sci.*, **9**, 1–11.

Zhang, Y., Liang, Z., Zong, Y., Wang, Y., Liu, J., Chen, K., Qiu, J.L. and Gao, C. (2016) Efficient and transgene-free genome editing in wheat through transient expression of CRISPR/Cas9 DNA or RNA. *Nat. Commun.*, **7**, 1–8.

Zhou, H., Liu, B., Weeks, D.P., Spalding, M.H. and Yang, B. (2014) Large chromosomal deletions and heritable small genetic changes induced by CRISPR/Cas9 in rice. *Nucleic Acids Res.*, **42**, 10903–10914.

Zhou, J., Peng, Z., Long, J., *et al*. (2015) Gene targeting by the TAL effector PthXo2 reveals cryptic resistance gene for bacterial blight of rice. *Plant J.*, **82**, 632–643

Supplementary information

Supplementary tables

Table S1. List of primers used in barley experiments.

Primer name	Forward primer	Reverse primer	Purpose	Remarks
ABF1-q	TGCAGAAGAAACAGGCTGAA	GACCGGTAAGGGTTCTTCTCA	qPCR	Transient assay
ABF2-q	GAGAGAAGGCAAAGGAGAATGA	CTTCAAGCTCCACGGTGTAAG	qPCR	Transient assay
ABF3-q	CGTTCTCAACCTGCAACACA	TCATAGGATGGTTATGAATTCCAAG	qPCR	Transient assay
ABF4-q	GCAACCTGGTGCTGGTATCC	TGTTCTAGGCAACGTCAACGA	qPCR	Transient assay
GUS-q	TTAACTATGCCGGAATCCATCGC	AACGCTGACATCACCATTGGC	qPCR	Transient assay
18S-q	GGTGGTAACGGGTGACGGAGAAT	CGCCGACCGAAGGGACAAGCCGA	qPCR	Transient assay
HvP5cs1-q	GCAGAGACCTTTCTACGTCAAG	CCTGTACTTATGCCAACCTCAG	qPCR	
HvElf4b-q	TCATGCCTGTGGGTTATGG	CTGGACGTACTCGTTGATGG	qPCR	
3-UTR-g	AAAGGGCAAATTGTGAATGG	CAAGAGCAAGCAAAACCACA	Marker-assisted backcrossing	
HvP5cs1-pSeq	CTGCCATCATTTGATTGTTAGG	AGCAGGGACGGGATAATCG	Promoter sequencing	
HvP5cs1-pSeqFside	GAGCTGCAATGGAGTGCCG		Promoter sequencing	
HvP5cs1-pSeqRside		CCGCTGACGTGCTCTGAGAT	Promoter sequencing	
T-DNA-g	TTTAGCCCTGCCTTCATACG	TTAATCATGTGGGCCAGAGC	CRISPR mutant genotyping	
HvABF-cr	TCCTCGGTCTACTCGCTCA	GGCCTCCGAAGAACATCAT	CRISPR mutant sequencing	
HvABI5-cr	CGTGAAGTTCTCCGACGAG	TGATCTCAGCCCACACCTC	CRISPR mutant sequencing	

Table S2. Summary statistics of the adaptive response of NIL-143 and Scarlett to drought stress at the seedling stage. The asterisks indicated significant genotype (G), treatment (T) and genotype by treatment interaction (G*T) effect (ns, non-significant; $P \leq 0.05$, *; $P \leq 0.01$, **; ***$P \leq 0.001$). EL, electrolyte leakage; RWC, relative water content; MDA, malondialdehyde; SPAD, soil plant analysis development; Y(II) effective quantum yield of photosystem II at steady-state photosynthesis under light conditions; NDVI, normalized differences vegetation index; SR, simple ratio index; Ctr2, Carter index 2; Lic1, Lichtenthaler index 1; SIPI, simple ratio pigment index; RDVI, renormalized differences vegetation index; V_{cmax}, maximum carboxylation rate of rubisco; J_{max}, maximum rate of electron transport during ribulose-1,5-biphosphate regeneration; g_s, stomatal conductance; E, transpiration rate; A, CO_2 assimilation rate.

DAS	Traits	Control		Drought		ANOVA		
		Scarlett	NIL-143	Scarlett	NIL-143	G	T	G*T
4 d	Proline	29.0	24.5	25.7	30.4	ns	ns	*
	EL	7.5	8.8	7.9	7.8	ns	ns	Ns
	RWC	92.2	94.3	94.2	93.1	ns	ns	Ns
	MDA	6.6	7.2	8.9	7.8	ns	ns	Ns
	SPAD	41.9	43.6	41.7	43.6	*	ns	Ns
	Y(II)	0.699	0.702	0.691	0.692	ns	ns	Ns
	NDVI	0.486	0.473	0.491	0.487	ns	ns	Ns
	SR	2.89	2.81	2.93	2.91	ns	ns	Ns
	Ctr2	0.417	0.426	0.412	0.410	ns	ns	Ns
	Lic1	0.526	0.517	0.531	0.519	ns	ns	Ns
	SIPI	0.524	0.515	0.531	0.518	ns	ns	Ns
	RDVI	0.453	0.441	0.459	0.445	ns	ns	Ns
	V_{cmax}	85.0	83.1	79.7	79.1	ns	ns	Ns
	J_{max}	212.1	195.4	219.5	202.9	ns	ns	Ns
	g_s	0.619	0.701	0.522	0.575	ns	*	Ns
	E	3.31	4.18	4.39	3.85	ns	ns	*
	A	20.1	20.3	20.5	20.2	ns	ns	Ns
5 d	Proline	31.8	27.9	46.2	112.1	ns	*	*
	SPAD	41.8	40.0	40.0	40.2	ns	ns	Ns
	Y(II)	0.697	0.696	0.635	0.686	ns	*	Ns
	NDVI	0.500	0.480	0.483	0.486	ns	ns	Ns
	SR	3.00	2.85	2.87	2.90	ns	ns	*
	Ctr2	0.403	0.421	0.415	0.410	ns	ns	Ns
	Lic1	0.538	0.521	0.524	0.527	ns	ns	*
	SIPI	0.537	0.529	0.528	0.535	ns	ns	Ns
	RDVI	0.459	0.446	0.449	0.456	ns	ns	*
	Proline	30.9	24.9	307.9	631.1	*	***	*
6 d	EL	9.6	10.0	11.7	10.3	ns	*	Ns
	RWC	93.4	93.7	71.1	78.6	ns	***	Ns
	MDA	6.8	8.3	13.6	11.4	ns	***	Ns

	SPAD	42.0	42.3	38.8	41.3	*	**	Ns
	Y(II)	0.688	0.688	0.576	0.636	ns	***	Ns
	NDVI	0.491	0.497	0.480	0.496	*	ns	Ns
	SR	2.93	2.98	2.85	2.97	*	ns	Ns
	Ctr2	0.415	0.404	0.421	0.401	**	ns	Ns
	Lic1	0.529	0.533	0.520	0.533	ns	ns	Ns
	SIPI	0.535	0.540	0.527	0.542	ns	ns	Ns
	RDVI	0.459	0.462	0.448	0.463	ns	ns	Ns
	V_{cmax}	87.0	73.7	40.6	49.4	ns	***	Ns
	J_{max}	189.3	186.3	153.3	166.2	ns	**	Ns
	g_s	0.731	0.701	0.484	0.533	ns	***	Ns
	E	6.72	6.28	2.02	2.80	ns	***	*
	A	24	23.4	18.5	19.5	ns	***	Ns
8 d	Proline	66.9	69.5	2384.4	5650.3	*	***	**
	EL	6.2	6.3	24.9	13.1	**	***	**
	RWC	94.9	93.9	30.0	32.9	ns	***	Ns
	MDA	6.5	5.7	18.4	15	ns	***	Ns
	SPAD	45.1	44.2	32.2	36.0	*	**	*
	Y(II)	0.697	0.699	0.331	0.452	***	***	**
	NDVI	0.504	0.500	0.386	0.430	*	***	*
	SR	3.04	3.01	2.26	2.52	*	***	*
	Ctr2	0.394	0.394	0.513	0.473	*	***	Ns
	Lic1	0.538	0.539	0.457	0.500	**	***	*
	SIPI	0.536	0.533	0.460	0.511	*	***	*
	RDVI	0.469	0.470	0.396	0.439	**	***	Ns
	V_{cmax}	57.5	57.1	16.4	32.6	ns	***	*
	J_{max}	145.6	153.2	93.5	133.4	ns	**	Ns
	g_s	0.593	0.575	0.115	0.176	ns	***	Ns
	E	5.77	6.34	1.41	2.05	*	***	Ns
	A	18.1	17.4	7.6	13.5	ns	***	*

Table S3. Summary statistics of the adaptive response of NIL-143 and Scarlett to drought stress under field conditions. The asterisks indicated significant genotype (G), treatment (T) and genotype by treatment interaction (G*T) effect (ns, non-significant; $P \leq 0.05$, *; $P \leq 0.01$, **; $P \leq 0.001$, ***). The asterisks indicated significant genotype (G), treatment (T) and genotype by treatment interaction (G*T) effect (ns, non-significant; $P \leq 0.05$, *; $P \leq 0.01$, **; ***$P \leq 0.001$). SPAD, soil plant analysis development; Y(II) effective quantum yield of phostosystem II at stead-state photosynthesis under light conditions; NDVI, normalised differences vegetation index; SR, simple ratio index; CRI, carotenoid index; Ctr2, Carter index 2; Lic1, Lichtenthaler index 1; SIPI, simple ratio pigment index; RDVI, renormalized differences vegetation index; OSAVI, optimized soil-adjusted vegetation index; GM2, Gitelson and Merzlyak index 2; Lic1, Lichtenthaler index; PRI, photochemical reflectance index; SPRI; simple ratio pigment index (SPRI); Zarco-Tejada and Miller index (ZMI).

DAS	Trait	Control		Drought		G	T	G*T
		Scarlett	NIL-143	Scarlett	NIL-143			
7 d	SPAD	57	58.5	55.9	57.4	*	ns	ns
	YII	0.605	0.602	0.45	0.43	ns	***	ns
14 d	SPAD	61.2	60	54.6	58.1	*	***	***
	YII	0.602	0.621	0.49	0.47	ns	***	ns
	CRI	1.6	1.5	1.6	1.5	ns	ns	ns
	Ctr2	0.335	0.322	0.334	0.33	*	ns	ns
	GM2	2.5	2.6	2.5	2.5	*	**	*
	Lic1	0.585	0.592	0.582	0.588	ns	ns	ns
	OSAVI	0.57	0.573	0.562	0.566	ns	*	ns
	NDVI	0.56	0.57	0.553	0.562	*	ns	ns
	PRI	0.031	0.03	0.029	0.029	ns	ns	ns
	SPRI	0.98	0.99	0.984	0.99	ns	ns	ns
	SR	3.5	3.7	3.4	3.6	*	*	ns
	SIPI	0.584	0.589	0.578	0.583	ns	ns	ns
	ZMI	1.8	1.9	1.8	1.8	*	**	*
21 d	SPAD	54.6	56.1	29.9	44.2	***	***	***
	YII	0.65	0.611	0.133	0.287	**	***	***
	CRI	1.6	1.5	1.3	1.6	*	ns	***
	Ctr2	0.37	0.357	0.5	0.428	*	***	*
	GM2	2.3	2.3	1.6	1.9	ns	***	**
	Lic1	0.564	0.565	0.481	0.535	*	***	***
	OSAVI	0.556	0.553	0.469	0.522	*	***	***
	NDVI	0.53	0.534	0.406	0.475	*	***	**
	PRI	0.024	0.023	0.006	0.016	ns	***	*
	SPRI	0.953	0.943	0.903	0.932	ns	*	*
	SR	3.3	3.3	2.4	2.9	ns	***	**
	SIPI	0.566	0.566	0.502	0.538	ns	***	**
	ZMI	1.7	1.7	1.4	1.5	ns	***	ns

Table S4. Summary statistics of yield and related traits of NIL-143 and Scarlett under field conditions. The phenotypic values averaged over the genotypes sharing a letter are not significantly different by Tukey-adjusted comparisons ($P \leq 0.05$). Rainfed refers to the plants grown in an open field, while irrigated and drought indicate the regular water plot and water-stress applied plot inside the rainout shelter, respectively. The experiment was performed in Campus Kleinaltendorf, Rheinbach, Germany. The asterisks indicated significant genotype (G), treatment (T) and genotype by treatment interaction (G*T) effect (ns, non-significant; $P \leq 0.05$, *; $P \leq 0.01$, **; $P \leq 0.001$, ***). G, genotype; T, treatment

Trait	Rainfed	Irrigated	Drought	G	T	G*T
Tiller number	15.6^{a}	13.9^{a}	5.8^{b}	ns	***	Ns
Ear number	11.2^{a}	9^{b}	4.2^{c}	ns	***	Ns
Grain weight (g)	8.2^{a}	6.6^{a}	2.7^{b}	ns	***	Ns
Grain number	17.2^{a}	15.7^{a}	16.3^{a}	**	ns	Ns
1000 grain weight (g)	42.3^{b}	46.5^{a}	40^{c}	*	***	Ns
Shoot weight (g)	10.4^{a}	12.4^{a}	4.2^{b}	ns	***	Ns
Harvest index	0.39^{a}	0.396^{a}	0.383^{a}	*	ns	Ns

Table S5. Summary of the number of raw and mapped reads count.

DataSet	Raw read	Trimmed reads	Filtered reads	Percent of reads aligned to the reference
hvabf C1	77084467	77042239	62413908	81.01
hvabf C2	77566198	77517118	62537592	80.68
hvabf C3	71573615	71531357	58227106	81.40
hvabf T1	65312542	65271252	54059494	82.82
hvabf T2	61559387	61522778	50789759	82.55
hvabf T3	72093072	72048439	59697815	82.86
hvabi5 C1	61477209	61437716	50248712	81.79
hvabi5 C2	90783502	90720219	74270745	81.87
hvabi5 C3	79380201	79326717	58227106	73.40
hvabi5 T1	67807743	67764362	55982436	82.61
hvabi5 T2	64867054	64823074	53955703	83.24
hvabi5 T3	69912560	69874159	57853185	82.80
GP C1	64535048	64493757	52627593	81.60
GP C2	54555636	54521903	44206661	81.08
GP C3	53781455	53751482	43760975	81.41
GP T1	73704665	73660886	60414369	82.02
GP T2	61014807	60975117	50040300	82.07
GP T3	60088200	60049795	49297230	82.09

Table S6. Summary statistics for the physiological and biochemical response of *hvabf* and *hvabi5* to drought stress. Means sharing a letter are not significantly different from Tukey-adjusted comparisons ($P \leq 0.05$). Electrolyte leakage (EL) and relative water content (RWC) is expressed as a percentage, malondialdehyde (MDA) as nmol g^{-1} fresh weight, and proline as µg g^{-1} fresh weight. The asterisks indicate significant genotype, treatment and genotype by treatment interaction effect (ns, non-significant; $P \leq 0.05$, *; $P \leq 0.01$, **; $P \leq 0.001$, ***). G, genotype; T, treatment

Days after stress	Trait	Control			Drought			ANOVA		
		GP	*hvabf*	*hvabi5*	GP	*hvabf*	*hvabi5*	G	T	G*T
6 d	EL	6.3	5.7	7.3	8.6	8.6	8.1	ns	***	Ns
	RWC	93.4	92.7	93.8	92.6	92	89.9	ns	***	*
	MDA	7.8	9.9	8.2	11.6	13.3	12.4	ns	***	Ns
	Proline	28.7	29.3	31.2	28.5	37.7	41.4	ns	**	*
9 d	EL	6.7	5.1	7	12	14.3	15.8	ns	***	Ns
	RWC	93.7	93.4	93.7	70.8	52	57.1	*	***	*
	MDA	11.9	15.7	8.2	25.1	30.5	32.5	ns	***	Ns
	Proline	29.5	25.8	24.8	589.3	1355.8	1580.2	*	***	*

Table S7. Gene ontology (GO) terms of differentially expressed genes between wild type and mutants. Adjusted *P*-value after false discovery rate (FDR) correction is indicated in the table (significance threshold set to $P \leq 0.05$). The probability of FDR is close to 0 for red cells and close to 0.05 for yellow cells, while grey cells indicate non-significant GO terms. Three GO terms are indicated in the table namely biological process (P), molecular function (M) and cellular component (C)

SN	GO Term	Ontology	Description	Down-regulated			Up-regulated		
				GP	*hvabf*	*hvabi5*	GP	*hvabf*	*hvabi5*
1	GO:0006468	P	protein phosphorylation						
2	GO:0016310	P	Phosphorylation						
3	GO:0036211	P	protein modification process						
4	GO:0006464	P	cellular protein modification process						
5	GO:0043412	P	macromolecule modification						
6	GO:0006793	P	phosphorus metabolic process						
7	GO:0006796	P	phosphate-containing compound metabolic process						
8	GO:0044706	P	multi-multicellular organism process						
9	GO:0009875	P	pollen-pistil interaction						
10	GO:0008037	P	cell recognition						
11	GO:0048544	P	recognition of pollen						
12	GO:0009856	P	Pollination						
13	GO:0044702	P	single organism reproductive process						
14	GO:0008152	P	metabolic process						
15	GO:0044703	P	multi-organism reproductive process						
16	GO:0051704	P	multi-organism process						
17	GO:0000003	P	Reproduction						
18	GO:0022414	P	reproductive process						
19	GO:0019538	P	protein metabolic process						
20	GO:0044267	P	cellular protein metabolic process						
21	GO:0032501	P	multicellular organismal process						

22	GO:0044699	P	single-organism process
23	GO:0007154	P	cell communication
24	GO:0071704	P	organic substance metabolic process
25	GO:0044710	P	single-organism metabolic process
26	GO:0004672	F	protein kinase activity
27	GO:0016773	F	phosphotransferase activity, alcohol group as acceptor
28	GO:0016301	F	kinase activity
29	GO:0016740	F	transferase activity
30	GO:0016772	F	transferase activity, transferring phosphorus-containing groups
31	GO:0003824	F	catalytic activity
32	GO:0032559	F	adenyl ribonucleotide binding
33	GO:0030554	F	adenyl nucleotide binding
34	GO:0017076	F	purine nucleotide binding
35	GO:0032555	F	purine ribonucleotide binding
36	GO:0032553	F	ribonucleotide binding
37	GO:0032550	F	purine ribonucleoside binding
38	GO:0001883	F	purine nucleoside binding
39	GO:0001882	F	nucleoside binding
40	GO:0032549	F	ribonucleoside binding
41	GO:0005524	F	ATP binding
42	GO:0097367	F	carbohydrate derivative binding
43	GO:0035639	F	purine ribonucleoside triphosphate binding
44	GO:0000166	F	nucleotide binding
45	GO:1901265	F	nucleoside phosphate binding
46	GO:0036094	F	small molecule binding
47	GO:0030246	F	carbohydrate binding
48	GO:0004674	F	protein serine/threonine kinase activity
49	GO:0001871	F	pattern binding
50	GO:0030247	F	polysaccharide binding

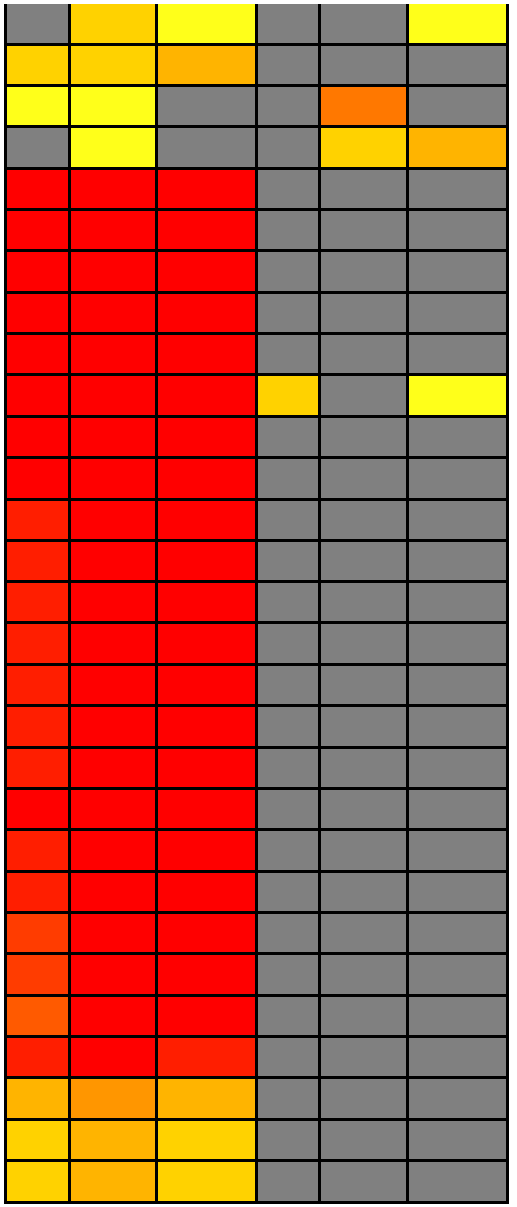

51	GO:0016705	F	oxidoreductase activity, acting on paired donors, with incorporation or reduction of oxygen	
52	GO:0046906	F	tetrapyrrole binding	
53	GO:0020037	F	heme binding	
54	GO:0016758	F	transferase activity, transferring hexosyl groups	
55	GO:0005506	F	iron ion binding	
56	GO:0016757	F	transferase activity, transferring glycosyl groups	
57	GO:0005509	F	calcium ion binding	
58	GO:1901363	F	heterocyclic compound binding	
59	GO:0097159	F	organic cyclic compound binding	
60	GO:0016491	F	oxidoreductase activity	
61	GO:0005215	F	transporter activity	
62	GO:0005200	F	structural constituent of cytoskeleton	
63	GO:0055085	P	transmembrane transport	
64	GO:0006810	P	Transport	
65	GO:0051234	P	establishment of localization	
66	GO:0051179	P	Localization	
67	GO:0071705	P	nitrogen compound transport	
68	GO:0006829	P	zinc II ion transport	
69	GO:0071577	P	zinc II ion transmembrane transport	
70	GO:0015849	P	organic acid transport	
71	GO:1905039	P	carboxylic acid transmembrane transport	
72	GO:1903825	P	organic acid transmembrane transport	
73	GO:0003333	P	amino acid transmembrane transport	
74	GO:0000041	P	transition metal ion transport	
75	GO:0070838	P	divalent metal ion transport	
76	GO:0072511	P	divalent inorganic cation transport	
77	GO:0030001	P	metal ion transport	
78	GO:0022857	F	transmembrane transporter activity	
79	GO:0022891	F	substrate-specific transmembrane transporter activity	

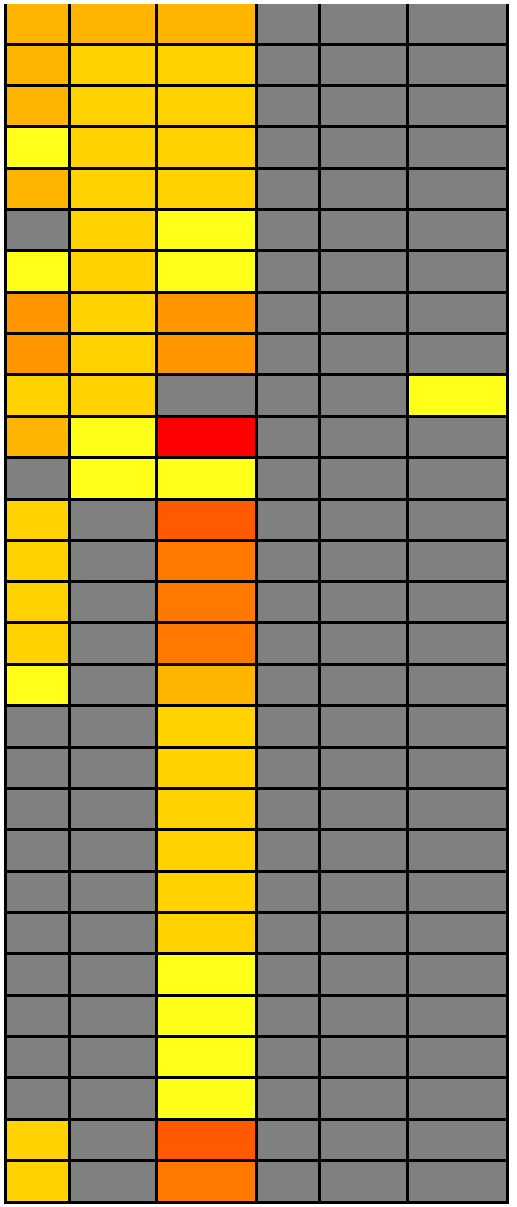

80	GO:0022892	F	substrate-specific transporter activity
81	GO:0005385	F	zinc ion transmembrane transporter activity
82	GO:0005342	F	organic acid transmembrane transporter activity
83	GO:0046943	F	carboxylic acid transmembrane transporter activity
84	GO:0015171	F	amino acid transmembrane transporter activity
85	GO:0046915	F	transition metal ion transmembrane transporter activity
86	GO:0072509	F	divalent inorganic cation transmembrane transporter activity
87	GO:0008519	F	ammonium transmembrane transporter activity
88	GO:0016020	C	Membrane
89	GO:0099512	C	supramolecular fiber
90	GO:0099513	C	polymeric cytoskeletal fiber
91	GO:0005874	C	Microtubule
92	GO:0055114	P	oxidation-reduction process
93	GO:0001071	F	nucleic acid binding transcription factor activity
94	GO:0003700	F	transcription factor activity, sequence-specific DNA binding
95	GO:0043565	F	sequence-specific DNA binding
96	GO:1901566	P	organonitrogen compound biosynthetic process
97	GO:1901564	P	organonitrogen compound metabolic process
98	GO:0043043	P	peptide biosynthetic process
99	GO:0043604	P	amide biosynthetic process
100	GO:0006412	P	Translation
101	GO:0006518	P	peptide metabolic process
102	GO:0043603	P	cellular amide metabolic process
103	GO:0009058	P	biosynthetic process
104	GO:0044249	P	cellular biosynthetic process
105	GO:0006807	P	nitrogen compound metabolic process
106	GO:1901576	P	organic substance biosynthetic process
107	GO:0044271	P	cellular nitrogen compound biosynthetic process
108	GO:0010467	P	gene expression

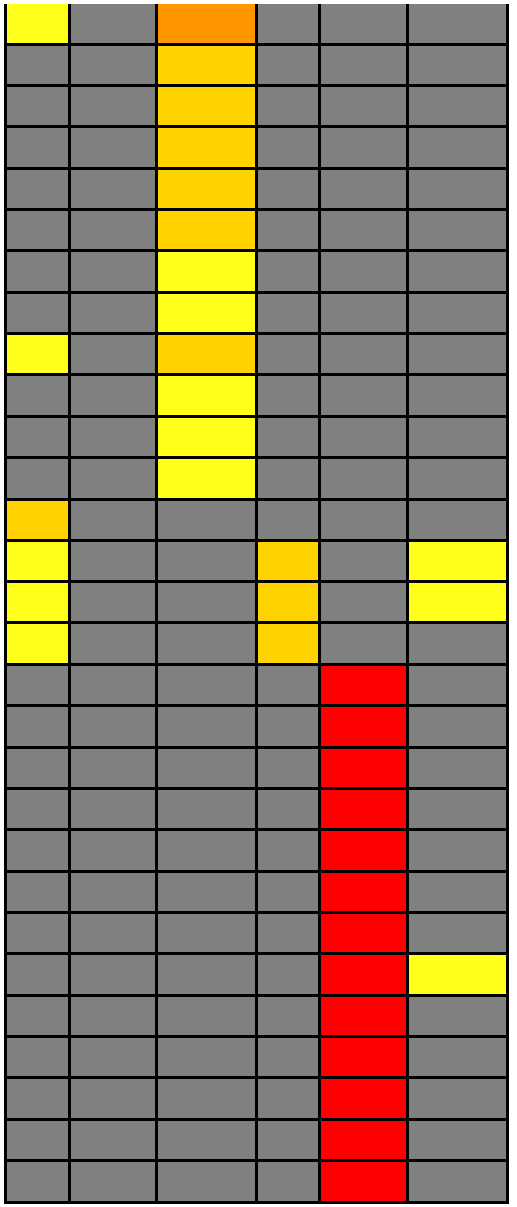

109	GO:0034641	P	cellular nitrogen compound metabolic process
110	GO:0034645	P	cellular macromolecule biosynthetic process
111	GO:0009059	P	macromolecule biosynthetic process
112	GO:0006082	P	organic acid metabolic process
113	GO:0044281	P	small molecule metabolic process
114	GO:0019752	P	carboxylic acid metabolic process
115	GO:0043436	P	oxoacid metabolic process
116	GO:0010035	P	response to inorganic substance
117	GO:1901700	P	response to oxygen-containing compound
118	GO:0009415	P	response to water
119	GO:0001101	P	response to acid chemical
120	GO:0044238	P	primary metabolic process
121	GO:0044711	P	single-organism biosynthetic process
122	GO:0042254	P	ribosome biogenesis
123	GO:0006520	P	cellular amino acid metabolic process
124	GO:0008652	P	cellular amino acid biosynthetic process
125	GO:0044237	P	cellular metabolic process
126	GO:0022613	P	ribonucleoprotein complex biogenesis
127	GO:0009628	P	response to abiotic stimulus
128	GO:0016053	P	organic acid biosynthetic process
129	GO:0006457	P	protein folding
130	GO:1901607	P	alpha-amino acid biosynthetic process
131	GO:0046394	P	carboxylic acid biosynthetic process
132	GO:1901605	P	alpha-amino acid metabolic process
133	GO:0044283	P	small molecule biosynthetic process
134	GO:0009790	P	embryo development
135	GO:0043648	P	dicarboxylic acid metabolic process
136	GO:0034660	P	ncRNA metabolic process
137	GO:0003735	F	structural constituent of ribosome

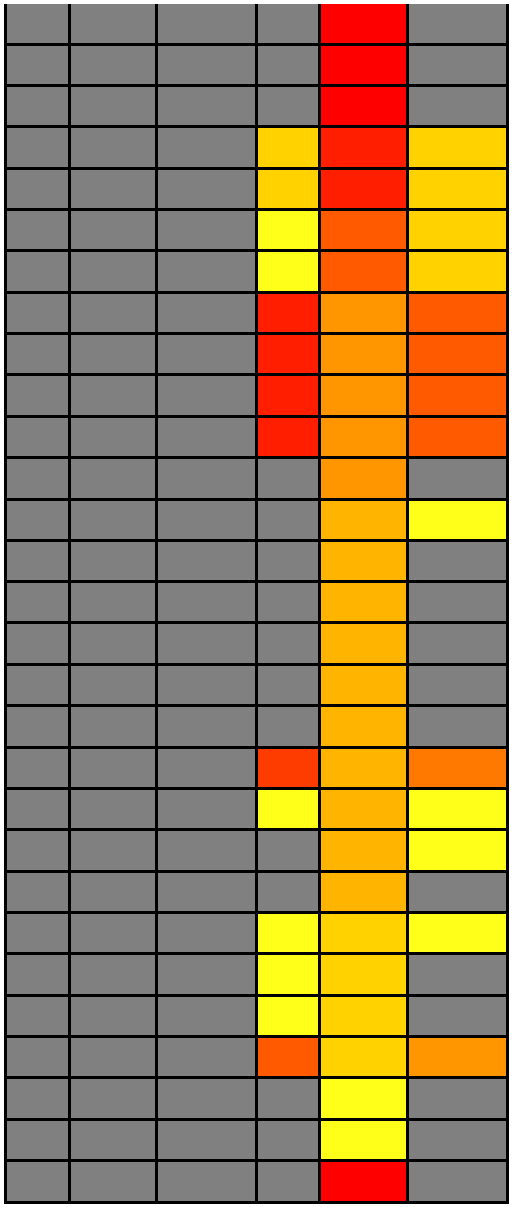

138	GO:0005198	F	structural molecule activity
139	GO:0003723	F	RNA binding
140	GO:0043168	F	anion binding
141	GO:0048037	F	cofactor binding
142	GO:0030170	F	pyridoxal phosphate binding
143	GO:0061135	F	endopeptidase regulator activity
144	GO:0004866	F	endopeptidase inhibitor activity
145	GO:0061134	F	peptidase regulator activity
146	GO:0030414	F	peptidase inhibitor activity
147	GO:0008483	F	transaminase activity
148	GO:0016769	F	transferase activity, transferring nitrogenous groups
149	GO:0016874	F	ligase activity
150	GO:0016903	F	oxidoreductase activity, acting on the aldehyde or oxo group of donors
151	GO:0008097	F	5S rRNA binding
152	GO:0004867	F	serine-type endopeptidase inhibitor activity
153	GO:0016614	F	oxidoreductase activity, acting on CH-OH group of donors
154	GO:1990904	C	ribonucleoprotein complex
155	GO:0030529	C	intracellular ribonucleoprotein complex
156	GO:0005840	C	Ribosome
157	GO:0005737	C	Cytoplasm
158	GO:0044444	C	cytoplasmic part
159	GO:0043232	C	intracellular non-membrane-bounded organelle
160	GO:0043228	C	non-membrane-bounded organelle
161	GO:0032991	C	macromolecular complex
162	GO:0044424	C	intracellular part
163	GO:0005622	C	Intracellular
164	GO:0043229	C	intracellular organelle
165	GO:0043226	C	Organelle
166	GO:0044464	C	cell part

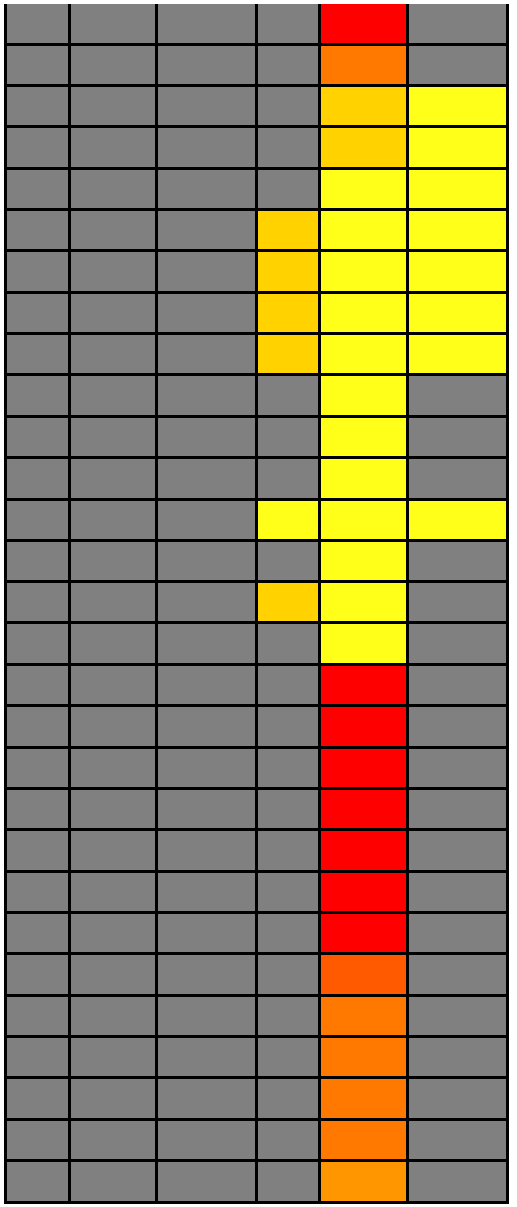

167	GO:0005623	C	Cell	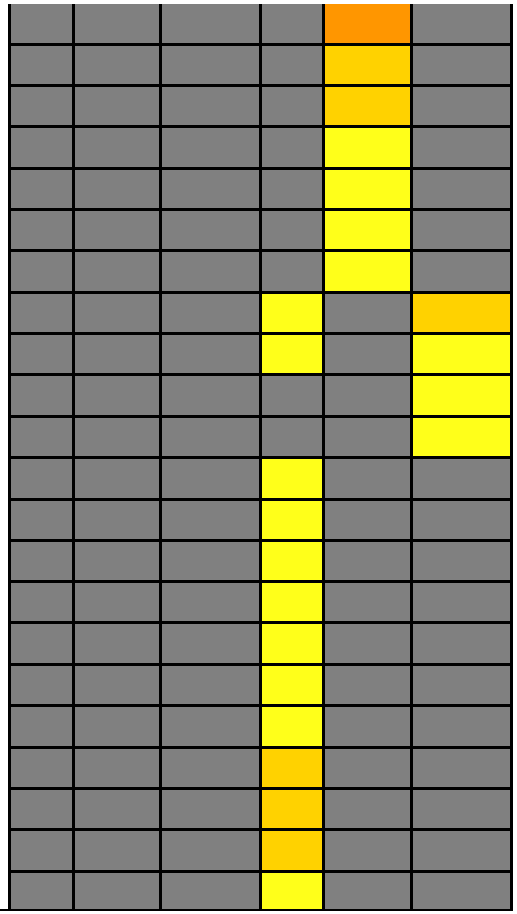
168	GO:0030684	C	Preribosome	
169	GO:0044391	C	ribosomal subunit	
170	GO:0032040	C	small-subunit processome	
171	GO:0033176	C	proton-transporting V-type ATPase complex	
172	GO:0015934	C	large ribosomal subunit	
173	GO:0033180	C	proton-transporting V-type ATPase, V1 domain	
174	GO:0006950	P	response to stress	
175	GO:0042221	P	response to chemical	
176	GO:0005975	P	carbohydrate metabolic process	
177	GO:0016620	F	oxidoreductase activity, acting on the aldehyde or oxo group of donors, NAD as acceptor	
178	GO:0044707	P	single-multicellular organism process	
179	GO:0007275	P	multicellular organism development	
180	GO:0032502	P	developmental process	
181	GO:0044767	P	single-organism developmental process	
182	GO:0048856	P	anatomical structure development	
183	GO:0009064	P	glutamine family amino acid metabolic process	
184	GO:0009611	P	response to wounding	
185	GO:0042578	F	phosphoric ester hydrolase activity	
186	GO:0003993	F	acid phosphatase activity	
187	GO:0016791	F	phosphatase activity	
188	GO:0016787	F	hydrolase activity	

Table S8. List of most significant upregulated and downregulated genes (top 20) in Golden Promise compared to *hvabf* under drought conditions. Molecular function and cellular component of annotated proteins are indicated. DEG, differentially expressed gene; GO, gene ontology

Gene ID	DEG direction	Gene annotation	GO: molecular function	GO: cellular component
HORVU6Hr1G011520	Downregulated	Histone 3	DNA binding	Nucleus
HORVU5Hr1G036670	Downregulated	SAM_MT_TRM5_TYW2 domain-containing protein	tRNA methyl transferase activity	Cytoplasm
HORVU5Hr1G004700	Downregulated	Terpene_synth domain-containing protein	terpene synthase activity	
HORVU6Hr1G017810	Downregulated	Uncharacterized		
HORVU2Hr1G077370	Downregulated	Uncharacterized		
HORVU5Hr1G005890	Downregulated	Uncharacterized		
HORVU7Hr1G077370	Downregulated	Uncharacterized		
HORVU6Hr1G093140	Downregulated	Protein kinase domain-containing protein	transmembrane receptor protein serine/threonine kinase activity	plasma membrane
HORVU2Hr1G043940	Downregulated	Uncharacterized		
HORVU6Hr1G053350	Downregulated	Uncharacterized		
HORVU5Hr1G059310	Downregulated	Peptidase C83 domain-containing protein	metal ion binding	
HORVU2Hr1G010030	Downregulated	Uncharacterized		
HORVU5Hr1G108870	Downregulated	Uncharacterized		
HORVU4Hr1G078950	Downregulated	Uncharacterized		
HORVU4Hr1G061900	Downregulated	Ubiquitin-like domain-containing protein	upiquitin protein ligase binding	nucleus
HORVU3Hr1G023590	Downregulated	Uncharacterized		
HORVU6Hr1G032080	Downregulated	Uncharacterized		
HORVU1Hr1G073460	Downregulated	TPR_REGION domain-containing protein		
HORVU3Hr1G105720	Downregulated	TF-B3 domain-containing protein	Transcription	nucleus
HORVU4Hr1G090780	Downregulated	Dirigent protein	carbohydrate binding	apoplast
HORVU7Hr1G097070	Upregulated	Uncharacterized		
HORVU6Hr1G018030	Upregulated	F-box domain-containing protein	protein binding	chloroplast
HORVU5Hr1G015140	Upregulated	Ferredoxin thioredoxin reductase catalytic beta subunit	oxidoreductase activity, acting on iron-sulfur proteins as donors	membrane
HORVU0Hr1G010880	Upregulated	Uncharacterized	oxidoreductase activity, iron-ion binding	membrane

HORVU5Hr1G005340	Upregulated	Uncharacterized		
HORVU5Hr1G106090	Upregulated	Catalytic activity	tryptophan synthase activity	chloroplast
HORVU7Hr1G073770	Upregulated		translation initiation activity	cytoplasmic stress granule
HORVU1Hr1G016840	Upregulated	peroxidase	peroxidase activity	extracellular region
HORVU4Hr1G001900	Upregulated	Uncharacterized		
HORVU6Hr1G059800	Upregulated	Galectin domain-containing protein	galactosyltransferase activity	golgi appratus
HORVU3Hr1G083190	Upregulated	peroxidase	peroxidase activity	extracellular region
HORVU0Hr1G005210	Upregulated	Uncharacterized		
HORVU1Hr1G047560	Upregulated	Uncharacterized		
HORVU5Hr1G009840	Upregulated	Guanosine nucleotide diphosphate dissociation inhibitor	GDP-dissociation inhibitor activity	intracellular
HORVU2Hr1G082740	Upregulated	Uncharacterized		
HORVU5Hr1G095630	Upregulated	VRN-H1	transcription factor activity	nucleus
HORVU5Hr1G019220	Upregulated	WD40/YVTN repeat-like domain	intracellular protein transport	golgi appratus
HORVU2Hr1G019900	Upregulated	Uncharacterized		
HORVU4Hr1G008700	Upregulated	Glutamate decarboxylase	glutamate decarboxylase activity	cytoplasm
HORVU5Hr1G088360	Upregulated	Uncharacterized		

Table S9. List of most significantly (top 20) upregulated and downregulated genes in Golden Promise compared to *hvabi5* under drought conditions. Molecular function and cellular component of annotated proteins are indicated. DEG, differentially expressed gene; GO, gene ontology

Gene	DEG direction	Gene annotation	GO: molecular function	GO: cellular component
HORVU6Hr1G050370	Downregulated	Integrase catalytic domain-containing protein	nucleic acid binding	
HORVU3Hr1G026670	Downregulated	DUF3474 domain-containing protein	oxidoreductase activity	membrane
HORVU6Hr1G010420	Downregulated	Ubiquitin-like domain-containing protein	ubiquitin-dependent protein catabolic process	
HORVU1Hr1G055350	Downregulated	Uncharacterized		
HORVU7Hr1G020180	Downregulated	Expressed protein	regulation of transcription	
HORVU2Hr1G109190	Downregulated	Expressed protein	regulation of transcription	

HORVU7Hr1G077370	Downregulated	Uncharacterized		
HORVU7Hr1G031680	Downregulated	PBPe domain-containing protein	ligand-gated ion channel activity	
HORVU4Hr1G052030	Downregulated	SWIM-type domain-containing protein	zinc ion binding	
HORVU2Hr1G077370	Downregulated	Uncharacterized		
HORVU6Hr1G017810	Downregulated	Uncharacterized		
HORVU6Hr1G093140	Downregulated	Protein kinase domain-containing protein	ATP binding	plasma membrane
HORVU6Hr1G053350	Downregulated	Uncharacterized		
HORVU2Hr1G013820	Downregulated	Uncharacterized		
HORVU6Hr1G078390	Downregulated	F-box-like domain superfamily	protein binding	
HORVU2Hr1G010030	Downregulated	Uncharacterized		
HORVU7Hr1G006630	Downregulated	Uncharacterized		
HORVU4Hr1G076610	Downregulated	Uncharacterized		
HORVU4Hr1G061900	Downregulated	Ubiquitin-like domain-containing protein	ubiquitin protein ligase binding	nucleus, cytoplasm
HORVU3Hr1G105720	Downregulated	TF-B3 domain-containing protein	DNA binding	nucleus
HORVU2Hr1G048610	Upregulated	Uncharacterized		
HORVU6Hr1G018030	Upregulated	Uncharacterized		
HORVU7Hr1G097070	Upregulated	Uncharacterized		
HORVU1Hr1G009980	Upregulated	Expressed protein	protein phosphatase inhibitor activity	
HORVU1Hr1G019640	Upregulated	Uncharacterized		
HORVU6Hr1G081270	Upregulated	Uncharacterized		
HORVU3Hr1G105760	Upregulated	Uncharacterized		
HORVU5Hr1G095580	Upregulated	Expressed protein	cysteine-type endopeptidase activity	extracellular
HORVU7Hr1G111960	Upregulated	Expressed protein	magnesium ion binding	
HORVU0Hr1G010880	Upregulated	Expressed protein	monooxygnogenase, oxidoreductase actiivity	membrane
HORVU6Hr1G059800	Upregulated	Expressed protein	galactosyltransferase activity	golgi apparauts, membrane
HORVU6Hr1G090470	Upregulated	Expressed protein	ATP binding/ defense response	
HORVU2Hr1G073210	Upregulated	Glyco_hydro_32N domain-containing protein	hydrolase activity, hydrolyzing O-glycosyl compounds	membrane
HORVU4Hr1G079600	Upregulated	Uncharacterized		
HORVU3Hr1G079180	Upregulated	VQ domain-containing protein	positive regulation of DNA-binding transcription factor activity	

HORVU3Hr1G046900	Upregulated	Glyco_tran_28_C domain-containing protein	transferase activity, transferring hexosyl groups	
HORVU4Hr1G044140	Upregulated	MGDG_synth domain-containing protein	transferase activity, transferring hexosyl groups	
HORVU3Hr1G036600	Upregulated	TLC domain-containing protein	phospholipid homeostasis	membrane
HORVU5Hr1G062450	Upregulated	Uncharacterized		
HORVU5Hr1G028140	Upregulated	Expressed protein	signaling receptor activity	

Table S10. List of primers used in experiments with Arabidopsis.

Primer name	Forward primer	Reverse primer	Purpose	Remarks
ELF4a-q	TCAGAAGGAGAGAGACGCCA	CACGGTTGTTGGGGAGATCA	qPCR	Feng et al. 2016
P5CS1-q	AAGAGCCCCATATCAGGATTCTTCT	GAGCGATGTTGAAGGTCTTTACACA	qPCR	Feng et al. 2016
S132819	CCGGTAAGGGTTCTTCTCAAG	AGAGGCAACAGACTTTAGGGG	SALK_132819	
S002984	TAATGGGAAATCTTGGTGCAG	TCTTTTGCATTTCCATGATCC	SALK_002984	
S09696	ACACTGTTATTAACGGCGGTG	CTTTCTCCAGAACTGCACCTG	SALK_096965	
S069523	TCCTCGATTAAGCACATACGG	GAACAAGGGTTTTAGGGCTTG	SALK_069523	
SALK_LB 1.3	ATTTTGCCGATTTCGGAAC		left border primer	
ABF1-semiRT	AGAGGCAACAGACTTTAGGGG	CCGGTAAGGGTTCTTCTCAAG	SALK_genotyping	Yoshida et al. 2015
ABF2-semiRT	GGTGGTCTTGTGGGACTTGGA	CTTCAAGCTCCACGGTGTAAG	SALK_genotyping	Yoshida et al. 2015
ABF3-semiRT	GCTGTTGGTGTGGGAGGAGAA	GGGCGCTCTTTGGAGTCAGAT	SALK_genotyping	Yoshida et al. 2015
ABF4-semiRT	GGGTTTTAGGGCTTGGATGCT	TTCACAGGCGCAGAAAATGCT	SALK_genotyping	Yoshida et al. 2015
bTUB-seimRT	ATCCCACCGGACGTTACAAC	TTCGTTGTCGAGGACCATGC	SALK_genotyping	Yoshida et al. 2015

Feng X.J., Li J.R., Qi S.L., Lin Q.F., Jin J.B. & Hua X.J. (2016) Light affects salt stress-induced transcriptional memory of P5CS1 in Arabidopsis. *Proceedings of the National Academy of Sciences of the United States of America* **113**, E8335–E8343.

Yoshida T., Fujita Y., Maruyama K., Mogami J., Todaka D., Shinozaki K. & Yamaguchi-Shinozaki K. (2015) Four Arabidopsis AREB/ABF transcription factors function predominantly in gene expression downstream of SnRK2 kinases in abscisic acid signalling in response to osmotic stress. *Plant, Cell and Environment* **38**, 35–49.

Table S11. Summary statistics of proline concentration and *P5CS1* mRNA expression in shoot under ABA treatment. Means sharing a letter are not significantly different from Tukey-adjusted comparisons ($P \leq 0.05$). The asterisks indicated significant genotype, treatment and genotype by treatment interaction effect (ns, non-significant; $P \leq 0.05$, *; $P \leq 0.01$, **; $P \leq 0.001$, ***). G, genotype; T, treatment

Mean values of shoot proline concentration (µg/ g Fresh weight)							
Hour	-ABA		+ABA		ANOVA		
	abf1 abf2 abf3 abf4	Col-0	*abf1 abf2 abf3 abf4*	Col-0	G	T	G*T
24	90^{a}	87^{a}	120^{a}	183^{b}	**	***	*
48	112^{ab}	92^{a}	170^{bc}	233^{c}	ns	***	Ns
72	118^{a}	107^{a}	209^{b}	448^{c}	*	***	*
96	131^{a}	135^{a}	259^{b}	847^{c}	***	***	***
Mean values of relative *P5CS1* expression (fold change to control)							
24	1.01^{a}	1.16^{a}	1.89^{a}	6.82^{b}	*	**	*
48	1.06^{a}	1.03^{a}	4.61^{b}	15.26^{b}	**	***	**
72	1.00^{a}	1.00^{a}	3.32^{b}	18.39^{c}	***	***	***
96	1.04^{a}	1.03^{a}	3.52^{b}	21.00^{c}	**	***	**

Table S12. Summary statistics of shoot proline concentration and *P5CS1* mRNA expression in shoot under acute dehydration treatment. Means sharing a letter are not significantly different by Tukey-adjusted comparisons ($P \leq 0.05$). The asterisks indicated significant genotype, treatment and genotype by treatment interaction effect (ns, non-significant; $P \leq 0.05$, *; $P \leq 0.01$, **; $P \leq 0.001$, ***). G, genotype; T, treatment

Mean values of shoot proline (µg/ g FW)							
Hour	Control		Dehydration		ANOVA		
	abf1 abf2 abf3 abf4	Col-0	*abf1 abf2 abf3 abf4*	Col-0	G	T	G*T
1	54.2^{a}	60.7^{a}	80.3^{ab}	94.8^{b}	**	**	**
2	62.2^{a}	66.8^{a}	114.7^{ab}	168.7^{b}	*	***	Ns
3	61.5^{a}	58.3^{a}	185.1^{b}	286.0^{c}	*	***	*
Mean values of relative *P5CS1* expression (fold change to control)							
1	1.1^{a}	1.1^{a}	1.22^{a}	4.1^{b}	**	**	**
2	0.9^{a}	1.1^{ab}	2.7^{bc}	6.9^{c}	***	***	***
3	1.14^{a}	1.0^{a}	3.5^{b}	13.5^{c}	***	***	***

Table S13. Summary statistics of shoot proline concentration under drought stress. Means sharing a letter are not significantly different by Tukey-adjusted comparisons ($P \leq 0.05$). The asterisks indicated significant genotype, treatment and genotype by treatment interaction effect (ns, non-significant; $P \leq 0.05$, *; $P \leq 0.01$, **; $P \leq 0.001$, ***). G, genotype; T, treatment

Day	Control		Drought		ANOVA		
	abf1 abf2 abf3 abf4	Col-0	*abf1 abf2 abf3 abf4*	Col-0	G	T	G*T
4	57^{a}	47^{a}	55^{a}	55^{a}	ns	ns	Ns
5	55^{a}	44^{a}	209^{b}	435^{c}	***	***	***
6	53^{a}	51^{a}	1226^{c}	1085^{b}	***	***	*
7	45^{a}	44^{a}	3013^{b}	3132^{b}	ns	***	Ns

Table S14. Summary statistics for the morphological and biochemical response to drought stress. Means sharing a letter are not significantly different by Tukey-adjusted comparisons ($P \leq 0.05$). The asterisks indicated significant genotype, treatment and genotype by treatment interaction effect (ns, non-significant; $P \leq 0.05$, *; $P \leq 0.01$, **; $P \leq 0.001$, ***). G, genotype; MDA, malondialdehyde; T, treatment

Trait	Control		Drought		ANOVA		
	Col-0	*abf1 abf2 abf3 abf4*	Col-0	*abf1 abf2 abf3 abf4*	G	T	G*T
Fresh weight (g)	177.5^{a}	165.9^{a}	56.6^{b}	21.5^{b}	*	***	ns
Dry weight (g)	11.85^{a}	12.24^{a}	7.55^{b}	3.86^{c}	*	***	*
MDA (nmol/ g fresh weight)	10.0^{a}	10.8^{a}	13.3^{a}	23.7^{b}	**	***	**
Electrolyte leakage (%)	5.3^{a}	5.1^{a}	7.46^{a}	14.69^{b}	**	***	**
Relative water content (%)	81.5^{a}	80.9^{a}	50.1^{b}	38.1^{c}	**	***	*

Table S15. List of high confidence genes present in the QTL (*QPro.S42-1H*) interval.

Gene ID	chromosome: start-stop	Description
HORVU1Hr1G071810	chr1H:494910477-494913834	Lung seven transmembrane receptor family protein
HORVU1Hr1G071840	chr1H:494959516-494983640	BTB-POZ and MATH domain 1
HORVU1Hr1G071880	chr1H:495195841-495196127	Endoribonuclease Dicer homolog 1
HORVU1Hr1G071890	chr1H:495203603-495210811	Phosphatidate phosphatase LPIN2
HORVU1Hr1G071930	chr1H:495404668-495410478	Metal tolerance protein 5
HORVU1Hr1G071950	chr1H:495547671-495548389	Histone H2A 7
HORVU1Hr1G071960	chr1H:495604804-495606122	Histone H2A 7
HORVU1Hr1G071980	chr1H:495746590-495746908	Histone H2A 12
HORVU1Hr1G072050	chr1H:495875162-495876936	HXXXD-type acyl-transferase family protein
HORVU1Hr1G072060	chr1H:495884739-495886729	30S ribosomal protein S8
HORVU1Hr1G072070	chr1H:495888795-495891818	Ras-related protein Rab-8B
HORVU1Hr1G072090	chr1H:496009174-496009886	Basic-leucine zipper (bZIP) transcription factor family protein
HORVU1Hr1G072110	chr1H:496080124-496083235	Coatomer subunit zeta-1
HORVU1Hr1G072120	chr1H:496087757-496093636	Basic-leucine zipper (bZIP) transcription factor family protein
HORVU1Hr1G072140	chr1H:496197194-496205312	Respiratory burst oxidase homologue D
HORVU1Hr1G072160	chr1H:496271629-496278858	Respiratory burst oxidase homologue D
HORVU1Hr1G072170	chr1H:496434857-496439629	Very-long-chain (3R)-3-hydroxyacyl-CoA dehydratase 2
HORVU1Hr1G072180	chr1H:496442865-496446585	Riboflavin biosynthesis protein RibBA
HORVU1Hr1G072190	chr1H:496445735-496446595	Histone H2B.11
HORVU1Hr1G072200	chr1H:496571925-496575026	Ubiquitin-conjugating enzyme 13
HORVU1Hr1G072210	chr1H:496657261-496660675	NAD-specific glutamate dehydrogenase
HORVU1Hr1G072220	chr1H:496657555-496660454	Heat shock 70 kDa protein
HORVU1Hr1G072230	chr1H:496745915-496749940	Tryptophan aminotransferase related 2
HORVU1Hr1G072250	chr1H:496810598-496812395	Chitinase 2
HORVU1Hr1G072270	chr1H:496930969-496933348	60S ribosomal protein L36-2
HORVU1Hr1G072280	chr1H:496941467-496941788	Fasciclin-like arabinogalactan family protein
HORVU1Hr1G072290	chr1H:497024084-497026746	Fasciclin-like arabinogalactan family protein

HORVU1Hr1G072300	chr1H:497034138-497035775	Disease resistance protein RPM1
HORVU1Hr1G072360	chr1H:497144523-497150811	O-fucosyltransferase family protein
HORVU1Hr1G072370	chr1H:497206745-497210574	Kinesin 4
HORVU1Hr1G072390	chr1H:497253090-497253683	Membrin 11
HORVU1Hr1G072400	chr1H:497334110-497336675	RING/U-box superfamily protein
HORVU1Hr1G072420	chr1H:497472764-497473345	SAUR-like auxin-responsive protein family
HORVU1Hr1G072430	chr1H:497663499-497669000	MYB domain protein 3r-5
HORVU1Hr1G072470	chr1H:497762541-497765213	Laccase 17
HORVU1Hr1G072490	chr1H:497889581-497943853	ATP-dependent zinc metalloprotease FtsH
HORVU1Hr1G072500	chr1H:498024404-498028438	Heavy metal transport/detoxification superfamily protein
HORVU1Hr1G072530	chr1H:498116203-498118620	Laccase 17
HORVU1Hr1G072560	chr1H:498200252-498207010	Protein S-acyltransferase 11
HORVU1Hr1G072570	chr1H:498202625-498207934	Peptidyl-prolyl cis-trans isomerase
HORVU1Hr1G072580	chr1H:498234638-498235317	ROTUNDIFOLIA like 8
HORVU1Hr1G072590	chr1H:498354627-498356343	Glycerol-3-phosphate acyltransferase 7
HORVU1Hr1G072610	chr1H:498424804-498425506	COX VIIa-like protein
HORVU1Hr1G072640	chr1H:498512017-498516380	Tetratricopeptide repeat (TPR)-like superfamily protein
HORVU1Hr1G072650	chr1H:498568088-498571507	Protein YIPF
HORVU1Hr1G072660	chr1H:498571915-498573497	Mitochondrial glycoprotein family protein
HORVU1Hr1G072670	chr1H:498578659-498581776	Aldose reductase
HORVU1Hr1G072680	chr1H:498614402-498618911	Aldose reductase
HORVU1Hr1G072690	chr1H:498650547-498655628	Aldose reductase A
HORVU1Hr1G072700	chr1H:498694753-498696867	Aldose reductase
HORVU1Hr1G072710	chr1H:498704314-498707100	CASP-like protein 16
HORVU1Hr1G072730	chr1H:498773732-498779589	Prenylated RAB acceptor 1.A3
HORVU1Hr1G072740	chr1H:498776551-498776708	Callose synthase 9
HORVU1Hr1G072750	chr1H:498780357-498783833	Uracil phosphoribosyltransferase
HORVU1Hr1G072780	chr1H:498975383-498982941	Gamma-glutamyl phosphate reductase
HORVU1Hr1G072810	chr1H:499154869-499157373	Transcription factor ILR3
HORVU1Hr1G072820	chr1H:499118472-499120282	Microtubule-binding protein TANGLED1

HORVU1Hr1G072850	chr1H:499314439-499319533	Homeobox protein BEL1 homolog
HORVU1Hr1G072910	chr1H:499643443-499646887	ROP guanine nucleotide exchange factor 5
HORVU1Hr1G072930	chr1H:499895459-499898412	DNA replication complex GINS protein PSF1
HORVU1Hr1G072970	chr1H:500134362-500136504	Auxin efflux carrier family protein
HORVU1Hr1G072990	chr1H:500387708-500391739	Guanylyl cyclase 1
HORVU1Hr1G073040	chr1H:500888949-500893295	Phosphatidylinositol:ceramide inositolphosphotransferase
HORVU1Hr1G073060	chr1H:500963868-500967622	Phosphatidylinositol:ceramide inositolphosphotransferase
HORVU1Hr1G073070	chr1H:501000400-501008184	Ankyrin repeat family protein
HORVU1Hr1G073080	chr1H:501108974-501110172	Yos1-like protein
HORVU1Hr1G073130	chr1H:501295170-501296366	Ataxin-3 homolog
HORVU1Hr1G073150	chr1H:501358479-501363313	O-fucosyltransferase family protein
HORVU1Hr1G073180	chr1H:501622052-501624694	Pentatricopeptide repeat-containing protein
HORVU1Hr1G073210	chr1H:501987914-501991647	phosphate transporter 4;2
HORVU1Hr1G073230	chr1H:502081021-502084952	Coronatine-insensitive protein homolog 1b
HORVU1Hr1G073280	chr1H:502236455-502240099	Glycosyl hydrolase family protein
HORVU1Hr1G073300	chr1H:502678559-502680680	MYB-like transcription factor family protein
HORVU1Hr1G073310	chr1H:502679642-502680604	ScMYB36 protein
HORVU1Hr1G073330	chr1H:503056222-503058634	HXXXD-type acyl-transferase family protein
HORVU1Hr1G073340	chr1H:503131338-503141099	Glycerol-3-phosphate acyltransferase 6
HORVU1Hr1G073400	chr1H:503256232-503257711	Tetratricopeptide repeat (TPR)-like superfamily protein
HORVU1Hr1G073460	chr1H:503312082-503313620	Tetratricopeptide repeat (TPR)-like superfamily protein
HORVU1Hr1G073480	chr1H:503410879-503413977	Indole-3-glycerol phosphate synthase
HORVU1Hr1G073490	chr1H:503418687-503424739	Auxin transporter-like protein 2
HORVU1Hr1G073500	chr1H:503498281-503505706	Arginyl-tRNA--protein transferase 1
HORVU1Hr1G073510	chr1H:503508154-503511215	Alpha-amylase
HORVU1Hr1G073540	chr1H:503657570-503662934	DNA glycosylase superfamily protein
HORVU1Hr1G073570	chr1H:503690353-503691345	ROTUNDIFOLIA like 8
HORVU1Hr1G073640	chr1H:504078029-504080009	60S acidic ribosomal protein family
HORVU1Hr1G073660	chr1H:504086268-504087584	Protein BUD31 homolog 2
HORVU1Hr1G073670	chr1H:504166593-504167486	Histone superfamily protein

HORVU1Hr1G073680	chr1H:504169057-504169904	Histone superfamily protein
HORVU1Hr1G073700	chr1H:504325276-504327646	Cytochrome P450 superfamily protein
HORVU1Hr1G073720	chr1H:504429876-504439484	Solute carrier family 35 member F2
HORVU1Hr1G073760	chr1H:504458555-504461395	Solute carrier family 35 member F2
HORVU1Hr1G073820	chr1H:504788299-504800017	Glucan endo-1
HORVU1Hr1G073840	chr1H:504803233-504805066	Ferredoxin 3
HORVU1Hr1G073870	chr1H:504928798-504933724	Transcription factor-related
HORVU1Hr1G073890	chr1H:505146277-505151971	Protein transport protein SEC24
HORVU1Hr1G073900	chr1H:505244500-505246396	NAC domain protein
HORVU1Hr1G073910	chr1H:505547459-505547581	D111/G-patch domain-containing protein
HORVU1Hr1G073920	chr1H:505648010-505648633	Voltage-dependent L-type calcium channel subunit alpha-1F
HORVU1Hr1G073940	chr1H:505808877-505810214	MYB-like transcription factor family protein
HORVU1Hr1G072100	chr1H:496076442-496076948	Zinc-finger protein 3
HORVU1Hr1G072870	chr1H:499380903-499382988	DNA/RNA helicase protein
HORVU1Hr1G073050	chr1H:500894039-500897338	RING/FYVE/PHD zinc finger superfamily protein
HORVU1Hr1G073170	chr1H:501616873-501619587	LSD1 zinc finger family protein
HORVU1Hr1G073320	chr1H:502805136-502805654	MYB/SANT-like DNA-binding domain protein
HORVU1Hr1G073710	chr1H:504428449-504428718	Ribosomal protein-like
HORVU1Hr1G071850	chr1H:494993135-494993649	Undescribed protein
HORVU1Hr1G071870	chr1H:495213284-495214402	Coffea canephora DH200=94 genomic scaffold
HORVU1Hr1G071910	chr1H:495399707-495401012	Plant protein 1589 of unknown function
HORVU1Hr1G071940	chr1H:495457089-495458502	Unknown function
HORVU1Hr1G072310	chr1H:497036811-497037092	Undescribed protein
HORVU1Hr1G072380	chr1H:497251503-497252565	Unknown function
HORVU1Hr1G072410	chr1H:497470161-497476191	BnaC04g25510D protein
HORVU1Hr1G072720	chr1H:498707615-498708832	Unknown protein
HORVU1Hr1G072840	chr1H:499252785-499253054	Unknown function
HORVU1Hr1G072890	chr1H:499562026-499563106	Unknown function
HORVU1Hr1G073010	chr1H:500581804-500637119	Unknown function
HORVU1Hr1G073120	chr1H:501127364-501127624	Undescribed protein

HORVU1Hr1G073190	chr1H:501967950-501971414	Protein of unknown function (DUF740)
HORVU1Hr1G073260	chr1H:502162131-502162328	Unknown function
HORVU1Hr1G073600	chr1H:503801465-503802031	Unknown function
HORVU1Hr1G073610	chr1H:503856778-503859409	Unknown function
HORVU1Hr1G073780	chr1H:504469909-504470151	Unknown function

Supplementary figures

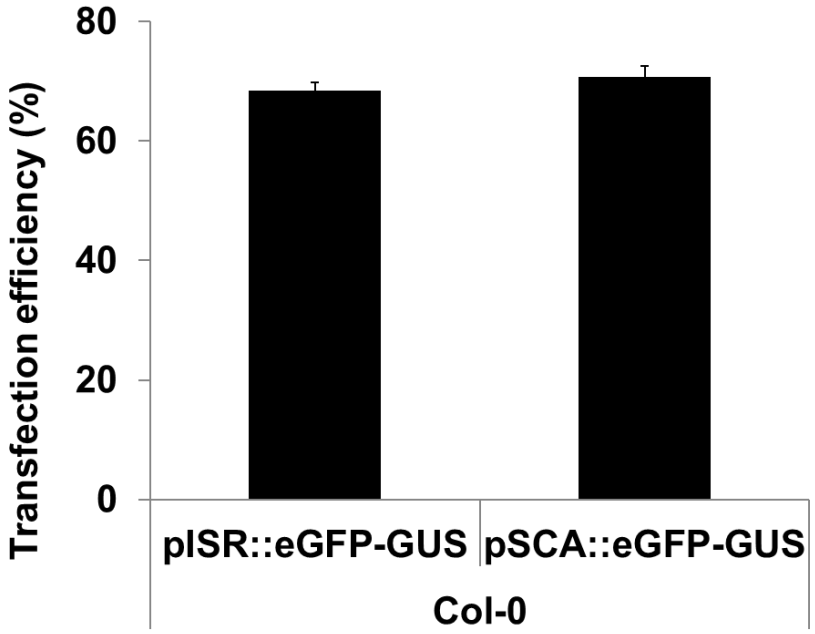

Figure S1. Transfection efficiency in Arabidopsis protoplast. The protoplast transfected with pISR::eGFP-GUS or pSCA::eGFP-GUS was checked for GFP signals using a confocal microscope. Transfection efficiency is expressed as a percentage. Bars indicate mean ± SE (n = 3).

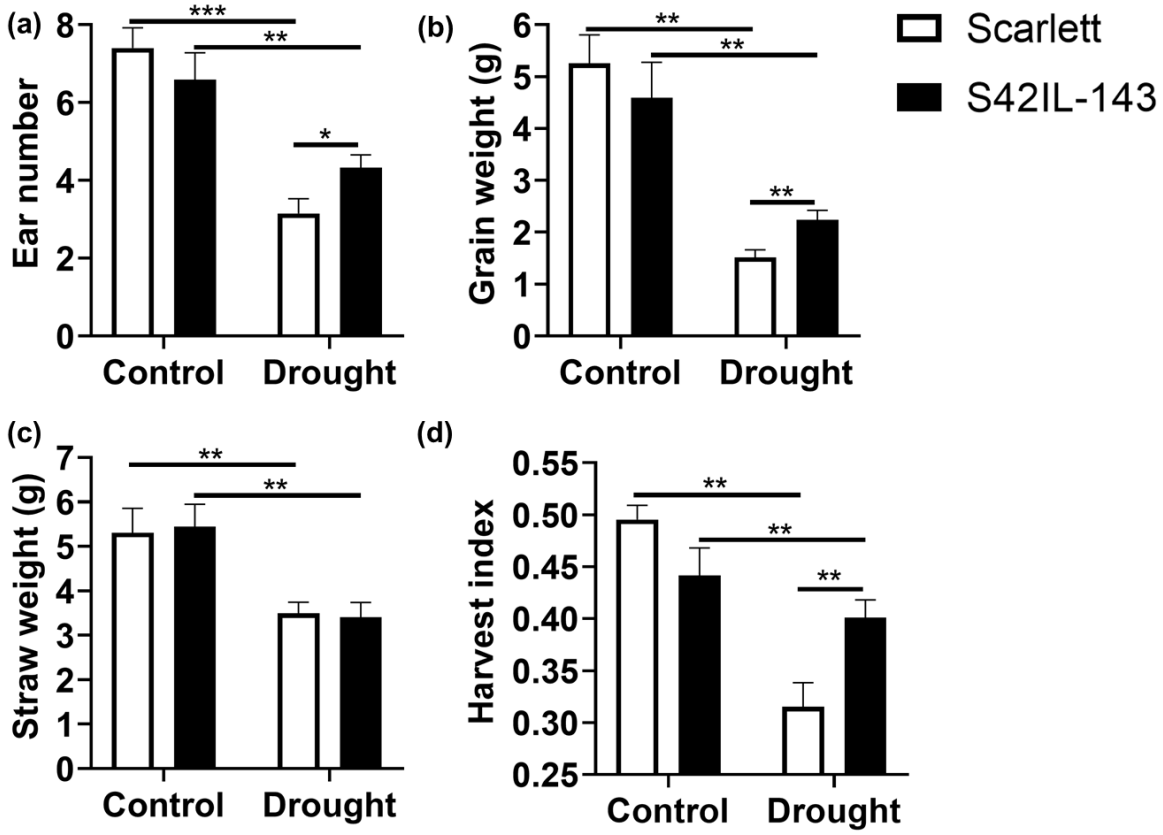

Figure S2. Yield and related traits of Scarlett and S42IL-143 in a pot experiment. Effect of drought stress on (a) number of ears per plant, (b) grain weight per plant (c) straw weight per plant, and (d) harvest index. Scarlett and S42IL-143 seeds were sown in a pot (22 × 22 × 26), and plants were watered three times a day using a drip irrigation system. Two drought stress treatments were applied at the tillering stage and before heading. Water supply was withheld for 14 d before rewatering. Matured panicles and straw were harvested, and oven-dried at 37°C for 72 h. The graph represents the mean ± SE (n = 20). Asterisks indicate significant differences between genotypes (**$P \leq 0.01$, ***$P \leq 0.001$) using a student's *t*-test.

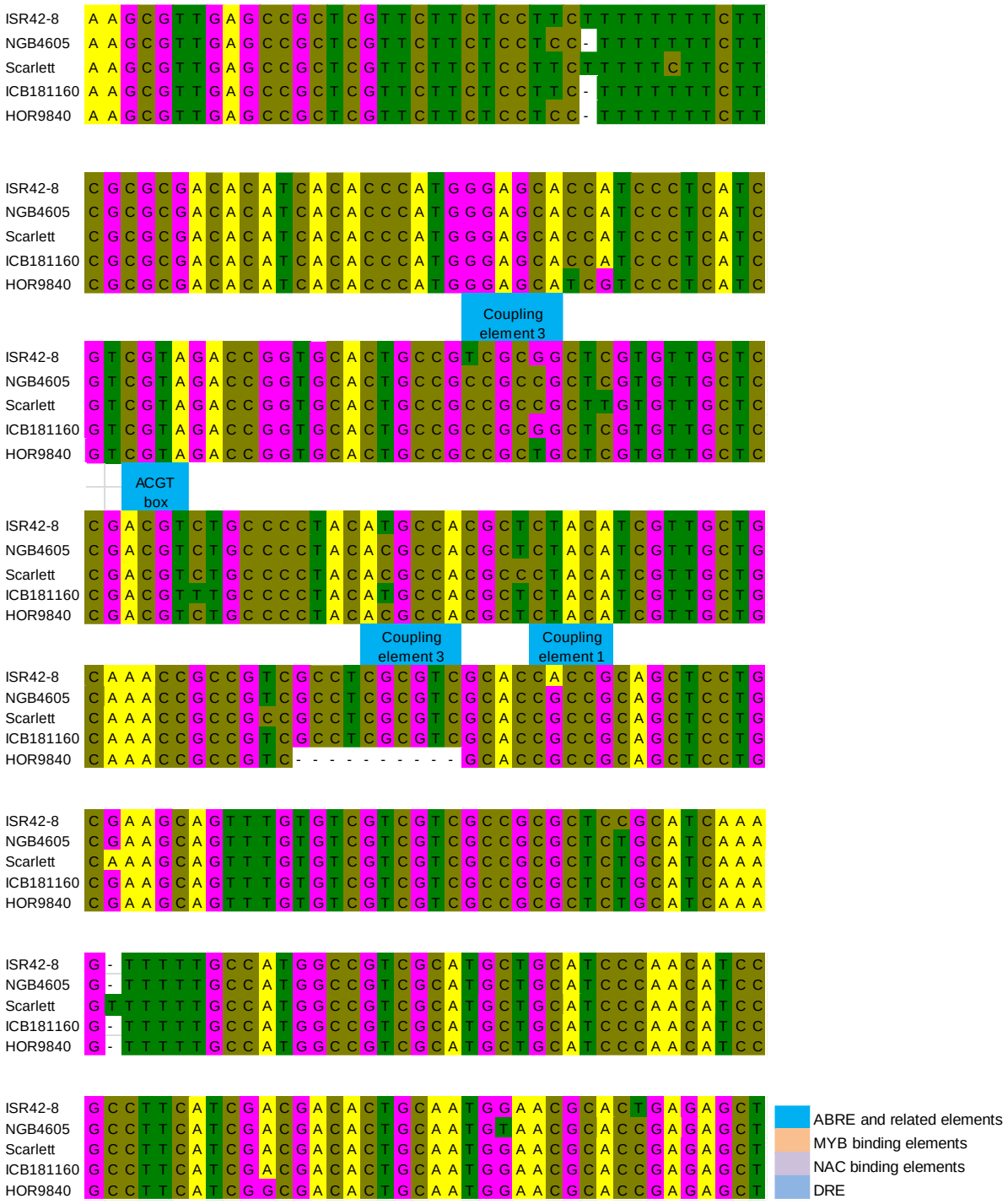

Figure S3. Sequence alignment of five barley genotypes (1450 bp upstream of the start codon). The name of the predicted binding motif is indicated above the sequence alignment. Only core motifs are indicated. Except for the first row with a start codon (9 bp), each row comprises of 40 bp. ABRE, ABA-responsive element; DRE, dehydration responsive element

Figure S3 continued

Figure S3 continued

Figure S3 continued

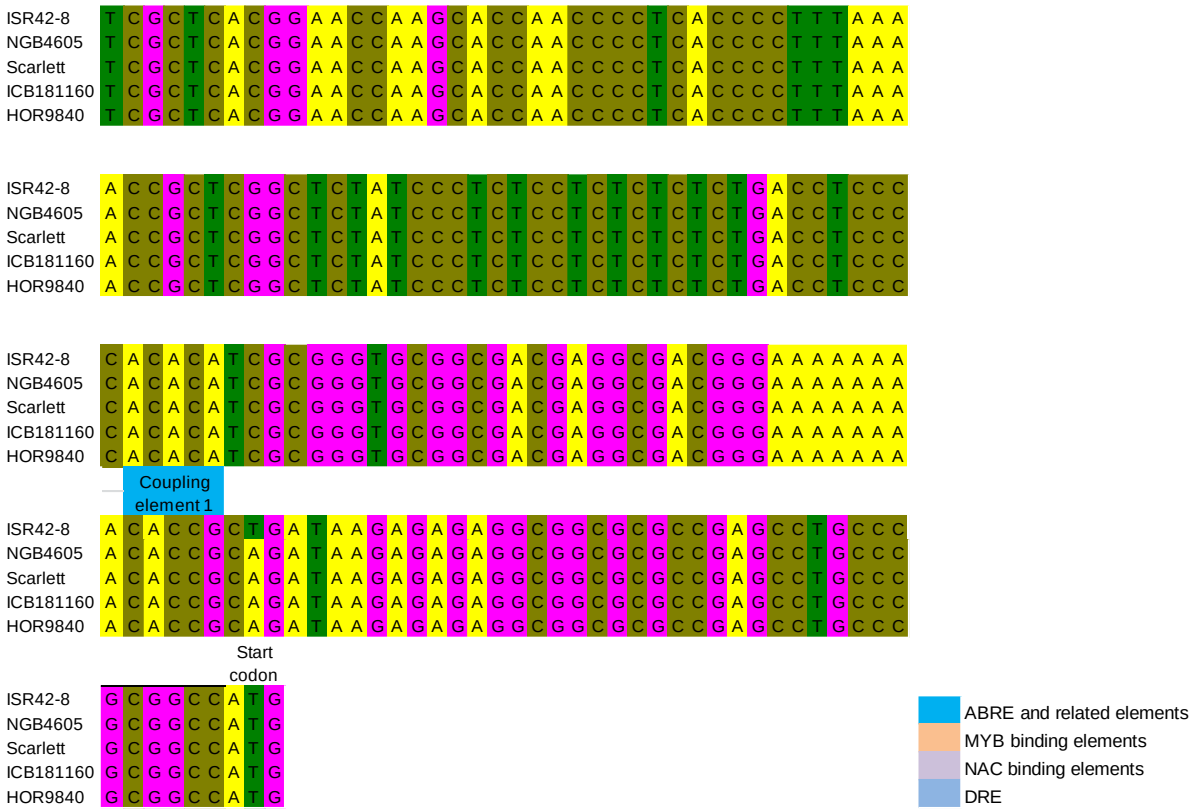

Figure S3 continued

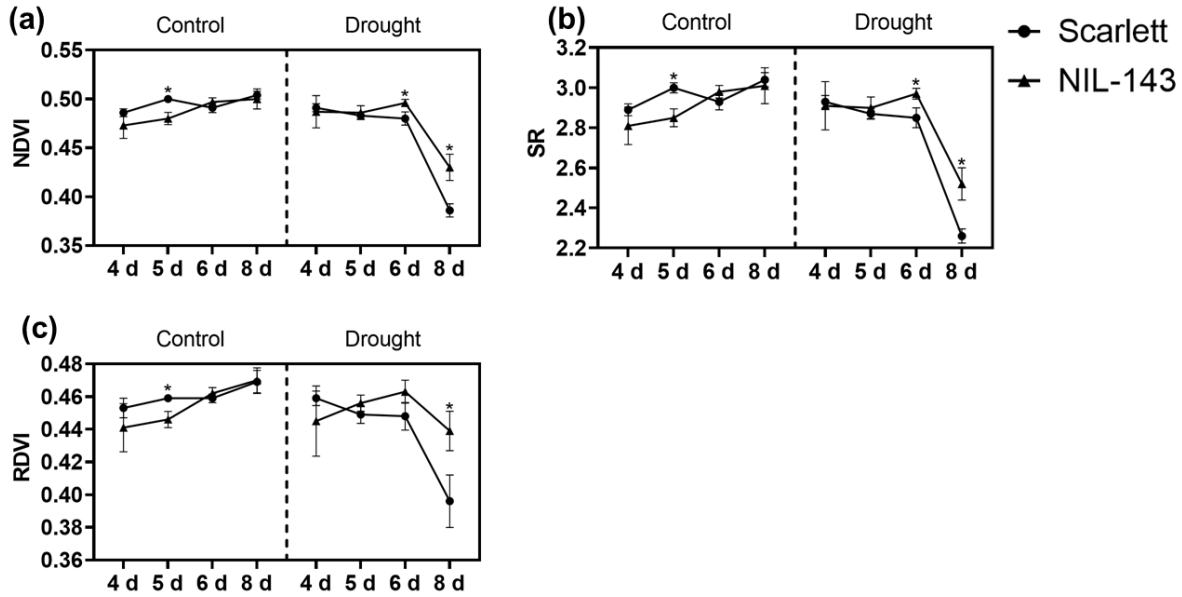

Figure S4. Vegetation index of Scarlett and NIL-143 under drought stress at the seedling stage. Effect of water stress on (a) Normalized differences vegetation index (NDVI) (b) simple ratio index (SR) (c) renormalized differences vegetation index (RDVI) and (d) Carter index 2 (Ctr2). Drought treatment was applied to two-week-old seedlings by terminating the water supply. Vegetation indexes were scored at 4, 5, 6 and 8 d after stress using SPAD meter and PolyPen. The graph indicates mean ± SE (n = 5). Asterisks indicate significant differences between genotypes (*$P \leq 0.05$) using student's *t*-test.

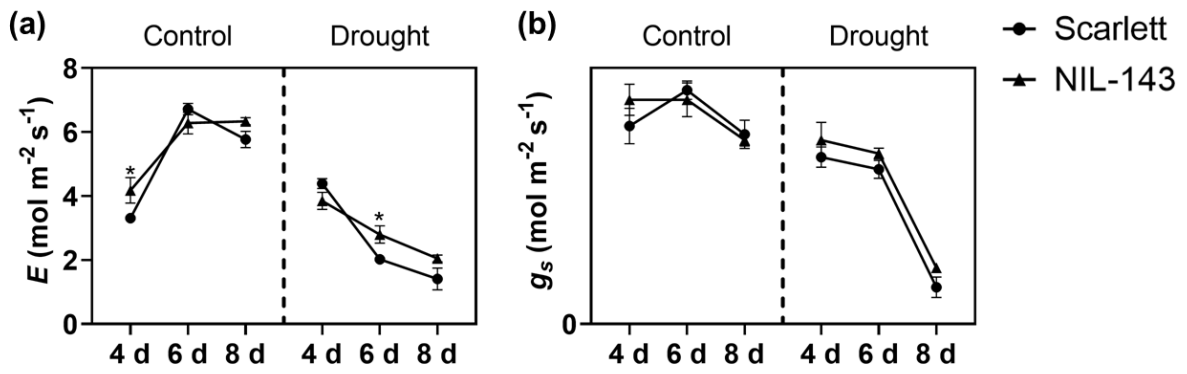

Figure S5. Photosynthetic traits in Scarlett and NIL-143 under drought stress at the seedling stage. Effect of water stress on (a) transpiration rate (*E*) and (b) stomatal conductance (g_s). Drought treatment was applied to two-week-old seedlings by terminating the water supply. Photosynthesis related traits were evaluated at 4, 6 and 8 d after stress using gas exchange analyzer by LI-COR. The graph indicates mean ± SE (n = 5). Asterisks indicate significant differences between genotypes (*$P \leq 0.05$) using student's *t*-test.

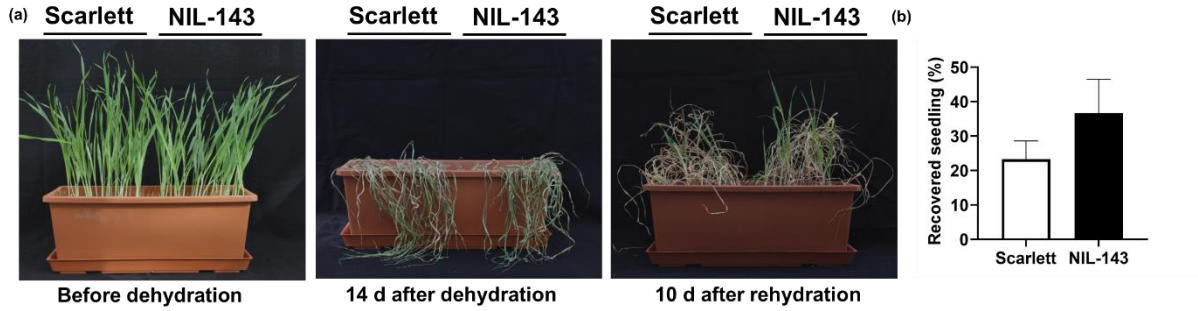

Figure S6. Stress recovery in Scarlett and NIL-143 at the seedling stage. Images of representative pots of (a) Scarlett and NIL-143 before the start of dehydration and after rehydration. Thirty seedlings were per genotype were grown in a pot for 14 d at 75% field capacity. Two-week-old seedlings were subjected to dehydration stress by withholding the water supply for 14 d. The images were taken 10 d after rewatering using Canon 750D. (b) The percentage of recovered seedlings was determined by counting the number of rejuvenated plants. Scoring was done 14 d after rewatering. The experiment was performed four biological replicates. The graph represents mean ± SE (n = 4).

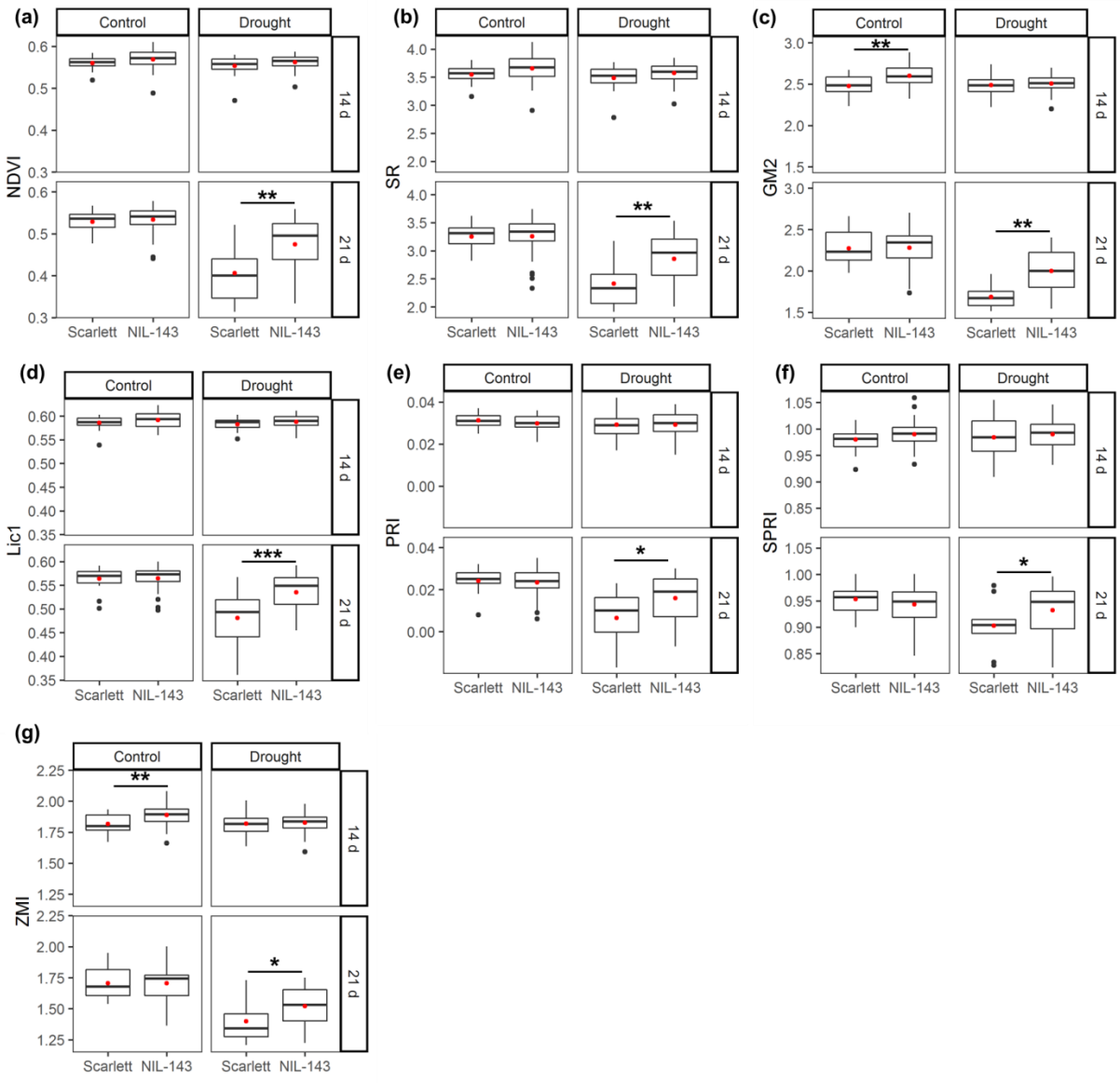

Figure S7. Vegetation index of Scarlett and NIL-143 under field conditions. Effect of water stress on (a) normalized differences vegetation index (NDVI) (b) simple ratio index (SR) (c) Gitelson and Merzlyak index 2 (GM2) (d) Lichtenthaler index (Lic1) (e) photochemical reflectance index (PRI) (f) simple ratio pigment index (SPRI) and (g) Zarco-Tejada and Miller Index (ZMI). Scarlett and NIL-143 were grown in 40 cm rows inside a rainout shelter. One plot was regularly irrigated, while drought stress was applied to another plot for 21 d at the heading stage (BBCH 41). Vegetation indexes were scored at 7, 14 and 21 d after stress. The red dot indicates the mean of the distribution. Asterisks indicate significant differences between genotypes (*$P \leq 0.05$, **$P \leq 0.01$, ***$P \leq 0.001$) using student's *t*-test (n = 19 to 45).

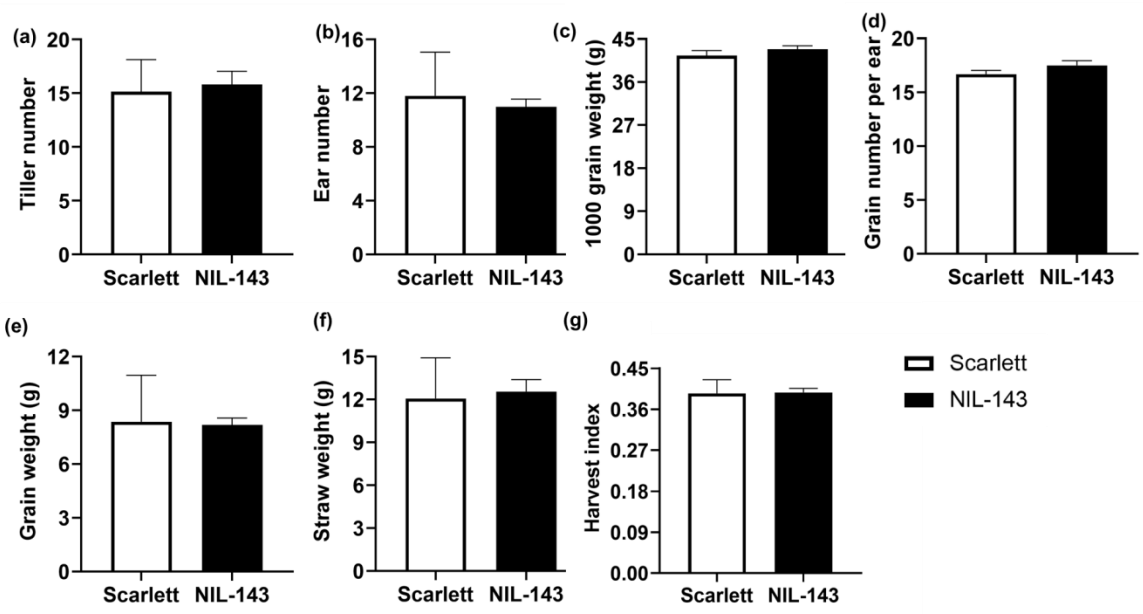

Figure S8. Yield and related traits of Scarlett and S42IL-143 under field conditions. Effect of drought stress on (a) tiller number (b) ear number per plant (c) grain number per ear (d) 1000-kernel weight (e) grain weight per plant (f) straw weight per plant and (g) harvest index. Scarlett and NIL-143 were grown in 40 cm rows under rainfed conditions in Campus Kleinaltendorf, Rheinbach, Germany. Matured panicles and straw were harvested, and oven-dried at 37°C for 72 h. The graph represents the mean ± SE (n = 10).

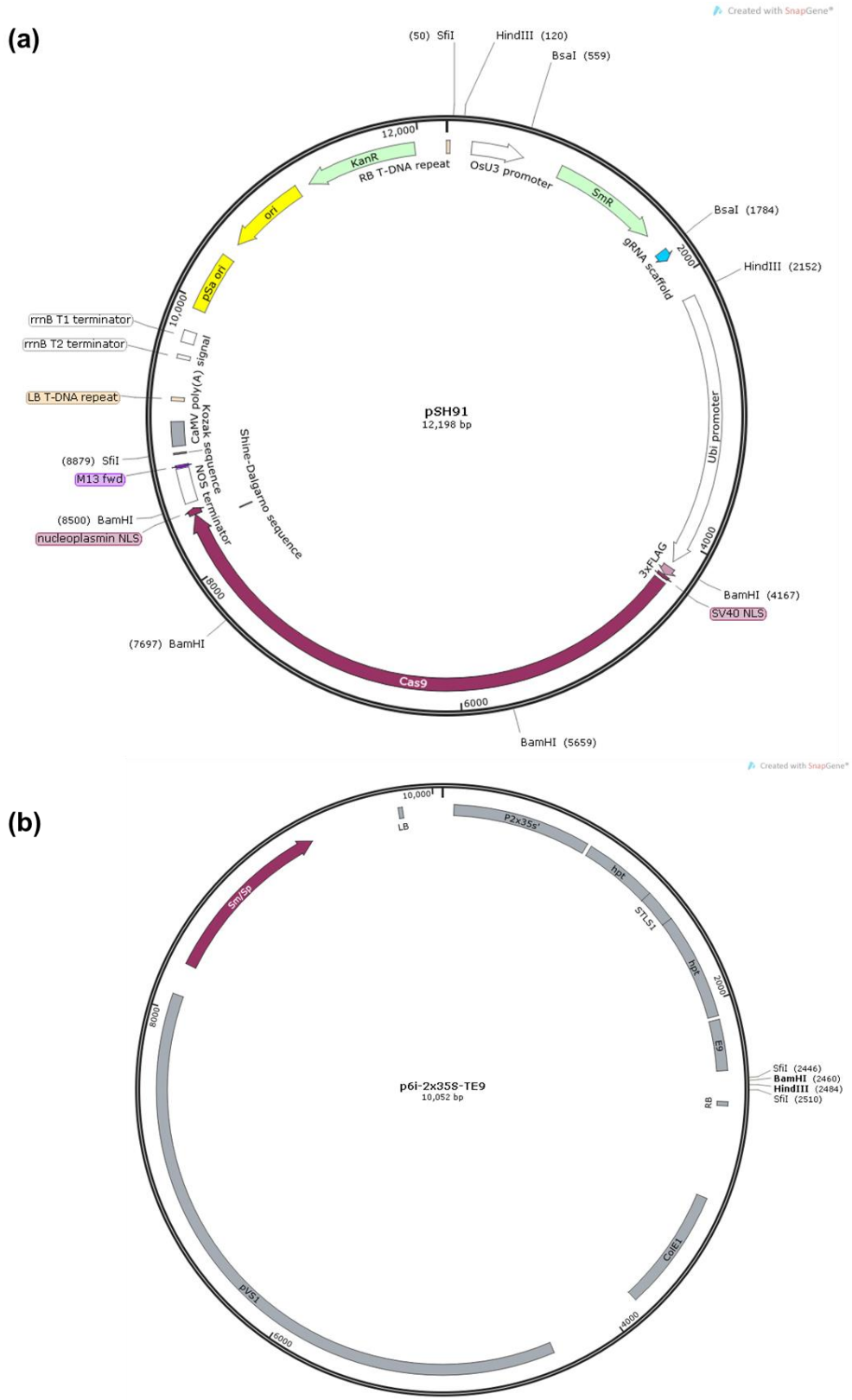

Figure S9. Structure of destination and binary vector used to develop plant transformation CRISPR RNA/Cas9 construct.

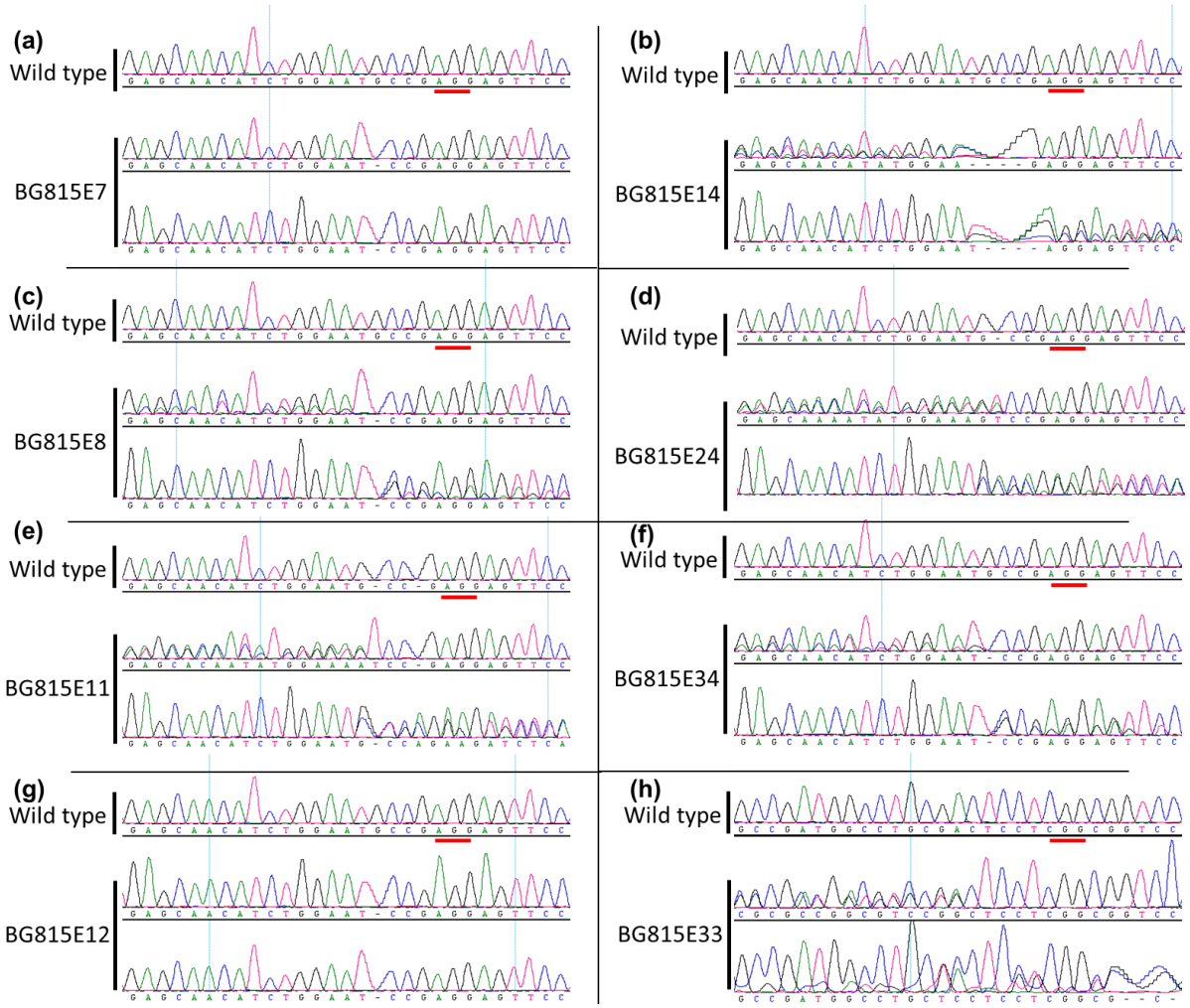

Figure S10. Site-directed mutagenesis detected in T_0 progenies through Sanger sequencing. The target site was PCR amplified, PCR product was purified and sent for Sanger sequencing. (a-h) The chromatogram of the target site of T_0 progenies generated after co-transformation with sgRNAbZIP-PS3 and sgRNAbZIP-PS4. We detected mutation events in T_0 progenies from (a-g) for HvABI5 and (h) for HvABF. Detection of multiple peaks around the PAM sequence was used as an indicator for the selection of T_0 progenies with possible mutation events. A homozygous mutation event was detected already in three T_0 progenies (a, c, and g). The nucleotides indicated with the red line is the protospacer motif.

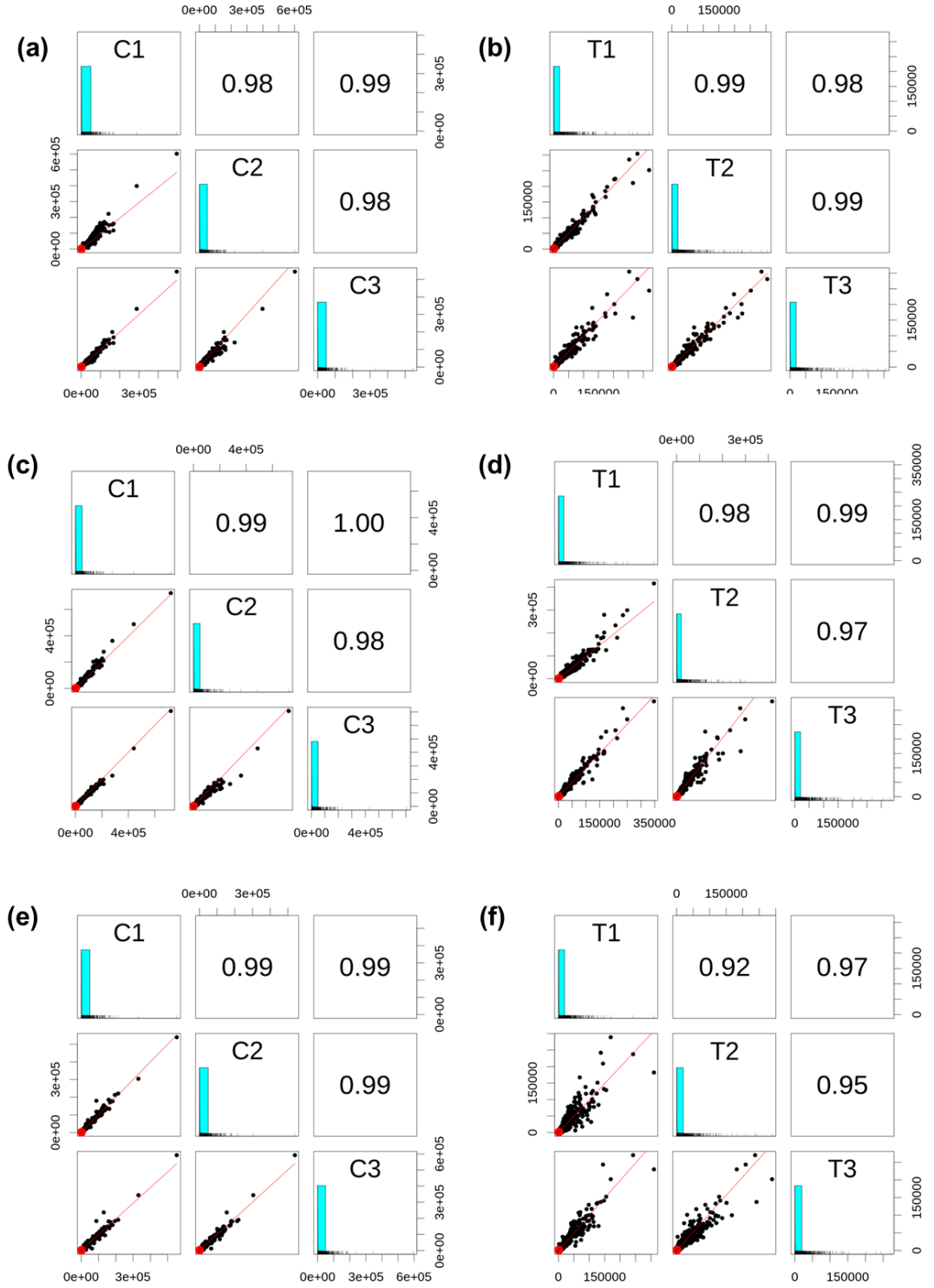

Figure S11. Correlation between the normalized expression value of the biological replicates. (a) Golden Promise under control conditions (b) Golden Promise under drought conditions (c) *hvabf* under control conditions (d) *hvabf* under drought conditions (e) *hvabi5* control conditions (f) *hvabi5* under drought conditions.

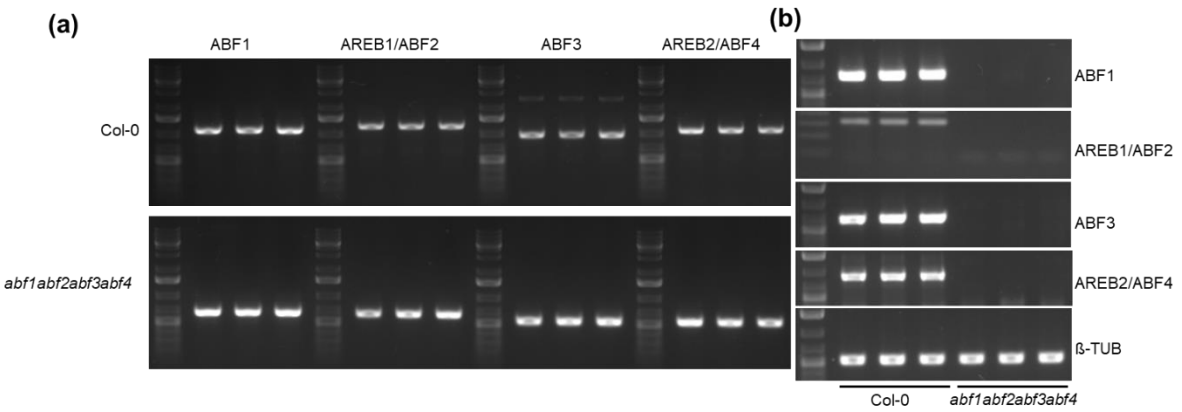

Figure S12. Genotyping of ABF mutants. (a) PCR products amplified from the genomic DNA of Col-0 and the *abf1 abf2 abf3 abf4* quadruple mutant using the genotyping primers for SALK_132819, SALK_002984, SALK_096965 and SALK_069523. (b) The presence/ absence analysis of gene expression of four ABFs (ABF1, AREB1/ABF2, ABF3, and AREB2/ABF4) was evaluated by semi-quantitative PCR. ß-TUB1 was used as a reference gene. Fifteen days old seedlings were dehydrated for 1h before RNA extraction.

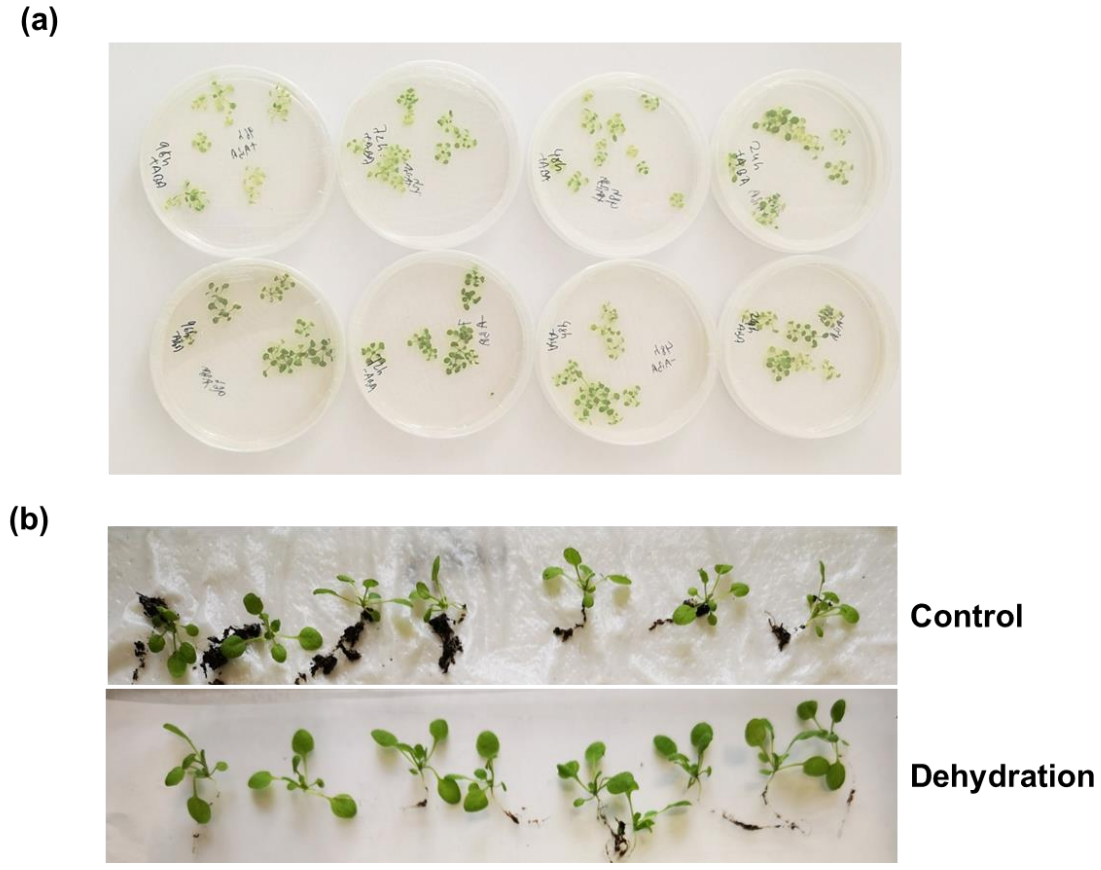

Figure S13. Experimental setup for (a) external ABA application and (b) acute dehydration.

Figure S14. Position of ABA-responsive elements (ABRE) motifs in the *P5CS1* promoter. The promoter motifs were predicted by plant promoter analysis navigator (PlantPAN 3.0) and plant cis-acting regulatory DNA elements (PLACE) databases.

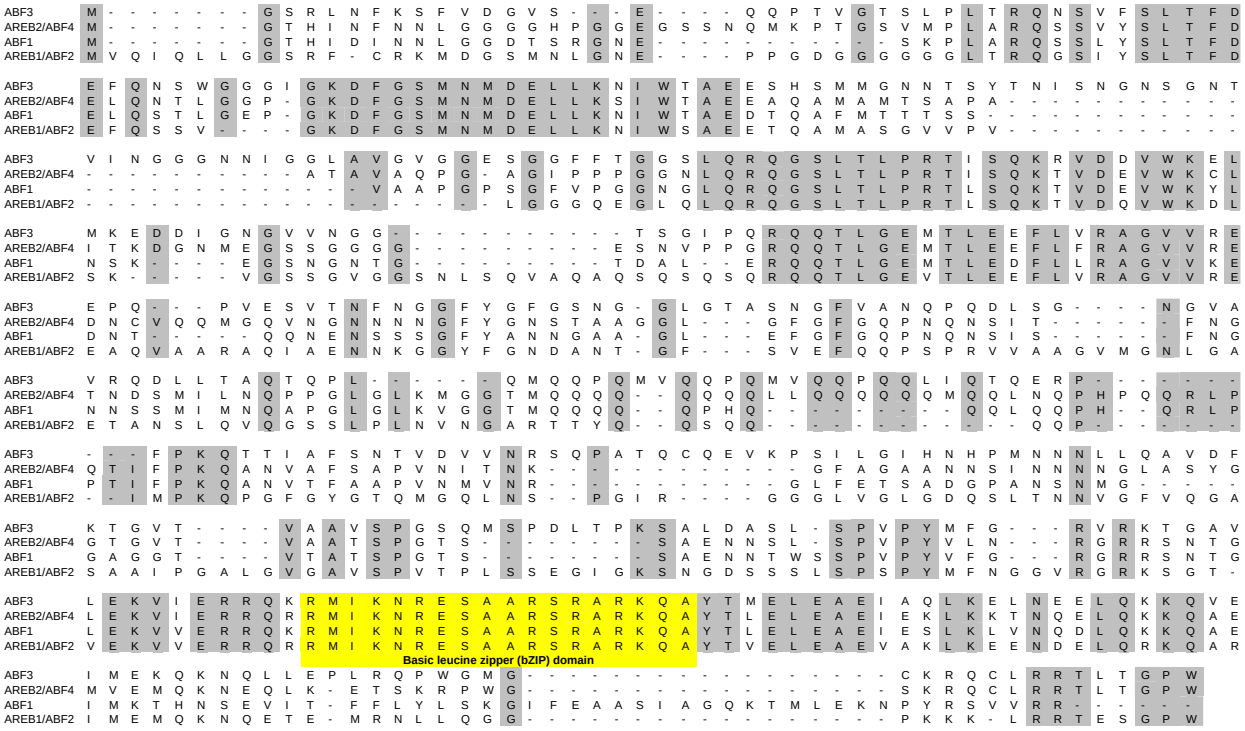

Figure S15. Protein sequence alignment of four ABA-responsive element binding factors in Arabidopsis. Basic leucine zipper domain is highlighted in yellow.

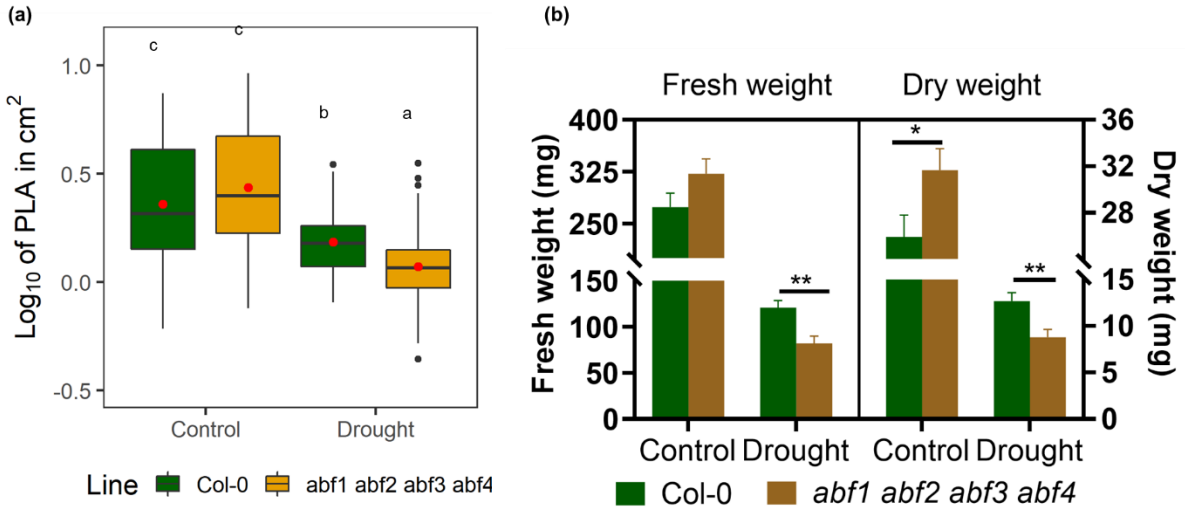

Figure S16. Shoot growth under constant drought stress in wild type and the *abf1 abf2 abf3 abf4* quadruple mutant. Watering was stopped at 24 d after seeding, and moderate drought (10% volumetric moisture content) was maintained until 36 d. PLA was recorded every day after drought treatment, and plants were re-watered when no further increase in PLA was observed under drought conditions. Plants were harvested 5 d after re-watering. (a) Boxplot for projected leaf area between 26 d and 36 d (duration of drought). The red dot indicates mean of the distribution (n = 180). Indexed letters above the bars indicate a significant difference between the genotypes ($P \leq 0.05$) using TukeyHSD test. (b) Effect of

moderate water stress on shoot fresh and dry weight. Bar indicates mean ± SE (n = 20). Asterisks indicate a significant difference between genotypes (*$P \leq 0.05$, **$P \leq 0.01$) using student's *t*-test.

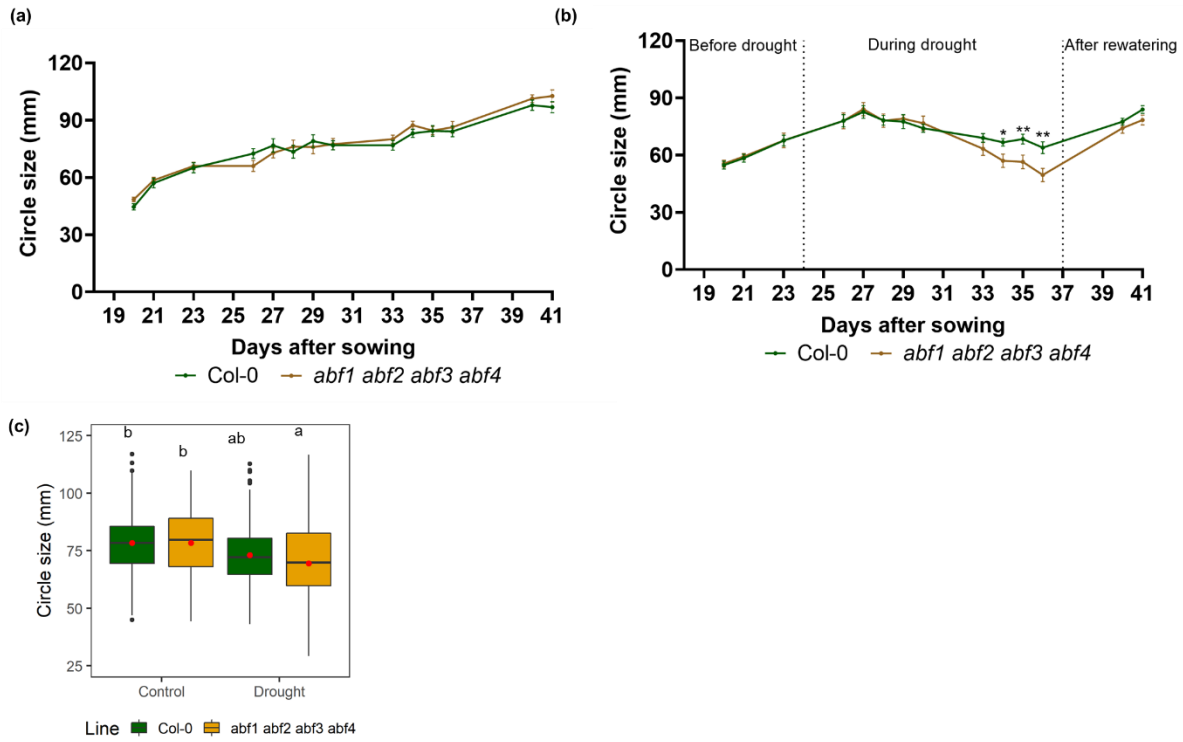

Figure S17. Rosette morphology under constant drought stress in wild type and the *abf1 abf2 abf3 abf4* quadruple mutant. Watering was stopped at 24 d after seeding, and moderate drought (10% volumetric moisture content) was maintained until 36 d. PLA was recorded every day after drought treatment, and the plants were re-watered when no further increase in PLA was observed under drought conditions. Estimated circle size of rosette under (a) control and (b) drought conditions. The line graph represents mean ± SE (n = 20). Asterisks indicate significance difference between genotypes (*$P \leq 0.05$, **$P \leq 0.01$, ***$P \leq 0.001$) using student's *t*-test. (c) Boxplot for estimated circle size of rosette between 26 d and 36 d (duration of drought). The red dot indicates mean of the distribution. Indexed letters above the bars indicate a significant difference between the genotypes ($P \leq 0.05$) using TukeyHSD test.

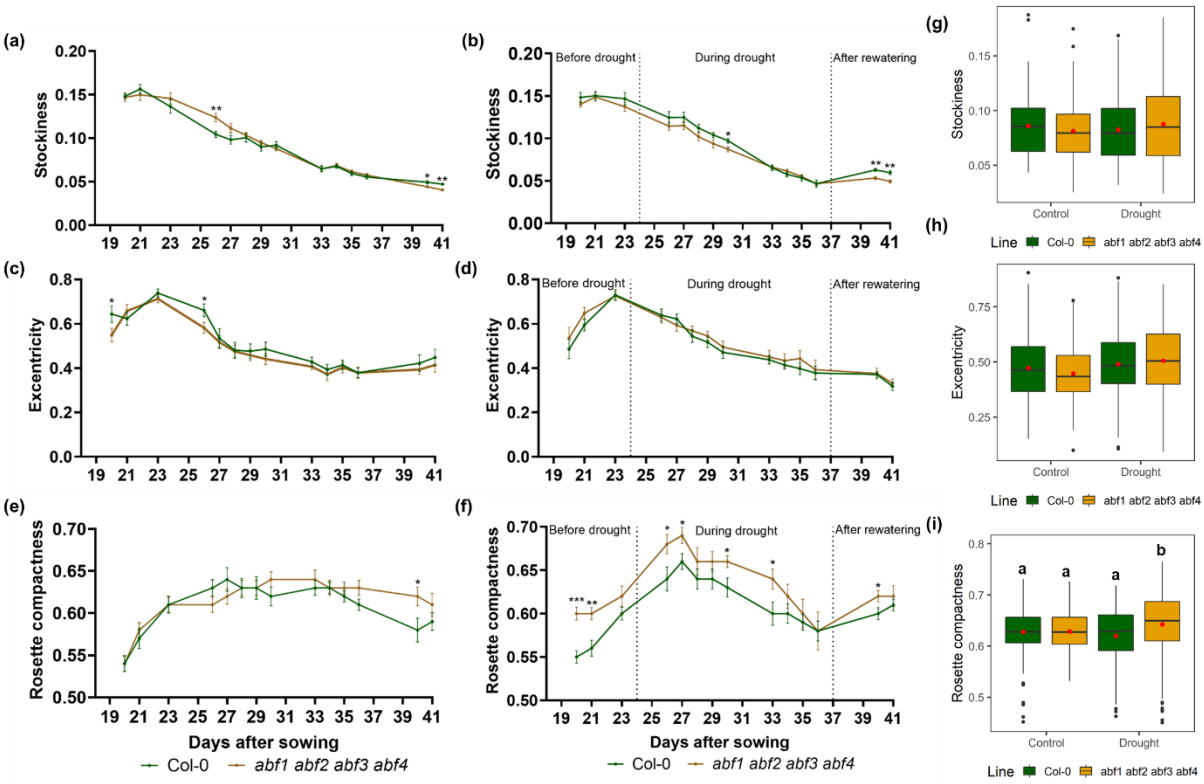

Figure S18. Rosette morphology under constant drought stress in wild type and the *abf1 abf2 abf3 abf4* quadruple mutant. Watering was stopped at 24 d after seeding, and moderate drought (10% volumetric moisture content) was maintained until 36 d. PLA was recorded every day after drought treatment, and the plants were re-watered when no further increase in PLA was observed under drought conditions. Stockiness under (a) control and (b) drought conditions. Excentricity under (c) control and (d) drought conditions. Rosette compactness under (c) control and (d) drought conditions. The points on the line graph represent mean ± SE (n = 20). Asterisks indicate a significant difference between genotypes (*$P \leq 0.05$, **$P \leq 0.01$) using student's *t*-test. Boxplot for estimated (g) rosette compactness (h) rosette stockiness (i) rosette excentricity between 26 d and 36 d (duration of drought). The red dot indicates mean of the distribution. Indexed letters above the bars indicate a significant difference between the genotypes ($P \leq 0.05$) using TukeyHSD test.

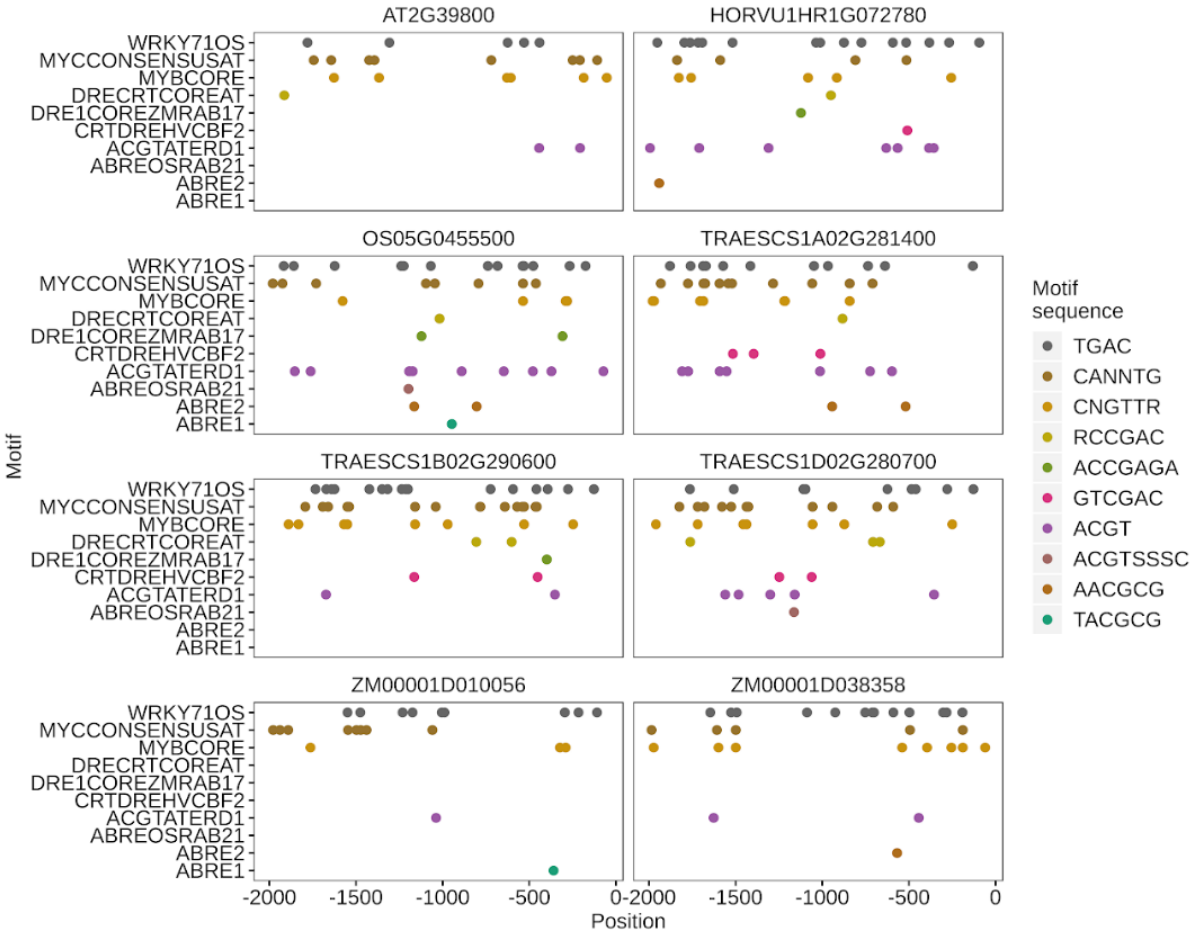

Figure S19. *Cis*-regulatory elements detected across *P5CS1* promoter in Arabidopsis, barley, rice, wheat and maize. A 2000 kb sequence upstream of the start codon was used to predict the motif. Dots indicate the position of the motif in the promoter region.

Publications

Muzammil S, **Shrestha A**, Dadshani S, Pillen K, Siddique S, Léon J, Naz A. 2018. An ancestral *P5cs1* allele promotes proline accumulation and drought adaptation in cultivated barley. Plant Physiology. /doi.org/10.1104/pp.18.00169. **(First author with equal contribution)**

Contributed to fine mapping of *QPro.S42-1H,* data analysis and manuscript preparation, performed transient assay, executed pot experiments for yield attributing traits.

Shrestha A, Cudjoe DK, Fiorani F, Siddique S, Léon J, Naz A. Drought inducible proline synthesis involves ABF-dependent signals in *Arabidopsis thaliana.* **(Manuscript in preparation)**

Leading the experiment, performed a large part of the experiments except GROWSCREEN phenotyping, data analysis and manuscript preparation.

Shrestha A, Fendel A, Kullik S, Adebay A, Nguyen T, Gaugler P, Frei M, Schaaf G, Léon J, Naz A. An exotic allele of wild barley promotes adaptive response and yield advantage under drought stress in barley. (**Manuscript in preparation)**

Leading the field experiment and ABA application experiment in barley, executed experiments at the seedling stage, performed data analysis and writing of the manuscript.

Shrestha A, Schneider M, Benndorf J, Sauer C, Nguyen T, Kumlehn J, Léon J, Naz A. A member of HvABF family confers drought stress tolerance in barley.

Leading the experiment, developed CRISPR constructs for plant transformation, performed genotyping of mutant pipelines, supervised students for a screening of mutant lines, executed RNAseq experiment and did part of RNAseq analysis, statistical analysis and writing of the manuscript. (**Manuscript in preparation)**